The Effects of Beta-Adrenergic Drugs on Proliferation and Differentiation of Mid-Gestation Ventricular Cells and Their Impact on Donor Cell Transplantation

by

Tiam Feridooni

Submitted in partial fulfilment of the requirements
for the degree of Doctor of Philosophy

at

Dalhousie University
Halifax, Nova Scotia
October 2014

Dedicated to my parents, Amir and Nahid, my brother, Hirad, and all those who made sacrifices for me to reach this far.

Table of contents

LIST OF TABLES

LIST OF FIGURES

ABSTRACT

Heart disease is the leading cause of death worldwide. Cell transplantation therapy is emerging as a method for regeneration of the heart muscle cells (cardiomyocytes) lost during disease. Despite several advances in cell transplantation field, there is no consensus on the type of donor cell or optimal conditions required for myocardial repair. Cardiac progenitor cells (CPC) present in mid-gestation ventricles exhibit unique attributes such as the ability to rapidly divide and subsequently differentiate into mature cardiomyocytes. The present study examined the effects of β-adrenergic receptor (β-AR) agonists and antagonists on proliferation and differentiation of mid-gestation ventricular cells *in vitro* as well as on intracardiac graft formation *in vivo*. Results showed that primary cultured or transplanted ventricular cells underwent a reduction in cell cycle activity following exposure to non-selective β-adrenergic stimulation via Isoproterenol (ISO). Further, administration of β_1-AR blocker Metoprolol rescued deleterious cell cycle effects associated with ISO treatment *in vitro* and *in vivo*. While β-AR stimulation increased the differentiation of CPCs into cardiomyocytes, β-AR blockers exhibited the opposite effect on CPC differentiation.

This study also tested the hypothesis that developmental stage and differentiation status of ventricular cells could impact on their engraftment potential *in vivo*. Results showed that mid-gestation ventricular cells could form larger intracardiac grafts when compared to ventricular cells from later developmental stages. Notably, mid-gestation ventricular cells can migrate to the injured myocardium and improve cardiac function more efficiently compared to cells from a later developmental stage. Further, this work also evaluated the potential of a novel mitochondrial dye (TMRM) based method to fractionate CPCs from cardiomyocytes. Results from TMRM based fractionation studies demonstrated that CPCs could be efficiently separated from cardiomyocytes and the fractionated CPCs have the potential to differentiate into cardiomyocytes with or without cardiomyogenic factors. Collectively, results from this thesis increased our current understanding of the mechanisms regulating proliferation and differentiation of cardiomyogenic donor cells. These findings could bridge the gap between the basic research and clinical use of myocardial cells derived from pluripotent stem cells and possibly aid in the development of new cell-based therapies for treating patients with severe heart disease.

LIST OF ABBREVIATIONS AND SYMBOLS USED

~	Approximately
Δ	Change
°	Degree
µL	Micro liter
µm	Micro meter
µM	Micro molar
#	Number
%	Percent
α	Alpha
α-CSA	α-cardiac sarcomeric actinin
α-MHC	α-myosin heavy chain
α-SMA	α-smooth muscle actin
β	Beta
β-AR	β-adrenergic receptor
βARKs	β-adrenergic receptor kinases
β-gal	β-galactosidase
AKAPs	A-kinase anchoring proteins
AM	Acetoxymethyl
AP	Action potential
ATP	Adenosine tri-phosphate
AC	Adenylyl cyclase
APS	Ammonium persulfate
ACE	Angiotensin converting enzyme
AHF	Anterior heart-forming field
AB/AM	Antibiotic antimycotic
AV	Atrioventricular
BMK1	Big MAP kinase-1
BMSC	Bone marrow stem cells
BMPs	Bone morphogenetic proteins
BMMNCs	Bone-marrow-derived mononuclear stem cells
JNK	c-Jun N-terminal kinases
Calcium	Ca^{2+}
CaMK-II	Ca^{2+}-calmodulin-dependent protein kinase II
CNCCs	Cardiac neural crest cells
CPCs	Cardiac progenitor cells
CMs	Cardiomyocytes
Cl^-	Chloride
cDNA	Complementary DNA
CHF	Congestive heart failure
Cx40	Connexin-40
Cx43	Connexin-43

CABG	Coronary artery bypass graft
Cre	Cre-recombinase
cAMP	Cyclic adenosine 3', 5'-monophosphate
HCN4	Potassium/sodium Hyperpolarization-activated cyclic nucleotide-gated channel
CDK4	Cyclin-dependant kinase 4
CYP2D6	Cytochrome p450 2D6
DCM	Dilated cardiomyopathy
DMSO	Dimethyl sulfoxide
DBH	Dopamine β-hydroxylase
Dox	Doxorubicin
DMEM	Dulbecco's modified eagle medium
ECG	Electrocardiogram
E	Embryonic day
ESC	Embryonic stem cell
EPC	Endothelial progenitor cell
EMT	Epithelial-mesenchymal transformation
EDTA	Ethylenediaminetetraacetic acid
E-C	Excitation-contraction
ERK	Extracellular signal-regulated kinases
FGF	Fibroblast growth factor
FLA 365	4-(2-aminopropyl)-3,5-dichloro-N,N-dimethylaniline
FHF	First heart field
FACS	Fluorescence activated cell-sorting
GRKs	G-protein-coupled receptor kinases
GPCRs	G-protein-coupled receptors
GAPDH	Glyceraldehyde 3-phosphate dehydrogenase
g	Grams
GDP	Guanosine diphosphate
GTP	Guanosine triphosphate
H_2O	Water
H_2O_2	Hydrogen Peroxide
EC_{50}	Half maximal effective concentration
t½	Half-life
HAND	Heart and neural crest derivatives expressed transcript
Hh	Hedgehog
Hours	Hrs
hESC	Human embryonic stem cell
hMSC	Human mesenchymal stem cell
IBMX	1-methyl-3-(2-methylpropyl)-7H-purine-2,6-dione
ICI	ICI-118, 551
iPSC	Induced pluripotent stem cell
IRES	Internal ribosomal entry sequence

$[Ca^{2+}]_I$	Intracellular Ca^{2+}
IP3R	IP3 binding receptor
ISO	Isoproterenol
KO	Knockout
L-DOPA	L-3,4-dihydroxyphenylalanine
LTCC	L-type Ca^{2+} channels
LV	Left ventricle
LIF	Leukemia inhibitory factor
isl1	LIM-homeodomain transcription factor islet-1
MSC	Mesenchymal stem cell
Mesp1	Mesoderm posterior 1
Meto	Metoprolol
Min	Minute
MAPK	Mitogen activated protein kinase
MEF	Myocyte enhancer factor
MyBP-C	Myosin binding protein-C
NAO	10-Nonyl Acridine Orange
nM	Nano molar
Nkx2.5	NK2 transcription-factor related, locus 5
NC	Nkx2.5-Cre
NMC	Nonmyocyte cell
NE	Norepinephrine
PM	Pharyngeal mesodermal
PBS	Phosphate buffered saline
PH3	Phospho-histone 3
PDGF	Platelet-derived growth factor
PCR	Polymerase chain reaction
K^+	Potassium
PS	Primitive streak
PI	Propidium iodide
PKA	Protein kinase A
qPCR	Quantitative polymerase chain reaction
ROI	Regions of interest
RNA	Ribonucleic acid
RL	Rosa LacZ
RyR	Ryanodine receptor
SERCA	Sarco/endoplasmic reticulum Ca^{2+}-ATPase
SL	Sarcolemma
MF20	Sarcomeric myosin heavy chain
SR	Sarcoplasmic reticulum
Scx	Scleraxis
SHF	Second heart field
Sema3D	Semaphorin3D

SA	Sinoatrial
Na^+	Sodium
SDS	Sodium dodecyl sulfate
SCNT	Somatic cell nuclear transfer
Sca-1	Stem cell antigen-1
SDF-1	Stromal cell-derived factor-1
SSII-RT	Superscript II reverse transcriptase enzyme
Tbx	T-box transcription factor
Bry	T-box transcription factor Brachyury/T
TUNEL	Terminal deoxynucleotidyl transferase dUTP nick end labelling
TEMED	Tetramethylethylenediamine
TMRM	Tetramethylrhodamine methyl ester perchlorate
C_T	Threshold cycle
LI	Thymidine-labeling index
T-Tubules	Transverse tubules
T-Tubules	Transverse tubules
VEGF	Vascular endothelial growth factor
VCS	Ventricular conduction system
vWF	Von Willebrand factor
WT	Wild-type
Wt1	Wilm's Tumour 1
X-Gal	5-bromo-4-chloro-3-indolyl-β-D-galactopyranoside

ACKNOWLEDGEMENTS

I would like to thank first and foremost my Supervisor Dr. Kishore Pasumarthi for his exceptional patience and mentorship throughout my doctoral studies. I owe my success as a graduate student to his undying curiosity, passion and enthusiasm for science. His dedication for my success, not only as a graduate student, but also as a future scientist was both motivational and inspirational. I am forever thankful and indebted to him for all of his hard work, advice and encouragement.

I would also extend thanks to all of the members of the Pasumarthi lab, past and present, for their assistance, insight and what I hope will be life-long friendship. A special thanks to Dr. Mark Baguma, Sarita Chini and Arun Govindapillai for their hard work and assistance during my graduate studies. Furthermore, special thanks to Dr. Adam Hotchkiss for his guidance and insight throughout my graduate studies and helping me mature not only as a scientist but in other aspects of life as well.

I would like to thank the member of my advisory committee, Dr. Chris Sinal, Dr. Christian Lehmann and Dr. Ryan Pelis as well our graduate coordinator Dr. Eileen Denovan-Wright for their valuable advice and support during my graduate studies. I would also like to thank the administrative staff in the Department of Pharmacology, Sandi Leaf, Luisa Vaughan and Cheryl bailey for all of their patience and assistance.

I would also like to express my sincere appreciation to my thesis examining committee, Dr. Christopher McMaster, Dr. Gregory Hirsch and Dr. Ren-Ke Li for reviewing my thesis work.

I would also like thank my colleagues and friends for their continuous support and encouragement throughout my graduate studies. Lastly, I would like to extend my deepest thanks to my parents and brother who have always played a significant role in my success in all aspects of life due to their continuous support, encouragement and understanding.

CHAPTER 1 INTRODUCTION

1.1 Thesis Overview

Every year, approximately 15 million new cases of myocardial infarction are reported worldwide. Myocardial infarction is the result of occlusion of one or more coronary arteries, which in turn results in interruption of coronary circulation leading to the loss of contractile myocardial tissue. Although the mammalian heart has adapted a variety of signaling pathways for maintaining cardiac output and systemic blood pressure in disease states, it lacks the intrinsic ability to replace lost and/or diseased myocardium due to a scant number of resident cardiac stem cells and low levels of cardiomyocyte cell cycle activity in post-natal life (Rosenthal, 2001). Additionally, prolonged activation of β-adrenergic receptors, in response to catecholamines (epinephrine and norepinephrine), has been shown to be directly toxic to cardiomyocytes (Lamba & Abraham, 2000). Thus, the collective loss of contractile myocardial tissue leads to activation of endogenous repair mechanisms where contractile tissue is replaced with non-contractile fibrotic tissue, ultimately leading to progressive heart failure (Zucker et al., 2012).

Despite advances in pharmacological and surgical therapies, the prognosis for patients with end-stage heart failure still remains grim. In fact, patients in end-stage heart failure have a 1-year mortality rate of approximately 50% and require intensive care and special therapeutic intervention. Although newly developed pharmacological therapies along with invasive surgical procedures have increased the survival of patients suffering from heart failure, these interventions fail to replace the myocardial scarring with new contractile tissue (Spargias et al., 1999). Thus, several new therapeutic strategies have been investigated to replace the diseased myocardium. Among those, cell transplantation therapy is emerging as a method for regeneration of myocardium lost due to

cardiovascular disease (Christoforou & Gearhart, 2007; Barile et al., 2007; Ni et al., 2014). Evidence suggests that transplanted cells are capable of improving the function of scarred myocardium by inducing angiogenesis, myogenesis and secretion of cardioprotective paracrine factors, which may collectively result in attenuation of the ventricular scar tissue and improved ventricular function (Dai et al., 2005; Orlic et al., 2003).

Although several studies have shown improvements in myocardial function following cell transplantation, initial benefits are lost over time due to loss of transplanted cells (Rosenthal, 2001). Furthermore, the ideal donor cell type required for optimal integration within the host myocardium or the conditions required for cell seeding to increase graft volume are yet to be determined. Recent advances in stem cell research have resulted in the generation of functional heart muscle cells from induced pluripotent stem cell cultures (iPS), which are derived from adult skin cells (Yu et al., 2007; Takahashi et al., 2007). Despite this discovery, there is a great degree of heterogeneity in the cells produced from iPS cultures, which typically consist of mature cardiomyocytes (CMs), cardiac progenitor cells (CPCs) as well as a variety of non-heart muscle cell types (Dambrot et al., 2011). We believe that CPCs hold unique qualities, which are essential to overcome existing hurdles in the cell transplantation field. These include (i) cardiomyogenic ability, (ii) higher cell cycle activity and (iii) inability to form teratomas**. Hence, development of optimal methods for enrichment of CPCs from a mixed population of heart cells hold great clinical significance and could bridge the gap between the basic research and clinical use of iPS-derived myocardial cells.** Furthermore, it has been reported that the β-adrenergic system plays an essential role in

the proper development of the embryonic heart; however, the role of the β-adrenergic system in the regulation of proliferation and differentiation of embryonic heart cells is poorly understood (Zhou et al., 1995; Rios et al., 1999; Kobayashi et al., 1995; Thomas et al., 1995). As stated earlier, local and systemic levels of catecholamines are highly elevated in cardiovascular (CV) patients in an effort to compensate for the lost function. **Hence, it is important to gain a clear understanding on the effects of widely used adrenergic drugs on potential donor cells such as embryonic or ES derived CPCs and CMs *in vitro* as well as on graft formation *in vivo*.**

Thus, the first hypothesis addressed in my doctoral work was that the β-adrenergic receptor (AR) signaling plays a critical role in the cell cycle regulation of embryonic ventricular CPCs and CMs. Towards this aim, my objectives were, (i) to investigate the expression of β_1 and β_2-ARs in cardiac ventricles from various developmental stages (ii) to determine whether β-AR stimulation plays a role in regulation of CPC and CM proliferation in mid-gestation ventricles and (iii) to determine the β-AR subtypes and signal transduction pathways involved in regulation of cell cycle events in E11.5 ventricular cells.

The second hypothesis addressed in my doctoral work was that the mid-gestational ventricular cells harboring a large number of CPCs can form larger grafts compared to cells derived from later stages of ventricular development and drugs acting on β-ARs will have a direct impact on graft size *in vivo*. Towards this aim, my objectives were, (i) to examine the grafting efficiencies of mid- and late-gestation ventricular cells in intramuscular and intracardiac transplantation models, (ii) to determine the effect of non-selective β-AR agonist Isoproterenol and β_1-adrenergic

antagonist Metoprolol on the graft size and differentiation of mid-gestation ventricular cells post-intracardiac transplantation and (iii) to examine the potential of tail vein infusion of mid- and late-gestation ventricular cells in angiogenesis and improvement of cardiac function in a doxorubicin-induced heart failure mouse model.

The third hypothesis addressed in my doctoral work was that embryonic CPCs and CMs could be enriched using a fluorescent mitochondrial marker (tetramethylrhodamine methyl ester perchlorate; TMRM) and known cardiomyogenic compounds can increase the differentiation potential of fractionated CPCs. Towards this aim, my objectives were, (i) to fractionate CMs and CPCs from embryonic mouse ventricles using TMRM staining and FACS sorting techniques (ii) to determine the differentiation potential of TMRM-low fraction into mature CMs overtime and (iii) to examine the effects of cardiomyogenic induction factors on differentiation of TMRM-low fraction into mature CMs.

The final hypothesis addressed in my doctoral work was that that β-AR signaling mediates differentiation of CPCs in TMRM low fractions into CMs. Towards this aim, my objectives were, (i) to compare the second messenger responses of β-AR stimulation between fractionated TMRM high and low fractions of E11.5 ventricular cells (ii) to compare and contrast the effects of β-adrenergic stimulation on intracellular Ca^{2+} levels of fractionated TMRM high and low fraction in response to isoproterenol stimulation and (iii) to examine the role of β-adrenergic system in differentiation of TMRM low fractions.

These studies aim to develop a method for the isolation of heart muscle precursor cells, provide new insights into the mechanisms underlying cell cycle regulation in

cardiomyogenic donor cells, increase graft volume following donor cell transplantation and possibly aid in the development of new cell-based therapies for treating patients with heart failure. The results from this thesis could bridge the gap between the basic research and clinical use of myocardial cells derived from iPS stem cells and possibly aid in the development of new methods for treatment of patients suffering from a host of cardiovascular diseases characterized by loss of functional heart muscle tissue.

1.2 Overview of the cardiovascular system

Throughout history, the heart has always been, and still is a source of mystery and wonder. It is safe to say that our understanding of the heart has come a long way from William Harvey's first discovery of the circulation of blood in the 17th century. Subsequent to Harvey's discovery, our knowledge of the heart increased with regards to descriptive anatomy and pathology in the 17th and 18th centuries, auscultation and correlations in the 19th century, understanding of cardiac disease and pathophysiology in the late 19th and 20th century, followed by advancements and protocols for treatment of cardiovascular disease into the 21st century (Silverman, 1999). The combination of evidence-based medical therapies and reductions in major risk factors has attributed to significant decrease in the number of mortalities caused by cardiovascular disease (Ford et al., 2007) in addition to an overall effort to increase the quality of patient care (Califf et al., 2002).

Even though, there has been an decrease in the mortality cardiovascular patients, the incidence of the cardiac diseases, such as heart failure and ischemic heart disease, is still increasing within the aging population (Califf et al., 2002). The prevalence of cardiovascular disease highlights the need for basic research, clinical trials and outcomes

research in hope to develop new therapeutics and tools that assist physicians and other healthcare providers to deliver high quality, equitable and effective health care to cardiovascular patients (Califf et al., 2002). Gaining a better understanding of the anatomy and physiology of the heart will provide the platform needed to better understand the pathophysiological origins of various forms of cardiovascular disease.

1.2.1 Basic cardiac structure and function

The mammalian heart is cone-like and consists of four muscular chambers. The right and left ventricles are the more muscular chambers responsible for pumping blood out of the heart, while the right and left atria are the less muscular chambers responsible for pumping blood into their respective ventricular chambers. The chambers of the heart are separated by the interventricular septum. The tip of the left ventricle, which points anteriorly and inferiorly to the left of the midline, is referred to as the apex, while the atria (mostly the left) form the base of the heart. The right atrium and ventricle make up the anterior while the left ventricle (and a small portion of the right ventricle) make up the posterior surface of the heart.

The heart consists of four major valves responsible for preventing backflow of the blood during atrial and ventricular contraction. The two atrioventricular valves, tricuspid and mitral valves are responsible for separating the right and left atria from their respective ventricles. The pulmonic and aortic semilunar valves separate the ventricles from the major arteries. The heart valves are attached to the cardiac skeleton, which is mainly composed of fibrous connective tissue and functions as a site of attachment for the valves and atrioventricular muscles.

Starting from the right atrium, deoxygenated blood from the body enters through the superior and inferior vena cava and accumulates within the right atrium. Upon contraction of the right atrium, the blood is then pumped through the tricuspid valve into the right ventricle, where it is pumped out through the pulmonic valve into the pulmonary artery and into the lungs. Oxygenated blood from the lungs is pumped from the pulmonary veins into the left atrium. Upon contraction of the left atrium the blood is pumped through the mitral valve into the left ventricle. When the left ventricle contracts the blood is pumped through the aortic valve into the aorta and subsequently distributed to the rest of the body.

The heart can be divided into three distinct layers, the endocardium, myocardium and epicardium. The endocardium is a single layer of endothelial cells that covers the interior surface of the heart chambers and the surface of the valves. Elastic and collagenous fibers, fibroblasts, nerves, veins, and branches of the conduction system make up the subendocardial tissue and are connected to the myocardium. The myocardium is the thickest layer of the heart consisting of bundles of cardiac muscle tissue. The outermost layer of the heart is the epicardium and it consists of a layer of connective tissue and adipose tissue, nerves and also the larger blood vessels responsible for providing the myocardial blood supply.

1.2.2 Cardiac innervation and conduction system

The heart is innervated by the autonomic nervous system, which consists of both sympathetic and parasympathetic nerves. The sympathetic and parasympathetic nervous systems control cardiac function by stimulation of adrenergic and muscarinic receptors of the heart (Brodde et al., 2001). Multiple autonomic receptor subtypes exist in the heart

which include α_1-, β_1-, β_2-adrenerenoceptors and M2-muscarinic receptors (Brodde et al., 2001). In the human heart the β_1- and β_2-adrenerenoceptors are evenly distributed, while a higher concentration of M2-receptors can be found in the atria compared to the ventricles (Brodde et al., 2001). Norepinephrine is the neurotransmitter used by the cardiac sympathetic system to increase heart rate (chronotropic), conduction velocity (dromotropic), myocardial contraction (inotropic) and myocardial relaxation (lusitrophic) by stimulating β_1-adrenerenoceptors (Kimura et al., 2012). Acetylcholine is the neurotransmitter used by the cardiac parasympathetic system to decrease heart rate and myocardial contraction by stimulating the M2-receptors (Olshansky et al., 2008).

At rest there is a tonic level of cardioinhibitory parasympathetic nerve firing, and an insignificant amount of sympathetic activity (Mendelowitz, 1999). The combination of decreased parasympathetic nerve firing and increased sympathetic activity results in the increase in heart rate (Mendelowitz, 1999). The preganglionic sympathetic neurons originate from the upper five to six thoracic level of the spinal cord synapse with second-order neurons in the cervical sympathetic ganglia, which travel within the cardiac nerves, terminating in the heart and great vessels. The preganglionic parasympathetic neurons originate from the dorsal motor nucleus of the medulla passing as branches of the vagus nerve where they synapse with second-order neurons located in the ganglia within the heart and great vessels. In the inferior and posterior regions of the ventricles, a large supply of afferent neurons responsible for mediating cardiac reflexes can be found. On the other hand, a large supply of vagal efferent neurons can be found in the sinoatrial (SA) and atrioventricular (AV) nodes of heart.

The SA node is responsible for generating the cardiac electrical impulses and is regarded as the pacemaker of the mammalian heart. The SA node is located in the right atrial endocardium between the upper and lower caval veins and consists of highly specialized cells capable of generating action potentials (Scicchitano et al., 2012). The AV node is located at the atrioventricular junction on the right side of the heart and is responsible for conduction of the action potential from the atria into the ventricles (Temple et al., 2013). Beneath the AV node is the bundle of His which is the insulated component of the AV conduction axis, providing the only conduction pathway in the ventricles of the normal heart (Dobrzynski et al., 2013). At the crest of the ventricular septum, the bundle of His bifurcates into the asymmetric left and right bundle branches which continue on towards the apex of the heart where the Purkinje network is formed (Dobrzynski et al., 2013). The main function of the His-Purkinje network is to propagate the action potential throughout the ventricles and to ensure correct sequential contraction of the ventricular muscles (Dobrzynski et al., 2013).

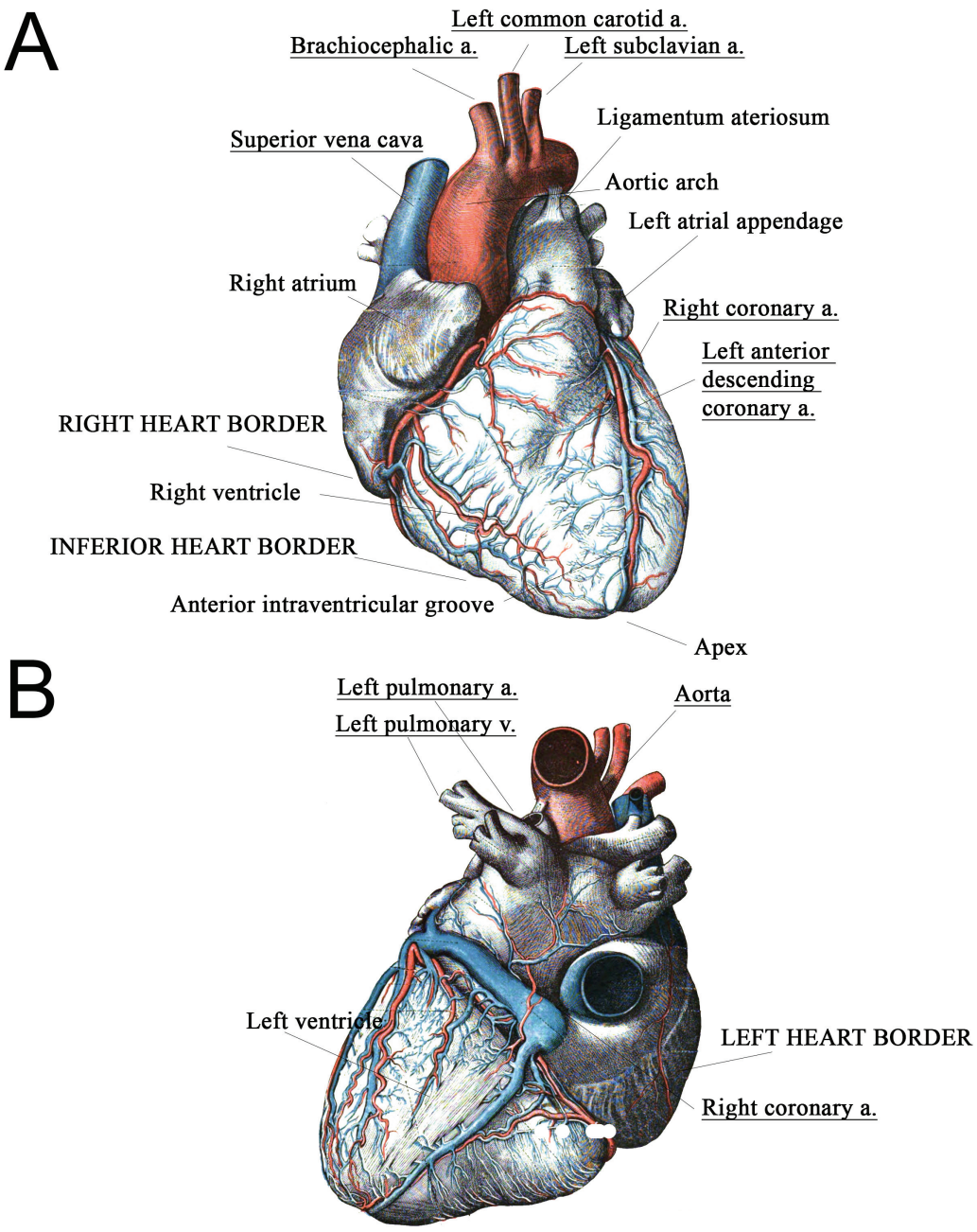

Figure 1.1: Schematic model of the external structures of the heart.
Above is a schematic representation of the anterior view **(A)** and posterior view **(B)** of the external structure of the mammalian heart. a, artery, v, veins. (Photo credit, Shutterstock #89021335, modified).

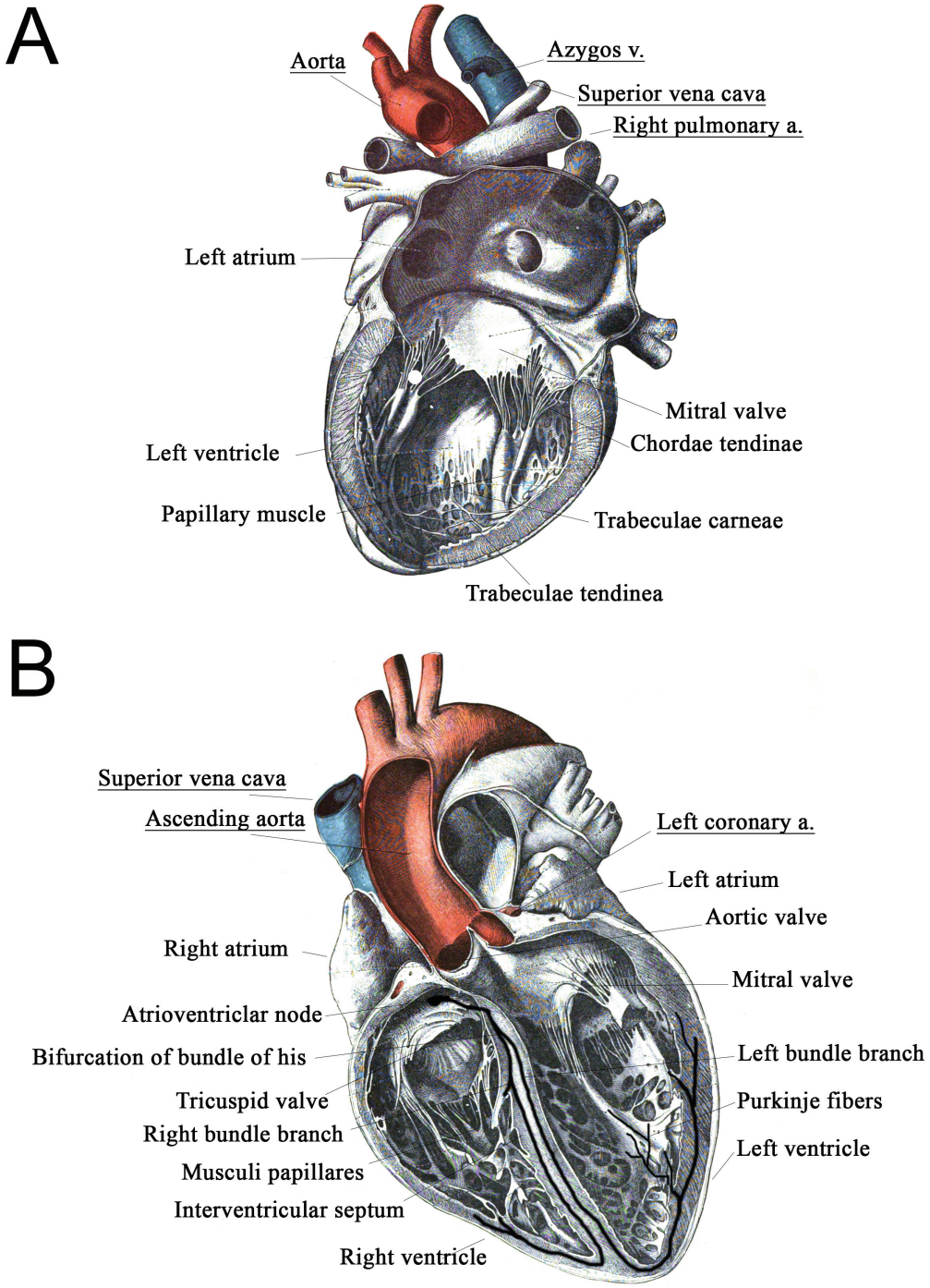

Figure 1.2 Schematic model of the internal structures of the heart.
Above is a schematic representation of the internal structures of the right and left atrium and ventricles **(A, B)**, and the main components of the conduction system **(B)** of the mammalian heart. a, artery, v, veins. (Photo credit, Shutterstock #89021335, modified).

1.2.4 Histology of myocardial cells

The cardiomyocyte is the fundamental work unit of the heart (Evans et al., 2010). Cardiomyocytes are responsible for 85% of the heart's mass and contain a large array of basic contractile units called myofibrils, which are long chains of sarcomeres (Maillet et al., 2013). The ventricular cardiomyocytes are rod-like cells measuring 20μm in diameter and 60-140μm in length, while the atrial cardiomyocytes are ellipsoidal shaped cells with diameter of 5μm and length of 10-20μm. Approximately 50% of the weight of the cardiomyocytes is occupied by the myofibrils, while the mitochondria occupy 25% of the cell and the nucleus, sarcoplasmic reticulum (SR) and the cytosol make up the remaining portion (Shintaro Nakano, 2012). The sarcomere consists of actin thin filament, myosin thick filament and titin, which stabilize the myosin at the Z-line. During systole and diastole, the length of the sarcomere ranges between 1.8-2.2μm in length (Shintaro Nakano, 2012).

In addition to the presence of various cell surface receptors and ion channels, the cardiomyocyte membrane also termed, the sarcolemma**,** consists of a series of gap-junction proteins creating intercalated disks, which are at the interface of adjacent cardiac fibers. Intercalated disks are responsible for maintaining cardiac structural and electrical continuity between adjacent cardiomyocytes. Furthermore, the transverse tubules (T-Tubules) form invaginations in the sarcolemma within the cardiomyocytes while separating the intra and extracellular space (Shintaro Nakano, 2012). T-tubules also play a role in maintaining the rapid transmission of the excitatory electrical impulses required for initiation of cardiomyocyte contraction.

The sarcoplasmic reticulum (SR) is an extensive intracellular tubular network that complements the T-Tubules both functionally and structurally. The SR functions as the

cardiomyocyte calcium storage unit. The release of SR calcium is essential for the activation of the contractile apparatus of the heart.

1.2.5 Excitation-contraction coupling

Excitation-contraction (E-C) coupling is a term that was coined in 1952 to describe conversion of an electrical signal into physical contraction of a myocyte (Sandow, 1952). E-C coupling in cardiomyocytes is initiated by a mechanism called calcium-induced calcium release (Fabiato, 1983). The E-C coupling of cardiomyocytes is initiated by action potentials (AP), which result from complex interactions among cellular electrical activity, cardiac tissue structure and electrical cell-cell communication (Kléber & Rudy, 2004). The contraction of the cardiomyocyte is initiated by an increase in intracellular calcium (Ca^{2+}) concentration due to the influx of Ca^{2+} through the sarcolemma and release from the SR (Cannell et al., 1994).

An AP is the result of dynamic changes in the ionic concentrations (Na^+, K^+ and Ca^{2+}) and their effects on the membrane currents (Kléber & Rudy, 2004). In working cardiomyocytes, each AP consists of four phases, subsequent to depolarization; the Na^+ influx results in a rapid increase in membrane potential (Phase 0), quickly followed by partial membrane repolarization due to transient outward K^+ efflux (Phase 1), plateau of membrane potential due to slow Ca^{2+} influx and low K^+ efflux (Phase 2), and rapid membrane repolarization due to K^+ efflux (Phase 3). The resting potential is also referred to as Phase 4 (Kléber & Rudy, 2004).

The opening of individual voltage sensitive L-type Ca^{2+} channels located in the T-tubules results in Ca^{2+} release from the SR Ca^{2+} release channels known as the ryanodine receptors (RyRs) located on the membrane of the SR (Greenstein & Winslow, 2002).

This results in an increase in intracellular Ca^{2+} levels, which in turn can activate the contractile components of the cell (Greenstein & Winslow, 2002). The coordinated contractions of the heart are the result of the anatomical, cellular composition and conduction pathways, which collectively form an efficient system capable of continuous contractions for billions of times over the individual's life span.

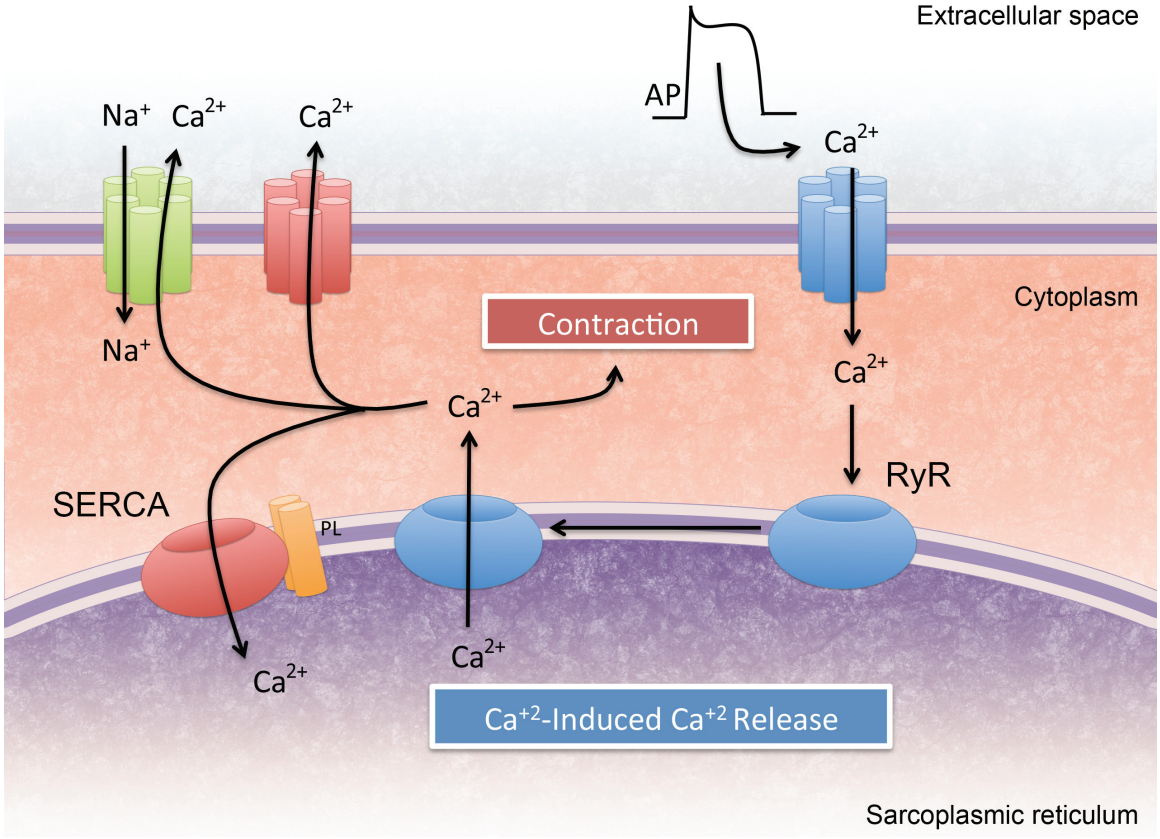

Figure 1.3 Simplified schematic representation of calcium movement within the cardiomyocyte during excitation and contraction.
In response to the action potential (AP), during phase 2, calcium (Ca^{2+}) enters the cell through Ca^{2+} channels triggering Ca^{2+}-induced Ca^{2+} release from the sarcoplasmic reticulum (SR) via ryanodine receptors. Cytosolic Ca^{2+} binds to troponin C enabling contraction. Subsequently, relaxation occurs as the Ca^{2+} is returned to the SR by the sarcoplasmic reticulum Ca^{2+} ATPase (SERCA), which is also regulated by phospholamban (PL). Sodium (Na^{+})-Ca^{2+} exchange proteins and Ca^{2+}-ATPases return the remaining intracellular Ca^{2+} to the extracellular space.

1.3 Cardiogenesis

The heart is the first organ to form during embryonic development, thus, all subsequent events in the life of the organism depend upon its proper development and function (Olson, 2004). The functional heart is composed of various different cell types, such as cardiomyocytes, fibroblasts, endocardial cells, conduction system cells, smooth muscle cells and endothelial cells. Cardiogenesis is dependent upon a combination of complex morphogenetic influences involving cells of various embryonic origins along with hemodynamic influences that play a role in proper formation of the heart (Srivastava, 2006a). Fortunately, many of the genetic mechanisms that mediate cardiogenesis are conserved across species (Srivastava & Olson, 2000), thus, facilitating the use of various genetic models to expand upon existing knowledge of the molecular mechanisms involved in differentiation and proliferation of embryonic cells involved during cardiogenesis (Srivastava & Olson, 2000).

The myocytes that the early embryonic heart is composed of originate from two separate sources of progenitor cells. The progenitor cells of the first heart field (FHF) give rise to the cardiac crescent and the primary heart tube, which begin to differentiate during the crescent stage (Prall et al., 2007). The progenitor cells of the second heart field (SHF) consist of a group of undifferentiated multipotent group of cells that contribute to formation of the heart tube, inflow and outflow poles, and are also responsible for giving rise to the majority of myocytes of the right ventricle and outflow track, atria and some of the left ventricle (Prall et al., 2007). Thus far, there have been three separate sources of heart precursor cell populations identified, the cardiogenic mesoderm cells (FHF and SHF), cardiac neural crest cells, and proepicardial cells. Collectively, these three different groups of progenitors give rise to the mammalian heart. The following section will

describe the journey of separate cardiac progenitor cells, highlighting factors involved in their specification and differentiation into mature cardiac cells.

1.3.1 The role of cardiogenic mesoderm cells in cardiogenesis and the molecular events responsible for differentiation and proliferation of cardiogenic mesoderm progenitors

Cardiac mesoderm cells are derivatives of the mesodermal layer, which have been shown to emerge from the anterior region of the primitive streak (PS) during gastrulation in both chick (Garcia-Martinez & Schoenwolf, 1993) and mouse embryos (Tam et al., 1997). While remaining uncommitted to any specific cardiogenic cell type, these groups of cells subsequently migrate from the PS and amalgamate in the anterior lateral region relative to the PS described as the splanchnic mesoderm (Francou et al., 2013). Later (mouse E7.5), the paired heart-forming fields on either side of the PS extend across the midline, forming the cardiac crescent. Around E7.5-8.0, fusion of the lateral wings of the cardiac crescent results in the formation of the primitive heart tube which consists of an outer myocardial layer and an inner epithelial layer (Zaffran et al., 2004). Around E9, the primitive heart tube undergoes rightward looping to form a C-shaped structure and subsequent ballooning of the heart tube results in the formation of the future atrial and ventricular chambers. Formation of the four chambered heart is considered to occur by E10.5, and is followed by septation and valve formation (Meilhac et al., 2003). The two essential mechanisms involved in the growth of linear heart tube include the proliferation of existing cells and recruitment of additional cells. Additional cells include cells of the final major heart segment, which are essential for formation of the cardiac outflow tract. Fate mapping has shown that such cells originate from the anterior heart-forming field (AHF, a subset of SHF), which is separate from the paired heart-forming fields

(Mjaatvedt et al., 2001). Furthermore, studies of mouse and chick embryos have suggested that cells that give rise to the arterial and venous poles of the linear heart tube originate from the pharyngeal mesodermal (PM) cells which collectively give rise to significant parts of the heart and pharyngeal muscles. Progenitor cells responsible for populating the cardiac outflow tract and the right ventricle and majority of the cells in the atria during the looping stage originate from the PM cells, also referred to as AHF, a subset of the SHF (Tzahor & Evans, 2011).

The completion of the heart tube extension by midgestation in the mouse, is followed by process termed ballooning morphogenesis during which highly regulated gene expression changes and cell proliferation lead to formation of left and right ventricles and atria and the outer curvature of the looped heart tube (Miquerol & Kelly, 2013). The collection of listed events involves the complex and delicate interaction between cardiomyocytes, epi- and endocardial cells, as well as cardiac neural crest cells.

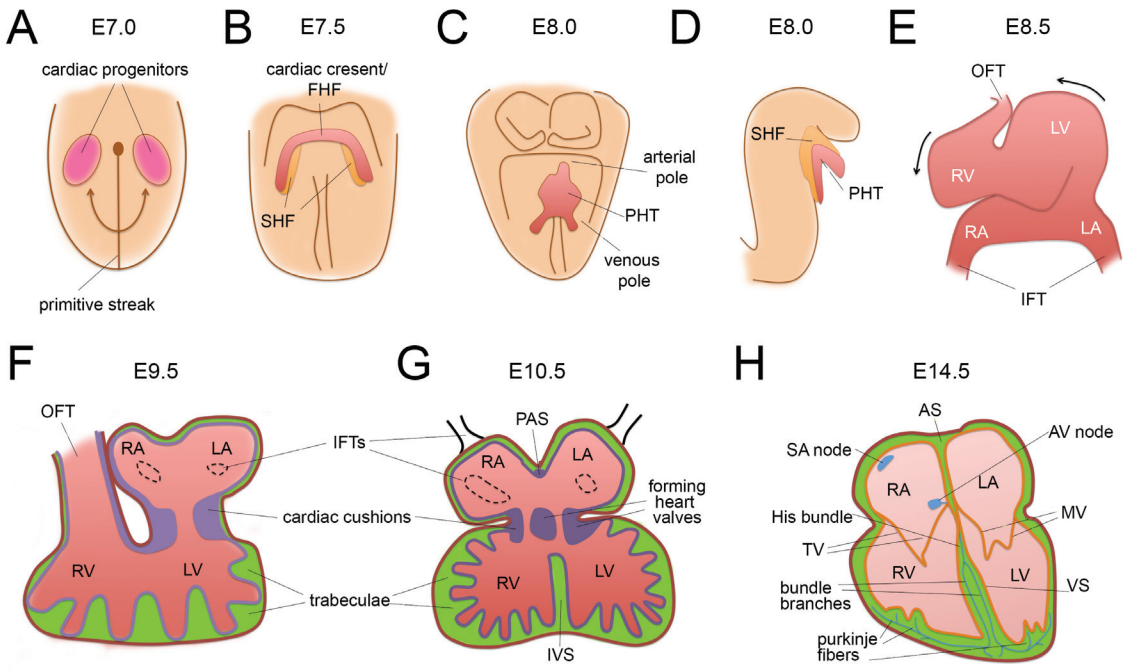

Figure 1.4 Schematic representation of embryonic development of the mammalian heart.

(A) Post ingression, CPCs migrate from the PS towards the anterior side of the embryo forming two separate populations of CPCs represented by pink. **(B)** The two cell populations come together to form two distinct heart lineages, FHF (red), also known as the cardiac crescent during this embryonic stage, and the SHF (orange). **(C)** The cells of FHF form the PHT with the arterial and venous poles located anterior and posterior to the embryo, respectively. **(D)** Lateral view of the heart. As the cells of the FHF form the PHT, cells of the SHF migrate into the PHT from both sides of the heart allowing for the ballooning of the heart. **(E)** Formation of the PHT and ballooning of the heart is followed by the looping process. During this stage, the heart loops to the right (black arrows) as the OFT and the IFT arise from the arterial and venous pole, respectively. **(F - H)** Transverse cross-section of the embryonic heart during embryonic development. **(F)** At this stage the heart consists of the epicardium (red), myocardium (green), and endocardium and cardiac jelly (purple). By undergoing EMT, cells of the epicardium make up the cells of cardiac jelly, a thick layer between the endocardium and myocardium. **(G)** At this stage, the cardiac chambers begin to develop trabeculae and the cardiac jelly and endocardium extend into the heart lumen to form heart valves. **(H)** The heart chambers are formed and are separated by AS and VS as well as MV and TV. Cardiac conduction originates from the SA node and is transmitted to the AV node, both located in the right atrium. The signal is then transmitted through the ventricles from the AV node through the His bundles, left and right bundle branches and purkinje fibers. FHF, first heart field; SHF, second heart field; PHT, primary heart tube; OFT, outflow tract; IFT, inflow tract; RV, right ventricle; LV, left ventricle; RA, right atria; LA, left atria; PAS, primary atrial septum; IVS, interventricular septum; MV, mitral valve; TV, tricuspid valve; VS, ventricular septum; AS, atrial septum; SA, sinoatrial node; AV, atrioventricular node. Figure redrawn and modified from (Gessert & Kühl, 2010).

Molecular mechanisms involved in induction of the mesoderm have been shown to be very conserved and tightly regulated by various signaling pathways. The current understanding of the mesoderm induction suggests that the Nodal family plays a significant role in mesodermal formation, the fibroblast growth factors (FGFs) and Wnts are also believed to be involved in maintaining the mesoderm state while the bone morphogenetic proteins (BMPs) are responsible for patterning the mesoderm (Kimelman, 2006). However, recent studies have suggested that a functional overlap may exist between each of these factors.

The direct target gene for Wnt/β-catenin signaling is the T-box transcription factor Brachyury/T (Bry), the expression of which is necessary for migration of mesodermal cells from the PS (Showell et al., 2004). Further, collective findings suggest that the Wnt/β-catenin signaling pathway has a biphasic function during cardiogenesis (Ueno et al., 2007), where the stimulation of the noncanonical Wnt signaling and inhibition of the canonical Wnt/β-catenin signaling is essential for commitment of Bry^+ mesodermal progenitor cells towards a cardiogenic fate (Gessert & Kühl, 2010). The Bry^+ mesodermal progenitor cells give rise to two distinct populations of cells, $Bry^+/Flk\text{-}1^-$ and $Bry^+/Flk\text{-}1^+$ (approximately E6.0 in mice). Without the presence of cytokines known to function during cardiogenesis the $Bry^+/Flk\text{-}1^+$ mesodermal progenitors are able to give rise to hematopoietic endothelial, vascular smooth muscle cells (Kattman et al., 2006). The $Bry^+/Flk\text{-}1^-$ population contains early stage cardiac progenitor cells that will undergo differentiation and give rise to contracting cardiomyocytes when cultured under appropriate conditions (Kouskoff et al., 2005). As development progresses, the down regulation of Bry is followed by activation of T-box transcription factor Eomesodermin

which acts upstream of mesoderm posterior 1 (Mesp1) (Costello et al., 2011). Lineage tracking has shown that Mesp1 is the earliest marker of cardiac progenitor cells (E7.0 in mice) and also a key regulator of cardiac progenitor cell specification and migration in vertebrates (Bondue & Blanpain, 2010).

The $Mesp1^{+}$ cells migrate to give rise to the cardiac crescent, at which time, the first and second heart fields can be distinguished. The position of progenitor cells of FHF in the cardiac crescent allows for the cells to be exposed to factors such as FGF (fgf8/acerebellar) (Reifers et al., 2000), BMP (BMP2/4) (Schultheiss et al., 1997) and inhibitors of the Wnt pathway such as, Dkk-1 and GSK3β which inhibit the β-catenin-mediated Wnt pathway (Marvin et al., 2001; Schneider & Mercola, 2001). Exposure of progenitor cells of the FHF to previously listed factors results in differentiation of progenitors into cardiomyocytes and smooth muscle cells which is marked by the expression of key lineage regulator markers such as homeobox gene Nkx2.5 (NK2 transcription-factor related, locus 5) (Lints et al., 1993), GATA4, 5 and 6 (Molkentin, 2000), MEF2b/c (myocyte enhancer factor) (Guo et al., 2014), Hand1/2 (heart and neural crest derivatives expressed transcript 1/2) (Srivastava et al., 1995) and Tbx5 and 20 (Bruneau et al., 1999; Meins et al., 2000).

The progenitor cells of SHF can be distinguished due to expression of a LIM homeodomain transcription factor termed Isl1, as the expression of Isl1 has been shown to be absent in differentiated FHF cells (Prall et al., 2007). Studies show that expression of Isl1 is essential for formation of outflow tract, right ventricle and the atria and essential for migration of cardiac progenitor cells into the heart during development (Cai et al., 2003). The expansion of $Isl1^{+}$ cardiac progenitor cells is dependent upon the Wnt/β-

catenin pathway (Ai et al., 2007), while the expression of Isl1 is diminished as the cardiac progenitors begin to differentiate (Cai et al., 2003). Lineage tracking studies have shown that the $Isl1^{+}/Nkx2.5^{+}/flk1^{+}$ cells are multipotent in nature and are able to give rise to cardiac, smooth muscle, endothelial, and conduction system cells (Moretti et al., 2006; Wu et al., 2006). More specifically, $Isl1^{+}/Nkx2.5^{+}/flk1^{-}$ cells are mainly committed to becoming smooth and cardiac muscle cells, contributing to proepicardium and endocardium during heart development (Zhou, Ma, et al., 2008; Zhou, von Gise, et al., 2008), while the $Isl1^{+}/Nkx2.5^{-}/flk1^{+}$ cells differentiate into smooth muscle and endothelial cells (Moretti et al., 2006). The differentiation fate of SHF progenitor cells is dependent upon various signaling pathways, for instance, the FGF signaling, canonical Wnt and Hedgehog (Hh) signaling inhibits differentiation and promotes proliferation of the progenitors (Kelly, 2012). Inversely, the noncanonical Wnt and Notch signaling pathways promote differentiation of SHF progenitors (Vincent & Buckingham, 2010).

Collectively, it can be concluded that the complex network of growth factors (BMP, FGF, and Wnt) and transcriptional regulators (Nkx2.5, GATA, MEF, HAND and Tbx) and the spatiotemporal alignment of the cells within the developing embryo direct the proper development of the progenitor cells of both FHF and SHF (Figure 1.5).

Figure 1.5 Lineage specification of cardiac cells during cardiogenesis.
Increased activity of various signaling pathways such as the Wnt/β-catenin, FGF, Nodal and BMP, are responsible for the induction of the mesoderm. The Brachyury (Bry) positive mesodermal precursors differentiate into $Bry^{+}/Flk\text{-}1^{+}$ hemangioblasts capable of differentiating into cells giving rise to endothelial and blood cell lineages. The up-regulation of noncanonical Wnt signaling and down-regulation of Wnt/β-catenin signaling results in the generation of a second wave of $Bry^{+}/Flk\text{-}1^{+}$ mesodermal progenitor cells. Increased Eomesodermin signaling is responsible for driving the mesodermal precursors into cardiogenic mesodermal cells marked by expression of mesoderm posterior 1 (Mesp1). The cardiogenic mesodermal ($Mesp1^{+}$) cells undergo further lineage differentiation and give rise to progenitor cells of the first and second heart field (FHF, SHF). Increased BMP and FGF signaling results in differentiation of the FHF progenitor cells into $Nkx2.5^{+}/Tbx5^{+}$ cells, capable of differentiating into cardiomyocytes and smooth muscle cells. The progenitor cells of the SHF marked by their expression of Isl1, Nkx2.5 and Flk-1, are kept in a proliferative state in response to FGF, Wnt/β-catenin and endodermal Shh signaling. As the cells of SHF contribute to the looping of the heart they further differentiate into two subpopulations marked by the expression of Isl1/Nkx2.5 and Isl1/Flk-1. The $Isl1^{+}/Flk\text{-}1^{+}$ cells are capable of differentiating into smooth muscle and endothelial cells, whereas, the $Isl1^{+}/Nkx2.5^{+}$ are capable of differentiating into smooth muscle cells and cardiomyocytes. Furthermore, the $Isl1^{+}/Nkx2.5^{+}$ give rise to two proepicaridal progenitor cells populations marked by their expression of Wnt1/Tbx18 and Scx/Sema3D. The Wnt1+/Tbx18+ and Scx+/Sema3D+ cells are capable of differentiating into smooth muscle and endothelial cells and fibroblasts. The BMP/Notch/noncanonical Wnt and Retinoic acid/TGF-β signaling, respectively, mediate the differentiation and patterning of SHF progenitors. Figure modified and redrawn from (Brade et al., 2013).

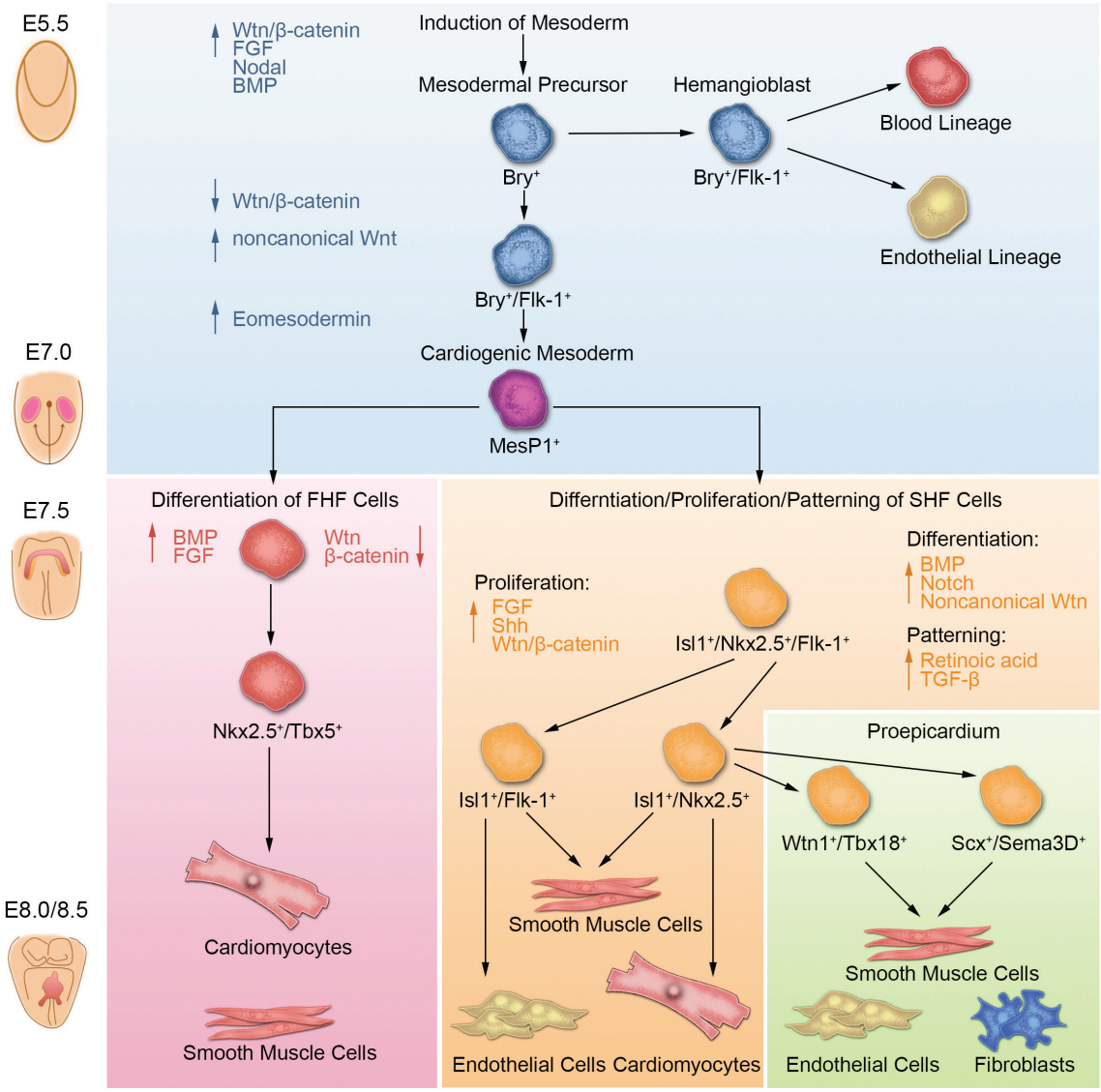
E5.5
Wtn/β-catenin
FGF
Nodal
BMP
Induction of Mesoderm
Mesodermal Precursor
Hemangioblast
Blood Lineage
Bry+
Bry+/Flk-1+
Wtn/β-catenin
noncanonical Wnt
Endothelial Lineage
Eomesodermin
Bry+/Flk-1+
E7.0
Cardiogenic Mesoderm
MesP1+
E7.5
Differentiation of FHF Cells
BMP
FGF
Wtn
β-catenin
Differntiation/Proliferation/Patterning of SHF Cells
Differentiation:
BMP
Notch
Noncanonical Wtn
Proliferation:
FGF
Shh
Wtn/β-catenin
Isl1+/Nkx2.5+/Flk-1+
Patterning:
Retinoic acid
TGF-β
Nkx2.5+/Tbx5+
Proepicardium
Isl1+/Flk-1+
Isl1+/Nkx2.5+
Wtn1+/Tbx18+
Scx+/Sema3D+
Smooth Muscle Cells
Smooth Muscle Cells
E8.0/8.5
Cardiomyocytes
Smooth Muscle Cells
Endothelial Cells
Cardiomyocytes
Endothelial Cells
Fibroblasts

1.3.2 Formation of epicardium and coronary vessels and the role of epicardium-derived cells in cardiogenesis

During cardiogenesis, the transition of the heart tube from a two-layered endocardium and the myocardium to a complex multi-layered organ coincides with the formation of the epicardium (Männer et al., 2001). The epicardium is described as an epithelial layer that covers the myocardium (van Wijk & van den Hoff, 2010). At E9.5 of mouse development, the splanchnic mesoderm that covers the vitelline veins at the inflow of the heart gives rise to the proepicardium (Männer et al., 2001). As the proepicardial cells migrate to cover the myocardium, a subset of the epithelial cells undergo epithelial-mesenchymal transformation (EMT) (Wessels & Pérez-Pomares, 2004). This population of EMT cells is responsible for giving rise to the nonmyocardial cells in the myocardium such as coronary smooth muscle and endothelial cells, cardiac fibroblasts, and atrioventricular cushion mesenchymal cells (Wessels & Pérez-Pomares, 2004). Similar to FHF and SHF, the induction, growth and maintenance of the proepicardium is dependent upon intricate signaling pathways which include opposing interactions between the BMP2 (responsible for myocardial differentiation) and the FGF2 (responsible for epicardial cell differentiation) signaling pathways (Kruithof et al., 2006).

Proepicardium progenitor cells can be distinguished via expression of the T-box transcription factor 18 (Tbx18) (Kraus et al., 2001) and transcription factor Wilm's Tumor 1 (Wt1) (Pérez-Pomares et al., 2002). Recent findings suggest that the proepicardial organ is indeed a multi-compartmentalized structure where the Tbx18/Wt1-progenitors were shown to give rise to vascular smooth muscle cells and a separate group of progenitors marked by their expression of Scleraxis (Scx) and Semaphorin3D (Sema3D) contribute to the formation of early sinus venosus and cardiac endocardium

The molecular mechanisms necessary for development of the coronary arteries vary significantly from vasculogenesis. Development of the coronary vasculature is dependent upon an intricate network, which involves communication between the epicardium, subepicardial mesenchyme, and the myocardium, and partially mediated by the action of secreted growth factors (Olivey & Svensson, 2010). This process begins at approximately E11.5 stage (in mouse embryos); the endothelial cells coalesce to form interconnected vascular tubes in the subepicardial space (Olivey & Svensson, 2010). Subsequently, the plexus is formed at the atrioventricular junction beginning from the inferior surface of the heart spreading towards the apex, nearly covering the right and left ventricles by E13.5 (in mice embryos) (Olivey & Svensson, 2010). Prior to connecting to the systemic circulation, the process of angiogenesis results in sprouting of new vessels from existing ones during which, smooth muscle cells and pericytes are recruited to form more coronary vessels (Olivey & Svensson, 2010). By E14.5 (in mouse embryos) the coronary arteries become fully connected to the systemic circulation and establish circulation by connecting to the base of the aorta through the left and right coronary ostia (Olivey & Svensson, 2010). The FGF-hedgehog (HH)-vascular endothelial growth factor (VEGF)/angiopoietin signaling pathway are the molecular pathways involved in the formation of the coronary vasculature system (Lavine & Ornitz, 2008). Furthermore, the differentiation of epicardial progenitor cells into vascular smooth muscle cells is regulated by Notch signaling (Grieskamp et al., 2011).

1.3.3 Cardiac neural crest progenitors and the molecular events that govern induction and migration of progenitors during cardiogenesis

Cardiac neural crest cells (CNCCs) originating from the dorsal neural tube between the mid-otic placode to the posterior border of somite three migrate ventrally and pause in the circumpharyngeal ridge prior to continuing into pharyngeal arch three, four and six (Keyte & Hutson, 2012). Even though the mesenchymal derivatives of the neural crest have been shown to contribute to the connective tissue and vasculature of the pharyngeal arches, and also play a role in septation of the outflow tract, they are not essential for the aortic arch artery formation (Bookman et al., 1987). Initially, the CNCCs are the first cells to differentiate into primary smooth muscle cells of the arch arteries, later; CNCCs differentiate into fibroblasts and smooth muscle and nonmuscle cells of the media and intima (Bergwerff et al., 1998). Migration of CNCCs is dependent upon various signaling pathways, which although not studied in the cardiac crest, are believed to be similar to the other regions of the crest (Scholl & Kirby, 2009). Cells are guided into the caudal pharynx in response to activation of Ephrin and Semaphorin receptors (Scholl & Kirby, 2009). Further, the combination of signaling from endothelin, platelet-derived growth factor (PDGF) and transforming growth factor- β/BMP signaling pathways, mediate key aspects of cardiac neural crest biology (Scholl & Kirby, 2009). Additionally, the gap junction protein connexin 43 has also been shown to play an essential role in mediating the signaling pathways required for polarized CNCC migration along their path between the endoderm and pharyngeal ectoderm (Miquerol et al., 2003).

1.3.4 Cardiac progenitor cell populations of embryonic and post-natal stage

Cardiac mesoderm progenitor cells are derivatives of the mesodermal layer, which have been shown to emerge from the anterior region of the PS during gastrulation (Tam et al., 1997). During cardiac development, due to a combination of activation and deactivation of various molecular pathways, these progenitor cells differentiate into the cells, such as mature cardiomyocytes, fibroblasts, smooth muscle cells and endothelial cells, that give rise to the mature heart (Buckingham et al., 2005; Zhang & Pasumarthi, 2007). Mid-gestation (E11.5) ventricles have been shown to contain a significant number of undifferentiated CPCs ($Nkx2.5^{+}/ANF^{-}/MF20^{-}$) with the potential to differentiate *in vitro* into cardiomyocytes, expressing the cardiac specific differentiation makers such as sarcomeric myosin, MLC2V and α-cardiac actin (McMullen, Zhang & Pasumarthi, 2009). In addition to these findings, recent studies have highlighted the presence of rare populations of CPCs in the postnatal myocardium (Oh et al., 2003; Martin et al., 2004; Hierlihy et al., 2002; Beltrami et al., 2003; Tomita et al., 2005; Laugwitz et al., 2005).

Various methods have been used to enrich specific cardiac progenitor cells from embryonic and post-natal hearts and investigated their differentiation potential. For instance, human fetal $Isl1^{+}$ cardiovascular progenitor cells were shown to be able to differentiation into cardiomyocytes, smooth muscle and endothelial cell lineage (Bu et al., 2009). Further, Garry and colleagues were able to investigate the role of Nkx2.5 gene in early-gestation (E8.0) using the combination of fluorescence activated cell sorting (FACS) and double-transgenic mouse model, where the expression of Nkx2.5 gene resulted in activation of fluorescent protein (EYFP) reporter (Caprioli et al., 2011). Other markers besides $Isl\text{-}1^{+}$, and Nkx2.5- have also been used couple to activated fluorescent protein reporters including the proto-oncogene c-kit, which produces the cell surface

marker used to enrich a specific group of CPCs. Various studies have identified the presence of c-kit$^+$/Nkx2.5$^+$ cell populations in both embryonic and adult hearts. For instance, FACS sorted E9.5 Nkx2.5-eGFP$^+$ cells also expressing c-kit demonstrated bipotential ability as they were shown to differentiate into myocardial or smooth muscle cell lineage *in vivo* (Wu et al., 2006). Additionally, Anversa and colleagues demonstrated the presence of c-kit$^+$ cells in adult myocardium, with a positive correlation with increasing age (Sanada et al., 2014). Further, intramyocardial injection of c-kit$^+$ cells has been shown to be beneficial in partially rescuing LV function in ischemic cardiomyopathy in animal and human studies (Chugh et al., 2012; Welt et al., 2013). Similar to c-kit$^+$ CPCs, the existence of another adult heart-derived CPC population expressing stem cell antigen-1 (Sca-1) has been reported. Cultured Sca-1$^+$ cells were shown to express cardiomyogenic genes, such as *Nkx2.5*, *Bmpr1a* and *cardiac MHC*, in presence of the cardiomyogenic compound 5-azacytdine (Oh et al., 2003).

Although, the presence of adult stem cells in the myocardium is quite exciting, recent findings suggest the lack of cardiomyogenic and developmental plasticity of certain stem cells *in vivo* (Wagers et al., 2002; Castro et al., 2002). Thus, there is a need for finding a progenitor cell type that is committed to the cardiac lineage, but has the capacity to differentiate into all or most cardiac cell types. Thus far there is a vast number of studies in which the potential of CPCs from early- and late-gestation or adult stages have been examined, yet, knowledge surrounding the differentiation potential of mid-gestation CPCs is lacking, which may be attributed to the lack of appropriate markers for enrichment of mid-gestation CPCs.

1.4 β-adrenergic signaling in the mammalian heart

The mammalian heart is supplied with numerous adrenergic nerves and the release of neurotransmitter norepinephrine (NE) is responsible for modulation of the contractile state of the heart (Spann et al., 1966). The human heart consists of three main adrenergic receptors, β_1, β_2 and α_1, which in response to adrenergic stimulation have been shown to be coupled to a positive inotropic response and cell growth. Although there is evidence of other sub-types of β-adrenergic receptors (β-AR) in the heart, such as β_3 (Kohout et al., 2001) and β_4 (Molenaar et al., 1997) their role appears to be less significant and are yet to be fully determined. The acute and long-term regulation of cardiac function, including diastolic and systolic function and metabolism is primarily controlled by the β_1- and β_2-AR signaling pathways.

1.4.1 β-adrenergic receptor structure and function

In early to mid 1970s, Lefkowitz and colleagues used a combination of radioligand binding and specific purification techniques to identify the molecular structure of β-AR (Lefkowitz, 2003). The β-ARs are among a superfamily of membrane bound proteins known as G-protein-coupled receptors (GPCRs). Both are coupled to adenylyl cyclase (AC), through the guanine nucleotide-binding regulatory protein G_s, which modulates AC function in response to receptor stimulation via catecholamines (Gilman, 1987).

The β-ARs are membrane proteins consisting of seven-transmembrane α-helices (I-VII) with alternating extracellular and cytoplasmic loops (Figure 1.6) with a molecular weight of approximately 67 kDa (Frishman, 2013). The α-helices of β-ARs are connected by three extracellular and intracellular loops, with extracellular amino terminus and an

intracellular carboxyl terminus (Frishman, 2013). Overall amino acid identity between the two receptors is 54%, the two receptors share a 71% highest region of identity in the putative transmembrane region (Dohlman et al., 1987).

There is a high degree of sequence homology in the transmembrane regions of adrenergic receptors. It has been suggested that the extracellular hydrophilic loops are not essential for ligand binding (Dixon et al., 1987), thus, the transmembrane helices are essential for forming the ligand-binding sites of these receptors (Frielle et al., 1988). Further, α-helices IV, VI and VII play the most significant role in receptor agonist binding affinity and are arranged very closely to form the ligand-binding pocket (Frielle et al., 1988).

Interestingly, β_1- and β_2-ARs have different affinities towards endogenous catecholamines (norepinephrine and epinephrine) and also various synthetic agonists and antagonists (Stiles & Lefkowitz, 1984). Epinephrine and norepinephrine are equipotent in competing with an antagonist radioligand for binding to the β_1-ARs, however, compared to norepinephrine, epinephrine is 15-times more potent in binding to β_2-ARs (Frielle et al., 1988). When comparing the β_1- and β_2-ARs sequences, it can be seen that there is significant differences between the α-helices IV, VI and VII, suggesting that pharmacological differences seen between the two receptors could be due the differences seen in these transmembrane domains (Frielle et al., 1988).

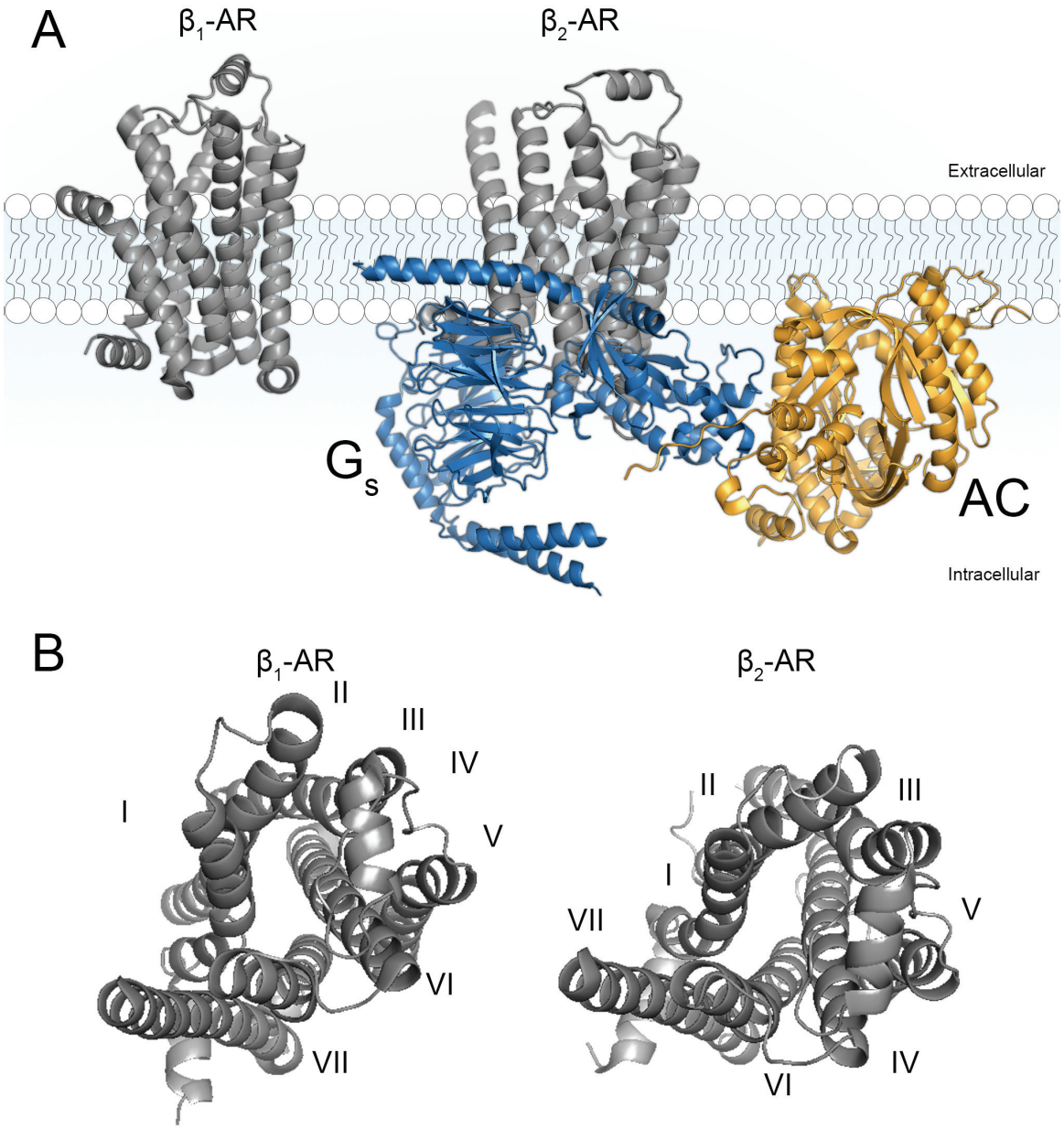

Figure 1.6 The proposed structures of β-adrenergic receptors, G proteins and adenylyl cyclase.
(A) The overall structure of β_1- and β_2-adrenergic receptors (gray), indicating the seven-transmembrane α-helices (I-VII) and their alternating extracellular and cytoplasmic loops and the extensive interaction of the β_2-AR with the Gαs (blue) and adenylyl cyclase (yellow). **(B)** Proposed arrangement of the β_1- and β_2-adrenergic receptors helices.

1.4.2 β-adrenergic receptor signaling via G-proteins

The current consensus is that binding of a ligand to the receptor causes a change in relative orientation of transmembrane domains causing conformational changes to the intracellular receptor surface, leading to productive coupling with heterotrimeric G-proteins (Wess, 1997). Heterotrimeric G-proteins consist of α, β and γ subunits. Upon coupling with the receptor, the G-protein bound guanosine diphosphate (GDP) is exchanged for guanosine triphosphate (GTP), leading to dissociation of the subunits into active Gα and Gβγ subunits that mediate downstream signaling pathways (Xiao, 2001). Furthermore, due to their amino acid sequences, the Gα subunits are divided into four subgroups, $G\alpha_i$, $G\alpha_s$, $G\alpha_q$ and $G\alpha_{12}$ (Rockman et al., 2002). In cardiomyocytes, the β_1-ARs are primarily bound to the G stimulatory (Gs) protein (Xiao, 2001), where, in addition to binding to Gs, β_2-ARs are also able to couple to pertussis toxin – sensitive G inhibitory protein (Gi) (Zamah et al., 2002). When activated, $G\alpha_s$ and $G\alpha_i$ modulate activation of effector molecules adenylyl cyclase (AC) (Xiao, 2001). It known that activation of $G\alpha_s$ results in activation of AC whereas activation of $G\alpha_i$ results in inhibition of AC. Upon activation, AC generates the secondary messenger cyclic adenosine monophosphate (cAMP) (Xiao, 2001). Generation of cAMP leads to activation of cAMP-dependent proteins such as phosphodiesterases, A-kinase anchoring proteins, Epac, and more importantly, cAMP-dependent protein kinases (Matsuda et al., 1990).

Protein kinase A (PKA) is a tetrameric holoenzyme with two catalytic subunits, PKAC, and a regulatory subunit dimer, PKAR (Canaves & Taylor, 2002). PKA is enzymatically inactive in the absence of cAMP, however, upon binding of four cAMP molecules, the enzyme dissociates into PKAR dimer with four cAMP molecules attached, and two free and active PKAC subunits (Canaves & Taylor, 2002). In cardiac cells,

cAMP-induced PKA activation leads to phosphorylation of various proteins that are essential for cardiomyocyte contractile function. Among these are, L-type calcium channels (Gerhardstein et al., 1999), Troponin I (Sulakhe & Vo, 1995), Ryanodine receptor-2 (RyR2) (Marx et al., 2000), myosin binding protein-C (MyBP-C) and protein phosphatase inhibitor-1 (Kunst et al., 2000). Activation of such proteins is essential for increase in Ca^{2+} influx (L-type calcium channels) (Gerhardstein et al., 1999), increase in Ca^{2+} reuptake into the sarcomeric reticulum (phospholamban/SERCA) (Simmerman & Jones, 1998) and modulation of myofilament Ca^{2+} sensitivity (troponin I and MyBP-C) (Sulakhe & Vo, 1995; Kunst et al., 2000).

Calcium is essential for cell function (Bers, 2002). The duration of Ca^{2+} increase within a cell can have different effects on a cell, for instance, long lasting Ca^{2+} increase results in activation of metabolic genes, while short lasting can trigger contraction (Berridge, 1997; Carafoli, 2002). In cardiomyocytes, the influx of external Ca^{2+} results in release of Ca^{2+} from SR, the internal Ca^{2+} store of cardiomyocytes, by activating two ligand-gated Ca^{2+} release channels, the RyR2 and the IP3 binding receptor (IP3R), in a process termed Ca^{2+} induced Ca^{2+} release (Marx et al., 2000). The Ca^{2+} channels can be activated via PKA, PKC and Ca^{2+}-calmodulin-dependent protein kinase II (CaMK-II) and are inhibited by high levels of Ca^{2+} and calmodulin (Ferguson, 1975; Kamp & Hell, 2000).

Additionally, G-proteins are capable of activating the monomeric GTPase Ras, which is a master switch for various cellular processes involved in cell growth and differentiation. Ras is able to relay the signal onto the nucleus via activation of the four mitogen activated protein kinase (MAPK) signaling cascades (Neves et al., 2002). Each

of the MAPK signaling pathways plays a significant role in cell function and health, for instance, modulation of (1) extracellular signal-regulated kinases (ERK), which regulate cardiac hypertrophy and apoptosis, (2) big MAP kinase-1 (BMK1), relays oxidative stress signals to the nucleus, (3) p38 MAPK isoform activation in response to environmental stress and cytokines, also involved in apoptosis, and (4) c-Jun N-terminal kinases (JNK) which play a significant role in transcription (Neves et al., 2002).

1.4.3 Regulation of β-adrenergic signaling

With regards to regulation of the β-adrenergic signaling, β_2-AR is the receptor that is most studied, and the general consensus is that regulatory pathways involved in regulating β_2-AR also apply to other β-ARs. Currently, there are four paradigms regarding the regulation of β_2-AR, generated using information gathered from *in vitro* wild type and mutant receptor mouse models.

(i) Over stimulation of the β-ARs, whether physiological, pharmacological or pathophysiological, may result in desensitization of the adrenergic receptors (Lamba & Abraham, 2000). Homologous desensitization involves G-protein-coupled receptor kinases (GRKs) also known as β-adrenergic receptor kinases (βARKs), phosphorylating consecutive serines (355 and 366) of the C-terminal region of the β_2-ARs causing receptor desensitization (Bünemann et al., 1999). The recruitment of GRKs from the cytoplasm to the membrane is initiated by Gβγ subunits (Bünemann et al., 1999). Further, GRKs are responsible for only phosphorylating ligand-bound receptors and are not responsible for regulation of antagonist-bound and inactive receptors, and are dependent on intermediary secondary messenger molecules (Bünemann et al., 1999). Phosphorylation of the β_2-ARs C-terminus causes binding of regulatory protein arrestin,

which along with the heterotetrameric adapter complex AP2, causes endocytosis of the receptor by delivering it to clathrin-coated pits (Mahan & Mangan, 1975). The β_2-ARs in the endosomes are dephosphorylated via phosphatases and returned to the cell membrane (Mahan & Mangan, 1975). β_2-ARs are degraded when endosomes containing β_2-ARs fuse with lysosomes (Bünemann et al., 1999). There is a degree of receptor-type specificity with regards internalization of receptors. In response to agonist stimulation β_2-ARs are internalized, while the β_1-ARs remain at the cell surface, even in the desensitized state (Bünemann et al., 1999).

(ii) As previously stated, β_2-AR is able to associate with $G\alpha_i$ and $G\alpha_s$. The G-protein specificity of β_2-ARs is partly determined by the type of agonist or antagonist bound to the receptor (Wenzel-Seifert & Seifert, 2000). Coupling of β_2-ARs to G-proteins is determined by phosphorylation of the intracellular loop of the C-terminus region (Wenzel-Seifert & Seifert, 2000). Heterologous desensitization of β-ARs does not require occupation of a ligand (Bünemann et al., 1999). PKA-dependent phosphorylation of serines 261, 262, 345 and 346 of the C-terminus of β_2-AR results in uncoupling of the receptor from the stimulatory $G\alpha_s$ and subsequent coupling to inhibitory $G\alpha_i$ thus, inhibiting AC and activating MAPK signaling cascade (Zamah et al., 2002).

(iii) Recent findings suggest that the β-ARs are capable of forming hetero- and homodimers (Angers et al., 2002). β_2-ARs have been shown to form dimers upon agonist activation, where, the dimer form of β_2-ARs is the active form of the receptor. It has been suggested that the sixth transmembrane domain is responsible for dimerization of the receptors (Angers et al., 2002). Interestingly, β_1-ARs and β_2-ARs are capable of forming heterodimers, and the heterodimerization of the two receptors inhibits agonist-induced

internalization of β_2-ARs and their ability to activate the MAPK signaling pathway (Lavoie et al., 2002).

(iv) GPCRs are able to interact with numerous cytoplasmic scaffolding proteins which are capable of linking the receptors to various signaling intermediates and intracellular effectors (Hall & Lefkowitz, 2002). GPCR-associated proteins have been shown to play four major roles with regards to receptor signaling. GPCR-associated proteins are able to (1) directly mediate receptor signaling with regards to G-proteins, (2) play a role in receptor localization and trafficking, (3) function as allosteric modulators for receptor conformation and (4) may act as scaffolds involved in increasing receptor efficiency or specificity (Milligan & White, 2001; Hall et al., 1999; Brzostowski & Kimmel, 2001). A group of PKA associated A-kinase anchoring proteins (AKAPs) have been shown to associate with the C-terminus of β_2-ARs and induce activation of the ERK signaling cascade (Steinberg & Brunton, 2001).

1.4.4 The role of β-adrenergic signaling in cardiac development

Knockout mouse models have been used to analyze the role of various players, such as the ligand, the receptors, G-proteins and regulatory proteins, of the β-adrenergic signaling system in cardiac development. The collective information gathered from these findings suggests that the adrenergic signaling system plays a significant role in cardiac development.

(i) In pregnant rats, where non-selective β-antagonist propranolol was used throughout fetal development, any developmental deficiencies induced due to β-AR blockade were resolved in post-natal life (Kudlacz et al., 1990). Further, there was no evidence in changes in litter size, birth weight, and number of stillbirths (Kudlacz et al.,

1990). However, mice lacking catecholamines die prior to birth due to cardiac abnormalities. For instance, mice lacking dopamine β-hydroxylase (*DBH-/-*), thus unable to synthesize norepinephrine and epinephrine, and those lacking tyrosin hydroxylase (*Th-/-*), unable to synthesize L-3,4-dihydroxyphenylalanine (L-DOPA), die in utero, with majority of the lethality observed in the *DBH-/-* and *Th-/-* knockout mice between embryonic day 11.5 – 15.5 stage (Zhou et al., 1995; Rios et al., 1999; Kobayashi et al., 1995; Thomas et al., 1995). Administration of L-Dopa to pregnant females was able to rescue mutant mice in utero, however, without further treatment mice died prior to weaning (Zhou et al., 1995). Mice lacking dopamine but not norepinephrine and epinephrine appeared to be viable (Zhou & Palmiter, 1995). Lastly, presence of β-agonist, isoproterenol increased the survival of *Th-/-* fetuses (Portbury et al., 2003).

(ii) Analysis of homozygous β_1-AR null mutant (β_1-AR$^{-/-}$) mice suggested that of ~70% of the β_1-AR$^{-/-}$ mice die in utero (Rohrer et al., 1996). Analysis of β_1-AR$^{-/-}$ frequencies among the different groups indicated no significant deviation from the Mendelian expectations (1:2:1 ratio) in E10.5 embryos, whereas E18.5 and post-natal mice deviated significantly from the expected Mendelian ratio (Rohrer et al., 1996). The β_1-AR$^{-/-}$ mice that survived to adulthood seemed normal, yet, lacked the chronotropic and inotropic responses seen in WT mice in the presence of the β_1-AR agonist isoproterenol (Rohrer et al., 1996). Interestingly, the resting heart rate and blood pressure does not significantly differ between WT and surviving β_1-AR$^{-/-}$ mice (Rohrer et al., 1998). However, the peak heart rate of β_1-AR$^{-/-}$ mice has been shown to be approximately 200 beats/min less than the WT during graded treadmill exercise with no reduction in maximal exercise capacity or metabolic indices, suggesting that β_1-AR may not be

essential for maintaining resting heart rate or maximally stressed cardiac performance (Rohrer et al., 1998). In contrast to the β_1-AR$^{-/-}$ mice, mice lacking β_2-ARs (β_2-AR$^{-/-}$) show no prenatal lethality associated with the loss of β_2-AR gene (Chruscinski et al., 1999). Furthermore, mature β_2-AR$^{-/-}$ mice appear grossly normal, show no abnormal behavior, and both male and female are fertile (Chruscinski et al., 1999). Additionally, β_2-AR$^{-/-}$ mice showed normal resting heart rate and blood pressure (Chruscinski et al., 1999). Interestingly, β_2-AR$^{-/-}$ mice showed lower respiratory exchange ratio, suggesting greater hypertensive response to epinephrine compared to the WT mice (Chruscinski et al., 1999). Exercise-induced cardiovascular stress and infusion of epinephrine led to development of a hypertensive state in β_2-AR$^{-/-}$ mice (Chruscinski et al., 1999). Mice lacking both β_1-AR and β_2-AR ($\beta_{1/2}$-AR$^{-/-}$ double KO) showed similar baseline heart rate, blood pressure and metabolic rate when compared to WT mice (Rohrer et al., 1999). However, during exercise-induced cardiovascular stress and β-AR agonist stimulation, the double knockout mice showed impaired chronotropic range, vascular reactivity and metabolic rate, yet, the maximal exercise capacity remained unchanged (Rohrer et al., 1999).

1.4.5 Basis for use of β-blockers for treatment of heart disease

Neurohormonal activation in response to congestive heart failure has been established as one of the hallmarks of compensatory mechanisms involved in maintaining cardiac output and systemic blood pressure (Zucker et al., 2012). During CHF, various hormonal substrates involved in vasoconstriction are elevated, including, angiotensin II of renin-angiotensin system (Zucker et al., 2014), endothelin-1 (Lehmann et al., 2014), vasopressin (Filippatos & Elisaf, 2013), and norepinephrine (Zucker et al., 2012).

Unable to maintain the contractility and heart rate, the failing human heart has been shown to increase its sympathetic nerve activity (Ferguson et al., 1990). Although this increase in circulating norepinephrine is initially supportive in CHF patients, it has been shown to play a pivotal role in the pathophysiology of this disease (Yu et al., 2007). There is overwhelming evidence suggesting that excessive stimulation of the β-adrenergic system results in cardiomyopathy, myocardial scaring eventually leading to CHF (Lamba & Abraham, 2000).

In the ventricles of healthy human heart, the relative proportion of β_1- and β_2-ARs ranges between 75% and 25% respectively (Brodde et al., 1986). Interestingly, in patients with end-stage CHF and ischemic cardiomyopathy, there appears to be a selective down-regulation in β_1-AR, where the β_2-AR subtype remains unaffected (Brodde et al., 1998; Brodde et al., 1986). Furthermore, in addition to down-regulation of β_1-AR subtypes, in patients with end-stage CHF, a significant increase in the $G\alpha_i$ and βAR kinase 1 (βARK1) levels is also evident (Madamanchi, 2007; Vatner et al., 2000). Collectively, the fluctuations in substrates of β-adrenergic signaling pathway results in diminished β-adrenergic signaling, largely due to elevated levels of catecholamines.

Various interacting pathways are activated in order to adapt to the increase in workload in a failing heart, hence, CHF is often proceeded by the onset of hypertrophic cardiomyopathy. In fact, studies have suggested that functional status and prognosis of patients with chronic CHF is closely associated with abnormalities of left ventricular diastolic filling (Hansen et al., 2001). It is believed that cardiac hypertrophy is initially an adaptive process to improve ventricular function, however, decreasing cardiac efficiency of hypertrophied heart is followed by increased sympathetic nervous system modulation

of cardiac function, which is inversely correlated to patient survival (Lamba & Abraham, 2000). In light of these findings, a new paradigm has been created in which it is suggested that activation of the sympathetic system in response to decreased cardiac function and over-stimulation of the signaling pathways involved may play a more prominent role in manifestation of heart failure. Thus, listed detrimental effects of increased norepinephrine in a failing heart set the foundation for the use of β-adrenergic blockers for the treatment of heart failure (Spargias et al., 1999).

1.4.6 Murine mouse heart failure models used to gain insight into the importance of molecular components of the β-adrenergic system

Genetically engineered murine mouse models have allowed for cardiovascular researchers to study various aspect of cardiac pathology. Cardiac specific genetically modified mouse models have become possible largely due to use of murine α-myosin heavy chain (α-MHC) gene promoter in ventricular myocytes (Rindt et al., 1995). The α-MHC promoter is activated post-birth in response to increased levels of circulating thyroid hormone, which voids the animals from any possible transgene-specific developmental complications (Rindt et al., 1995). Genetically modified mouse models have provided insight into various elements of β-adrenergic signaling system such as, β_1- and β_2-ARs, and β-adrenergic receptor kinase (βARK) and their potential role in pathophysiology of heart failure.

The α-MHC promoter was used to generate mice with cardiac-specific overexpression of β_1-AR, increasing its expression levels 5 to 15-fold (Engelhardt et al., 1999). Transgenic mice with overexpressing β_1-AR showed increased basal contractile function and an increase in response to isoproterenol (a non-selective β-AR agonist) in

young animals (Engelhardt et al., 1999). However, contractility was reduced by approximately 50% in 35-week-old mice, and a decrease in left ventricular ejection fraction of 20% was evident (Engelhardt et al., 1999). It was concluded that overexpression of β_1-AR in the heart may result in initial short-lived improvements in cardiac contractility but long-term effects proved to be detrimental as the decrease in cardiac function was shown to be associated with progressive myocyte hypertrophy and fibrosis (Engelhardt et al., 1999). Additionally, in another study where α-MHC promoter was used to overexpress human β_1-AR 24-46-fold, older mice showed increase in ventricular chamber size and histopathological analysis indicated myocyte hypertrophy, myofibril disarray, and large areas of fibrosis (Bisognano et al., 2000). Furthermore, regions of fibrosis were accompanied by increased pre-apoptotic marker, Bax, and apoptotic index, measured using TUNEL staining (Bisognano et al., 2000).

Transgenic mouse models have made it very clear that although very similar in structure and function, β_1-AR and β_2-AR signaling significantly differ. Unlike β_1-AR, the effect of β_2-AR overexpression on myocytes is dose-dependent. The α-MHC promoter was used to generate mice overexpressing β_2-AR 60, 100, 150 and 350-fold (Liggett et al., 2000). Mice with lower levels of β_2-AR overexpression (60-fold) showed enhanced basal cardiac function without any increase in mortality and any apparent pathophysiological consequences within a 1-year period (Liggett et al., 2000). However, higher levels of β_2-AR overexpression resulted in delayed (100-fold) or rapidly progressive (350-fold) cardiac and myocyte hypertrophy, myocardial fibrosis, and reduced survival as mice with 100-fold died at 41 weeks and those with 350-fold died at 25 weeks (Liggett et al., 2000). Further, mice with 200-fold overexpression of β_2-AR

showed worse prognosis post aortic stenosis as the β_2-AR hyperactivity led to exacerbation of the transition from hypertrophic heart to heart failure (Du et al., 2000). The "dose-response" effect seen in β_2-AR overexpression is attributed to the ability of β_2-AR to couple with both G_i and G_s (Xiao et al., 1995). β_2-AR coupling to G_i allows for suppressing the pro-apoptotic pathways mediated by G_s (Xiao et al., 1999).

The uncoupling of β-AR during heart failure is due to increased expression and activity of βARK1 (Ungerer et al., 1993). Two transgenic mouse models were used to investigate the role of βARK1 with regards to heart failure, transgenic mouse overexpressing βARK1 and mice overexpressing βARK inhibitor (βARKct). βARKct corresponds to the carboxyl-terminal 194 amino acids of βARK1 and contains the binding domain for the $G_{\beta\gamma}$ subunits, required for βARK1 membrane translocation and activity (Koch et al., 1994; Pitcher et al., 1992). βARKct inhibits βARK1 activity by competing with endogenous βARK1 for $G_{\beta\gamma}$ binding (Akhter et al., 1999). Transgenic mice with myocardial 3- to 5-fold overexpression of βARK1 showed reduced contractile function (Akhter et al., 1999), thus, suggesting that overexpression of βARK1 is sufficient to induce cardiac dysfunction (Koch et al., 1995). Inversely, overexpression of the inhibitor, βARKct, prevented cardiomyopathy in a model of murine heart failure ($MLP^{-/-}$), as mice showed normal LV chamber size and function (Rockman et al., 1998). In a rabbit MI-induced heart failure model, adenoviral-mediated gene delivery of βARKct at the time of infarction prevented a rise in βARK1 activity, maintained β-AR density and improved cardiac function (White et al., 2000). The positive effects associated with use of βARKct may not be fully due to inhibition of βARK1, and could partially be due to βARKct ability to interfere with $G_{\beta\gamma}$ subunits effecting alternative $G_{\beta\gamma}$ pathways.

Inhibition of $G_{\beta\gamma}$ subunits resulted in enhanced contractility of cardiomyocytes to the same extent seen in βARKct (Li et al., 2003). Thus, inhibition of βARK1, via βARKct, could hold as a potential therapeutic option for treatment of heart failure.

1.4.7 Brief overview of pharmacokinetics and pharmacodynamics of different classes of β-adrenergic blockers

Thus far, there have been three different classes/generations of β-blockers used clinically for treatment of various cardiovascular diseases, including, the first generation, non-selective (such as propranolol), second generation, β_1-selective (such as Metoprolol), and the third generation β-blocker/vasodilator (such as Carvedilol).

First generation / non-selective β-blockers*:* Of the first generation drugs, propranolol was the first to be introduced into clinical practice in 1968 as an anti-anginal and anti-hypertensive therapeutic. To determine the distribution of propranolol, tissue studies were performed in beagle dogs, where high concentration of propranolol was found in the lungs, followed by relatively high concentrations in the brain, heart, liver, and kidneys (Hayes & Cooper, 1971). Propranolol undergoes "first pass metabolism" in the liver. Hence, due to this hepatic elimination, a six- to ten-fold higher dose is required for oral administration compared to intravenously administered drug (Forrest et al., 1970). The plasma half-life (t½) for propranolol was calculated to range between 2hrs20min to approximately 5hrs, where the longer half-lives were seen mainly in patients who received propranolol intravenously (Forrest et al., 1970). The drugs t½ is the result of very high hepatic extraction rate of about 70% in humans (Shand & Rangno, 1972). It should be noted that patients with liver disease and heart failure show variable

responses to propranolol, and that the drug is contraindicated in patients with severe heart failure (Nies & Shand, 1975).

The negative inotropic effects of propranolol last for about 12-15hrs, while the negative chronotropic effects last about 24-36hrs (Boudoulas et al., 1977). Additionally, it has been suggested that propranolol plays a role in inhibition of renin secretion (Bühler et al., 1972). In a study where the antihypertensive effects of propranolol was tested in patients with high, normal and low plasma renin activity, it was found that propranolol alone was able to lower plasma renin activity by approximately 63%, and it also, to a lesser extent, was able to suppress aldosterone secretion in patients with high renin activity (Bühler et al., 1972).

Even though excessive sympathetic activation in response to decreases in heart function is proven to be detrimental to the heart, the failing heart is still dependent on the adrenergic support (Gaffney & Braunwald, 1963; Stephen, 1966). Acute administration of first generation β-adrenergic blockers, such as propranolol, have been shown to decrease contractile state of the heart and cause a simultaneous increase in vascular resistance (Armstrong et al., 1977; Bristow et al., 1998), resulting in a significant decrease in cardiac output (Metra et al., 2001). For the reasons mentioned, an intolerance of drug is seen in approximately 20% of patients prescribed with first generation β-adrenergic blockers, such as propranolol (Talwar et al., 1996).

Second generation / β_1-selective blockers*:* It was initially believed that using β-blocking agents that selectively antagonized β_1-ARs, the human heart could be selectively targeted (Bristow et al., 1986). It was also perceived that lack of β_2-blockade would reduce some of the perivascular and pulmonary side effects associated with non-selective

β-blocking agents. Of the second generation of β_1-blocking agents, practolol was the first to be introduced, but was clinically unsuccessful (Dunlop & Shanks, 1968). Soon after, Metoprolol was introduced as a selective β_1-blocker.

Metoprolol is a β_1-AR antagonist with very little β_2-AR selectivity which was evident due to little effect on the β_2-ARs in the bronchi and peripheral vessels, compared to the non-selective drugs, such as propranolol, discussed previously (Formgren, 1976) (Pietschmann et al., 1991). Metoprolol in Dilated Cardiomyopathy (MDC) was the first placebo-controlled multicenter trail with a β-adrenergic antagonist, where Metoprolol tartrate was compared to placebo in patients with symptomatic heart failure from idiopathic dilated cardiomyopathy (Waagstein et al., 1993). It was found that, compared to the placebo group, patients treated with Metoprolol showed significant improvements in exercise time at 12 months, improved symptoms and cardiac function and lowered clinical deterioration (Waagstein et al., 1993).

In pharmacokinetic studies of Metoprolol, it was found that when administered orally Metoprolol is rapidly and completely absorbed, with a bioavailability of approximately 40% of the intravenously administered dose (Regårdh et al., 1974). It was also found that the drug is distributed to extravascular tissues within 12min, the plasma t½ was calculated to be approximately 3hrs, and the drug is metabolized in the liver, and the remaining metabolites were excreted through the kidneys as approximately 95% of the dose was excreted through the urine within 72hrs of administration (Regårdh et al., 1974). Metoprolol is one of the only β-blockers that undergoes oxidative metabolism, as a result, Metoprolol exhibits sensitivity to cytochrome p450 2D6 (CYP2D6) type of

genetic polymorphism where poor hydroxylators tend to exhibit a 6-fold higher plasma concentration and a 3-fold increase in t½ of the drug (Lennard et al., 1982).

Furthermore, Metoprolol has been shown to exert inverse agonistic activity on the β-ARs. When the β-ARs are unoccupied, the intrinsic a basal level of adenylyl cyclase (AC) activity results in basal cAMP levels. The ability of β-blockers to reduce the basal AC activity and levels of secondary messenger molecules is referred to as "inverse agonistic activity". Metoprolol has been shown to decrease basal force of contraction by 15% in left ventricular papillary muscle strips in patients with terminal heart failure (Maack et al., 2000). Thus it has been suggested that Metoprolol is an inverse agonist that stabilizes the inactive form of β-ARs (Maack et al., 2000). Thus, resulting in possible attenuation of phosphorylation of the β-AR via the β-AR kinases, and subsequent desensitization and possible down-regulation (Maack et al., 2000).

Compared to the first generation drugs, second-generation β_1-blocker Metoprolol show significantly improved drug tolerability (Bristow et al., 1998). Although, use of second-generation β_1-blockers proved to be more beneficial in comparison to the first generation non-selective β-blockers, second generation agents failed to improve patient outcomes with regards to sudden death post-myocardial infarction (Eichhorn & Bristow, 1997).

ICI-118, 551 (erythro-dl-1-(7-methylindan-4-yloxy-3-isopropylaminobutan-2-ol, ICI) is a β_2-blocker. When compared to propranolol, ICI demonstrated a similar and membrane-stabilizing action, yet, a 50-fold higher β_2-selectivity (Bilski et al., 1983). Further, ICI is >500-fold more selective towards β_2-AR than β_1- and β_3-AR (Baker, 2005). The selectivity of ICI towards the β_2-AR, has made it a great candidate for use

when studying the role of β_1-AR and β_2-ARs in different tissues (O'Donnell & Wanstall, 1980).

***Third-generation / non-selective or selective β-blockers with vasodilator properties**:* Initially, the third-generation of β-blockers with vasodilator properties were developed to treat hypertension, yet several have undergone extensive evaluation for treatment of CHF (Bristow et al., 1998). Among most third-generation β-blockers (such as labetalol (Johnson et al., 1988) and nebivolol(Cockcroft et al., 1995)), Carvedilol is one β-blocker that has been extensively examined in treatment of patients with heart failure.

Carvedilol, a non-selective β-blocker and a selective α_1-blocker, with vasodilator capabilities and no intrinsic sympathomimetic activity, is effective in treating hypertension, coronary artery disease and congestive heart failure (Ruffolo & Feuerstein, 1997; Packer et al., 1996). Due to being both a β-blocker and a vasodilator, Carvedilol is able to decrease workload of the heart by reducing all three major components of oxygen demand, heart rate, contractility and wall tension, which collectively have resulted in maintained or increased stroke volume and cardiac output in patients (Ruffolo & Feuerstein, 1997). It is now believed that at clinically used doses, Carvedilol is an antagonist for β_1- β_2- and α_1-ARs with some calcium channel blockade capabilities in vascular smooth muscles (Nichols et al., 1991). Yet, it is imperative to note that the arterial vasodilation observed is largely attributed to selective α_1-AR blockade, with little or no contribution from the calcium channel blockade ability of Carvedilol (Nichols et al., 1991). Lastly, it has been shown that some of the cardioprotective properties seen with Carvedilol are due to its antioxidative properties (Carreira et al., 2006). In isolated

heart mitochondria, it was found that Carvedilol is able to inhibit mitochondrial oxygen consumption and superoxide production due to calcium overload (Kametani et al., 2006). The antioxidative property of Carvedilol is a property that other β-blockers such as Metoprolol lack (Brixius et al., 2007).

Carvedilol is a high affinity competitive blocking agent with a descending rank order of potency ratio for β_1, α_1 and β_2-ARs of 1:2:7 respectively (Yoshikawa et al., 1996). Furthermore, compared to the large inverse agonist activity of previously listed drugs, Metoprolol and propranolol, Carvedilol has low level of inverse agonistic capabilities (Yoshikawa et al., 1996).

Approximately 20-25% of the drug is systemically available after oral administration and the t½ is 6-7hrs (Neugebauer et al., 1987; von Möllendorff et al., 1987). Further, the 20-25% bioavailability of the drug is mainly due to hepatic "first-pass" metabolism, as only about 1% of the unchanged drug was excreted through the urine (Neugebauer et al., 1987; von Möllendorff et al., 1987). About 16% of the metabolites are excreted through the urine, and majority of the other metabolites (up to 60%) through the fecal route (Neugebauer et al., 1987). Interestingly, compared to healthy volunteers, the plasma concentrations of Carvedilol was 30-40% higher in patients with heart failure, suggesting that heart failure may potentially have a role on the pharmacokinetics of the drug (Tenero et al., 2000).

Due their ability to, block both β_1- and β_2- along with the α_1-receptors, reduce the cardiac adrenergic drive, and the fact that they do not affect the regulation/expression of β-receptors in the heart, the third generation β-blockers, such as Carvedilol, are used

more often as they provide a more comprehensive anti-adrenergic function compared to the other classes/generation of β-blockers.

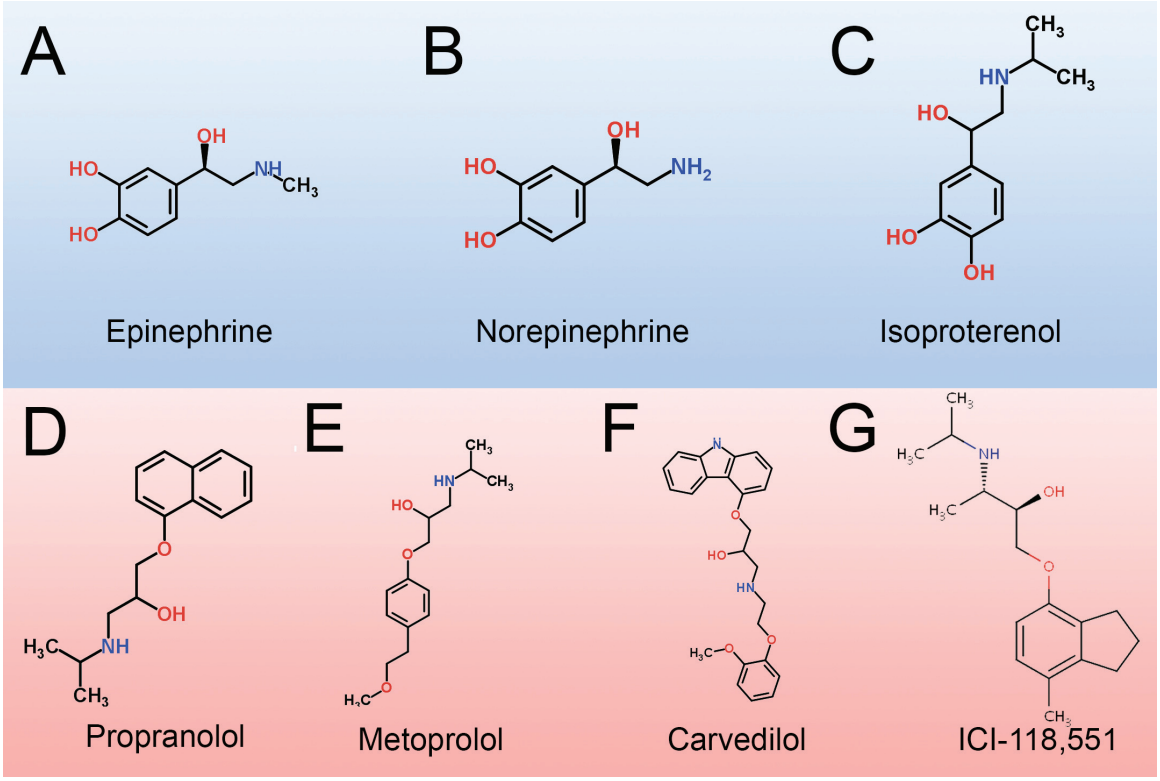

Figure 1.7 Chemical structures of β-adrenergic receptor agonists and antagonists. Chemical structures of β-AR **(A-C)** agonists and **(D-G)** antagonists. Naturally present β-AR agonist **(A)** epinephrine and **(B)** norepinephrine, and the synthesized **(C)** isoproterenol. The chemical structure of first generation, non-selective β-AR antagonist **(D)** propranolol, **(E)** second generation β1-AR selective antagonist Metoprolol, **(F)** the third generation non-selective β-AR antagonist Carvedilol and **(G)** β_2-AR antagonist, ICI-118,551. Chemical structures obtained from ChemSpider.com.

1.4.7 Beneficial effects of β-adrenergic antagonists in heart failure

Although benefits of β-blockade with regards to improvement of cardiac contractility and patient survival in heart failure was well established, the mechanisms underlying observed favorable responses were poorly understood. Initially it was believed that the beneficial effects of β-adrenergic blockers was mainly due to decrease in heart rate, however, various studies have suggested that some other mechanisms may also be equally responsible. For instance, when cardiac hemodynamic effects of Metoprolol was compared to ivabradine, a pure heart rate-reducing agent, it was found that although both had beneficial effects with regards to cardiac hemodynamics, Metoprolol also prevented left ventricular dilation and hypertrophy in MI-induced rats (Maczewski & Mackiewicz, 2008). It was found that compared to ivabradine treated rats, better contractility and Ca^{2+} handling was evident in cardiomyocytes of post-infarction rat hearts treated with Metoprolol (Maczewski & Mackiewicz, 2008). This suggests that reducing heart rate alone does not account for the full effects of β-adrenergic blockade in post-infarction setting.

It has been suggested that heart failure can result in alterations in sarcolemma (SL) calcium handling which are believed to be attributed to decreased calcium channel density and also decreased SL Ca^{2+}-ATPase activity (Colston et al., 1994). Certain β-blockers, such as propranolol, have been shown to have biphasic properties with regards to SL Ca^{2+} pump activities, where lower concentrations were shown to have stimulatory properties and higher concentrations were shown to be inhibitory (Dzurba et al., 1984). Hyperadrenergic state of heart failure results in PKA-induced hyperphosphorylation of the cardiac ryanodine receptors (RyR2) resulting in dissociation from the regulatory subunit, FK506 binding protein, FKBP12.6 (Marx et al., 2000). FKBP12.6 depletion

from the RyR2 complex results in defective channel function due to increased sensitivity to Ca^{2+}-induced activation (Marx et al., 2000). In a clinical study, it was shown that systemic β-blockade results in up-regulation of β-AR density and restoration of normal macromolecular complex composition and function of RyR2 channels in human failing hearts (Reiken et al., 2003). Moreover, cardiac function improvements associated with use of Metoprolol in heart failure are attributed to the drug's ability to attenuate the decrease of the amplitude of calcium transients, RyR2 expression and the ratio of SERCA2a and Na^{+}-Ca^{2+} exchanger (Zou et al., 2007). Cardiac improvements associated with use of Carvedilol are partially due to the drug's capacity to depress L-type Ca^{2+} channel currents thereby decreasing Ca^{2+} overload and PKA activation (Yao et al., 2003). Furthermore, it has been shown that Carvedilol corrects defective interdomain interactions of RyR2 complex in failing hearts (Mochizuki et al., 2007). Compared to Metoprolol, Carvedilol use has also been shown to result in more significant improvements in expression of SERCA (Sun et al., 2005). It could be concluded from these findings that improvements in heart function attributed to use of β-blockers in heart failure could be partially due to restoration in function of channels and complexes involved in Ca^{2+}-handling in cardiomyocytes.

Recent findings have suggested alterations in myofilament function in human myocardium, which may potentially contribute to diastolic dysfunction observed in heart failure patients (Brixius et al., 2002). A significant increase in Ca^{2+} sensitivity of myofibrillar function is evident in heart failure patients without β-blocker treatment (Brixius et al., 2002). As previously indicated, even though Metoprolol and Carvedilol have been successful in prolonging survival of patients with heart failure, there are

distinct pharmacodynamics differences between the two drugs. It was found that Metoprolol is able to restore myofibrillar function by improving phosphorylation of troponin I resulting in decreased myofibrillar Ca^{2+} sensitivity (Brixius et al., 2007). However, Metoprolol failed to improve myofibrillar economy as it failed to alter myofibrillar ATP consumption (Brixius et al., 2007). On the other hand, Carvedilol was able to improve myofibrillar ATP consumption by improving maximal Ca^{2+} – dependent tension and significantly decreased tension-dependent ATP consumption without altering myofibrillar Ca^{2+} sensitivity (Brixius et al., 2007). Furthermore, phosphorylation of troponin I was also improved in patients treated with Carvedilol (Brixius et al., 2007). The difference seen between the two β-blockers is believed to be due to the antioxidative properties of Carvedilol (Flesch et al., 1999). Lastly, clinical findings suggest that use of either Metoprolol or Carvedilol results in increased mRNA expression of α-myosin heavy chain and decreased mRNA expression of β-myosin heavy chain (Lowes et al., 2002). Thus, it could be concluded that improvement of cardiac function due to β-blocker treatment in CHF patients could be partially due to reduction of cardiac remodeling.

1.5 Intracardiac cell transplantation for myocardial regeneration

Every year, there are >15 million new cases of myocardial infarction worldwide. Myocardial infarction is the result of an occlusion of the one or more coronary arteries by an atherosclerotic plaque, resulting in interruption of blood flow generally leading to loss of contractile cardiomyocyte tissue. Thus, loss of cardiomyocytes leads to activation of endogenous repair mechanism, where contractile tissue is replaced with non-contractile fibrotic tissue, which ultimately will lead to progressive heart failure.

There are several new strategies being investigated to replace the diseased myocardium, these include, abrogation of myocardial cell death or reviving apoptotic cardiomyocytes (Masri & Chandrashekhar, 2008; van Empel et al., 2005; Kang & Izumo, 2003), regulation of MicroRNAs during cardiac hypertrophy and heart failure (Cheng & Zhang, 2010; Jazbutyte & Thum, 2010), reactivation of the cardiomyocyte cell cycle activity (MacLellan & Schneider, 2000) and donor cell transplantation (Christoforou & Gearhart, 2007; Barile et al., 2007; Ni et al., 2014). Evidence suggests that transplanted cells are capable of improving the function of scarred myocardium by inducing angiogenesis, myogenesis and secretion of paracrine factors, which may result in attenuation of the ventricular scar tissue (Dai et al., 2005; Orlic et al., 2003).

1.5.1 Mammalian heart's capacity for regeneration post-infarction

The initial notion that the mammalian heart was terminally differentiated and incapable of regeneration has been challenged by various findings (Orlic et al., 2001). For instance, by taking advantage of carbon-14 integration in the DNA of human cardiomyocytes due to nuclear bomb testing during the cold war, it was found that the heart is able to renew itself at a rate of 1% at age 25, with the rate dropping to 0.4% by age 75 (Bergmann et al., 2009). In a comparative study, when hearts of patients that had died due to MI were compared with those of control patients that had died due to unrelated causes, it was found that 4% of cardiomyocytes were engaged in mitosis in the region adjacent to the infarct, approximately 80-fold higher compared to the control hearts, and in 1% of cells in regions distant from the infarct (Beltrami et al., 2001). Although initially very exciting, these findings did not indicate whether cell division subsequently occurred as approximately 25% of the cells in the myocardium are

binucleated, furthermore, the level of cardiomyocyte proliferation reported would not be sufficient to counter the level of cell loss followed by infarction (Rosenthal, 2001). In a clinical study, where male patients received hearts from a female donor, the Y-chromosome was used to detect migration of undifferentiated cells expressing stem cell antigens from those of the donor (Quaini et al., 2002). It was found that approximately 7-10% of the myocytes, coronary arterioles and capillaries had the Y-chromosome in the donor heart after transplantation and were also highly proliferative (Quaini et al., 2002). Furthermore, undifferentiated cells expressed cardiogenic markers, such as MEF2, GATA-4 and Nestin, and endothelial markers, such as Flk1, yet, were negative for markers of bone marrow origin (Quaini et al., 2002).

Collectively, these findings suggest that the heart may have some intrinsic mechanisms for self-regeneration; however, it is imperative to note that the cell types seen within these infarct regions have the capacity to differentiate into various different cell types, including endothelial cells and smooth muscle cells, and may not become cardiomyocytes (Rosenthal, 2001). The grim outcome that most patients face after a myocardial infarction is clear evidence that those mechanisms are not enough for replenishing the massive loss of contractile tissue, but only beneficial for prevention of ventricular remodeling and slowing the progression of heart failure (Rosenthal, 2001).

1.5.2 Sources of donor cells previously used for myocardial transplantation

The concept of cell based therapy for myocardial repair is a very complex one. Not only do we need to have an understanding of the environment into which the cells are to be transplanted (the infarct or the infarct boarder), but we also need to have a full understanding of the cell type to be transplanted, the effects of the infarct environment on

viability, proliferation and differentiation of these cells, and the effects of different drugs used to treat cardiovascular diseases on the infarct zone, and the transplanted cells. **The main goals of cell-based therapies are to improve cardiac function by (1) replacing lost, necrotic or apoptotic cardiomyocytes, (2) increase number of contractile cells, (3) promote angiogenesis and (4) induce cardiac protection** (Schwartz & Kornowski, 2003)**. To achieve these goals, various cell types have been suggested and used in animal and clinical settings. The following overview highlights the pros and cons of different cell types previously suggested for intracardiac transplantation for myocardial regeneration.**

(i) Skeletal myoblasts: The first cell-based therapy for cardiac regeneration began with the use of skeletal muscle satellite cell progenitor cells (commonly referred to as myoblasts), which are generally involved in the regeneration of skeletal muscle. Intracardiac transplantation of skeletal myoblasts showed promising results in normal and diseased adult murine hearts (Chiu et al., 1995; Koh et al., 1993). The transplanted myoblasts were able to form viable grafts and improve the function of the host myocardium in rabbits in which myoblasts were incorporated (Taylor et al., 1998). Although initial findings suggested that the engrafted myoblasts trans-differentiated into cardiomyocytes, it was found that none of the transplanted cells expressed β-MHC, cardiac troponin I, atrial natriuretic peptide, nor do they express the gap-junction proteins (N-cadherin and connexin 43), required for electromechanical coupling between one another and the host myocardium (Reinecke et al., 2002). Additionally, using a 2-photon analysis of skeletal myoblasts expressing EGFP reporter, it became evident that majority of the transplanted myoblasts are functionally isolated from the host myocardium

(Leobon et al., 2003). Further analysis indicated that grafted myoblasts differentiate into peculiar hyperexcitable myotubes with a contractile activity fully independent form the host myocardium (Leobon et al., 2003).

The functional improvements seen in the original animal studies are also believed to be due their ability to reduce ventricular dilation, and not due to electromechanical coupling of grafted and host cells (Leobon et al., 2003). Despite this gap in knowledge, in June 2000 the first operation was performed, launching 3 surgical studies of small cohorts of patients with low left ventricular ejection fraction (LVEF) who received intracardiac transplantation of autologous myoblasts along with coronary artery bypass surgery (CABG) (Siminiak et al., 2004; Dib et al., 2005). The autologous cells were isolated from skeletal biopsy samples and approximately $4x10^5 – 5x10^7$ cells were administered into the akinetic area during the CABG surgery (Siminiak et al., 2004). Out of the 10 patients, one died 7 days postoperatively due to infarction in an area, which was not previously targeted by cell injection. In the 9 remaining patients, improvements in the ejection fraction and a decrease in number of dyskinetic segments were observed (Siminiak et al., 2004). In a similar study, histological evaluation in hearts of patients who underwent heart transplantation, indicated that survival and engraftment of skeletal myoblasts within the infarcted myocardium (Dib et al., 2005). In one of the trials, four of the ten patients experienced delayed episodes of sustained ventricular tachycardia and recieved implanted internal defibrillators (Menasché et al., 2003). The Myoblast Autologous Grafting in Ischemic Cardiomyopathy (MAGIC) trial (Menasché et al., 2008) investigated the potential of intracardiac transplantation of skeletal myoblasts in a HF-setting.

Unfortunately, the MAGIC trial had to be terminated, as the occurrence of arrhythmias in myoblast-treated patients was twice the untreated patients (Menasché et al., 2008).

(ii) Embryonic stem (ES)-derived cells: Despite the ethical and political issues surrounding ES cells, their unlimited ability for self-renewal (Amit et al., 2000) and well established protocols for their derivation, propagation and cardiomyogenic differentiation make them an attractive source for cell-based cardiac therapies (Mummery et al., 2012). ES cells are derived from the inner cell mass of developing blastocysts and maintained in their undifferentiated state in presence of leukemia inhibitory factor (LIF), and in absence of LIF are able to differentiate into ecto-, endo-, and mesodermal cell lineages (with exception of yolk sac cells) (Doetschman et al., 1985). Human ES (hES) cell-derived cardiomyocytes have been shown to express markers that are reminiscent of cardiomyocytes such as cardiac α-MHC, cardiac troponin I and T, atrial natriuretic factor, cardiac transcription factors such as GATA-4, Nkx2.5, and MEF-2 (Xu et al., 2002). Additionally, hES- cell derived cardiomyocytes were shown to express gap junction proteins, such as connexin 43, along with other molecular elements that are required for successful electromechanical coupling with host myocardium (Westfall et al., 1997). Furthermore, the cardiomyocyte differentiation of hES cells was improved with treatment of 5-aza-2'-deoxycytidine but not dimethyl sulfoxide (DMSO) or retinoic acid (Xu et al., 2002).

Due to the ethical controversies surrounding use of ES cells, alternative methods have been developed, where adult somatic cells are genetically reprogrammed into pluripotent stem cells via somatic cell nuclear transfer (SCNT) (Pralong et al., 2005). Recent advances in molecular biology has lead to successful reprogramming of adult

human fibroblasts into pluripotent, embryonic stem cell-like cells from human cells (iPSC) (Yu et al., 2007; Takahashi et al., 2007). The first iPSC line was generated from fibroblasts using γ-retroviral vectors by introducing OCT3/4, SOX2, KLF4, and c-Myc (Takahashi et al., 2007), or OCT4, SOX2, NANOG and LIN28 (Yu et al., 2007). Additionally, generation of mammalian cardiomyocytes from fibroblasts *in vitro* was made possible by introducing core cardiac transcription factors GATA4, MEF2C and TBX5 (Olson, 2004; Qian et al., 2012). The combination of these two newly developed methods allows us to circumnavigate around the political and ethical issues that surround use of embryonic stem cells. It is important to note that even though it is easy for us to get excited about these technologies; they are far from being applicable in clinical settings. First, we must find alternative methods for generation of iPSCs due to limited efficiency (Dambrot et al., 2011). Secondly, protocols must be established to enable the enrichment of induced cardiomyogenic cells from culture since undifferentiated cells risk the generation of tumors within the host upon transplantation (Dambrot et al., 2011).

(iii) Bone marrow stem cells: It has been reported that upon transplantation of human heart there is a high induction of circulating bone marrow stem cells (BMSC) (Quaini et al., 2002). Further, some classes of bone marrow stem cells have been shown to have immunomodulatory properties where they are able to actively inhibit immune responses due to their ability to modulate T-cell phenotype, and hypoimmunogenic ability (Atoui & Chiu, 2012). Furthermore, it has been suggested that direct transplantation of BMSCs ($Lin^-/c\text{-}kit^+$) into infarct areas of mouse hearts can generate de novo myocardium, where it was found that 68% of the regenerated myocardium was occupied by the transplanted bone marrow cells (Orlic et al., 2001). However,

independent studies have refuted the cardiogenic potential of BMSCs ($Lin^-/c\text{-}kit^+$), suggesting that transplanted BMSCs adopt the phenotype of other cells as a result of spontaneous fusion (Murry et al., 2004). It was found that upon transplantation, transplanted BMSCs fuse with Purkinje fibers, cardiomyocytes and hepatocytes (Alvarez-Dolado et al., 2003). Recently it has been demonstrated that the migration of transplanted bone marrow stromal cells towards the areas of the heart with myocardial infarction is mediated by the stromal cell-derived factor-1 (SDF-1) and its receptor CXCR4 through the activation of the PI3K/Akt pathway (Yu et al., 2010). Regardless of the controversy surrounding the true function of BMSCs, these cells have undergone a variety of clinical trials. The outcome of these trials has been very hard to interpret because most of these trials were combined with other surgical therapies (CABG, stenting) and due to lack of proper controls (Balsam & Robbins, 2005). Despite the controversy on cardiomyogenic ability, BMSC transplantation was shown to increase angiogenesis and improve cardiac function by several investigators (Kocher et al., 2001; Sun et al., 2012). Table 1.1 and 1.2 summarize the list of clinical trials in which BMSCs were used.

(iv) Mesenchymal stem cells: Mesenchymal stem cells (MSCs) generally can be found in the bone marrow's stromal compartment, and they have been shown to be able to produce growth factors and cytokines that induce hematopoiesis *in vivo* and *in vitro* (Tocci & Forte, 2003). Other studies soon followed that showed MSCs are capable of replicating in their undifferentiated state, and also have the potential to differentiate into cells of osteoblasts, adipocytes, and chondrocytes osteocytic lineage (Pittenger et al., 1999). Treatment of enriched MSCs with 5-aza-2'deoxycytidine prior to intracardiac transplantation resulted in engrafted cells with myotube-like phenotype, elongated nuclei

and cells also expressed the cardiomyocyte-specific marker troponin I-C (Bittira et al., 2002). On the other hand, untreated MSCs were poorly differentiated and at times expressed non-cardiomyocyte phenotypes (Bittira et al., 2002). Furthermore, *in vitro*, untreated MSCs show fibroblast-like morphology, however, when treated with 5-azacytidine, approximately 30% of the cells began forming myotube-like structures, and began to beat spontaneously after two weeks, and showed synchronized beating after three weeks (Makino et al., 1999). Differentiated cells expressed myosin, desmin, actinin, atrial and brain natriuretic peptide, and contractile protein genes including myosin heavy and light chain and α-actinin which were similar to that of fetal ventricular cardiomyocytes (Makino et al., 1999). Prior to 5-azacytidine treatment MSCs expressed Nkx2.5/Csx, GATA4, TEF-1 and MEF2C mRNA, and when treated with 5-azacytidine MSCs also expressed MEF-2A and 2D (Makino et al., 1999).

These findings were then followed by evidence that direct transplantation of MSCs into the heart post-infarction can improve ventricular function in both rats (Dawn et al., 2005) and in swine (Shake et al., 2002), however, even though these cells stained for several muscle markers, their morphology resembled that of fibroblasts and they showed no electromecahnical junctions with other graft cells or the host myocardium (Shake et al., 2002). Table 1.1 and 1.2 summarize the list of clinical trials in which MSC were used.

(v) Resident postnatal cardiac progenitor cell: The adult heart is not known for its ability to self-regenerate. However, three different progenitor populations have been identified, all with different cardiomyogenic potential. The first of these cells are the Lin^- /c-kit^+ cells that were isolated from adult rat heart. When injected into an acutely

ischemic myocardium $Lin^-/c\text{-}kit^+$ cells or their clonal progeny were able to differentiate into myocardium, smooth muscle cells and blood carrying new vessels (Beltrami et al., 2003). In fact, transplantation of $Lin^-/c\text{-}kit^+$ cells in rats subjected to coronary occlusion resulted in a 29% decrease in the infarct size (Dawn et al., 2005). Furthermore, it was found that intravascular injection of $Lin^-/c\text{-}kit^+$ cells resulted in decrease infarct size, LV remodeling and amelioration of LV function (Dawn et al., 2005).

The second progenitor cell type was isolated from adult mouse heart based on stem cell antigen-1 (Sca-1) expression (Oh et al., 2003). Initially, Sca-1 cells did not express any cardiac structural genes nor did they express cardiac-specific transcription factor Nkx2.5, however, they were shown to differentiate in vitro in response to 5-azacytidine (Oh et al., 2003). When given intravenously after ischemia/reperfusion, Sca-1 cells tend to home to injured myocardium (Oh et al., 2003). Furthermore, genetic deletion of Sca-1 resulted in early-onset of cardiac contractile deficiency and age-associated hypertrophy in mice (Oh et al., 2003). The $Sca\text{-}1^+$ cardiogenic cells closely resemble the highly myogenic cells in the skeletal muscle discussed earlier that are also $Sca\text{-}1^+$, $CD45^-$, $CD34^-$, and $c\text{-}kit^-$ (Oh et al., 2003).

The third of the progenitor population are thought to be the cells expressing the LIM-homeodomain transcription factor islet-1 (isl1) (Cai et al., 2003). These $isl1^+$ cells are believed to play a role in heart development as mice lacking the Isl1 transcription factor also completely lack an outflow track, right ventricle and much of the atria (Cai et al., 2003). Even though they initially do not express any cardiac markers, purified $isl1^+$ cells are capable of being expanded without differentiation in cultures and can be rapidly differentiated into cardiomyocyte lineage when introduced to other cardiomyocytes (Cai

et al., 2003; Laugwitz et al., 2005). Co-culturing of isl1^{+} cells with neonatal myocytes indicated that isl1^{+} cells are capable of differentiating into cardioblasts, expressing myocytic markers and capable of generating action potentials with intact Ca^{2+} cycling (Laugwitz et al., 2005). As it stands today, these three different types of resident postnatal cardiac progenitor cells are believed to be different from one another such that Sca-1^{+} cells are c-kit^{-}, c-kit^{+} cells are Sca-1^{-} and isl1^{+} cells are c-kit^{-} and Sca-1^{-} (Laugwitz et al., 2005).

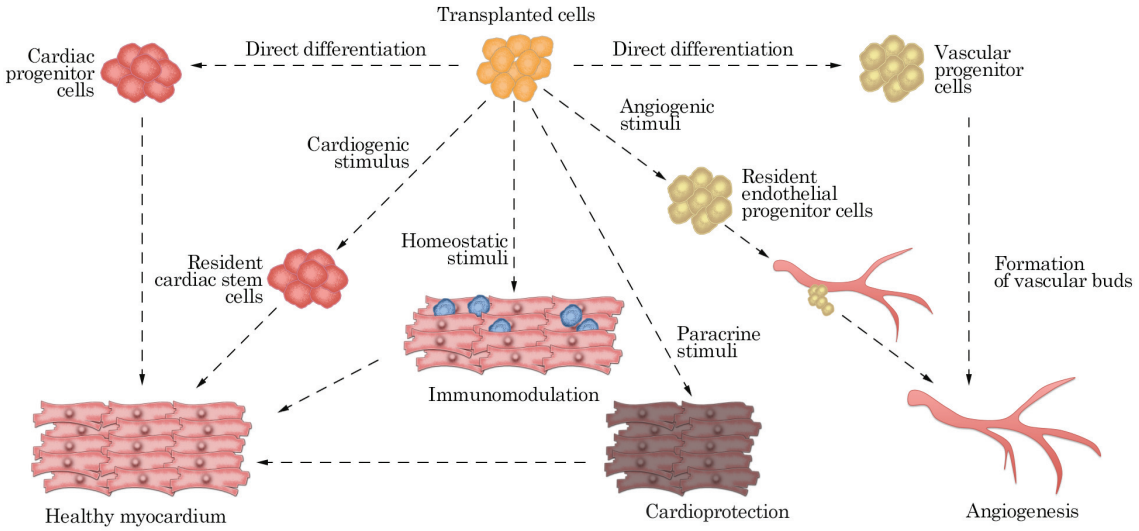

Figure 1.8 The fate and potential benefits of intracardiac transplanted cells. Transplantation of cells could have both direct and indirect benefits on the damaged myocardium. The progenitor cells could differentiate into vascular tissue and cardiomyocytes in order to replace the lost contractile tissue and provide the regenerated tissue with nutrients. Transplanted cells could indirectly improve cardiac function by releasing cardiogenic, homeostatic, paracrine or angiogenic stimuli, which collectively could recruit resident cardiac stem cells, reduce immune response, increase cardioprotective pathways and induce formation of new vasculature, respectively. Image modified and redrawn from (Behfar et al., 2014).

1.6 Clinical trials utilizing cell-based therapies for myocardial regeneration

Current clinical investigations of the potential of cell-based therapies for myocardial regeneration fall within two main categories, cardioprotective and cardiorestorative. The main focus of cardioprotective therapy is intended to limit the damage induced by acute myocardial infarction. In contrast, the main focus of cardiorestorative therapy is to restore the myocardial function in failing hearts. Due to their established reputation of being safe and relatively easy to use, bone-marrow-derived mononuclear stem cells (BMMNCs) have thus far been the most commonly used cell type for cell-based clinical trials.

1.6.1 Critical assessment of first-generation clinical trials

There are several issues surrounding the field of stem cell-based therapies for myocardial regeneration, which makes it difficult for investigators to reach a concrete conclusion and consensus. There is a large variability between different clinical trials with regards to handling of the cells, delivery of the cells and also characterization of the cells used, as is evident in the variability of outcomes of the first generation clinical trials (Table 1.1). When looking at the overall picture, there is a great degree of variability with regards to the time of harvest of cells, method of purification, incubation time, the vehicle used, the number of cells, and the methods used for functional assessments within each study. Although all studies categorize the cells used as BMMNCs, it would be difficult to assume that each patient was given similar cell product and equal cell number within each treatment. For instance, to date, cell surface profiles and/or colony-forming unit quantification, which have initially been established for hematological and not an organ-failure setting, have been used to distinguish BMMNCs (Løkkegaard et al., 2004).

Further, It has been suggested that the differential findings between the REPAIR-AMI and the ASTAMI trials could strictly be due to the differences in number of cells and handling of the cells prior to intracoronary infusion (Wollert & Drexler, 2010). Furthermore, special attention needs to be given to the vehicle used for intracoronary infusion of cells. For instance, the use of heparin in the vehicle solution, as seen in BOOST, ASTAMI and TOPCARE-CHD trial, has raised some concerns. It has been shown that heparin blocks the SDF-1/CXCR4 signaling as it binds to both the ligand and the receptor, thereby, inhibiting migration and homing of intracoronary infused BMMNCs (Seeger et al., 2012).

Additionally, patient inclusion criteria are often based on LVEF immediately after AMI, which has been shown to be not a good predictor of patient survival as functional improvements in response to PCI alone has been shown to be variable in patients (Ottervanger et al., 2001). Thus, the increase in function recorded in response to cell-based therapy may not be due to the therapy itself but may be due to the ventricular remodeling that occurs post-AMI (Ottervanger et al., 2001). Furthermore, BMMNC-therapy was most beneficial in patients with more extensive infarct damage (Wollert & Drexler, 2010), where on the other hand, a patient population has been characterized who do not respond to BMMNC-therapy (Janssens et al., 2006). Thus, better prognostic tools may be needed for patient selection and determining benefits of cell-based therapies. It is imperative to note that cell-based therapies follow the organ transplantation paradigm, as unlike small-molecule drugs or biological agents, they are a live functional entity, which are expected to provide a positive clinical outcome. Thus, there are still various clinical

questions that need to be addressed, such as, the best time for cell delivery and whether a dose-response relationship exists (Dimmeler et al., 2008).

1.6.2 Second generation clinical trials of cell-based therapies for myocardial regeneration

The second-generation therapies (Table 1.3) have focused on using more specific cell types rather than the generalized heterogeneous population of cells used in the first-generation clinical trials previously described. The rationale for use of purified stem-cell cultures is to eliminate the variability due to presence of other cell types, which has led to the variability in findings in the first-generation clinical trials. There are two populations of cells from the heterogeneous population of bone marrow cells, which have been extensively used in recent clinical trials, the human mesenchymal stem cells (hMSCs) and the $CD34^+$ endothelial progenitor cells (EPCs).

The potential of hMSCs for myocardial regeneration was first realized in a series of pre-clinical trial findings, suggesting that hMSCs have the capacity to differentiate at the single cell level into visceral mesoderm, neuroectoderm and endoderm *in vitro* (Jiang et al., 2002). Furthermore, it was found that hMSCs have the capacity to differentiate into functional smooth muscle cells (Ross et al., 2006) and hepatocytes (Schwartz et al., 2002). Additionally, it was demonstrated that transplantation of MSCs in mice had the capacity to repair infarcted myocardium and prevent ventricular remodeling, especially when genetically enhanced with Akt1 (Mangi et al., 2003).

Collectively, cell-based clinical studies have been able to establish safe methods of cell delivery in both AMI and HF settings. However, there is considerable amount of variability, which can be attributed to lack of understanding regarding time of cell

harvest, quality control procedures to ensure quality and potency of cells, dosing of cells, specific cell types and stem-cell delivery methods (Behfar et al., 2014). Even though there is still much work left to be done, lessons learned from clinical trials provide the groundwork where future investigators can build upon.

Table 1.1 First-generation clinical trials evaluating the regenerative potential of BMSCs in patients suffering from myocardial infarction, EF= Ejection Fraction

Study Name	Cell Type	Description	EF
Transplantation of Progenitor Cells and Regeneration Enhancement in Acute Myocardial Infarction (TOPCARE-AMI) (Assmus et al., 2002)	Bone marrow-derived progenitor cells or circulating blood-derived progenitor cells	Patients (n=20) with perfused AMI received cells ($7.3x10^{6}$) into the infarct artery ~3-5-days post AMI. An improved left ventricular function was seen, due to the significant increase in the myocardial viability in the infarct zone.	No change Some positive
BOne marrOw transfer to enhance ST-elevation infarct regeneration (BOOST) (Wollert et al., 2004)	Bone marrow-derived progenitor cells	Patients (n=60) with elevated ST-segment AMI received cells ($2.4x10^{9}$) into the infarct artery ~5-days post AMI. 6-months post transplantation compared to the control group a significant increase in the mean global LVEF was observed in BMMNC-treated group.	Positive
Reinfusion of Enriched Progenitor Cells and Infarct Remodeling in Acute Myocardial Infarction (REPAIR-AMI) (Schächinger et al., 2006)	Bone marrow aspirate including hematopoietic, mesenchymal and other progenitor cells.	Patients (n=204) with AMI received cells ($1.98x10^{8}$) into the infarct artery ~3-6-days post AMI. At 4-months a significant improvement in the LVEF was seen in the BMMNC-treated group compared to the control group.	Positive
FINnish stem CELL (FINCELL) (Huikuri et al., 2008)	Bone marrow-derived progenitor cells	Patients (n=80) with STEMI ($3.6x10^{9}$) into the infarct artery. At 6 months post intracoronary infusion of BMMNC cells, compared to the control group, the BMMNC-treated group had a greater absolute increase of global LVEF.	Positive
Leuven-AMI (Janssens et al., 2006)	Bone marrow-derived progenitor cells	Patients (n=67) 4 days post-PCI patients were infused ($4.8x10^{8}$) BMMNCs or placebo through the coronary arteries. At 4 months no difference between the groups was evident.	No change
Autologous Stem-Cell Transplantation in Acute Myocardial Infarction (ASTAMI) (Lunde et al., 2006)	Bone marrow-derived progenitor cells	Patients (n=100) 4-7 days post-anterior wall AMI were transplanted ($6.8x10^{7}$) BMMNCs or placebo through the coronary arteries. At 6 months no difference between the groups was evident.	No change
HEPE (Hirsch et al., 2011)	Bone marrow-derived progenitor cells	Patients (n=200) 3-8 days post-PCI were transplanted ($2.96x10^{9}$) BMMNCs or placebo through the coronary arteries. At 6 months no difference between the groups was evident.	No change
Timing In Myocardial infarction Evaluation (TIME) (Traverse et al., 2012)	Bone marrow-derived progenitor cells	TIME trial concluded that intracoronary infusion of BMMNCs ($1.5x10^{8}$) 3 or 7 days was insufficient for myocardial regeneration in patients (n=120).	No change
Late-TIME (Traverse et al., 2011)	Bone marrow-derived progenitor cells	Late-TIME trial concluded that intracoronary infusion of BMMNCs ($1.5x10^{8}$) 2-3 weeks was insufficient for myocardial regeneration in patients (n=120).	No change

Table 1.2 First-generation clinical trials evaluating the regenerative potential of BMSCs in patients suffering from congestive heart failure, EF= Ejection Fraction

Study Name	Cell Type	Description	EF
Transplantation of Progenitor Cells and Recovery of LV Function in Patients with Chronic Ischemic Heart Disease (TOPCARE-CHD) (Assmus et al., 2006)	BMMNCs or circulating blood-derived progenitor cells	Patients (n=92) were transplanted 3 months post MI. At the 3-month follow-up period, it was found that contrary to patients treated with circulating progenitor cells ($2.2x10^{\wedge 7}$) and those untreated, BMMNC-treated patients ($2.1x10^{\wedge 7}$) showed a moderate but significant improvement of LVEF over baseline.	Positive / No change
First Bone Marrow Mononuclear Cell United States Study-CCTRN (FOCUS-CCTRN) (Perin et al., 2012)	BMMNCs	Study concluded that in patients (n=92) with chronic ischemic HF, transednocaridial injection of BMMNCs ($1.00x10^{\wedge 8}$) does not improve left ventricular end-systolic volume, maximal oxygen consumption and reversibility. Furthermore, no differences were found in secondary outcomes such as percent myocardial infarct, total infarct size, fixed infarct size, regional wall motion and clinical improvements.	No change

Table 1.3 Second-generation clinical trials evaluating the regenerative potential of BMMNC and hMSCs in patients suffering from congestive heart failure, EF= Ejection Fraction

Study Name	Cell Type	Description	EF
The Prevention of Contrast renal Injury with Different Hydration Strategy (POSEIDON) (Hare et al., 2012)	BM-derived allogeneic and autologous MSCs	During the study patients were given one of three different doses (20, 100 or 200 million cells) of either allogeneic or autologous MSCs via transendocardial injections into 10 LV sites. No difference in ventricular arrhythmic serious adverse events between the allogeneic and autologous MSC-treated groups after a 1-year follow up period was evident. The low concentration treatment produced the greatest effects in patients.	Positive / No change
Transendocardial Autologous Mesenchymal Stem Cells and Mononuclear Bone Marrow Cells in Ischemic Heart Failure Trail (TAC-HFT) (Heldman et al., 2014)	BMMNCs and culture-expanded mesenchymal stem cells	This study was able to conclude that use of hMSCs and BMMNCs were safe for patients (n=65) with chronic ischemic HF. Additionally, the study found that compared to the untreated and BMMNC-treated group, the hMSC-treated patients showed improvements in cardiac function	Positive / No change
ACT34-CMI (Losordo et al., 2011)	Circulating $CD34^+$ EPCs	Patients (n=168) were either treated with one of two doses (100 or 500 thousand) or vehicle. It was found that those treated with lower dose of EPCs showed significantly lower angina frequency and improved exercise tolerance compared to the untreated and higher dose-treated patients.	Angina frequency was reduced
Stem Cell Infusion in Patients with Ischemic cardiOmyopathy (SCIPIO) (Bolli et al., 2011)	c-kit+ cardiac stem cells (CSC)	CSCs were obtained from atrial tissue samples, enriched, and 1 million autologous CSCs were administered via intracoronary infusion approximately 100 days post coronary artery bypass surgery (CABG) (n=16). Some CSC-treated patients showed improved LVEF function.	Positive
CArdiosphere-Derived aUtologous stem CELLs to reverse ventricular dySfunction (CADUCEUS) (Makkar et al., 2012)	Autologous cardiosphere-derived cells (CDCs)	Patients (n=31) were treated with (1.3-2.5x10^7) CDCs 2-4 weeks post MI. By 6 months, CDC-treated patients showed reduced scar mass, increased viable heart mass, regional contractility and systolic wall thickening, however, the findings failed to find any statistically significant changes in LVEF between different treatment groups.	No change
Cardiopoietic stem Cell therapy in heart failURE (C-CURE) (Bartunek et al., 2013)	Cardiopoietic hMSCs	Harvested hMSCs (0.6-1.2x10^9) were exposed to the cardiogenic cocktail, and administered via endomyocardial injections in LV of patients (n=45) with chronic HF were It was found that compared to the control group, patients treated cardiopoietic stem cells showed a significant increase in LVEF.	Positive

1.6.3 Drug interactions and donor cell transplantation

Undoubtedly any patient suffering from cardiovascular disease that would require donor cell transplantation will also rely on a variety of pharmacological therapeutics (such as diuretics, ACE inhibitors, β-adrenergic blockers, etc.) (McKelvie et al., 2013). Further, to date the current focus of most clinical trials has been changes in ventricular function via intracardiac or intracoronary cell transplantation in combination with or without surgical interventions (McMullen & Pasumarthi, 2007). However, the depth of knowledge surrounding the effects of various cardiovascular drugs on the survival, proliferation and differentiation of intracardiac or intracoronary cell transplanted cells is quiet shallow (McMullen & Pasumarthi, 2007).

There is some evidence that interactions between pharmacological therapies and transplanted cells have significant impact on the effectiveness of intracardiac transplantation therapies. For instance, the graft volume after intracardiac transplantation of embryonic ventricular cells was significantly reduced in mice treated with the L-type Ca^{2+} channel blocker Nifedipine (Hotchkiss et al., 2014). Secondly, use of heparin in the BOOST (Wollert et al., 2004) and CADUCEUS trial (Makkar et al., 2012) has come to question, as recent findings suggest that heparin interferes with the migration and homing potential of BMCs, and use of the anticoagulant bivalirudin instead of heparin was suggested (Seeger et al., 2012). Hence, future studies focused on characterizing the effects of other clinically used cardiovascular drug classes such as diuretics, ACE inhibitors, β-adrenergic blockers, etc., on proliferation and differentiation of intracardiac and intracoronary transplanted stem cells would bring to light whether those drugs would have beneficial or detrimental effects of such drugs on transplanted cells.

CHAPTER 2 MATERIALS AND METHODS

2.1 Animal Maintenance and Mouse Strains

All experimental protocols regarding the use of animals were previously approved by the Dalhousie University Committee on Laboratory Animals and were performed in agreement with the Canadian Council on Animal Care Guide to Care and Use of Experimental Animals (CCAC, Ottawa, ON: Vol.1.1, 2nd edition, 1993; Vol 2, 1984). All animals were maintained on a 12-hour light/dark cycle and housed in the Carleton Animal Care Facility at Dalhousie University.

C57Bl/6 and **CD1** mouse strains were purchased from Charles River Laboratories (Montreal, Quebec, Canada). The **R26R** reporter mouse strain (designated as Rosa *LacZ* and abbreviated as RL) was obtained from Jackson Laboratories, (Bar Harbor, Main, USA). The **Nkx2.5-Cre** mouse strain (abbreviated as NC) was obtained from Dr. Richard Harvey (Victor Chang Cardiac Research Institute, University of South Wales, Australia; (Stanley et al., 2002). The NC mice were engineered to have an internal ribosomal entry sequence (IRES) and a Cre-recombinase (Cre) coding sequence inserted into the 3' untranslated region of the Nkx2.5 gene. All transgenic mouse lines were maintained in C57Bl/6 background. Unless otherwise stated, CD1 mice were used for all experimental procedures.

2.2 Genomic DNA Extraction

Genomic DNA was extracted from ear-punch biopsy samples of all transgenic mouse strains using the Sigma REDExtract-N-AMP tissue PCR Kit (Sigma, Oakville, Ontario, Canada), according to the manufacture's instructions. Tissue samples were placed in 50µl of DNA extraction solution (10µl Tissue Preparation Solution: 40µl

Extraction Solution), ground manually using a sterile pipette tip and incubated for 10min at room temperature and heated to 95°C in a block heater. Next, 10µl of Neutralization Buffer was added to each sample and mixed. Later, the samples were centrifuged to pellet undigested tissue and the supernatant was used directly for polymerase chain reaction (PCR).

2.3 Genotyping by Polymerase Chain Reaction (PCR)

PCR was performed using REDExtract N-AMP kit (Sigma) with a total reaction volume of 10µl. Primers were ordered from Invitrogen (Burlington, Ontario, Canada), and primer sequences are listed in Table 2.1. Each PCR mixture was a combination of 5µl REDExtract N-AMP PCR mix, 0.5µl of each primer (50ng each) and 2µl of tissue extract and a final volume of 10µl was achieved by adding 2.5µl of water. For **Rosa-*LacZ* genotyping** PCR reaction were performed for 30 cycles: 30sec at 94 °C, 30 at 60°C and 60sec at 72°C with expected PCR product sizes of 650 bp for wildtype 320 bp for knockin allele. For **Nkx2.5-Cre genotyping** PCR reaction were performed for 30 cycles: 30sec at 94°C, 20 at 60°C and 60sec at 72°C with expected PCR product sizes of 264 bp for wildtype and 583 bp for knockin allele. No template controls were routinely performed in PCR reactions to rule out false positive results.

To ensure phenotype integrity, the atria of E11.5 ventricular cells were stained with X-Gal (goldbio, Missouri, USA). The atria of ventricles were placed in an X-Gal solution for 1hr in X-Gal solution and incubated in 37°C. X-Gal solution was prepared as follows: the primary X-Gal solution was prepared by adding 0.01g of X-Gal powder to 2.5mL of N, N-Dimethyl Formamide (DMF, Sigma) and added drop-wise to an 80mL PBS solution containing 200µL of 1M $MgCl_2$, 0.164g potassium ferricyanide, and 0.212g

potassium ferrocyanide. The following day, the X-Gal was removed and slides were washed in PBS and subjected to immunolabelling protocol exactly as described above.

2.4 Total RNA Extraction from Cells and Tissues

Cultured E11.5 ventricular cells were lysed directly in 35mm culture dishes by adding 1mL of TRIzol reagent (Invitrogen) and passing the cell lysates through a pipette tip and incubated at room temperature for 5min to allow dissociation of nucleoprotein complexes. Next, 0.2mL chloroform was added to the samples and shaken vigorously by hand for 15sec, incubated at room temperature for 3min and centrifuged at 13,000 rpm for 15min at 4°C. Following the centrifugation, the colorless aqueous phase containing the RNA was removed and transferred to fresh tubes and precipitated by adding 0.5mL isopropyl alcohol, incubated at room temperature for 10min, and centrifuged at 13,300 rpm for 10min at 4°C. The pellet was washed with 75% ethanol in nuclease free H_2O (Ambion), air dried and solubilized in nuclease free H_2O (Ambion). Later, using a spectrometer (SmartSpec^{TM} Plus, Bio-Rad, Mississauga, Ontario, Canada), the RNA content was quantified by measuring the absorbance at 260nm and 280nm.

2.5 RNA Quality Control

To ensure the purity of the acquired RNA, only samples with a 260:280 ratio >1.6 were used in gene expression experiments. Furthermore, to ensure a high level of RNA integrity, 2µg of RNA was electrophoresed on an agrose gel and stained with ethidium bromide and only samples which displayed two bands corresponding to predominant ribosomal RNAs at ~2kb (18S) and ~5kb (28S) were used. Thus, samples that met these

quality control experiments were immediately converted into cDNA sequences and stored in -20°C until used for real time quantitative PCR (qPCR) gene expression analysis.

2.6 Real Time Quantitative Polymerase Chain Reaction (RT-qPCR)

Complementary DNA (cDNA) from RNA samples was generated by adding 1µg of RNA to 1µL of 10mM dNTPs (Invitrogen), 250ng of random primers (Invitrogen), and RNAse-free H_2O (Ambion) to a total of 12µL, and then the mixture was heated for 5 minutes at 65°C. Next, 4µL of 5X Superscript II first strand buffer (Invitrogen), 1µL of 0.1M Dithiothreitol (Invitrogen) and 1µL RNAse OUT (Invitrogen) were added to each separate mixture, and samples were incubated at room temperature for 2min. Following this step, 100U of Superscript II reverse transcriptase enzyme (SSII-RT) (Invitrogen) was added and mixed gently, and the samples were incubated for 10min at 25°C and 42°C for 50min and heat inactivated at 70°C for 15min.

The primers used to amplify the cDNA via RT-qPCR were listed in Table 2.1. The primers for β_1 and β_2-adrenergic receptors, TBX 5, MEF2c, GATA4, HAND2, Cyclin D1, CDK4, Cyclin B1, P27, and GAPDH were generated using the NCBI primer design tool (http://www.ncbi.nlm.nih.gov/tools/primer-blast or http://mouseprimerdepot.nci.nih.gov). Later, qPCR efficiency experiments were then performed to determine optimal annealing temperatures for each of the primer pairs listed above. An annealing temperature of 60°C was used for all primer pairs. PCR products were purified using Axygen purification kit (Union City, California, USA) according to the manufacturer's instructions, followed by generation of 10X serial dilution series of purified product, which were subjected to the qPCR analysis. The primer pair efficiency was calculated using a previously described method (Taylor et al., 2010). An annealing

temperature that yielded efficiency between 90-110% was used for the subsequent experiments described below.

Each of the qPCR reaction mixtures consisted of: 1.0µL of forward and reverse primers (2.5µM), 1.0µL of 5X EVOlusion EvaGreen® qPCR mix (Montreal Biotech Inc., Quebec City, Canada), 2.0µL RNAse/DNAse free H2O (Ambion) and 1.0µL of cDNA product. All qPCR reactions were performed using an ECO thermocycler (Illumina, San Diego, California, USA) for 40 cycles: 15sec at 95°C, 60sec at 60°C. Next, the melt curve which was used to confirm the amplification of a single primer product was generated via an extra cycle using the following conditions: 15sec at 95°C, 15sec at 60°C and 15sec at 95°C. Subsequently, to confirm the expected amplicon seizes, the qPCR amplification products were resolved on a 1.5% agarose gel.

The gene expression findings were normalized to the control housekeeping gene glyceraldehyde 3-phosphate dehydrogenase (GAPDH) using the $\Delta\Delta C_T$ method (Livak and Schmittgen, 2001). The threshold cycle (C_T) value was determined by setting the threshold of fluoresce (dRN) to 0.1, and they represent the number of cycles at which the amplification plot of a gene of interest intersects the dRN threshold.

To compare the relative expression of two genes, the following calculations were performed to determine the $2^{-\Delta\Delta CT}$ values for each gene. First, to determine the ΔC_T value for each gene, the C_T value of the control GAPDH gene was subtracted from the C_T value of the corresponding gene, the ΔC_T of all genes were then averaged and subtracted from the ΔC_T values of each individual gene to generate $-\Delta\Delta C_T$ values. Next, the $2^{-\Delta\Delta CT}$ values of each gene was calculated and the relative expression of each gene was obtained by dividing the $2^{-\Delta\Delta CT}$ values obtained from each gene by the $2^{-\Delta\Delta CT}$ value of the selected

gene which allowed for the data to be expressed as relative expression of each gene relative to the one selected gene, which was set to the value of 1.0.

Table 2.1 List of primers used for genotyping and real time quantitative PCR and expected amplicon sizes

Primer Name	Primer Sequence (5'→3')	Expected band sizes (bp)	
Nkx2.5-S **Nkx2.5-AS** **Cre-S**	GCCCTGTCCCTCGGATTTCACACC ACGCACTCACTTTAATGGGAAGAG GATGACTCTGGTCAGAGATACCTG	583	264
Rosa 1 **Rosa 2** **Rosa 3**	AAAGTCGCTCTGAGTTGTTAT GCGAAGAGTTTGTCCTCAACC GGAGCGGGAGAAATGGATATG	320	650
GAPDH-F **GAPDH-R**	TCGTCCCGTAGACAAAATGG TTGAGGTCAATGAAGGGGTC	132	
Cyclin D1-F **Cyclin D1-R**	CTCCTCTCCAAAATGCCAG GGGTGGGTTGGAAATGAACT	112	
CDK4-F **CDK4-R**	TGCCAGAGATGGAGGAGTCT TTGTGCAGGTAGGAGTGCTG	109	
p27-F **p27-R**	GTGGACCAAATGCCTGACTC TTCTTCTGTTCTGTTGGCCC	126	
Cyclin B1-F **Cyclin B1-R**	TGTGTGAACCAGAGGTGGAA GGCTTGGAGAGGGATTATCA	114	
MEF2c-F **MEF2c-R**	TGGAGAGATGAAGTGAAGCG GCACAGCTCAGTTCCCAAAT	93	
GATA4-F **GATA4-R**	CTGGAAGACACCCCAATCTC CCATCTCGCCTCCAGAGT	100	
TBX5-F **TBX5-R**	TGGTTGGAGGTGACTTTGTG GGCAGTGATGACCTGGAGTT	101	
HAND2-F **HAND2-R**	CGGAGATCAAGAAGACCGA TGGTTTTCTTGTCGTTGCTG	96	
β_1-AR-F **β_1-AR-R**	CGAGCTCTGGACTTCGGTAG TCAGCAAACTCTGGTAGCGA	119	
β_2-AR-F **β_2-AR-R**	ATTTTGGCAACTTCTGGTGC TAGCGATCCACTGCAATCAC	97	

2.7 Timed Pregnant Female Mice

Breeding pairs (male or female NC with male or female RL mice) were placed in the same cage overnight, and the females were examined for the presence of a vaginal plug the next morning. A successful copulation was indicative of the presence of white/yellow fibrous plug in the female vagina. The morning, which the plug was detected, was considered to be embryonic day (E) 0.5. Timed pregnant female mice were anesthetized using inhalation of 4% isoflurane and sacrificed by cervical dislocation and embryos were isolated from uterine horns from various developmental stages (E11.5, E14.5 and E17.5) using a Leica MZ16SF stereomicroscope (Leica Microsystems, Richmond Hills, Ontario, Canada).

2.8 Embryonic Ventricular Primary Culture and Drug Treatments

The embryos (E11.5, E14.5 and E17.5) were removed from the uterus along with the placenta and placed in a warm PBS supplemented with 1X antibiotic/antimycotic (Gibo, Burlington, Ontario, Canada). Next, whole hearts were extracted and the left and right ventricles were placed into 0.2% v/v type I Collagenase (Worthington Biochemical Corp., Lakewood, New Jersey, USA) in PBS (PBS: 138 mM NaCl, -2.7 mM KCl, pH 7.4) and rocked at 37°C for 30min to digest the ventricular tissue. Following the 30min incubation, using a 200µl pipette tip the tissue was triturated to dissociate the cells from the remaining tissue pieces. Cells were then centrifuged at 4,000 rpm for 4min, and the pellet was neutralized with two subsequent washes of 10% DMEM (Dulbecco's Modified Eagles Medium; Wisent, Saint Bruno, Quebec, Canada) Containing 10% fetal bovine serum (FBS; Wisent). A hemocytometer was used to determine the total number of cells. Cells were plated on fibronectin (Sigma) coated 4-well chamber slides (Nunc, Rochester,

New York, USA), or 35mm dishes (Corning, Corning, New York, USA) at various cell densities ($1.2x10^5$ and $2.0x10^5$ cells, respectively).

Isoproterenol (Sigma) and Metoprolol (Sigma) stock solutions used to treat the ventricular cultures were prepared fresh by mixing the powder in sterile water and diluting the stock into 1µM working solutions in fresh medium. For ventricular cells treated with ICI 188,551 hydrochloride (referred to as ICI) (Sigma) treatment, a final concentration of 1µM was achieved by adding diluting 1.0M stock solution into 1µM working solutions using fresh medium. For ventricular cultures treated with 2.8mM and 1% DMSO (Thermo Fisher Scientific, Nepean, Ontario, Canada), 8.4µl and 30µl of DMSO was diluted in 3mL of fresh medium, respectively. 1µM stock solution of Retinoic Acid was diluted by adding 30µl of the stock solution to 3mL of fresh medium to make a 10nM working solution. Finally, 0.64M stock solution of Dynorphine B was diluted by adding 1µl of stock to 6mL of fresh medium to make the 100nM working solution.

2.9 Tritiated-Thymidine Labeling

In some experiments, at the end of the drug treatment period, medium was extracted and fresh medium supplemented with tritiated [^{3}H]-thymidine (GE Healthcare Life Sciences, New Jersey, USA) was added to each well at a concentration of 1.0µCi per 1mL of medium for six hours at 37°C. After six hours, the medium was removed, and the cells were rinsed with PBS three times and then fixed with ice cold methanol for 15min at 4°C, followed by three additional washes of PBS and processed for immunofluorescence and autoradiography.

2.10 Immune Cytochemistry

After fixation (1% paraformaldehyde [1gram of paraformaldehyde in 100mL of PBS, pH adjusted to 7.4, using NaOH] for 3min), primary cultures were permeabilized in 0.1% v/v Triton X-100 (Sigma) for 4min, followed by three consecutive 2min PBS washes. The cells were then covered in blocking buffer solution [10% v/v goat serum (Gibo), 1% w/v bovine serum albumin (BSA; Thermo Fisher Scientific) in PBS] for an hour. After, 1hr, blocking buffer solution was removed and replaced with blocking buffer containing primary antibodies of choice according to the concentrations listed in Table 2.2, for 1hr at room temperature. Next, the slides were washed with PBS three times for 3min each and incubated with secondary goat anti-mouse antibodies conjugated to Alexa Fluor 488 (1:200) and goat anti-rabbit antibodies conjugated to Alexa Fluor 555 (1:200) in blocking buffer for one hour. Cells were then washed three times (at 3min increments) and cell nuclei were counterstained by immersion in a solution of 1µg/mL of Hoechst 33258 (Sigma) in PBS. Finally the walls of the chamber slides were removed and the slides were air dried and prepared for autoradiography described in the following section (Section 2.11).

Final processing step for all experiments consisted of slides being washed in PBS and mounted with 0.1% propyl gallate (Sigma) solution [(0.1% w/v propyl gallate, 50% v/v glycerol (Thermo Fisher Scientific), 50% v/v PBS]. Slides were then examined using the Leica DM2500 Fluorescence microscope and images were captured using a Leica DFC 500 digital acquisition system.

Table 2.2 Primary antibodies and dilutions used for immunofluorescence experiments.

Primary Antibody	Dilution	Source / Catalogue #
α-Cardiac sarcomeric actinin	1:50	Sigma Aldrich Catalogue #: AEA-53
α-Smooth muscle actin	1:50	Sigma Aldrich Catalogue #: A5228
Akt	1:100	Cell Signaling Catalogue#: 4691
Phospho-Akt	1:100	Cell Signaling Catalogue#: 4060
β_1-adrenergic receptor (Cy5)	1:50	Antibodies-Online Inc. Catalogue#: ABIN669355
β_2-adrenergic receptor	1:50	Abcam Laboratories Catalogue#: ab36956
β-galactosidase	1:100	Chappel ICN Catalogue #: 55976
Cluster of differentiation 31	1:50	Developmental Studies Hybridoma Catalogue #: 2H8-c
Connexin 40	1:100	Alpha Diagnostics Catalogue #: Cx40-A
Connexin 43	1:100	BD transduction laboratories Catalogue #: 610061
Discoidin domain receptor 2	1:50	Santa Cruz Biotechnology Catalogue #: sc-8989
p-44/42 MAPK (ERK1/2)	1:100	Cell Signaling Catalogue#: 9102
Phospho-p-44/42 MAPK (p-ERK1/2)	1:100	Cell Signaling Catalogue#: 9101
GAPDH	1:100	Santa Cruz Biotechnology Catalogue #: sc-25778
HCN4	1:100	Alamone Laboratories Catalogue #: APC-052
Nestin	1:100	Developmental Studies Hybridoma Catalogue #: rat-401
Nkx2.5	1:50	Santa Cruz Biotechnology Catalogue #: sc-14033
Sarcomeric myosin (MF20)	1:100	Developmental Studies Hybridoma Catalogue #: MF-20
Vimentin	1:10 (concentrate)	Developmental Studies Hybridoma Catalogue #: 40E-C
Von Willebrand Factor	1:50	Santa Cruz Biotechnology Catalogue #: sc-14014

2.11 Tritiated-Thymidine Autoradiography

Upon completion of the immunofluorescence labeling protocol, slides were brought into a darkroom where they were coated with Kodak autoradiography emulsion type NTB (MarketLINK Scientific, Burlington, Ontario, Canada) and kept in a light-tight box at 4°C for a span of 3 days. After 3 days, slides were developed in a darkroom by placing them in Kodak D-19 developer (Sigma) for four minutes, followed by a rinse in ddH_2O, followed by immersing them in Ilford rapid fixer (Polysciences, Pennsylvania, USA) for 4 minutes. Next, the slides were washed in warm ddH_2O and mounted using 0.1% propyl gallate solution. Cells undergoing DNA synthesis during the S-phase of the cell cycle would incorporate thymidine in their nuclear DNA in the form of silver grains, thus, cells containing more than fifteen silver nuclear grains were considered to be undergoing DNA synthesis.

2.12 Protein Extraction and SDS-PAGE electrophoresis

Cultured CD1 E11.5 ventricular (left and right) cells (treated and untreated) were lysed in the 35mm dish, using 1mL Tumor Lysis Buffer (1% NP40, 5mM EDTA, 150mM NaCl, 50mM Tris/HCl pH8.0, 1.0µL PMSF and 1.0µL Aprotinin) and left on ice for 15min and centrifuged at 13,300 rpm for 15min at 4°C in order to separate the soluble cytosolic and insoluble membrane fractions. The Bradford Assay was then used to estimate the protein concentration of the protein extracts against a BSA standard curve. The principle of the Bradford Assay is based on the shift in absorbance maximum of Coomassie Blue (Pierce, Rockford, Illinois, USA) from 465nm to 595nm when bound to protein resulting in a color shift from brown to blue, which is measured via a spectrophotometer. The protein extracts were then denatured in Laemmli buffer [0.02%

w/v bromophenol blue, 2% w/v sodium dodecyl sulfate (SDS), 62.5mM Tris-HCl pH 6.8, 25% v/v glycerol, 0.5mL of β-mercaptoethanol and ddH_2O] and samples were boiled at 95°C for 3min and stored at -80°C.

Protein (total of 40µg) was separated on a 12.5% SDS-polyacrylamide gel [0.375M Tris/HCl pH 8.8, 0.08% w/v SDS, 0.2% v/v ammonium persulfate (APS), 12.5% acrylamide, 40µL TEMED] in a 1X Tris-Glycine migration buffer (190mM glycine, 25mM Tris base and 0.1% SDS at pH 8.3) at 100 volts for approximately 1hr in a Mini-PROTEAN 3 gel electrophoresis unit (Bio-Rad, Mississauga, Ontario, Canada). Subsequently, the separate proteins were transferred onto a nitrocellulose membrane (GE Healthcare Life Sciences) in Transfer buffer (190mM glycine, 25mM Tris base and 20% methanol at pH 8.3) for 1hr while applying a constant current of 100 volts. Nitrocellulose membranes were then rinsed in ddH_2O and air dried and prepared for western blot analysis.

2.13 Western Blot Analysis

To detect the protein of interest the nitrocellulose membrane was immersed in blocking buffer (3% w/v BSA and 5% w/v powder milk in PBS with 0.1% w/v tween) for two 30min washes. Later, the membrane was incubated in blocking buffer with the primary antibody of interest for 1hr. Primary antibodies used for western blot analysis include, rabbit polyclonal p44/42 MAPK (Erk1/2) (Cell Signaling, Catalogue #9102), rabbit polyclonal phospho-p44/42 MAPK (Erk1/2) (Thr202/Tyr204) (Cell Signaling, Catalogue #9101), rabbit polyclonal Akt (pan) (C67E7) (Cell Signaling, Catalogue #4691), rabbit polyclonal phospho-Akt (Ser472) (D9E) XP® (Cell Signaling, Catalogue #4060), and rabbit polyclonal GAPDH (FL-335) (Santa Cruz, Catalogue #Sc-25778).

After one hour of incubation with the primary antibodies, the membranes were washed three times in 1% Tween in PBS (0.1% PBST) in 10min increments and then incubated for 1hr in secondary antibody goat-anti-rabbit (1:2000) (Bio-Rad, Catalogue #172-1019) conjugated to horse radish peroxidase diluted in blocking buffer. Next, the nitrocellulose membrane was washed three times in 0.1% PBST for 10min increments and the protein bands were detected by enhanced chemiluminescence method using ECL Plus Western Blotting Detection System (GE Healthcare Life Sciences) according to the manufacturer's instructions.

2.14 Second Messenger Assay: cAMP

Ventricles (left and right) of CD1 embryos (E11.5, E14.5 and E16.5) were isolated and digested in 0.2% Type I collagenase (Worthington) for 30min (for E11.5 ventricles) and 45min (for E14.5 and E17.5 ventricles) at 37°C. The cells were then centrifuged and neutralized via 10% DMEM as previously described (Section 2.5). In order to determine the cAMP levels of embryonic ventricular cells, cAMP competitive immunoassay was performed using the two-step protocol of the cAMP *htrf* assay kit (Casibo, Bedford, Massachusetts, USA Catalogue #62AM4PEB) according to the manufacturer's instructions summarized below. The principle of this assay is based on the competition between a d2-dye labeled cAMP analogue (d2-cAMP) and endogenous cAMP for binding to the binding sites of monoclonal antibodies (anti-cAMP) labeled with Cryptate (mAb-Cryptate) where the signal generated due to transfer of energy between the d2-cAMP and mAb-Cryptate is inversely proportional to the concentration of endogenous cAMP within the experimental setting.

The two-step process involved in the detection of cAMP consisted of a stimulation and a detection step. **Step 1-Stimulation:** 5µL of dilution buffer consisting of the drug compound of interest was added to 5µL of cells (4,000 cells) in experimental wells of 384-well volume plates (Greiner Bio-One Catalogue #784075) to achieve a total volume of 10µL/well. In order to prevent degradation of the cAMP product, 500µM of broad substrate phosphodiesterase inhibitor 3-isobutyl-1-methylxanthine (IBMX, Sigma) was added to the dilution buffer. The plate was then sealed, and incubated at room temperature for 30min. **Step 2-Detection:** to each well, 5µL of d2-cAMP diluted in lysis buffer and 5µL of mAb-Cryptate was added to achieve a total volume of 20µL, and the plate was sealed and incubated at room temperature for 1hr. To determine non-specific signal, d2-cAMP was omitted in the negative control wells. Later, the plate was read on a POLARstar Omega plate reader (BMG Labtech). The d2-cAMP fluorophore was excited at 337nm and emission was detected at 665nm and 620nm and the results were calculated using the 665nm/620nm ration and expressed as Delta F values as described below. First, the 665nm/620nm ratio for each well was multiplied by 10^4 and an average value for each replicate well was calculated. Next, subtracting the negative control 665nm/620nm ratio value from the sample 665nm/620nm ratio, then dividing by the 665nm/620nm ratio of the negative control and multiplying by 100 obtained the Delta F value. The cAMP concentration values were obtained by extrapolating the respective Dalta F values from the standard curve, which covered a range of 0.17-712nM (final concentration of cAMP/well).

2.15 CyQUANT Cell Proliferation Assay

CyQUANT cell proliferation assay (Invitrogen) was used to measure E11.5 ventricular myocyte proliferation according to the manufacturer's instructions. Cells were seeded on fibronectin (Sigma) coated 96-well plate (UV-Star microplate, Greiner Bio One, Catalogue #655809). A standard curve was generated using known number of E11.5 ventricular cells and the resulting fluorescence was measured via a plate reader. For our experiments, 16,000 cells were plated per well in 10% FBS-DMEM for 4hrs. In order to examine the effects of β_1 and β_2-AR agonist and antagonists on proliferation of E11.5 ventricular cells, cells were treated with or without the following drugs: 1μM ISO, 1μM ISO + 1μM Meto and 1μM ISO + 1μM ICI. After, 18hrs the cells were washed with PBS and plates were frozen at -80°C in order to assist with cell lysis.

Later, plates were thawed at room temperature and 200μL of CyQUANT GR dye diluted in cell lysis buffer (Invitrogen) was added to each well. Later, plates were incubated in the dark at room temperature for 2min prior to measuring fluorescence. A plate reader was used to take fluorescence readings at an excitation of 485nm and an emission of 530nm using top optics. Fluorescence readings were used to calculate number of cells using the standard curve by linear regression using Graphpad Prism Version 5.01 (Graphpad Software).

2.16 Fluorescence Activated Cell Sorting and cell staining for adrenergic receptors, TMRM and cellular proliferation

Embryonic ventricular cells were isolated (E11.5 and E17.5) and digested via 0.2% Type I collagenase (Worthington) for 30min (for E11.5 ventricles) and 45 minutes (for E17.5 ventricles) at 37°C and the pellets were obtained and neutralized with 10%

DMEM as described in Section 2.14. To ensure that single-cell suspension was obtained, the cells were passed through a 40μM mesh filter, and centrifuged at 4000rpm for 4min. In experiments in which E11.5 ventricular myocytes were used, generally 6-8 pregnant mice were sacrificed and approximately 10 embryonic hearts were obtained per pregnancy resulting in ~$4.5x10^6$ cells prior to preparations for FACS analysis. In experiments in which E17.5 ventricular myocytes were used, generally 1-2 pregnant mice were sacrificed and approximately 10 embryonic hearts were obtained per pregnancy resulting in ~$5.0x10^6$ cells prior to preparations for FACS analysis.

For TMRM staining (Tetramethylrhodamine Methyl Ester Perchlorate) cells were incubated in 50nM of TMRM solution (Molecular Probes Inc., 29851 Willow Creek Road, Eugene, OR USA, Catalogue#T668) diluted in PBS at 37°C for 30min, washed in PBS, centrifuged at 4000rpm for 4min and reconstituted in FACS-Buffer (4% BSA in PBS).

For experiments where cells were analyzed for cell surface expression of **β_1 and β_2-adrenergic receptors**, unfixed cells were suspended in blocking buffer and incubated at room temperature for 45min. For β_1-adrenergic receptor staining, cells were incubated for 1 hour in rabbit polyclonal β_1-adrenergic receptor antibody conjugated to Cy5 (Antibodies-Online Inc. Dunwoody Park, Suit 145, Atlanta GA, USA, Catalogue #ABIN669355), centrifuged at 4000rpm for 4min, washed once in PBS, centrifuged at 4000rpm for 4min and reconstituted in FACS-Buffer (4% BSA in PBS). For β_2-adrenergic receptor staining, cells were incubated for 1hr in rabbit polyclonal β_2-adrenergic receptor antibody (Abcam, Toronto, ON, Canada, Catalogue# ab36956), centrifuged at 4000rpm for 4min, washed once in PBS, centrifuged at 4000rpm for 4min,

and incubated for 1hr in secondary goat anti-mouse antibodies conjugated to Alexa Fluor 488 (1:200). The cells were then washed in PBS and reconstituted in FACS-Buffer (0.1% BSA in PBS).

The cells were then placed in ice and promptly used for flow cytometry analysis (FACSAria, BD Biosciences, Franklin Lakes, New Jersey, USA). The sorted cells were centrifuged at 4000rpm for 4min and cultured for further analysis.

TMRM fractions were routinely isolated from ~60-80 E11.5 embryonic ventricles and consisted approximately $1.0x10^6$ TMRM-high and $2.5x10^6$ of TMRM-low cells. Cells sorted based on TMRM staining were cultured for 4hrs and subsequently treated for 48hrs with various drug combinations including, 1μM Metoprolol (Sigma), 1μM ICI (Sigma), 1μM Isoproterenol (Sigma), 2.8mM and 1% dimethyl sufoxide (DMSO) (Sigma), 10nM Retinoic Acid, 1μM Dynorphin B (Sigma) and TMRM-high 48hr Media.

The number of cardiomyocytes (CMs) ($MF20^+$ cells) and nonmyocytes (NMCs) ($MF20^-$ cells) were quantified and represented as number of cells per millimeter squared. The number of CMs and NMCs were counted per field and divided by the area of the field (calculated using Colour-Subtractive Computer Assisted Image Analysis as previously described (Gaspard & Pasumarthi, 2008)).

Propidum iodide (PI) staining was used as a DNA content method for determining the effects of ISO on cell proliferation, as previously described (Baguma-Nibasheka et al., 2007). Initially, mid-gestation ventricular myocytes were cultured as described in Section 2.8 and treated with 1μM ISO or 1μM ISO + 1μM Meto for 18hrs. Next, adherent cells were washed with PBS, and trypsinized (1X, for 3min in 37°C), spun (2400rpm, 6min, 4°C), re-suspended in PBS, cell number was counted using a

hemocytometer and spun again. The cells were then re-suspended in PBS and fixed by addition of ice-cold 70% ethanol (drop-wise) and stored in 4°C overnight. The next day, samples were incubated in PI solution (PI powder 50ng/mL [Invitrogen; Catalogue#: P3566] and 100units/mL ribonuclease A [Catalogue#: R-4875] in PBS) at room temperature for 30min. Later, fluorescence intensities were determined using a Becton Dickinson FACSCalibur^{TM} flow cytometer. The proportion of cells in different phases of cell cycle was estimated using the ModFit program (ModFit LT, version 4, Verity Software House).

2.17 Cell Transplantation and Drug Treatments

Prior to intracardiac transplantation of embryonic ventricular NCRL cells, ventricles of E11.5, E14.5 or E17.5 were isolated, pooled, and digested in 0.2% Type I collagenase (Worthington) for 30min (for E11.5 ventricles) and 45min (for E14.5 and E17.5 ventricles) at 37°C and the pellets were obtained and neutralized with 10% DMEM as described in Section 2.14 and diluted in concentration of $6x10^5$ cells/μL in sterile PBS. Adult C57Bl/6 male mice between the ages of 11-15 weeks were used as recipients for embryonic ventricular NCRL cells. Mice were anesthetized via administration of 2.5% isoflurane, and using thoracotomy, the trachea was exposed and the animals were intubated (100-cycles/min and 0.4cc volume) via an animal volume-controlled ventilator (Harvard Apparatus Small Animal Ventilator Model 687, Holliston, Massachusetts, USA). Small retractors were used to expose the heart and for each experiment, $3x10^5$ cells (suspended in 5μL of PBS) were injected directly into the left ventricle of mice using a 28-gauge insulin ½ cc syringe. The incisions were then closed using interrupted 4-0 sutures, and the ventilator tube was retracted to allow the animal to resume voluntary

respiration. Post-surgical care included injection of analgesics, Bupomorphine (0.03-0.05mg/kg body weight, IP) and Ketoprofen (2mg/kg body weight, administered via SC route) once every 12 hours until the end-date of experimental protocol.

Mini-osmotic pumps (Model 2001, Alzet, Copertino, CA, USA) were used to continuously administer Isoproterenol (0.025g/mL) and Metoprolol (0.0684g/mL) @ 1µl per hour in mice with intracardiac transplanted NCRL cells. Post-transplantation, an incision was made in the back of the animal and the pump was placed in a pocket in the back of the mouse and the incision was closed using interrupted 4-0 sutures. Three days post surgery, the animals were sacrificed and the hearts were extracted and processed for quantification of graft volume as described in Section 2.18.

For the hind-limb model, NCRL embryonic ventricular cells were injected intramuscularly into the right hind limb of anesthetized C57/BL6/J recipient mice ($8x10^5$ cells in 30µl of PBS/recipient). For the doxorubicin (Dox)-injury model, C57BL6/J male mice (aged 11-15 weeks) were injected intraperitoneally with a single dose of Doxorubicin Hydrochloride [20 mg/kg, Mayne Pharma, Montreal, QC, (Feridooni et al., 2011)]. Dox-injected mice were allowed to recover for three days and subsequently used as recipients for systemic cell injection experiments. NCRL embryonic ventricular cells were injected into the tail veins of anesthetized C57/BL6/J recipient mice ($5x10^5$ cells in 30µl of PBS/recipient) as described previously (Murry et al., 2004; Rubart et al., 2003). After 3 or 7 days post cell injections, recipient quadriceps or hearts were collected and fixed in Flow fix and prepared for quantification as described in Section 2.17.

2.18 Quantification of Graft Volume

In order to determine the graft volume and area, adult mice were sacrificed via cervical dislocation 3 days post surgery. The recipient quadriceps and hearts were excised, washed in PBS and stored in Flow Fix (previously described in section 2.7) and rocked at 4°C for 48hrs. Motorized advanced vibroslice (MA725 Campden Instruments Ltd., Lafayette, Indiana, USA) was used to generate 25µm thick tissue sections in a PBS tissue bath. The tissue sections were then rocked at 37°C overnight in X-Gal solution to elicit a blue chromogenic signal as a result of transplanted embryonic ventricular NCRL cells. Colour-Subtractive Computer Assisted Image Analysis as previously described (Gaspard and Pasumarthi, 2008) was used to quantify the intracardiac grafts of the 25µm tissue sections. First, the surface area of the grafts were calculated by calculating the area occupied by the blue chromogenic signal due to NCRL cell engraftment from photomicrographs using image processing software developed by Reindeer Graphics (Ashville, North Carolina, USA). Next, the total volume of the grafts was calculated by multiplying the surface area of each section by 25µm of all heart sections stained positive for β-Gal staining. The collective volume of all heart sections was then calculated to give an approximate total volume of the graft in each recipient heart. Later, the tissue sections were placed in 30% sucrose solution in 4°C overnight and placed in OCT medium (Sakura Finetek, Torrance, California, USA) and stored in -80°C for further sectioning and processing.

Similarly, Colour-Subtractive Computer Assisted Image Analysis as previously described (Gaspard and Pasumarthi, 2008) was used to quantify the intramuscular grafts of the 10µm thin sections obtained from X-gal positive hind limb tissues. Later, the sections were stored in -80°C for further sectioning and processing.

For our tail vein injury model, the percent of NCRL donor cells in recipient hearts were determined by firstly, generating 50µm using motorized advanced vibroslice (MA725 Campden Instruments Ltd.), stained with X-Gal and 10µm thin sections were generated as previously described. X-Gal positive cells were reported as a percentage of positive cells out of total nuclei (Hoechst 33258) in the field.

2.19 Immunostaining of Histological Sections

Thin cryostat sections were first hydrated with PBS for 5 min, and fixed with ice cold methanol for 5min at 4°C. For sections that were immunolabelled, similar steps were followed as listed in Section 2.10, using the same primary antibodies and antibody concentrations listed in Table 2.1. For sections that were incubated with vWF (Santa Cruz) antibody the Vectastain ABC system (Vector Labs) was used. After fixation, the sections were immersed in 0.3% H_2O_2 (hydrogen peroxide in PBS), followed by two consecutive 2min PBS washes, and then covered in blocking buffer solution [10% v/v goat serum (Gibo), 1% w/v BSA (Thermo Fisher Scientific) in PBS] for 5hrs at room temperature. After, 5hrs, blocking buffer solution was removed and replaced with blocking buffer containing primary antibodies of choice according to the concentrations listed in Table 2.2, overnight at 4°C. Next day, the slides were washed with PBS three times for 3min each and immersed in the secondary antibody (75µL of horse serum, 25µL of anti-rabbit biotinylated [from the kit] in 5mL of PBS) for 30min at room temperature, followed by two consecutive 2-min PBS washes. Next, the sections were immersed in ABC mix (2 drops of solution A and solution B [from the kit] in 5mL of PBS) for 30min at room temperature. Next, the slides were immersed in DAB solution (1 DAB [3,3'-diaminobenzidine] tablet in 0.375g of ammonium nickel (II) sulfate in

62.5mL of 1xTBX [4.0g of NaCl, 0.1g KCl, 1.5g Tris Base, pH adjusted to 7.4 using HCl] pH adjusted 8.0 and 1mL of 3% H_2O_2 [in PBS]) for 2min. Slides were then subsequently dehydrated in ascending grade of 70, 90 and 100% ethanol for approximately 2min and mounted in cytoseal-60.

The final processing step for all experiments consisted of slides being washed in PBS and mounted with 0.1% propyl gallate (Sigma) solution [(0.1% w/v propyl gallate, 50% v/v glycerol (Thermo Fisher Scientific), 50% v/v PBS]. The NCRL cultures used to [^{3}H]-thymidine incorporation assay were then examined using a Leica DM2500 Fluorescence microscope and images were captured using a Leica DFC 500 digital acquisition system.

2.20 Pico Sirius Red Fast Green (SR+FG) Staining on Adult Heart Sections

In order to determine the extend of fibrosis due to Dox treatment, cryosections were processed for Pico Sirius Red Green staining as previously described (Gaspard & Pasumarthi, 2008; Feridooni et al., 2011). Cryosections were initially fixed in 50mL of Bouins solution (35.7mL of water saturated Picric acid, 1.16mL of 37% formaldehyde, 10.7mL of ddH_2O and 2.41mL of Glacial acetic acid) at 55°C for 1hr, washed with water, and stained with 0.1% Fast Green (diluted in H_2O; Sigma) for 10min at room temperature. Next, the sections were rinsed with 0.1% acetic acid for 2min, and stained with 0.1% Sirius Pico Red (Sigma-Direct red 80 in saturated aqueous picric acid) for 30min at room temperature. Slides were then subsequently dehydrated in ascending grade of 70, 90 and 100% ethanol for approximately 2min and mounted in cytoseal-60. Areas occupied by the green and red represent healthy myocardium and fibrotic tissue, respectively.

2.21 Hematoxylin & Eosin (H&E) Staining on Adult Heart Sections

Engrafted heart sections were placed in OCT and cut into 10μm sections using a Leica CM3050S Cryostat and placed onto Superfrost® Plus Slides (Fisher Scientific). The slides containing the heart sections were then immersed in instant Hematoxylin solution (Thermo Electron Corporation, Pittsburg, Pennsylvania, USA) for 2min, rinsed under water, immersed in 0.25% HCl, rinsed under water, and immersed in bluing agent (0.05% lithium carbonate). Next, the slides were subsequently immersed in 95% ethanol, 95% ethanol, 100% ethanol, and xylenes and mounted with Cytoseal-60 (Richard-Allan Scientific, Kalamazoo, Michigan, USA). Once the slides were air-dried they were examined by light microscopy using a Leica DM2500 microscope.

2.22 Electrocardiogram (ECG)

Animals were anesthetized using 1.5% isoflurane and the ECG signal was obtained using a bipolar 3-electrode 3-lead system (AD Instruments Inc., Colorado Springs, USA). The positive and negative leads were placed under the skin of the left and right pectoral muscle of mice and the ground lead was placed under the skin of the left hind limb. ECG signals were recorded using a Bio AMP and Power Lab 8/30 hardware and analyzed via Lab Chart 7 v.7.3.7 software (AD Instruments). For each animal the ECG signal was recorded for 20min, and at least 10 beats were averaged to determine the heart rate, PR, RR, QRS, QT and P duration. During ECG analysis, the mice body temperature was maintained at 37°C using a small animal heating plate (Physitemp, Instruments, Inc. Clifton, New Jersey, USA, Model #TCAT-2LV) while a rectal probe was used to continuously monitor the body temperature.

2.23 Echocardiogram

Animals were anesthetized via 1% isoflurane and transthoracic echocardiography was performed using a high-resolution transducer and a GE Vivid 7 ultrasound machine (GE Healthcare). Cardiac function and structure was assessed by measuring 2 dimensional M-Mode images from the parasternal short axis at the level of midpapillary muscle and the parasternal long axis.

2.24 Confocal Microscopy and Calcium Imaging

Embryonic ventricular cells were isolated (E11.5) and FACS sorted as described in Section 2.16 and cells from TMRM high and low fractions cells were plated on fibronectin (Sigma) coated Delta T Dishes (Bioptechs Inc. 3560 Beck Rd. Butler, Pa 16002, USA. www.bioptechs.com) at various densities ($1.0\text{-}2.0\text{x}10^5$) and incubated at 37°C for 24hrs and 72hrs time periods.

Ca^{2+} imaging of TMRM high and low cell cultures using Fluo-8: The effects of β-adrenergic stimulation on intracellular Ca^{2+} influx (designated as ($[Ca^{2+}]_I$)) and fluctuations were determined using the Screen Quest^{TM} Fluo-8 NW Calcium assay (AAT Bioquest Inc. California, USA), according to the manufacturer's instructions. Fluo-8 is a Ca^{2+} indicator molecule, which readily crosses the membrane due to the presence of a nonpolar Acetoxymethyl (AM) ester. Once inside the cell, the AM ester groups are cleaved via non-selective esterase enzymes resulting in a polar Fluo-8 molecule unable to leave the cell. Upon binding to Ca^{2+}, Fluo-8 undergoes an immense increase in fluorescence, which is detected at an emission wavelength of 514nm. This increase in fluorescence can be used to determine Ca^{2+} fluctuations and $[Ca^{2+}]_I$. In order to calculate

$[Ca^{2+}]_I$ and Ca^{2+} fluctuations, TMRM high and low fractions were cultured in Delta T Dishes (Bioptechs Inc.) for 24 and 72 hours in 10% FBS-DMEM, respectively. Later, the cells were loaded with Fluo-8 dye loading solution (10μL of Fluo-8 stock solution into 5mL of 1X assay buffer consisting of: 4.5mL Hank's buffer with 20mM HEPES and 0.5mL Pluronic F127 Plus) at 37°C for 15min. The fluorescence intensity corresponding to $[Ca^{2+}]_I$ and Ca^{2+} fluctuations in response to 1μM ISO treatment in TMRM high and low fraction cell cultures were measured using Zeiss Cell Observer Spinning Disk confocal microscope (Carl Zeiss Microscopy GmbH, 07745 Jena, Germany. www.zeiss.com). The fluorescence intensity was quantified according to the intensity of green pixels (corresponding to Ca^{2+} sensitive Fluo-8 dye signal) was quantified using the Ziess Zen lite software (Carl Zeiss, 2012).

Visualization of the mitochondrial content of TMRM high and low cell cultures: To visualize the mitochondrial content of TMRM high and low fractions, cells were cultured for 24hrs, and stained with mitochondria content marker, TMRM, and cell viability dye, Calcein-AM (Life Technologies Inc. 5250 Mainway, Burlington, ON, L7L 5Z1, Canada. www.lifetechnologies.com). Cultured TMRM high and low fractions were stained for 30minutes with 50nM TMRM and 30nM Calcein in Kreb's buffer (1mM $CaCl_2$, 132mM NaCl, 4mM KCl, 1.2mM Na_2HPO_4, 1.4mM $MgCl_2$, 6mM Glucose, 10mM HEPES, pH7.4) for 30min. Images were collected using Zeiss Cell Observer Spinning Disk confocal microscope (Carl Zeiss) and images were processed using the Ziess Zen lite software (Carl Zeiss, 2012).

2.25 Statistical Analysis

Statistical analysis was performed using the Graphpad Prism Version 5.01 (Graphpad Software, San Diego, USA). Data are presented as mean ± standard error of the mean (SEM). Multiple group comparisons were analyzed by ANOVA and Tukey multiple comparison post hoc test. A two-tailed unpaired t-test was used to compare between two groups. Significance for all analyses was assigned at $p<0.05$. For each experiment, the number of experiments/replicates is represented in the corresponding figure legends.

CHAPTER 3 THE ROLE OF β-ADRENERGIC RECEPTOR SIGNALING IN THE REGULATION OF CELL CYCLE ACTIVITY AND DIFFERENTIATION OF MID-GESTATION VENTRICULAR CELLS

3.1 Background and Hypothesis

The beta-adrenergic receptors (β_1 and β_2-AR) belong to a large family of G-protein coupled receptors and are the main mediators of endogenous catecholamine-stimulated positive chronotropy and inotropy in the heart (Rockman et al., 2002; Ahlquist, 1980). The β_1- and β_2-ARs and the catecholamine ligands are shown to be present in the heart as early as embryonic day 8 (E8) (Chen et al., 1982; Portbury et al., 2003). Previous studies have demonstrated the importance of the β-adrenergic signaling pathways in development of embryonic heart (Zhou et al., 1995; Kudlacz et al., 1990; Portbury et al., 2003; Thomas et al., 1995).

The β-adrenergic system response is mediated through the second messenger cyclic adenosine 3', 5'-monophosphate (cAMP), which is responsible for various cardiac physiological functions (Keys & Koch, 2004). The cAMP is produced in response to activation of G_s protein-coupled to β-AR (Keys & Koch, 2004). Depending on the cell type, cAMP inhibits or stimulates cell proliferation. In Swiss 3T3 fibroblasts, cAMP induced transition from G_0-G_1 (Schwartz & Rubin, 1983), whereas in NIH 3T3 fibroblasts (Mitsuzawa, 1994; Pastan et al., 1975) and smooth muscle cells (Indolfi et al., 1997; Assender et al., 1992) increased cAMP levels resulted in decreased proliferation. While it is clear that the adrenergic system plays an important role in the development of embryonic heart, the role of β-AR signaling in the regulation of cell cycle events in the embryonic heart is still unclear. Targeted disruption of tyrosine hydroxylase (TH), the rate limiting enzyme in catecholamine biosynthesis, was shown to cause early embryonic

lethality between E11.5 and E15.5 possibly due to cardiac structural defects (Zhou et al., 1995). Histological examination of homozygous TH mutant embryos revealed improper organization of cardiomyocytes suggesting a role for catecholamines in cardiomyocyte proliferation and differentiation (Zhou et al., 1995). In previous studies, we showed that embryonic ventricles at E11.5 stage have both cardiac progenitor cells (CPCs) and mature cardiomyocytes (CMs), whereas the number of CPCs precipitously decreases in later stages of heart development (McMullen, Zhang, Hotchkiss, et al., 2009; Zhang & Pasumarthi, 2007). Because TH KO mice die at E11.5 stage, it is possible that catecholamines may regulate cell cycle events in the embryonic heart. **Thus, we hypothesized that the β-AR signaling regulates proliferation and differentiation of CPCs and mature CMs in the embryonic ventricles.**

3.2 Specific Aims

1. Investigate the expression of β_1- and β_2-ARs in cardiac ventricles from various developmental stages.
2. Determine whether β-AR stimulation plays a role in regulation of CPC and CM proliferation and differentiation in mid-gestation ventricles (E11.5 stage).
3. Determine the β-AR subtypes and signal transduction pathways involved in regulation of cell cycle events in E11.5 ventricular cells.

3.3 Results

3.3.1 Quantification of β_1 and β_2-adrenergic receptor expression during mouse ventricular development

The primary goal of this study was to determine the role of β-Adrenergic Receptors (β-ARs) in proliferation and differentiation of embryonic CPCs. Therefore, we first sought to determine the expression levels of β_1-AR and β_2-ARs in ventricular

myocytes from different developmental stages. Using quantitative polymerase chain reaction (qPCR), we determined the mRNA abundance of β_1-AR and β_2-AR receptors in E11.5 embryonic ventricular cardiomyocytes and also at later developmental/post-natal stages. In previous studies, we determined that the glyceraldehyde 3-phosphate dehydrogenase (GAPDH) mRNA expression levels remained unchanged throughout ventricular developmental (Hotchkiss et al., 2014). Therefore, we used GAPDH as an internal control gene to normalize data by correcting for variations in quantities of cDNA. A progressive increase of β_1-AR mRNA expression was evident throughout development of ventricular myocytes. We found that β_1-AR mRNA expression in cardiac ventricles significantly increased approximately 3-fold at E14.5 and E16.5, and approximately 5-fold at neonatal and adulthood compared to E11.5 stage (Figure 3.1 A). In contrast, the levels of β_2-AR mRNA expression remained unchanged throughout embryonic development; however, a 4-fold increase in mRNA expression in the ventricles was evident in adult mice (Figure 3.1 B). Notably, the β_1-AR mRNA levels were significantly higher when compared to β_2-AR mRNA levels at all stages of cardiac development (Figure 3.1 C). The fold difference in the expression of β_1- and β_2-ARs ranged from 4-5 fold at E11.5 and adult stages Vs. 17-34 fold at E14.5 and neonatal stages (Figure 3.1 C).

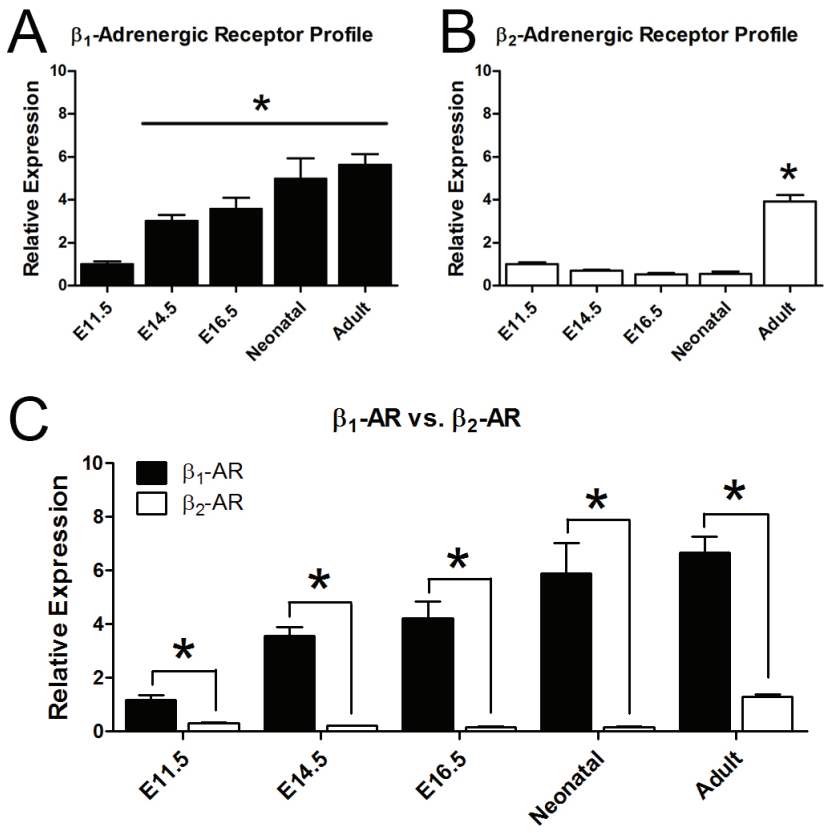

Figure 3.1 Quantification of mRNA levels of β_1- and β_2-adrenergic receptors throughout development of the heart ventricular cells.
Quantitative polymerase chain reaction (qPCR) of myocardial mRNA from different developmental stages, embryonic day (E) 11.5, E14.5, E16.5, neonatal, and adult demonstrating the expression profile for **(A)** β_1-adrenergic receptor (AR), **(B)** β_2-AR, and **(C)** β_2-AR expression compared to β_1-AR. Expression levels were normalized to GAPDH. The relative expression of β_1- and β_2-ARs was determined in relation to the E11.5 stage. Panel A: $*p < 0.05$ compared to E11.5, Panel B: $*p < 0.05$ compared to all stages; One way ANOVA, Tukey's multiple comparisons test. Panel C: $*p < 0.05$ β_1-AR vs. β_2-AR unpaired student's t-test. Each bar represents mean ± SEM, N=3 independent RNA extractions/developmental stage, duplicates.

3.3.2 Characterization of cell surface expression of β_1- and β_2-adrenergic receptors in E11.5 and E17.5 ventricular cells

Previously, we have shown that at E11.5 approximately half of the ventricular cells are Nkx2.5$^+$ CPCs with the potential to differentiate into CMs and conduction system cells albeit, at E17.5 majority of the cells are differentiated CMs (Zhang & Pasumarthi, 2007; McMullen, Zhang, Hotchkiss, et al., 2009). To determine whether cell surface expression of β_1- and β_2-AR in ventricular myocytes correlates with our mRNA expression findings (Section 3.3.1), we decided to compare receptor expression between early (E11.5) and late (E17.5) embryonic developmental stages. Using extracellular domain specific antibodies, we determined the number of cells positive for β_1- and β_2-AR protein in E11.5 and E17.5 embryonic ventricular cells. Unfixed and non-permeabilized cells were immunostained and processed for fluorescence activated cell sorting (FACS). Scatter plots gathered from the FACS analysis indicated significant number of E11.5 and E17.5 ventricular cells expressing β_1- and β_2-AR on their cell surface (Figure 3.2 A and C). Quantification of the FACS results indicated that 25.8±2.5% of E11.5 and 15.1±2.5% of E17.5 ventricular cells express β_1-AR on their cell surface, while the remaining cells are either β_1-AR negative or have very little β_1-AR on their cell surface (Figure 3.2 B). Furthermore, it was found that 10.3±1.7% of E11.5 and 9.9±0.7% of E17.5 ventricular cells express β_2-AR while the remaining cells are either β_2-AR negative or have very little β_2-AR on their cell surface (Figure 3.2 D).

To determine the distribution of CMs and nonmyocyte cells (NMC) within each sub-population of β_1-AR and β_2-AR positive and negative cells, FACS sorted cell fractions were immunolabelled with antibodies specific for sarcomeric myosin (MF20). Cells positive for MF20 were noted as CMs (MF20$^+$) and those negative for MF20

marker were noted as NMCs ($MF20^-$) (Figure 3.3). Immunolabelling of fractionated β_1-AR positive and β_1-AR negative embryonic ventricular heart cells indicated a mixed population of CMs ($MF20^+$) and NMCs ($MF20^-$) (Figure 3.3 A-F). Similarly, immunolabelling of fractionated β_2-AR positive and β_2-AR negative embryonic ventricular heart cells indicated a mixed population of CMs ($MF20^+$) and NMCs ($MF20^-$) as well (Figure 3.3 G-L). These data suggest that although β_1- and β_2-ARs are present on the cell surface of embryonic ventricular cells, neither of those markers can be used to fractionate pure populations of CMs and NMCs.

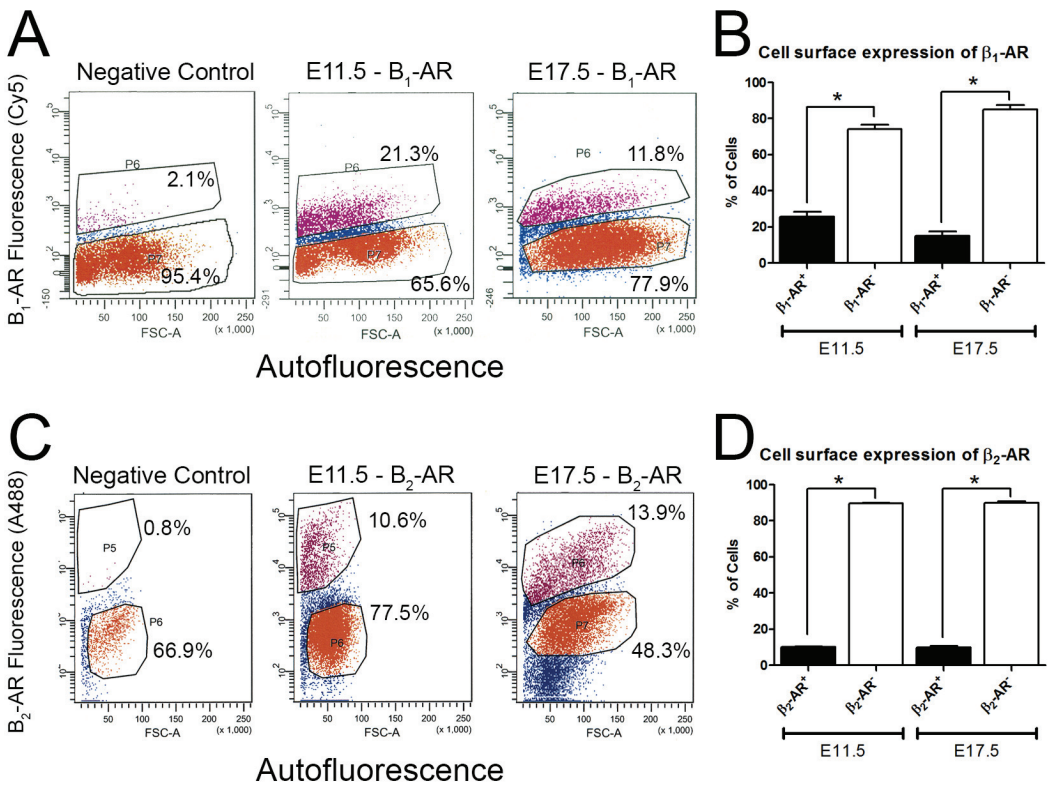

Figure 3.2 Characterization of cell surface expression of β_1- and β_2-adrenergic receptors in unfixed and non-permeabilized embryonic ventricular cells.
(A) Scatter plots of fluorescence activated cell sorted (FACS) embryonic day (E) 11.5 and E17.5 ventricular cells representing the percentage of cells expressing β_1-adrenergic receptor (AR) in E11.5 and E17.5 ventricles. In Panel A, unstained E11.5 cells lacked the conjugated β_1-AR antibody. **(B)** Graphical representation of percentage β_1-AR positive and negative cells in E11.5 and E17.5 embryonic ventricles. Unpaired student's t-test, $*p < 0.05$ β_1-AR$^+$ vs. β_1-AR$^-$. Each bar represents mean ± SEM, N=3 independent experiments. **(C)** Scatter plots of FACS sorted embryonic E11.5 and E17.5 ventricular cells representing the percentage of cells expressing β_2-AR. In Panel C, unstained E11.5 cells lacked the Alexa Fluor 488 secondary antibody. **(D)** Graphical representation of percentage β_2-AR positive and negative cells in E11.5 and E17.5 unfixed and non-permeabilized embryonic ventricular cells. Unpaired student's t-test, $*p < 0.05$ β_2-AR$^+$ vs. β_2-AR$^-$. Each bar represents mean ± SEM, N=3 independent experiments.

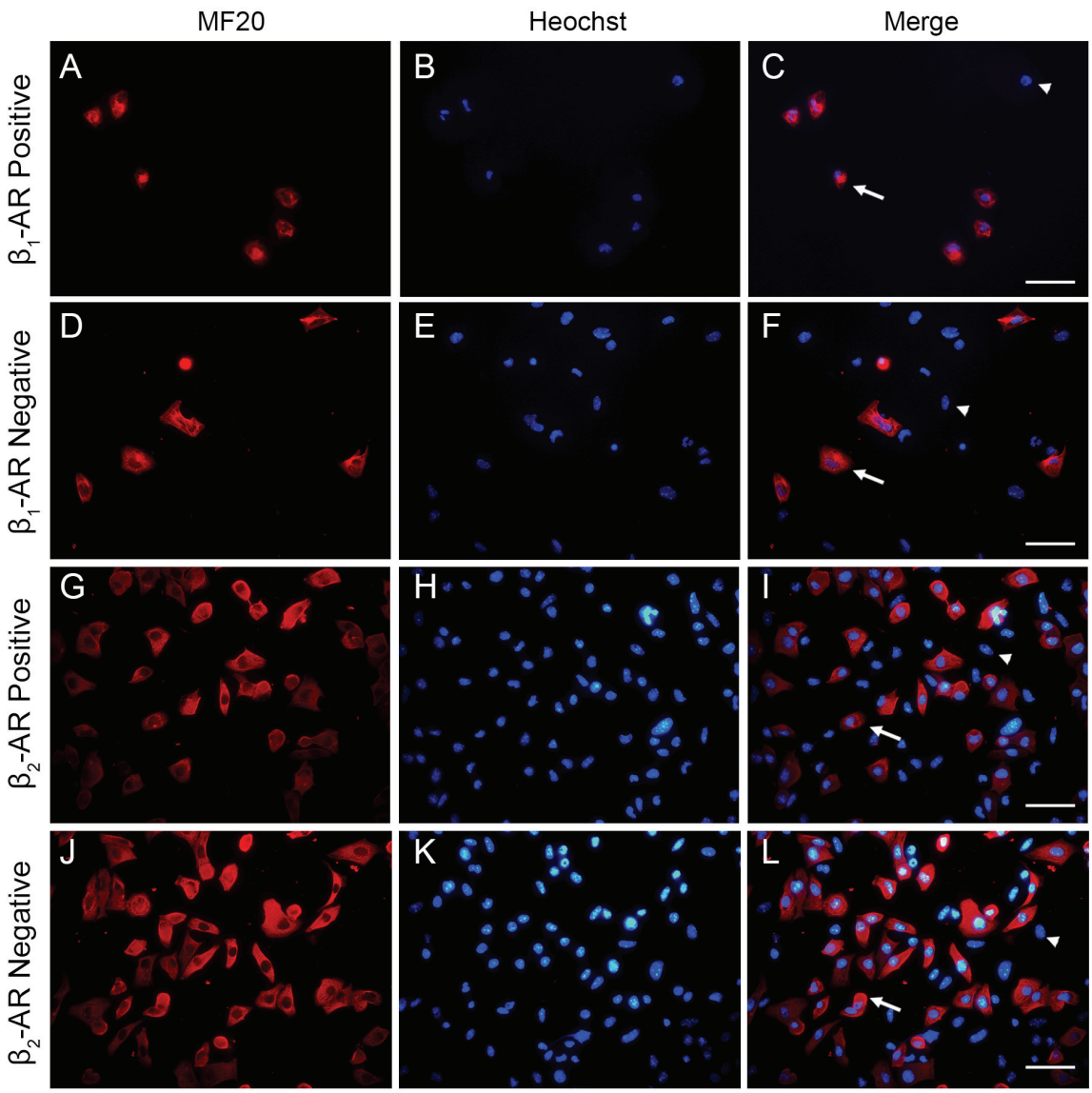

Figure 3.3 Characterization of FACS sorted embryonic ventricular cell cultures according to cell surface expression of β_1- and β_2-adrenergic.
Cultures of β_1- and β_2-adrenergic receptor (AR) fluorescence activated cell sorted (FACS) embryonic ventricular heart cells were immunolabelled to characterize the presence of cardiomyocytes (CMs; $MF20^+$) and nonmyocytes (NMCs; $MF20^-$). The first column shows representative fields of cells stained with MF20, the second column shows representative fields stained with Hoechst and the third column shows a merged image. Blocks are representative images of **(A-C)** β_1-AR^+, **(D-F)** β_1-AR^-, **(G-I)** β_2-AR^+ and **(J-L)** β_2-AR^-. In the merged image, the CMs are marked with an arrow, and the NMCs are marked with an arrowhead. Scale bar = 50μm.

3.3.3 Assessment of second messenger responses in embryonic ventricular cells after β-adrenergic receptor stimulation

Although gene expression studies established that mRNA levels of β_1- and β_2-ARs are lower in early stages of ventricular development, FACS analysis confirmed that there is no significant difference with regards to their cell surface expression between E11.5 and E17.5 stages. We next examined whether there are any differences in β-AR responses in cells isolated from different stages of developing ventricles. To do so, we used Isoproterenol (ISO), a non-selective β-AR agonist to determine the levels of cAMP produced in ventricular cells. E11.5, E14.5 and E17.5 ventricular cells were treated with different concentrations of ISO (0-100μM) and dose response curves were generated after normalizing responses to the cell number. Based on these responses, we determined the half maximal effective concentration (EC_{50}) of each developmental stage. The EC_{50} values for E11.5, E14.5 and E17.5 ISO responses were found to be 1083, 838.9, and 90.5 nM respectively (Figure 3.4 A). Furthermore, it was evident that the basal cAMP levels of E11.5 ventricular cells (0.55±0.28nM) are significantly lower compared to the E17.5 ventricular cells (2.64±0.34nM) (Figure 3.4 B). Notably, these results suggest that ISO acts more potently on E17.5 ventricular cells (~9-12 fold) compared to E11.5 or E14.5 cells.

We next determined whether the ISO responses seen in embryonic ventricular cells were due to β_1- or β_2-AR activation. For these experiments, E11.5 cells were treated with 1μM ISO (~EC_{50}) in the presence or absence of varying concentrations (0.1, 1 and 10μM) of the β_1-AR blocker Metoprolol (Meto) or the β_2-AR blocker ICI 188,551 (ICI) and the cAMP levels were measured (Figure 3.5). As expected, a significant increase in cAMP concentration was evident in cells treated with 1μM ISO (16.7±4.7 nM) compared

to the basal untreated group (4.46±0.6 nM), whereas co-treatment of cells with 1μM ISO and 1 or 10μM of the β_1-blocker Meto significantly reduced the cAMP levels back to basal levels (Figure 3.5 A). E11.5 ventricular cells co-treated with 1μM ISO and 0.1, 1 and 10μM of the β_2-blocker ICI showed significant reduction in cAMP levels compared to the ISO only group (Figure 3.5 B). Collectively, these results suggest that both β_1- and β_2-ARs are involved in ISO mediated cAMP generation in E11.5 ventricular cells.

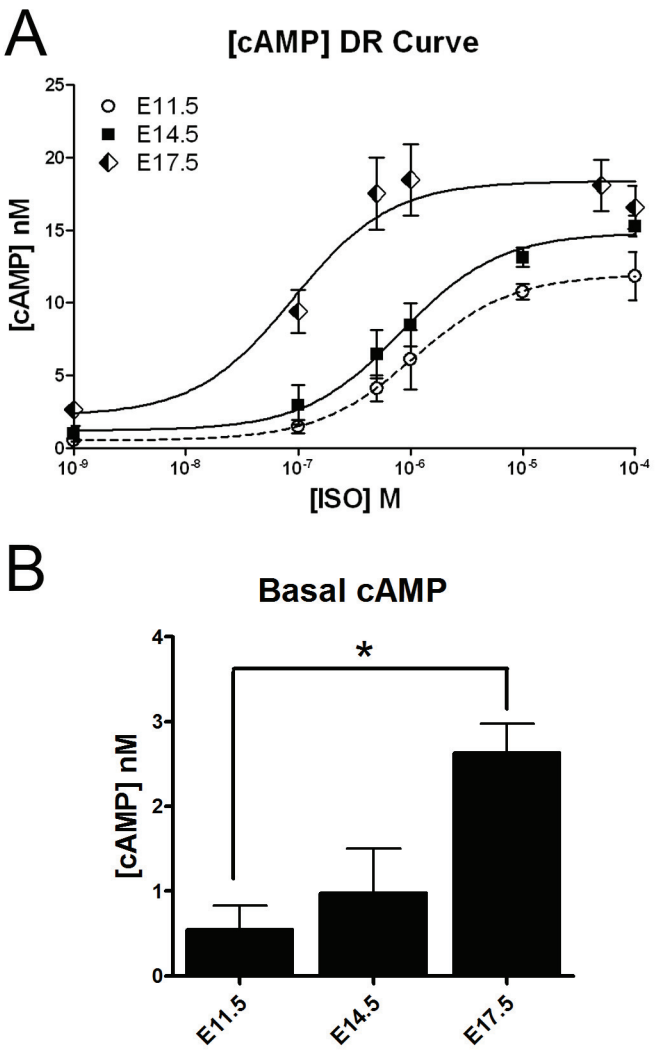

Figure 3.4 Dose-response curves for Isoproterenol (ISO) with E11.5, E14.5, and E17.5 ventricular cells using heterogeneous time resolved fluorescence based cAMP assay.

(A) It was found that the half maximal effective concentration (EC_{50}) of ISO for embryonic day (E) 11.5, E14.5, and E17.5 to be 1083, 838.9, and 90.5 nM respectively. **(B)** Basal 3'-5'-cyclic adenosine monophosphate (cAMP) levels of embryonic ventricular cells from embryonic day (E) 11.5, E14.5 and E17.5 ventricular cells. The basal cAMP levels of E17.5 ventricular cells were found to be significantly higher in comparison to the E11.5 ventricular cells. One way ANOVA, Tukey's multiple comparisons test N=3 - 5 independent experiments, each bar represents mean ± SEM, performed in duplicate wells *$p < 0.05$ vs. E11.5.

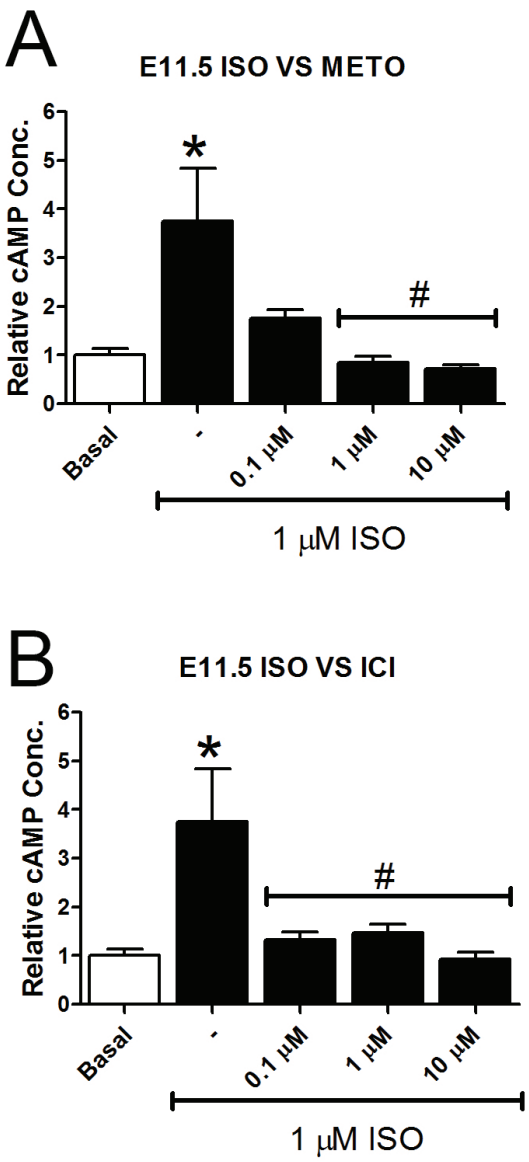

Figure 3.5 The effects of β-adrenergic receptor stimulation and inhibition on cAMP production in E11.5 ventricular cells.
Using a 3'-5'-cyclic adenosine monophosphate (cAMP) competitive immunoassay, basal cAMP levels were set to a value of 1.0 and data represent fold changes in cAMP in response to Isoproterenol (ISO) with or without β-adrenergic receptor (AR) blockers. **(A)** Stimulation with 1μM ISO was associated with ~4-fold increase in cAMP. Co-treatment of embryonic day (E) 11.5 cells with ISO and the β_1-AR selective antagonist Metoprolol (Meto) abolished the increase in cAMP production observed with ISO alone. **(B)** Co-treatment of E11.5 cells with ISO and the β_2-AR selective antagonist ICI also abolished the increase in cAMP production observed with ISO alone. One way ANOVA, Tukey's multiple comparisons test N=3 - 5 independent experiments, each bar represents mean ± SEM, performed in duplicate wells *$p < 0.05$ vs. basal, #$p < 0.05$ vs. ISO alone.

3.3.4 Lineage tracking of Nkx2.5^{+} myocardial cells in E11.5 ventricles

Since the TH homozygous knockout embryos display abnormal cardiomyocyte organization and mid-gestational embryonic lethality phenotype (between E11.5 and E15.5 stages; (Zhou et al., 1995)), we sought to examine the role of β-AR signaling in proliferation and differentiation of E11.5 ventricular cells. We have previously shown that E11.5 ventricles consist of Nkx2.5^{+} CMs and CPCs and Nkx2.5^{-} nonmyocyte population (McMullen, Zhang, Hotchkiss, et al., 2009; McMullen, Zhang & Pasumarthi, 2009). In order to distinguish Nkx2.5^{+} myocardial cells from nonmyocytes, we have used a previously published lineage tracking approach, which relied on crossing two knockin mouse strains Nkx2.5-Cre and ROSA-lac Z (Stanley et al., 2002).

The *Nkx2.5-Cre* knockin strain (designated NC) consists of an internal ribosomal entry sequence (IRES) and a Cre-recombinase coding sequence (Cre) from bacteriophage P1, inserted within the 3'-untranslated region of the *Nkx2.5* gene (Stanley et al., 2002). The expression of *Nkx2.5* gene results in expression of recombinase protein from the bacteriophage P1, Cre, which is responsible for mediating site-specific recombination between specific DNA sequences known as LoxP sites.

The ROSA-*LacZ* mouse strain (designated RL) was engineered to have a transcriptional terminator stop cassette proximal to the β-galactosidase (*LacZ*) coding sequence (Soriano, 1999). This stop cassette consists of a neomycin selection gene plus triple polyadenylation sites, and is flanked by LoxP sites. In double knockin mice, expression of *Nkx2.5* gene followed by the co-translation of Cre results in excision of the floxed stop cassette from the ROSA-*LacZ* transgene, thus resulting in the expression of *LacZ* reporter gene in all *Nkx2.5*$^{+}$ cells (Figure 3.6). Homozygous NC and RL mice were routinely crossed to obtain E11.5 embryos heterozygous for both genes (NCRL). This

allowed the detection of *Nkx2.5*$^{+}$ cells in embryonic ventricular cells by immunolabelling with β-galactosidase (β-Gal) antibodies or by incubating cells in 5-bromo-4-chloro-indolyl-β-D-galactopyranoside (X-Gal) solution which resulted in generation of visible insoluble blue product (5,5'-dibromo-4,4'-dichloro-indigo) (Figure 3.6). To further confirm the phenotype of NCRL embryonic hearts, atria were removed and incubated with X-Gal to ensure the development of blue color reaction product as described earlier (Hotchkiss et al., 2014).

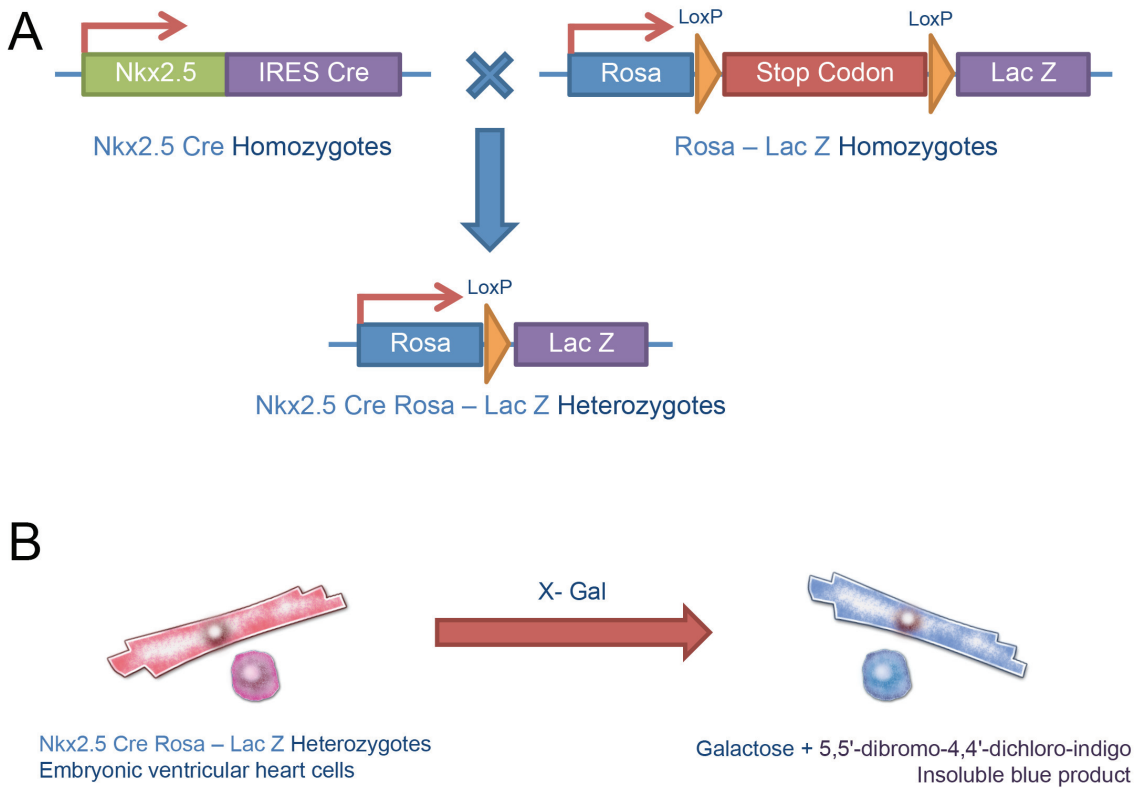

Figure 3.6 Conditional activation of the LacZ reporter gene in order to genetically label cells of Nkx2.5 cell lineage.
(A) A schematic representation of the result of genetic cross between the Nkx2.5-Cre (NC) mice with an internal ribosomal entry sequence (IRES) and Cre-recombinase (Cre) coding sequence inserted into the 3' untranslated region of the Nkx2.5 gene and the Rosa-*LacZ* (RL) mice with a transcriptional terminator stop cassette proximal to the β-galactosidase (*LacZ*) gene flanked LoxP sites. The crossing of NC and RL mice results in the generation of double transgenic NCRL embryos with an activated *LacZ* gene in cells of $Nkx2.5^{+}$ cell lineage. **(B)** Incubation of double transgenic NCRL embryonic ventricular heart cells in X-Gal solution results in hydrolysis of X-Gal by the β-galactosidase enzyme generating galactose and an insoluble blue product, detected via microscopy.

3.3.5 Stimulation of β_1- and β_2-adrenergic receptors in E11.5 ventricular cultures leads to decreased DNA synthesis in both CPCs and CM populations

To investigate the role of β_1- and β_2-ARs and their signaling cascades on cell proliferation kinetics, primary cultured E11.5 ventricular cells were treated with 1μM ISO alone or in combination with 1μM β_1-blocker Meto or 1μM β_2-blocker ICI for 24 hrs. In order to distinguish CPCs from CMs, we have used our previously published method which combines the Cre-LoxP based Nkx2.5$^+$ cell tracking and sarcomeric myosin antibody (MF20) staining (Hotchkiss et al., 2014).

Cells positive for β-Gal only were distinguished as CPCs (β-Gal$^+$/MF20$^-$) since it has been previously demonstrated that Nkx2.5$^+$/MF20$^-$ cells have the potential to differentiation into MF20$^+$ expressing cardiomyocytes in vitro (McMullen et al., 2009). Additionally, cells positive for both β-Gal and MF20 were distinguished as CMs (β-Gal$^+$/MF20$^+$) (Figure 3.7 A-B). Lastly, cells negative for both β-Gal and MF20 (β-Gal$^-$/MF20$^-$) were designated as non-cardiomyogenic cells (NMC).

Following the drug treatment and [^{3}H]-thymidine labeling period, cell cycle activity of E11.5 ventricular cells was determined using an *in situ* autoradiography method. The principle of this assay is based on the fact that cells undergoing *de novo* DNA synthesis during the S-phase of cell cycle will take up the radiolabelled thymidine analogue, [^{3}H]-thymidine. Thus, cells undergoing DNA synthesis (S-phase) can be detected due to the development of silver grains in the nucleus via autoradiography (Figure 3.7 A-B). The thymidine-labeling index (LI) is assessed as the percentage of cells positive for nuclear silver grains out of total cells counted in each experiment.

In untreated (Control) embryonic ventricular cells, the thymidine LI values were found to be 54.4 ± 1.1% for CPCs (Figure 3.7 C) and 22.4 ± 2.1% for CMs (Figure 3.7

D). These results indicate that E11.5 CPCs exhibit higher cell cycle activity compared to CMs. In response to 1μM ISO treatment, there was a significant decrease (~2.5-3 fold) in the levels of DNA synthesis in both CPCs and CM fractions. The LI for CPCs decreased to 19.7 ± 7.5% (Figure 3.7 C), while the LI for CMs decreased to 8.0 ± 2.2% (Figure 3.7 D) after ISO treatment. Co-treatment of cells with ISO in the presence of β_1-blocker Meto resulted in a significant increase in the thymidine labeling of CPCs (73.8 ± 2.2%; Figure 3.7 C) compared to that of ISO treated or untreated groups, however, a similar effect was not seen in the CM population (15.1 ± 2.0%; Figure 3.7 D). Co-treatment of cells with the β_2-blocker ICI and ISO fully rescued the inhibitory cell cycle effects mediated by ISO alone in both CPC (62.0 ± 2.0%; Figure 3.7 C) and CM (23.2 ± 1.8%; Figure 3.7 D) populations.

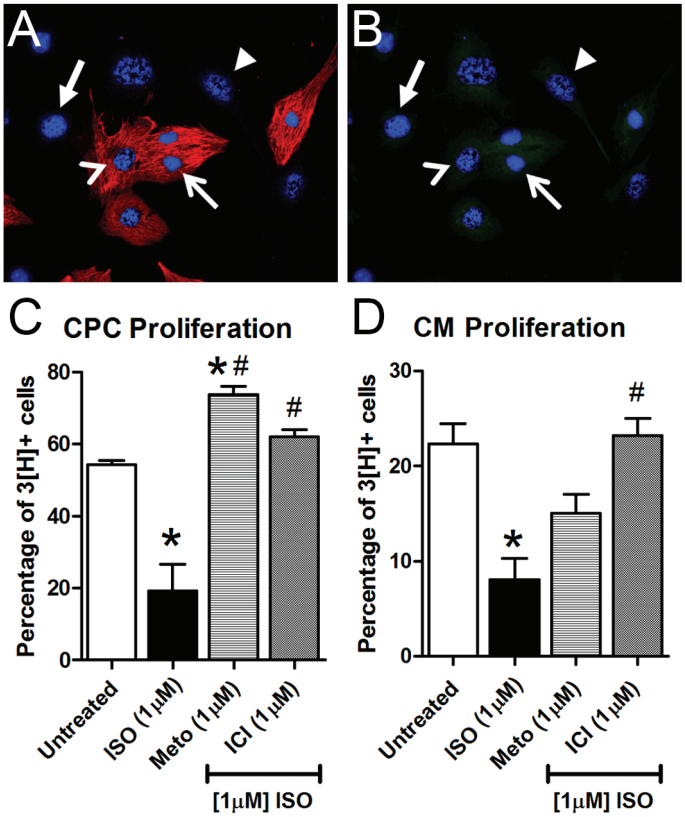

Figure 3.7 Proliferation kinetics of E11.5 cardiac progenitor cells and cardiomyocytes in response to β-adrenergic stimulation and inhibition.
(A, B) Double transgenic embryos (Nkx2.5 Cre X Rosa-lacZ) were generated in order to genetically label Nkx2.5^{+} lineage (express β-gal) in embryonic day (E) 11.5 primary ventricular cell cultures. [^{3}H]-thymidine incorporation assay enabled cells in the S-phase to be detected by the presence of silver grains in the nucleus. **(A)** Cells lablled for sarcomeric myosin (MF20; red). **(B)** The same field of cells labelled with β-galactosidase antibodies (β-Gal; green). Cells positive for MF20 and β-Gal (β-Gal^{+}/MF20^{+}) were considered to be mature cardiomyocytes (CM; open-head arrow), while cells positive for β-Gal only (β-Gal^{+}/MF20^{-}) were classified as cardiac progenitor cells (CPCs; solid arrowhead). Cells negative for both β-Gal and MF20 (β-Gal^{-}/MF20^{-}) were classified as non-cardiomyogenic cells (arrow). The CPC indicated by the solid arrowhead is also [^{3}H]$^{+}$ based on the presence of silver grains in the nucleus. **(C)** In the CPC population, a significant reduction in proliferation occurred in response to stimulation with isoproterenol (ISO). Pre-treatment with selective antagonists for either the β_1-AR (Metoprolol; Meto) or β_2-AR (ICI-118,551; ICI) abolished the anti-proliferative effect of ISO. **(D)** In the CM population, a significant reduction in proliferation occurred in response to ISO stimulation. Pre-treatment with Metoprolol or ICI partially inhibited the effects of ISO, but these results did not reach statistical significance. One way ANOVA, Tukey's multiple comparisons test N=5 independent experiments, each bar represents mean ± SEM, performed in duplicate wells *$p < 0.05$ vs. basal, #$p < 0.05$ vs. ISO alone.

3.3.6 ISO treatment decreases cell proliferation and increases the number of cells arrested in G_1/S phase in E11.5 ventricular cultures

Since stimulation of β-AR with ISO led to a significant decrease in the number of E11.5 ventricular cells undergoing DNA synthesis (Figure 3.7), we further determined if ISO treatment resulted in decreased proliferation and whether the ISO treated cells are arrested in G_1/S phase or the G_2/M phase of cell cycle. Firstly, in order to confirm the effects of ISO on cell proliferation, mid-gestation ventricle cells (E11.5) were seeded and were treated with ISO alone or in combination with either β_1-blocker Meto or β_2-blocker ICI for 18 hours. Subsequently, these cultures were subjected to a CyQUANT cell proliferation assay to assess changes in cell number. Cell numbers were determined by extrapolating fluorescence intensities using a standard curve as described in methods section. Statistical analysis indicated that compared to the control group, the number of cells in cultures treated with ISO alone was significantly lower (Control: 47708 ± 763 cells Vs. ISO: 41104 ± 1823 cells, Figure 3.8). Co-treatment of cells with the β_1-blocker Meto and ISO fully rescued the inhibitory effect on cell proliferation mediated by ISO alone, whereas, co-treatment of cells with the β_2-blocker ICI and ISO failed to rescue inhibitory effect on cell proliferation induced by ISO (ISO: 41104 ± 1823 cells Vs. ISO+Meto: 51315 ± 480 cells Vs. ISO+ICI: 42739 ± 1206 cells, Figure 3.8).

Next, cells treated with or without 1μM ISO were stained with propidium iodide (PI) and cellular DNA content frequency histograms were generated using FACS analysis. Further analysis of these histograms using a deconvolution software revealed relative cell distributions in G_1/S and G_2/M stages (Figure 3.9 A). The percentage of cells in G_1/S phase was significantly higher in ISO treated cells compared to control cultures (ISO: 79.4 ± 0.8% Vs. Control: 73.8 ± 1.8%; Figure 3.9 B). In contrast, the percentage of

cells in G_2/M phase was significantly lower in ISO treated cells compared to control cultures (ISO: 79.4 ± 0.8% Vs. Control: 73.8 ± 1.8%; Figure 3.9 C). Co-treatment of cells with the β_1-blocker Meto and ISO fully rescued the inhibitory cell cycle effects mediated by ISO alone and the percentage distribution of cells in co-treated cultures was not significantly different to that seen with control cultures (ISO+Meto: G1/S: 74.5 ± 0.2%; G2/M: 25.5 ± 0.2%; Figure 3.3.7 C, D). From these results, it is apparent that stimulation of β-AR by catecholamines can delay the progression of cell cycle in E11.5 cultures by arresting them at G_1/S phase.

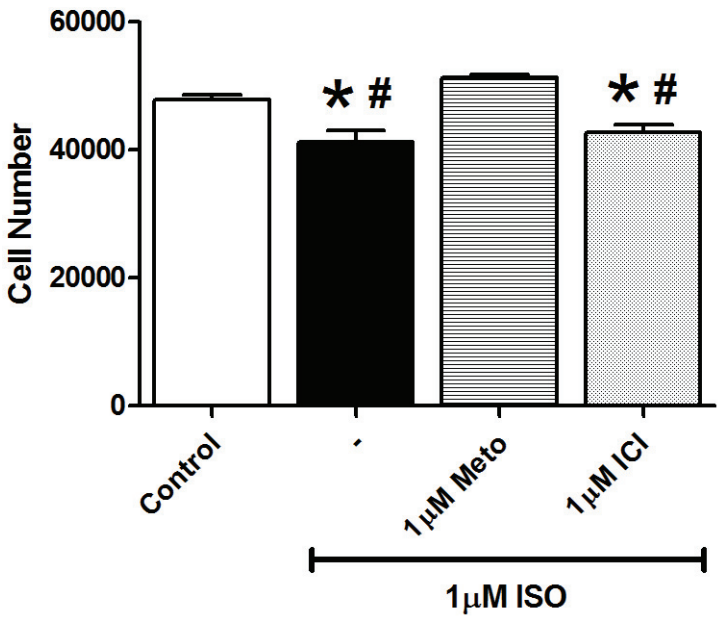

Figure 3.8 Stimulation of β_1-adrenergic receptor results in decreased proliferation of mid-gestation ventricular cells.

Mid-gestation ventricular cells (Embryonic day 11.5) were treated with 1μM of β-adrenergic receptor (AR) agonist Isoproterenol (ISO) in the presence and absence of either 1μM of β_1-antagonist Metoprolol (Meto) or β_2-antagonist ICI-118,551 (ICI) for 18 hours at which point proliferation was assessed with a CyQUANT cell proliferation assay. Continuous non-selective stimulation of β-AR via ISO decreased proliferation. While co-treatment of cells with Meto was sufficient in rescuing proliferation of cells in presence of ISO, co-treatment with ICI was not. *p <0.05 vs. Control, #p <0.05 vs. 1μM Meto, one-way ANOVA with Tukey's multiple comparison test. Results are mean ± SEM of 4 experiments/group.

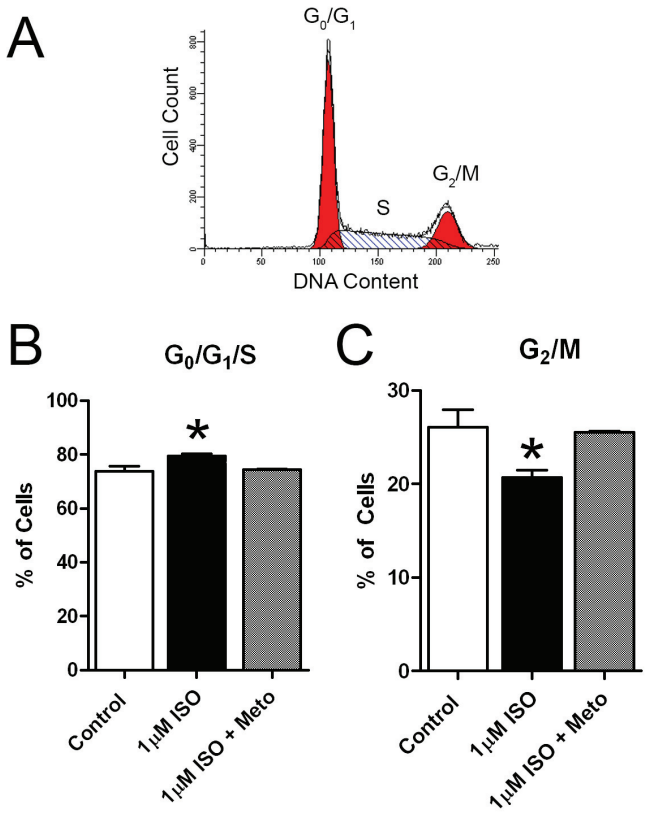

Figure 3.9 FACS analysis of proliferation kinetics of E11.5 cardiac progenitor cells and cardiomyocytes in response to β-adrenergic stimulation and inhibition.
Based on propidum iodide (PI) staining, fluorescence activated cell sort (FACS) data was used to measure the fraction of cells in different phases of cell cycle using ModFit LT software. **(A)** Representative histogram of the number of cells and their PI fluorescence intensity in E11.5 ventricular myocytes. **(B, C)** Mid-gestation ventricular cells (E11.5) were treated with 1μM Isoproterenol (ISO) in the presence or absence of 1μM Metoprolol (Meto) for 18 hours at which point proliferation was assessed using PI. **(B)** Compared to the control group, a significant increase in cells in the $G_0/G_1/S$ phase was evident in cells treated with 1μM ISO **(C)** accompanied by a significant decrease in cells in the G_2/M. **p* <0.05 vs. 1μM ISO, one-way ANOVA with Tukey's multiple comparison test. Results are mean ± SEM of 5 independent experiments/group.

3.3.7 β-Adrenergic receptor stimulation leads to decreased levels of phosphorylated-ERK and phosphorylated-AKT in E11.5 ventricular cultures

To determine the cellular mechanisms underlying cell cycle inhibition mediated by ISO, we examined if there are any changes in the levels in mitogenic proteins ERK and AKT. ERK and AKT are regulators of cell proliferation and cell survival and both are activated via phosphorylation. E11.5 ventricular cells were treated with or without 1μM ISO for various time points (10min, 30min, 1hr and 18hrs) and protein lysates were processed for western blotting with antibodies specific for total and phosphorylated forms of ERK and AKT. Densitometric analysis revealed that there was no significant difference in the expression levels of total ERK or AKT between control and ISO treated samples (data not shown). In contrast, there was a decreasing trend in the phosphorylation levels of ERK 30min post ISO treatment. Normalization of pERK levels using densitometric values for total ERK revealed a significant decrease in the pERK levels 1hr post ISO treatment (Figure 3.10 A). The pERK levels in ISO treated cells returned to the control levels 18hrs post drug treatment. Similarly, a significant decrease in pAKT levels was evident 30min post treatment with 1μM ISO (Figure 3.10 B). However, the pAKT levels returned to control levels at 1hr time point, but significantly increased compared to control levels 18hrs post treatment (Figure 3.10 B).

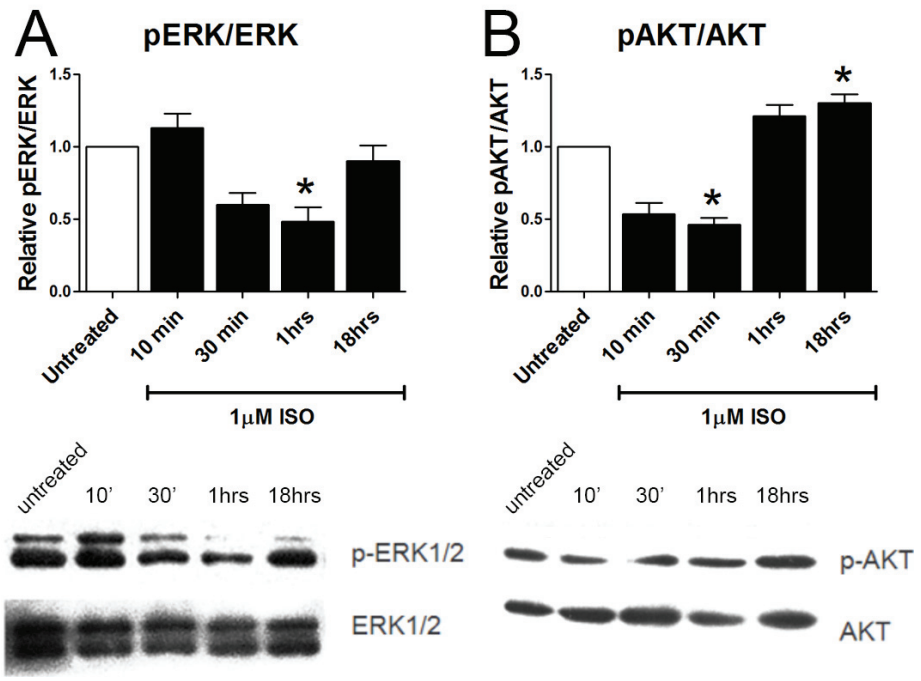

Figure 3.10 The effect of β-adrenergic stimulation on phosphorylation of pro-mitogenic proteins AKT and ERK.
Using western blot analysis, the relative levels of phosphorylated ERK and AKT were determined in cultured embryonic day (E) 11.5 ventricular cells treated with 1μM Isoproterenol (ISO) for various time periods. **(A)** The ratio of phosphorylated ERK1/2 (p-ERK) to total ERK1/2 significantly decreased within 1hr of 1μM ISO treatment compared to the untreated cultured E11.5 ventricular cells. **(B)** The ratio of phosphorylated AKT (pAKT) to total AKT significantly decreased within 30min of 1μM ISO treatment of cultured E11.5 ventricular cells and showed significant increase after 18hrs of continuous treatment compared to the untreated E11.5 ventricular cells. One-way ANOVA with Tukey's multiple comparison test, results are mean ± SEM of 3 independent experiments/group, analyzed in duplicate for each experiment, *$p < 0.05$ vs. untreated.

3.3.8 ISO treatment of E11.5 ventricular cultures decreases the expression of G_1/S cell cycle regulatory genes but not that of cardiomyogenic genes

Since pERK and pAKT play important roles in the regulation of gene expression, we next sought to characterize the effects of β-AR stimulation on the expression of several cell cycle regulatory genes and cardiomyogenic genes in E11.5 ventricular cultures treated with or without ISO for 18hrs. In addition, ISO effects on feedback regulation of β_1- and β_2-AR expression were also examined. QPCR analysis was used to determine changes in mRNA expression and the data was normalized using the expression levels of housekeeping gene, glyceraldehyde 3-phosphate dehydrogenase (GAPDH) as described earlier. Significant decreases in the mRNA levels of Cyclin D1 (Control: 1.108 ± 0.11% Vs. ISO: 0.6968 ± 0.07%) and CDK4 (Control: 1.094 ± 0.14% Vs. ISO: 0.6809 ± 0.10%) were noted in cultures treated with ISO compared to controls (Figure 3.11 A). No significant changes were evident in the mRNA levels of p27 and Cyclin B1 (QPCR results are summarized in Figure 3.11 B). It also became evident that ISO treatment led to a significant decrease in the expression of β_1-AR while the expression of β_2-ARwas unchanged (Figure 3.11 A). Notably, we did not find any significant changes in the mRNA levels of MEF2C, GATA4, TBX5, and HAND2 in ISO-treated cultures compared to the untreated cells (Results are summarized in Figure 3.11 B). Collectively, our results suggest that activation of β-ARs can decrease cell cycle activity of in mid-gestation ventricular cells via down regulation of cell cycle genes involved in G_1/S checkpoint regulation.

A

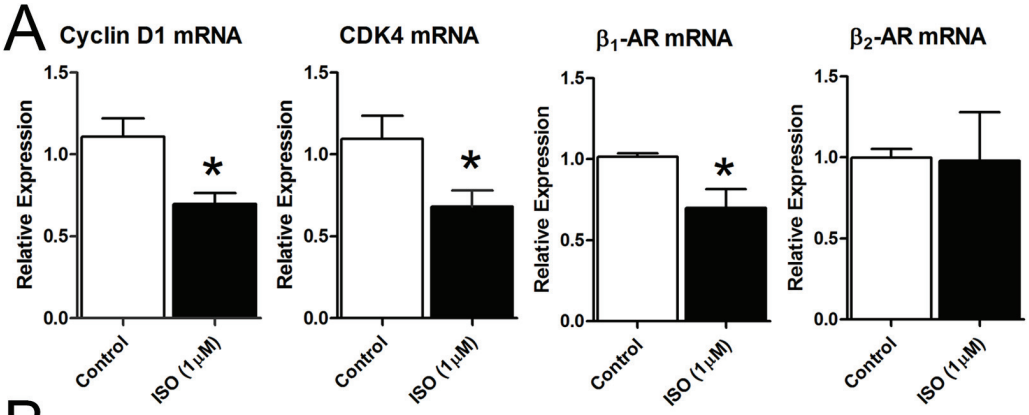

B

Gene	Control	ISO (1 μM)	Significance
MEF2c	1.15 ± 0.16	1.14 ± 0.40	NS
GATA4	1.00 ± 0.10	1.08 ± 0.01	NS
TBX5	1.05 ± 0.05	0.93 ± 0.02	NS
HAND2	1.07 ± 0.09	1.20 ± 0.11	NS
Cyclin D1	1.11 ± 0.11	0.70 ± 0.07	*S*, P<0.05
CDK4	1.10 ± 0.14	0.68 ± 0.10	*S*, P<0.05
p27	1.17 ± 0.19	1.23 ± 0.32	NS
Cyclin B1	1.23 ± 0.24	0.83 ± 0.22	NS

Figure 3.11 The effects of Isoproterenol on expression of cell cycle regulating genes and cardiogenic transcription factors.
Quantitative polymerase chain reaction (qPCR) method was used to determine gene expression levels of cell cycle regulating genes and cardiogenic transcription factors. Expression was normalized to GAPDH. **(A)** Compared to vehicle treated control cultures, treatment of embryonic day (E) 11.5 ventricular cell cultures with 1μM Isoproterenol (ISO) was associated with significant reductions in expression of the positive cell cycle regulators Cyclin D1 and Cyclin-dependent kinase 4 (CDK4) and a significant down regulation of β_1-AR mRNA. (**B)** Summary of the effects of ISO on expression of a panel of cardiogenic transcription factors and cell cycle regulating genes. Unpaired student's t-test, N=3 independent experiments/treatment group, analyzed in duplicate for each experiment, *$p < 0.05$ vs. Control. NS: not significant; S: significant.

3.3.9 Effect of Isoproterenol treatment on cellular differentiation in E11.5 ventricular cultures

Since we established that stimulation of β-AR with ISO led to a significant decrease in proliferation of mid-gestation ventricular cells, we next sought to determine whether any differences exist in cell differentiation between untreated and ISO-treated cultures. Given the heterogeneous nature of mid-gestation ventricular cells, cell differentiation status in E11.5 cell cultures was assessed by immunofluorescence using various cell lineage specific antibodies. Our results indicated that both control and ISO treated cultures were negative for the endothelial cells marker vWF (Figure 3.12 and 3.13 A-C) and less then 1% of the cells were positive for CD31 in both cultures (Figure 3.12 and 3.13 D-F). Immunolabelling of cultures with the fibroblast marker DDR2 indicated that both cultures consisted of approximately 50% DDR2 positive cells (Figure 3.12 and 3.13 G-I). Additionally, the majority of cells (>95%) were positive for the mesenchymal cell marker Vimentin (Figure 3.12 and 3.13 J-L).

Immunolabelling of cultures with cardiac progenitor and early cardiomyocyte marker Nkx2.5 indicated that approximately ~50% of the cells in both cultures were positive for Nkx2.5 (Figure 3.14 and 3.15 A-C). Furthermore, Both cultures were positive for the cardiac conduction cell marker HCN4 (Figure 3.14 and 3.15 G). Additionally, immunolabelling with the CM marker MF20 indicated that although both cultures possessed $MF20^{+}$ cells, compared to the untreated cultures, cultures treated with ISO seemed to have a higher number of $MF20^{+}$ cells (Figure 3.14 and 3.15 D-F). Quantification of CPCs and CMs in untreated and ISO-treated ventricular cultures indicated that compared to the untreated cell cultures, a significant reduction in the number of CPCs and a significant increase in the number of CMs were apparent in ISO-

treated cultures (Figure 3.16). Quantification of CPCs and CMs in untreated and ISO-treated ventricular cultures indicated that compared to the untreated cell cultures, a significant reduction in number of CPCs (Figure 3.16 A) and a significant increase in the number of CMs in ISO-treated cultures (Figure 3.16 B). Collectively, these findings suggest that β-AR stimulation with ISO may perhaps play a role in inducing differentiation of CPCs into conduction system CMs.

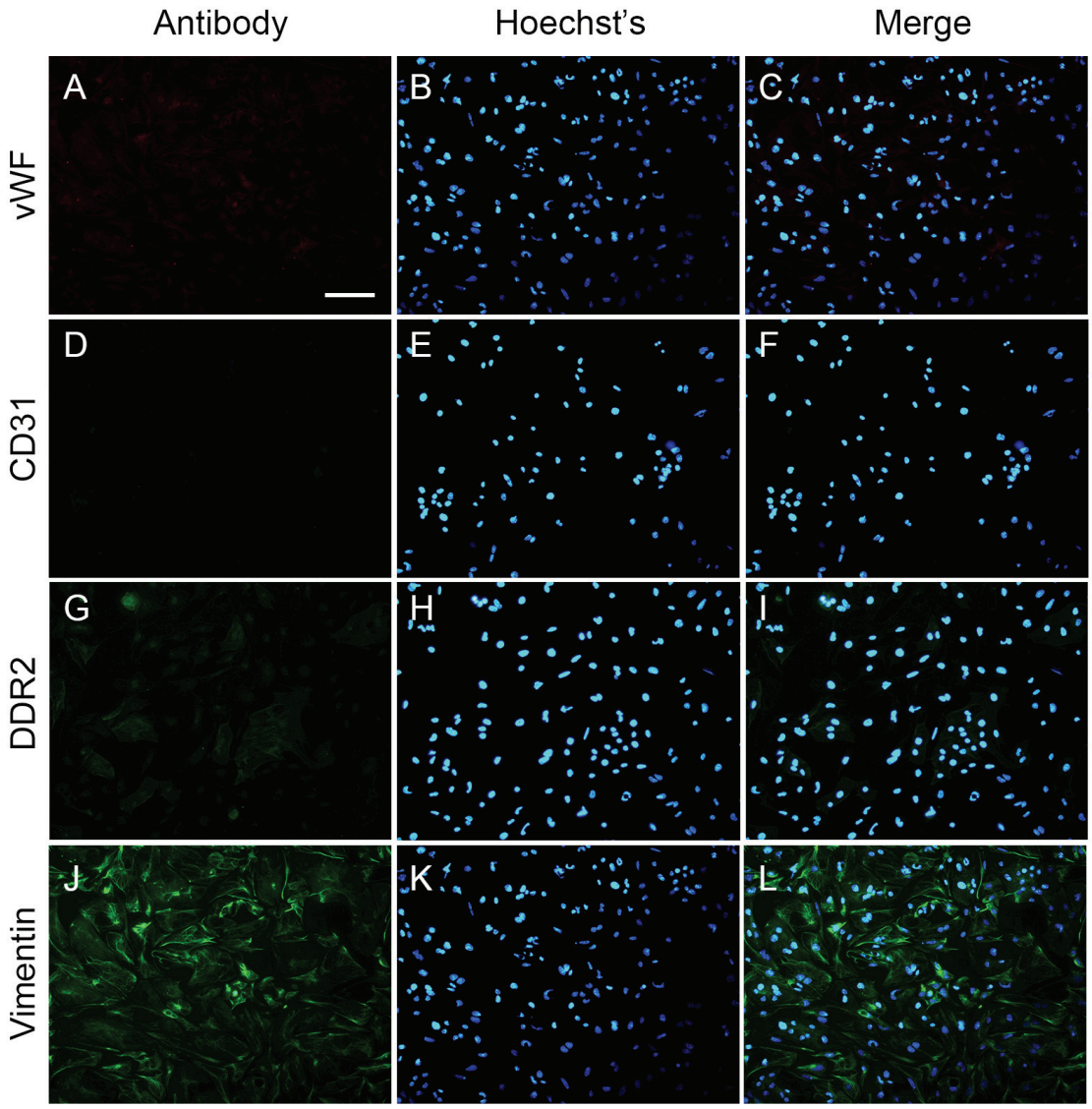

Figure 3.12 Characterization of untreated heterogeneous mid-gestation E11.5 myocytes cultures using endothelial, fibroblast and mesenchymal markers.
Embryonic day (E) 11.5 ventricular myocytes were cultured and then immunolabelled in order to characterize cell types present. The first column shows representative images of antibody of interest, second column shows the same field stained with Hoechst's nuclear stain, and the third column shows a merged image. Cells were labeled with **(A-C)** von Willebrand factor (vWF), **(D-F)** cluster of differentiation 31 (CD31), **(G-I)** Discoidin domain receptor 2 (DDR2), and **(J-L)** Vimentin to distinguish the phenotype of the nonmyocytes seen in cultures. CD31 and vWF were used to identify endothelial cells, and Vimentin was used to distinguish cells of mesenchymal origin. DDR2 immunolabelling indicated fibroblast cells. Scale bars = 100μm for A-L.

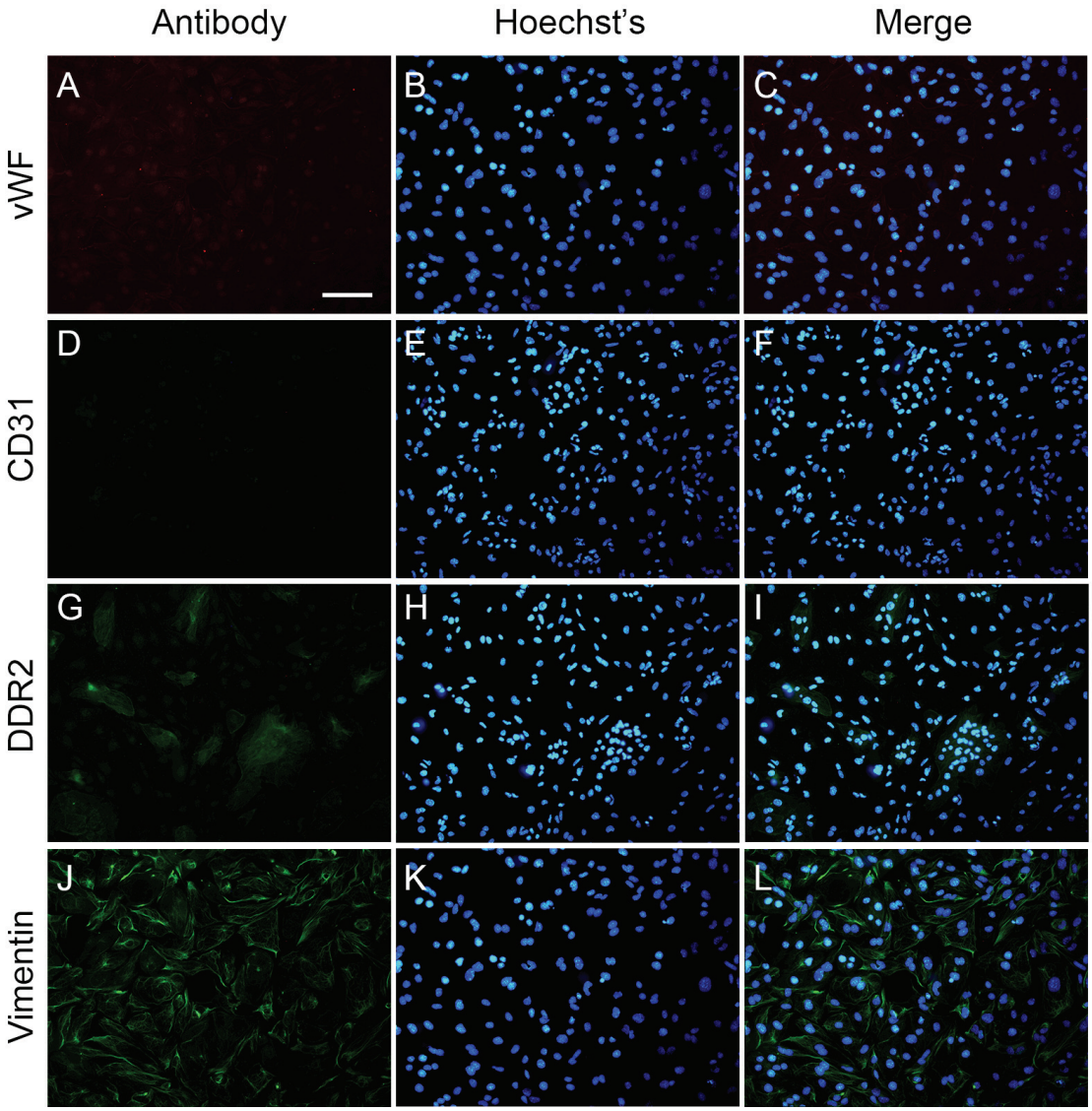

Figure 3.13 Characterization of Isoproterenol-treated heterogeneous mid-gestation E11.5 myocytes cultures using endothelial, fibroblast and mesenchymal markers. Embryonic day (E) 11.5 ventricular myocytes were cultured, treated with 1µM isoproterenol (ISO) and then immunolabelled in order to characterize cell types present. The first column shows representative images of antibody of interest, second column shows the same field stained with Hoechst's nuclear stain, and the third column shows a merged image. Cells were labeled with **(A-C)** von Willebrand factor (vWF), **(D-F)** cluster of differentiation 31 (CD31), **(G-I)** Discoidin domain receptor 2 (DDR2), and **(J-L)** Vimentin to distinguish the phenotype of the nonmyocytes seen in cultures. CD31 and vWF were used to identify endothelial cells, and Vimentin was used to distinguish cells of mesenchymal origin. DDR2 immunolabelling indicated fibroblast cells. Scale bars = 100µm A-L.

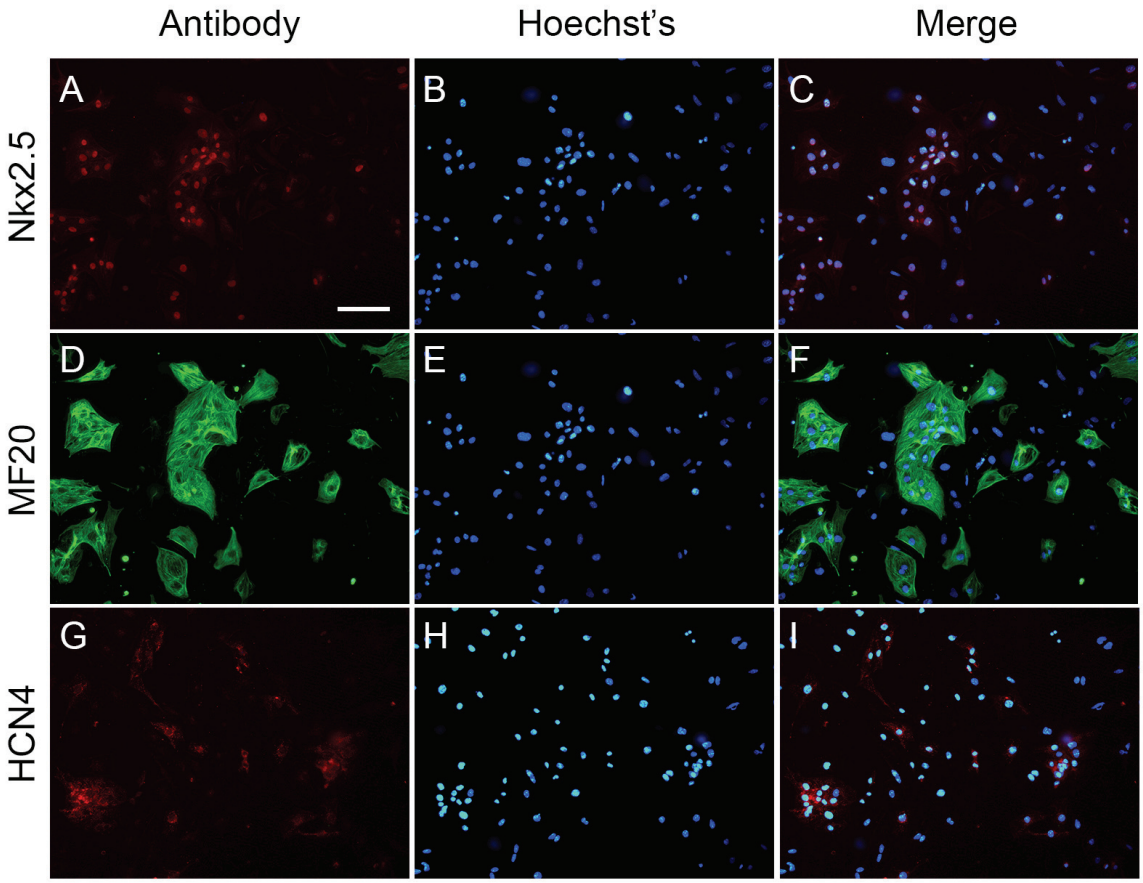

Figure 3.14 Characterization of untreated heterogeneous mid-gestation E11.5 myocytes cultures using cardiomyocyte specific markers.
Embryonic day (E) 11.5 ventricular myocytes were cultured and then immunolabelled in order to characterize cell types present. The first column show representative images of antibody of interest, second column shows the same field stained with Hoechst's nuclear stain, and the third column shows a merged image. Cells were labeled with **(A-C)** Nkx2.5, **(D-F)** sarcomeric myosin (MF20) and **(G-I)** Potassium/sodium Hyperpolarization-activated cyclic nucleotide-gated channel (HCN4) to distinguish the phenotype of the cells seen in cultures. Nkx2.5 was used to identify cells expressing a homeobox transcription factor, and MF20 was used to identify CMs. HCN4 was used to indicate first heart field and conduction system cells. Scale bars = 100μm A-I.

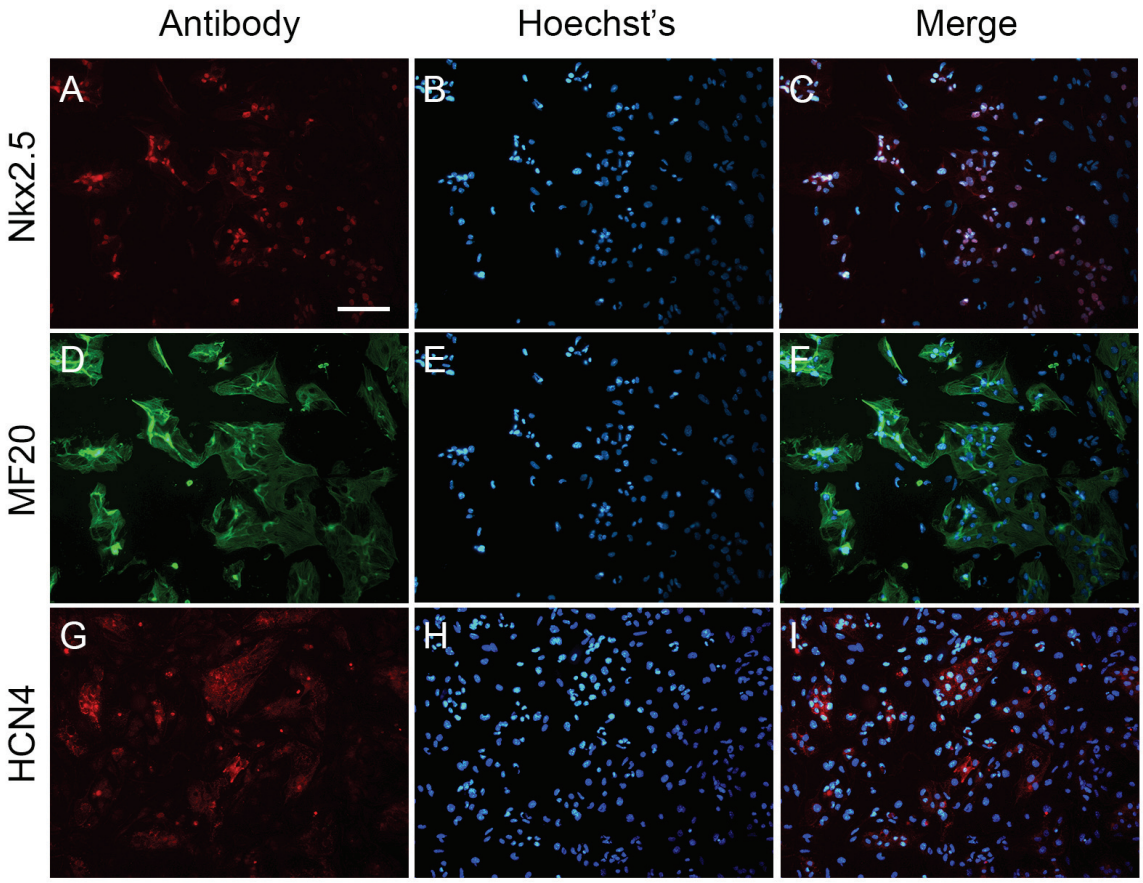

Figure 3.15 Characterization of Isoproterenol-treated heterogeneous mid-gestation E11.5 myocytes cultures using cardiomyocyte specific markers.
Embryonic day (E) 11.5 ventricular myocytes were cultured, treated with 1μM Isoproterenol and then immunolabelled in order to characterize cell types present. The first column show representative images of antibody of interest, second column shows the same field stained with Hoechst's nuclear stain, and the third column shows a merged image. Cells were labeled with **(A-C)** Nkx2.5, **(D-F)** sarcomeric myosin (MF20) and **(G-I)** Potassium/sodium Hyperpolarization-activated cyclic nucleotide-gated channel (HCN4) to distinguish the phenotype of the cells seen in cultures. Nkx2.5 was used to identify cells expressing a homeobox transcription factor, and MF20 was used to identify CMs. HCN4 was used to indicate first heart field and conduction system cells. Scale bars = 100μm A-I.

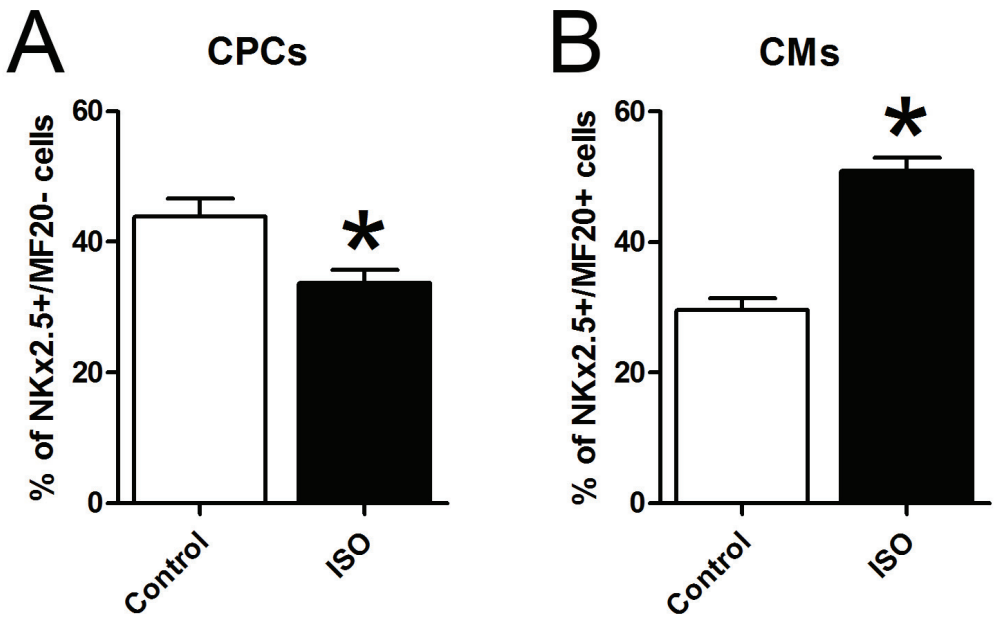

Figure 3.16 Quantification of Isoproterenol-treated heterogeneous mid-gestation E11.5 myocytes cultures using cardiomyocyte specific markers.
Double transgenic embryos (Nkx2.5 Cre X Rosa-lacZ) were generated in order to genetically label Nkx2.5^{+} lineage (expressing β-galactosidase; β-gal) in embryonic day (E) 11.5 primary ventricular cell cultures. Using cardio-specific markers, β-gal and sarcomeric myosin (MF20), **(A)** cardiac progenitor cells (CPCs) (β-gal^{+}/MF20^{-}) and **(B)** cardiomyocytes (CMs) (β-gal^{+}/MF20^{+}) were quantified in untreated and treated with 1μM Isoproterenol (ISO)-treated mid-gestation ventricular cell cultures. Unpaired t-test, N=5 independent experiments/treatment group, *$p < 0.05$ vs. Control.

CHAPTER 4 COMPARSION OF GRAFTING EFFICIENCIES OF MID- AND LATE-GESTATION VENTRICULAR CELLS AND THE EFFECTS OF ADRENERGIC DRUGS ON CELL TRANSPLANTATION

4.1 Background and Hypothesis

Cardiovascular disease remains a leading cause of death among both men and women worldwide (Zhang & Pasumarthi, 2008). Despite advances in pharmacological and surgical therapies, the prognosis for patients with end-stage heart failure remains grim, thus, there is a definite need for new therapies for various cardiovascular disorders. Cell transplantation therapy is emerging as a method for regeneration of myocardium lost to cardiovascular (CV) disease (Doss et al., 2008). Transplantation of fetal or embryonic stem cell (ES)-derived cardiomyocytes (CMs) was shown to confer protection against the induction of ventricular tachycardia in small animal myocardial injury models (Shiba et al., 2012; Roell et al., 2007). In contrast to small animal studies, transplantation of human ES derived CMs into infarcted primate hearts led to incomplete graft maturation and non-fatal arrhythmias (Chong et al., 2014). Moreover, limited survival of transplanted cells in the myocardium has been identified as a major challenge for cell based therapies (Reinecke & Murry, 2002). Since there are several unresolved issues, additional studies are warranted to increase the efficacy and safety parameters for intra-cardiac cell transplantation.

It has been shown that mid-gestational ventricles (E11.5 stage) contain both CPCs and CMs (McMullen, Zhang, Hotchkiss, et al., 2009; Zhang & Pasumarthi, 2007). Moreover, E11.5 CPCs were shown to differentiate into functional CMs but not other cell lineages using real-time imaging techniques (McMullen, Zhang, Hotchkiss, et al., 2009). Studies from the previous chapter suggest that E11.5 ventricular cells are less responsive

to β-AR stimulation compared to ventricular cells from later stages of development. Furthermore, E11.5 ventricular cells (both CPC and CM) exhibit higher proliferation rates compared to cardiomyocytes derived from later stages of development (data not shown). Notably E11.5 CPCs exhibit higher cell cycle activity compared to E11.5 CMs (~2.5 fold; see section 3.3.5, chapter 3). Based on these unique attributes, E11.5 ventricular cells may form larger myocyte grafts compared to donor cells derived from later stages of development.

Cardiac output is generally decreased in severe forms of heart disease, which results in increased sympathetic nervous system activity leading to increased levels of local and systemic catecholamines and subsequently increased myocyte death (Schlaich et al., 2003). It is possible that the low β-AR expression of E11.5 ventricular cells could protect these cells after intracardiac transplantation from the detrimental effects of catecholamines, thus facilitating larger graft formation. Results from the previous chapter also suggest that β-AR blockers can abrogate the detrimental effects of isoproterenol (ISO), a non-selective β-AR agonist, on ventricular cell cycle *in vitro*. To date, there is no information regarding the protective or detrimental effects of β-AR agonists or blockers on donor cell transplantation.

For studies described in this chapter**, we hypothesized that (i) E11.5 ventricular cells can form larger grafts compared to cells derived from later stages of ventricular development, (ii) chronic stimulation of recipients with β-AR agonist, ISO, after cell transplantation can decrease the graft size and (iii) β-AR blockers can protect E11.5 cell grafts from the effects of systemic catecholamines**.

4.2 Specific Aims

1. Examine the grafting efficiencies of mid- and late-gestation ventricular cells in intramuscular and intracardiac transplantation models.

2. Determine the effect of non-selective β-adrenergic agonist Isoproterenol and β_1-adrenergic antagonist Metoprolol on the graft size and differentiation of mid-gestation ventricular myocytes post-intracardiac transplantation.

3. Examine the potential of tail vein infusion of mid- and late-gestation ventricular cells in angiogenesis and improvement of cardiac function in doxorubicin-induced heart failure mouse model.

4.3 Results

4.3.1 Intramuscular transplantation of mid-gestation ventricular cells results in a larger graft formation compared to late-gestation ventricular cells

We have previously shown that the numbers of ventricular cardiac progenitor cells ($Nkx2.5^+/MF20^-$) significantly decrease from the mid-gestation (E11.5) to late-gestation (E14.5 and E17.5) and there is a significant increase in the population of mature cardiomyocytes ($MF20^+/Nkx2.5^+$) (McMullen, Zhang, Hotchkiss, et al., 2009). Furthermore, *in vitro* data in Chapter 3 indicates that compared to mature CMs, CPCs possess a higher rate of proliferation. Based on this knowledge, we hypothesized that intramuscular transplantation of E11.5 ventricular cells would result in a larger graft formation compared to intramuscular transplantation of E14.5 ventricular cells. To test this hypothesis, ventricular cells were isolated from E11.5 and E14.5 NCRL embryos and approximately $8x10^5$ ventricular cells were injected in the hind limb of healthy C57Bl/6 mice (Figure 4.1 A). Recipient mice were then sacrificed 3 or 7 days post-surgery and the hind-limbs were processed for fixation and placed in X-Gal overnight to visualize the intramuscular transplanted ventricular cells indicated by a blue reaction product (Figure

4.1 B). Cryosections (10μm) obtained from engrafted areas revealed X-Gal positive cells within the skeletal fibers of recipient limbs (Figure 4.1 C). Furthermore, 3 and 7 days post-surgery, the intramuscular transplanted cells expressed cardiac myocyte specific marker α-cardiac sarcomeric actinin (α-CSA) (Figure 4.2 A-B) and the gap junction protein connexin 43 (Figure 4.2 C-D). Further examination of the grafts via H&E staining revealed that the intramuscular transplanted ventricular cells did not fuse with the skeletal myocytes (Figure 4.3 A-B).

Areas occupied by the blue X-Gal staining in cryosections were quantified to determine the total graft areas using the Colour-Subtractive Computer Assisted Image Analysis software (Gaspard & Pasumarthi, 2008). Intramuscular transplantation of E11.5 ventricular cells after 3 day and 7 day time points resulted in significantly larger graft volumes in comparison to the E14.5 ventricular cells of 7 day (~3 fold), but not compared to the 3 day time point (Figure 4.4). Interestingly, no significant difference was noted between the E11.5 graft areas at 3 and 7 day times points, however, the graft areas of E14.5 at 3 day time point was significantly larger compared to the 7 day time point (Figure 4.4).

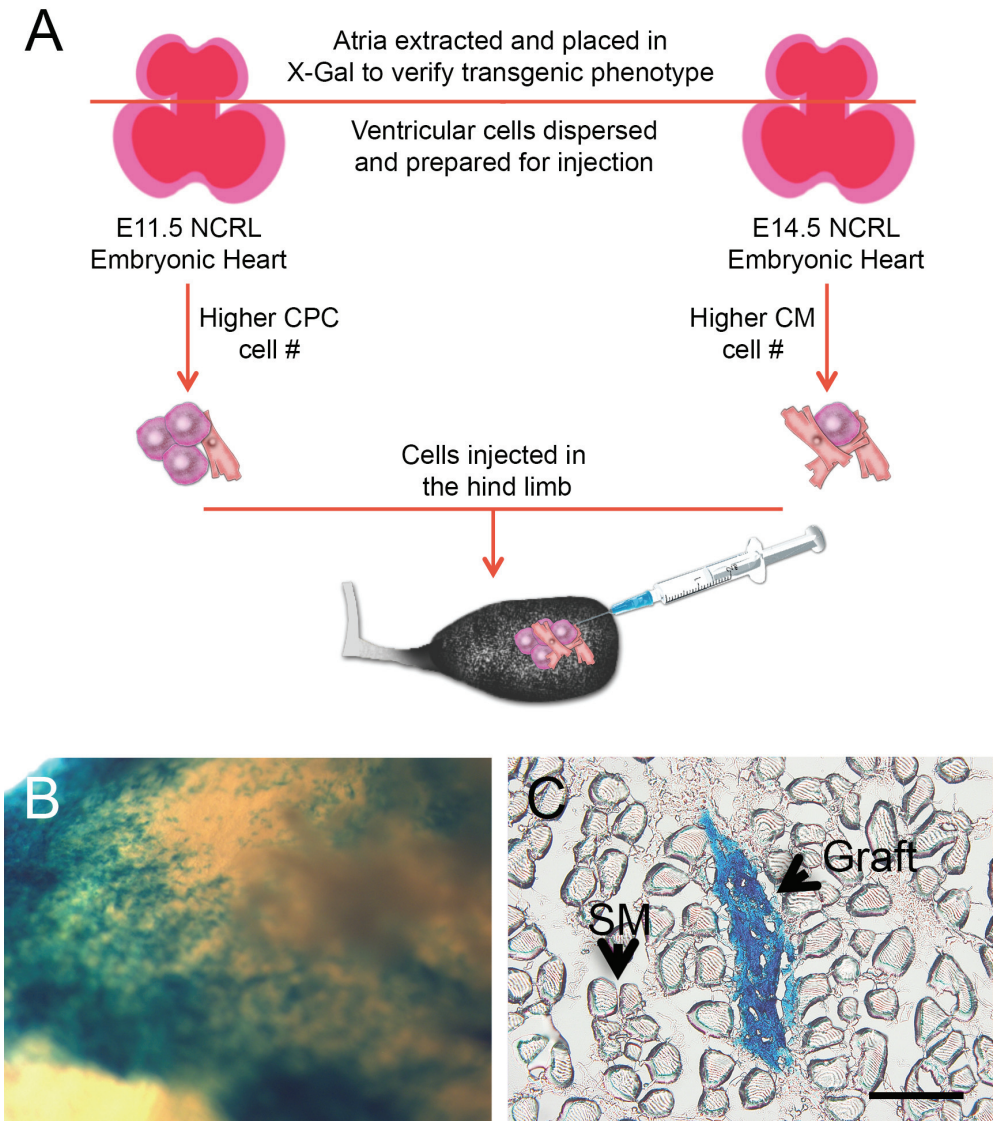

Figure 4.1 Hind limb mouse model used for intramuscular engraftment of E11.5 and E14.5 ventricular myocytes.

The double knockin embryos of (NCRL) mice were generated in order to genetically label and track intramuscular transplanted cells of Nkx2.5^{+} lineage. **(A)** Embryonic hearts of embryonic day (E) 11.5 and/or E14.5 mice were extracted, the atria was placed in X-Gal to verify the phenotype, while the cells of the ventricule were dispersed. Approximately 8x10^{5} cells were transplanted via direct intramuscular transplantation into the hind limb of healthy recepient C57BL/6 mice. **(B)** Recipient mice were sacrificed 3 or 7 days post transplantation and the recipient limbs were excised, minced and placed in X-Gal solution in order to visualize the transplanted NCRL cells within the recipient animal's hind limb. **(C)** Next, the muscle tissue containing the X-Gal^{+} cells were cryoprotected in 30% sucrose tissue over night, and cryosectioned into 10µm thin slices for quantification of graft volume. SM= Skeletal muscle. Bar = 50µm.

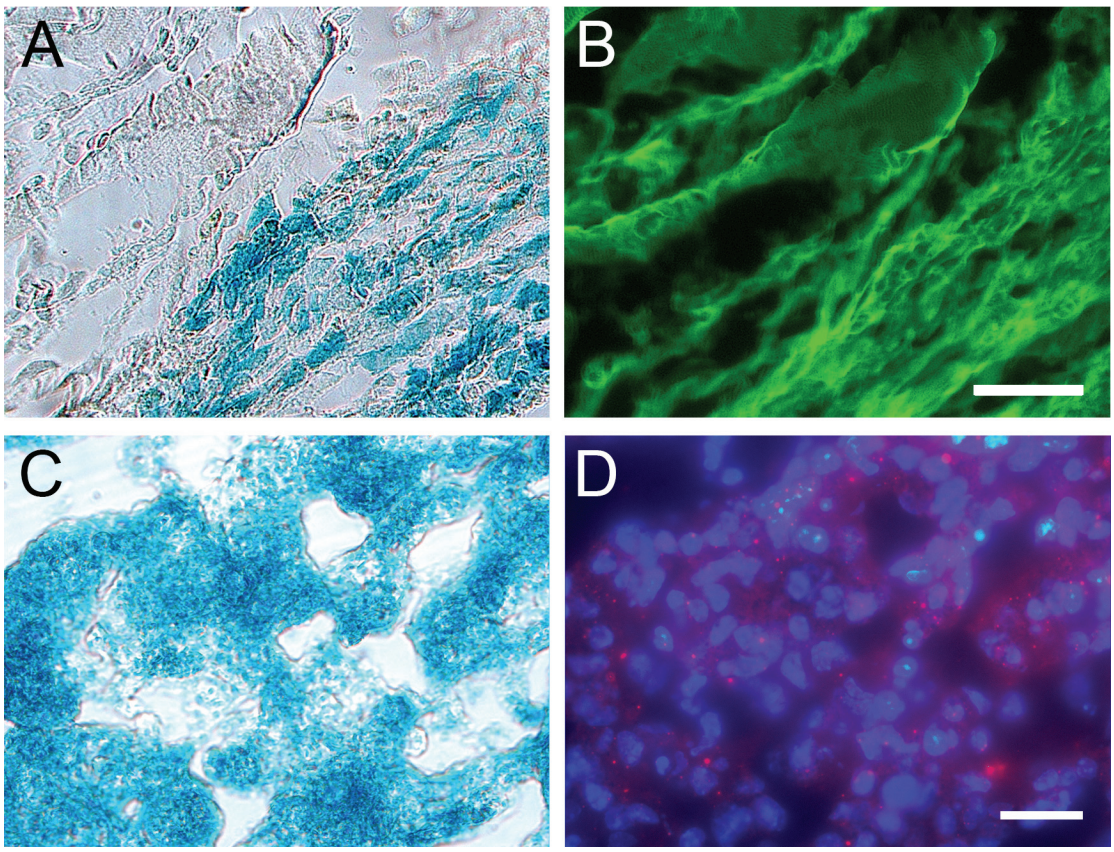

Figure 4.2 Intramuscular transplanted ventricular myocytes are capable of expressing α-CSA and Cx43.
The cryosections obtained from recipient mice with intramuscular transplanted NCRL embryonic ventricular myocytes were immunolabelled for gap junction protein connexin 43 (Cx43) and the cardiac differentiation marker, α-cardiac sarcomeric actinin (α-CSA). **(A, C)** Engrafted NCRL ventricular myocytes positive for X-Gal staining (Brightfield) expressed **(B)** α-CSA (green; bar = 50μm) and **(D)** Cx43 (red; bar = 20μm).

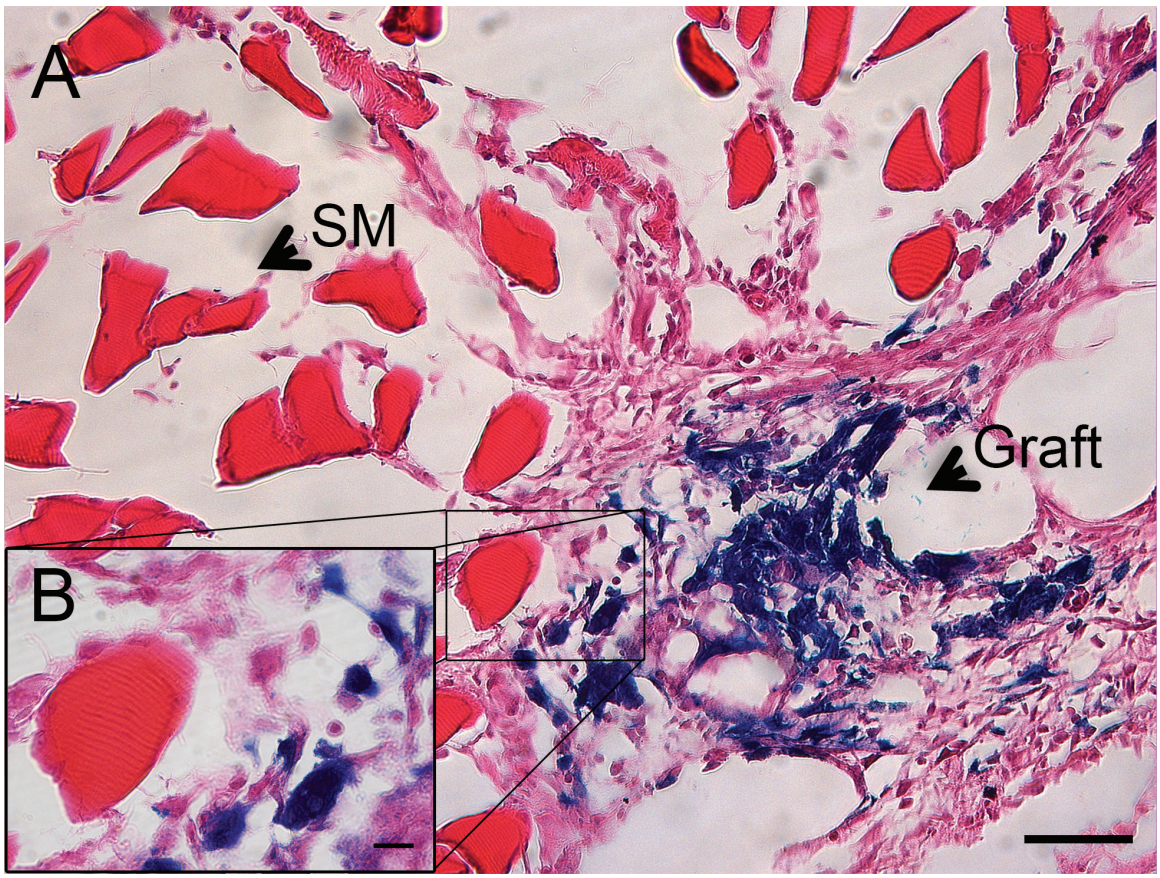

Figure 4.3 Intramuscular transplanted embryonic ventricular myocytes do not fuse with host muscular tissue.
(A) Hematoxylin and eosin (H&E) staining of cryosections obtained from recipient mice with intramuscular NCRL cell transplants indicated that the transplanted ventricular cells do not fuse with the host skeletal myocytes (SM). **(B)** Larger magnification of the area indicated by the square. Bar = 50μm.

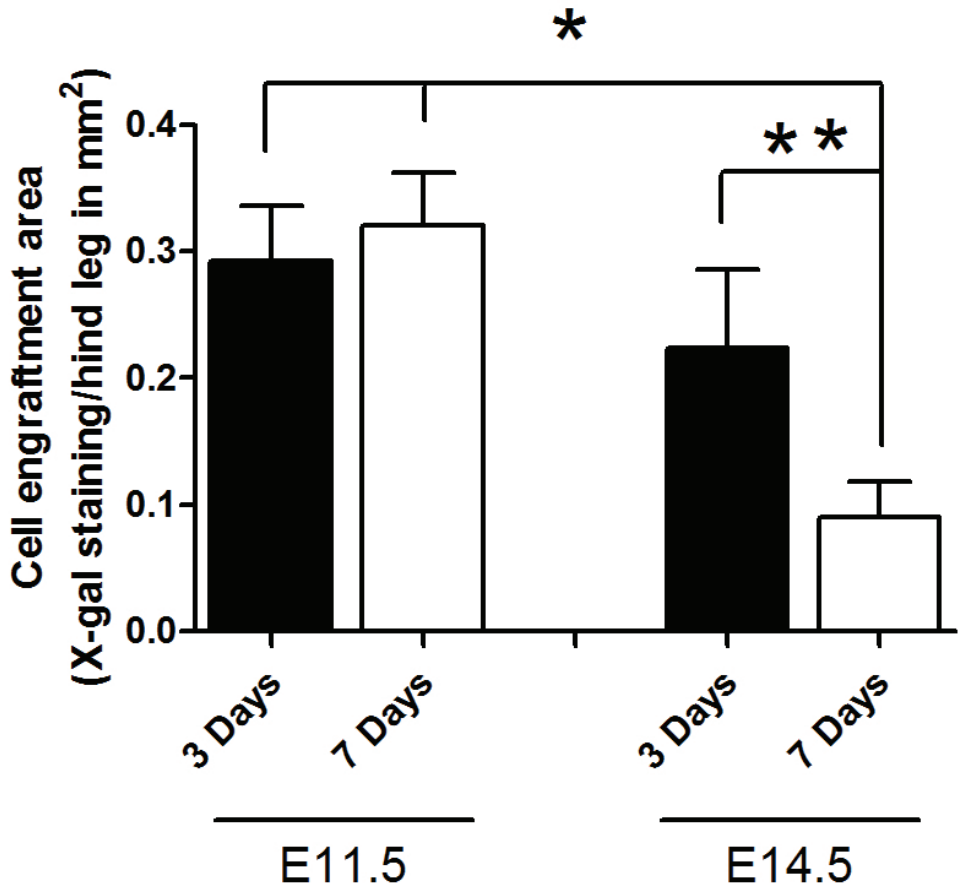

Figure 4.4 Quantification of intramuscular transplanted E11.5 and E14.5 ventricular cells 3 and 7 days post cell injections.
Quantification of graft area indicated that the graft area of embryonic day (E) 11.5 day ventricular cells (3 and 7 days) was significantly higher compared to the graft area of E14.5 day ventricular cells 7 days post transplantation. Further, the graft area of 3 days E14.5 ventricular cells was significantly larger compared to 7 days. *p <0.05 and **p <0.005 vs. E14.5 3 days, one-way ANOVA with Tukey's multiple comparison test. Results are mean ± SEM of 3 experiments/group.

4.3.2 Intracardiac transplantation of mid-gestation ventricular cells results in a larger graft formation compared to late-gestation ventricular cells

The combination of *in vitro* cell cycle data from Chapter 3 and *in vivo* data from the intramuscular transplantation from Section 4.3.1 indicated that the intracardiac transplantation of mid-gestation (E11.5) ventricular cells would result in a larger graft volume in comparison to the late-gestation (E14.5 and E17.5) ventricular cells. To test this hypothesis, ventricular cells were isolated from E11.5, E14.5 and E17.5 NCRL embryos and approximately $3x10^5$ ventricular cells were injected in the left ventricle of healthy C57Bl/6 mice (Figure 4.5 A). Animals were sacrificed 3-days post surgery and the hearts were excised and processed for quantification of graft volume. First, the hearts were sliced into 25μm sections and placed in X-Gal solution to help visualize the engrafted embryonic ventricular NCRL cells via a blue reaction product and for quantification of graft volume (Figure 4.5 B). Sections of hearts from control mice injected with the vehicle (PBS) alone did not reveal any blue staining when placed in the X-Gal solution (Figure 4.5 B). The samples were then sliced into 10μm sections and X-Gal positive engrafted areas were used for histology (Figure 4.5 C). Furthermore, no overt electrocardiogram (ECG) abnormalities were observed in recipient mice after intracardiac transplantation of E11.5 (Figure 4.5 D), E14.5 or E17.5 (data not shown) ventricular cells compared to sham injection controls (Figure 4.5 D).

X-Gal stained 25μm sections obtained from the recipient hearts (Figure 4.6 A-B) were used to quantify the volume of blue intracardiac grafted cells using the Colour-Subtractive Computer Assisted Image Analysis software (Gaspard & Pasumarthi, 2008). Quantification of the graft volumes indicated that intracardiac transplantation of mid-gestation E11.5 ventricular cells resulted in a significantly larger graft volume compared

to transplantation of late-gestation E14.5 (~7 fold) and E17.5 (~10 fold) ventricular myocytes (Figure 4.6 C). H&E staining indicated that the transplanted embryonic ventricular cells are well integrated within the host myocardium (Figure 4.6 D) and subsequent immunostaining for the gap junction protein Cx43 indicated that as transplanted cells adjoining the host myocardium also expressed Cx43 which is a prerequisite for functional coupling of donor cells with the host myocardium (Figure 4.6 E-F).

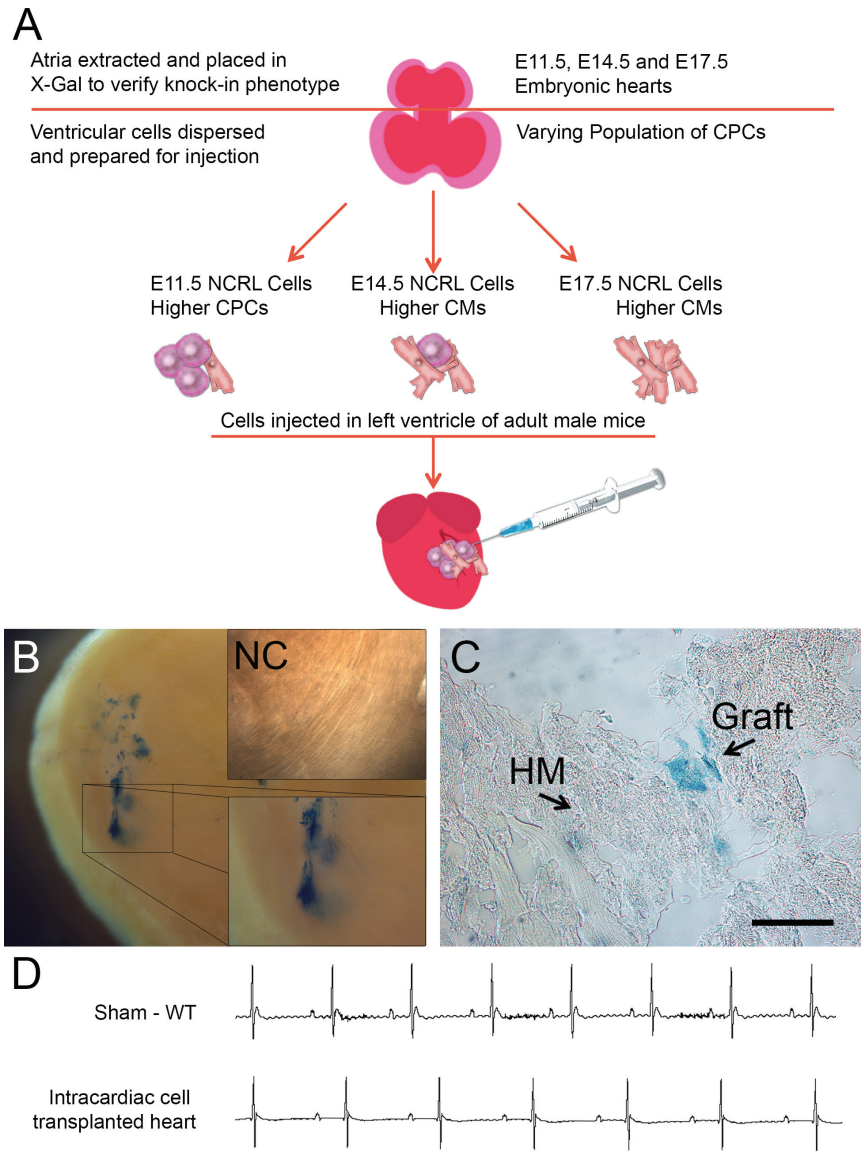

Figure 4.5 Intracardiac transplantation of embryonic ventricular cells from different embryonic stages.
(A) Embryonic hearts of NCRL embryonic day (E) 11.5, E14.5 and/or E17.5 mice were extracted, the atria was placed in X-Gal to verify genetic phenotype, while the cells of the ventricle were disperced. Approximatly $3x10^5$ cells were transplanted via direct intracardiac transplantation into the left ventricle of healthy recipient C57BL/6 mice. **(B)** The recipient hearts were excised and sectioned into 25µm thin sections and placed in X-Gal solution in order to visualize the transplanted NCRL cells wihtin the recipient animal's left ventricle. NC = Negative Control **(C)** The heart tissue containing the X-Gal$^+$ cells were cryosectioned into 10µm thin slices for quantification of graft volume. Bar = 100µm. **(D)** Electrocardiography (ECG) recording comparisons between sham (WT) mice and those with intracardiac transplanted NCRL cells showed no difference between the electrical activity of the hearts. HM= Host myocardium.

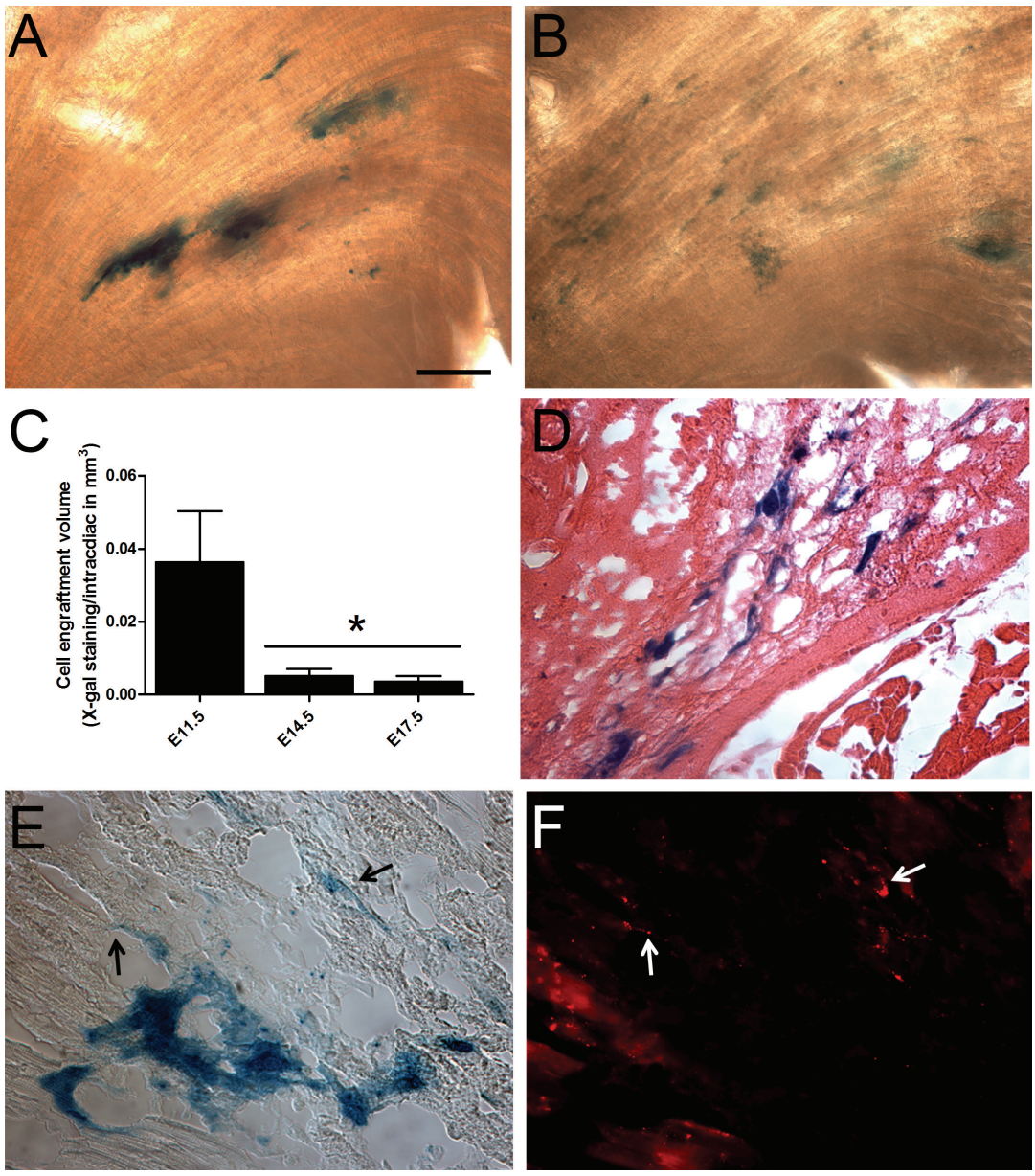

Figure 4.6 Quantification of graft volumes of intracardiac transplanted E11.5, E14.5 and E17.5 ventricular cells 3 days post transplantation.
(A, B) Representitive micrographs of X-Gal stained thick sections of reciepient hearts of mice transplanted with **(A)** embryonic day (E) 11.5 and **(B)** E14.5 ventricular cells. **(C)** Representitave graph of quantification of graft volumes of intracardiac transplanted embryonic ventricular cells. *p <0.05 vs. E11.5, one-way ANOVA with Tukey's multiple comparison test. Results are mean ± SEM of 3-4 independent experiments/group. **(D)** Hematoxylin and eosin (H&E) staining of cryosections obtained from recipient mice with intracardiac transplanted NCRL embryonic ventricular cells. **(E)** The donor cells are identified by X-Gal staining in 10µm cryosections and **(F)** Connexin 43 (Cx43) expression between the host myocardial tissue and donor cells is indicated by white arrows. Bar = 100µm **(A-B, D-F)**.

4.3.3 Continuous infusion β-adrenergic receptor agonist Isoproterenol decreases graft size and co-treatment with β_1-antagonist Metoprolol rescues detrimental effect of Isoproterenol following intracardiac cell transplantation

The *in vitro* data from Chapter 3 suggested that non-selective β-AR agonist Isoproterenol (ISO) significantly decreases the cell cycle activity of both E11.5 CPC and CM populations and the β_1-adrenergic antagonist Metoprolol (Meto) could play a protective role in rescuing these cells from the deleterious effects of continuous β-AR stimulation. We next tested the hypothesis that the detrimental effect of ISO and the protective effect of Meto seen *in vitro* could be translated to *in vivo* following intracardiac transplantation of E11.5 ventricular cells. To test this hypothesis, similar to Section 4.3.2, ventricular cells were isolated from E11.5 NCRL embryos and approximately $3x10^5$ ventricular cells were injected in the left ventricle of healthy C57Bl/6 mice and animals were treated with ISO, Meto, or ISO+Meto via mini-osmotic pumps for a period of 3 days. Upon completion of the study duration, animals were sacrificed 3-days post surgery and the hearts were excised and processed for quantification of graft volume. Next, the recipient hearts were sliced into 25μm sections and placed in X-Gal solution to help visualize the engrafted embryonic ventricular NCRL cells and to quantify the volume of blue intracardiac grafted cells as previously described (Gaspard & Pasumarthi, 2008), in response to different treatments.

Similar to our *in vitro* data, quantification of the graft volumes indicated that compared to the untreated group (Figure 4.7 A), systemic infusion of ISO (Figure 4.7 B) significantly reduced the graft volume (~10-fold decrease in graft volume). On the other hand, compared to the untreated group, treatment of recipient animals with Meto alone (Figure 4.7 C) had no significant effect on the graft volume compared to untreated group, however, the graft volume was significantly larger compared to the ISO treated group

(~10 fold increase in graft volume; Figure 4.7 E). Co-treatment of recipient animals with ISO+Meto (Figure 4.7 D) resulted in significant increase in graft volume compared to the ISO treated group (~10 fold increase in graft volume; Figure 4.7 E). Collectively, these results suggest that use of β_1-AR blocker Meto could remove deleterious effects of β-AR antagonist ISO on graft formation.

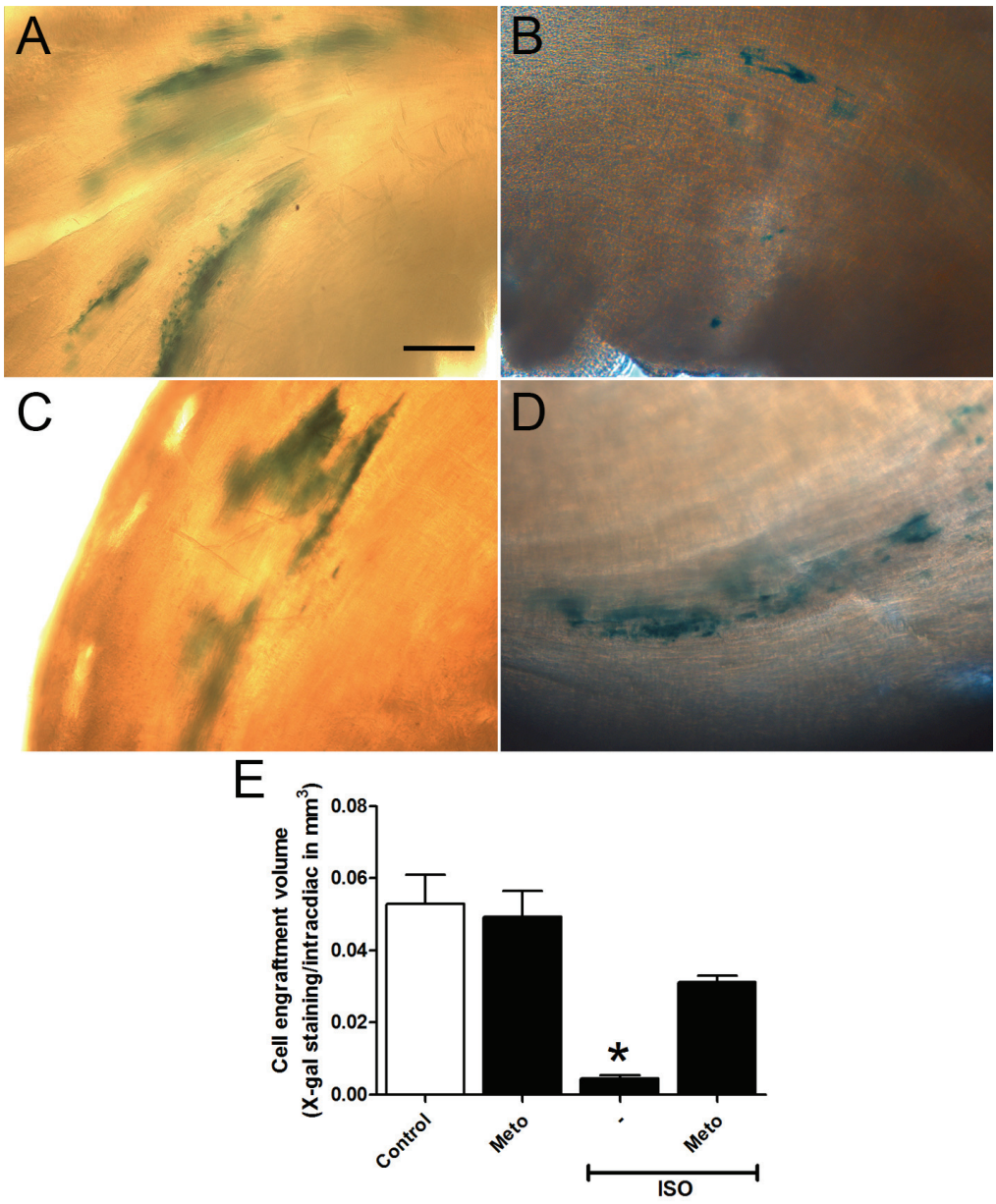

Figure 4.7 Quantification of graft volumes of intracardiac transplanted E11.5 ventricular cells, in recipient mice treated with or without β-adrenergic a agonist and antagonist.

(A) Representative micrographs of X-Gal thick stained sections of recipient hearts transplanted with embryonic day (E) 11.5 ventricular cells. Recipient mice were either untreated **(A)**, or treated with **(B)** Isoproterenol (ISO), **(C)** Metoprolol (Meto) or **(D)** ISO + Meto. **(E)** Quantification of graft volume of intracardiac transplanted embryonic ventricular cells indicated that the graft volumes of the untreated, Meto, and ISO + Meto treated groups were significantly larger than then the ISO treated group. **p* <0.05 vs. all other groups, one-way ANOVA with Tukey's multiple comparison test. Results are mean ± SEM of 3-4 experiments/group. Bar = 100µm **(A-D)**.

4.3.4 Embryonic ventricular cells can home to injured myocardium and increase angiogenesis

Progenitor cells are generally known to migrate to the injured tissues (Smart & Riley, 2008). Since the E11.5 ventricular cells harbor a large number of CPCs compared to later stages of development (Zhang & Pasumarthi, 2007), we sought to compare the homing efficiencies of E11.5 and E14.5 ventricular cells to the injured myocardium. We recently characterized a doxorubicin (Dox) induced cardiomyopathy model (Feridooni et al., 2011). Dox is a topoisomerase II inhibitor. Ultrastructurally, distinct types of Dox-induced morphological changes were seen during cardiomyocyte loss and vascular degradation (Billingham et al., 1978). In addition to these findings, we established that there is a significant increase in interstitial and vascular fibrosis in recipient C57/BL6/J mice 3 days post-injection (Feridooni et al., 2011). The increased fibrosis levels seen in recipient mice could be attributed to increased generation of reactive oxygen and nitrogen species (ROS/RNS), leading to release of cytochrome c from the mitochondria resulting in activation of apoptotic pathways (Feridooni et al., 2011).

To examine the homing properties, the unfractionated E11.5 and E14.5 ventricular cells obtained from NCRL embryos were injected in the tail veins of normal mice or mice treated with Dox. The recipient hearts were harvested 3 or 7 days after cell injections, cryosections were prepared and processed for X-Gal staining (Figure 4.8 A, B). We observed only a limited number of donor cells in normal recipient hearts with E11.5 ventricular cells but no grafts were found with E14.5 cells (Figure 4.8 A). By contrast, systemic delivery of both E11.5 and E14.5 donor cells led to formation of significantly larger intracardiac grafts in Dox treated mice at 3 day time points (Figure 4.8 B). While the E11.5 graft sizes remained similar at both 3 or 7 day points, the seeding

efficiency of E14.5 cells was significantly lower than that of E11.5 cells at both time points tested (~2-6 fold difference; Figure 4.8 G). Engrafted cells were frequently found in the areas of Dox-induced fibrosis and inflammation (Figure 4.8 C, D).

We next examined whether engrafted E11.5 or E14.5 ventricular cells can increase new blood vessel formation in recipient hearts. Histological sections were processed for immunostaining with vWF antibodies and X-Gal staining to identify vascular structures in the engrafted areas (Figure 4.8 E, F). The number of vWF positive vascular structures was significantly higher in recipient hearts with E11.5 or E14.5 cell transplants compared to the control animals, which received no cell transplantation (~2-3 fold increase; Figure 4.8 H). Notably, the number of blood vessels per cross sectional area at day 7 was significantly higher with E11.5 cell injections compared to E14.5 cell injections at both time points examined (~1.5 fold increase; Figure 4.8 H).

Figure 4.8 Comparison of homing efficiencies of E11.5 and E14.5 ventricular cells in the host myocardium by tail vein injection method.

(A-D) Representative micrographs from X-Gal stained sections of cell injection experiments. Recipient mice were treated with **(A)** Saline or **(B)** Doxorubicin (Dox) for 3 days, donor cells were injected 3 days later in the tail veins and recipient hearts were processed after 3 days for X-Gal, or **(C)** Sirius red and Fast green (SR+FG) and **(D)** Hematoxylin and Eosin staining (H&E). Arrows indicate engrafted X-Gal positive donor cells in panels **A** and **B**. **(C)** Fibrotic myocardium after Dox treatment is revealed by a red stain, indicated by the arrow. **(D)** Engrafted cells were found frequently in areas of inflammation (arrows indicate small inflammatory cells and arrowheads indicate X-Gal positive donor cells). **(E-F)** Representative cryosections sequentially process for von Willebrand factor (vWF) and X-Gal staining. **(E)** Note absence of X-Gal positive donor cells in blood vessel compartments indicated by the arrows. **(F)** Note donor cells in the interstitial space between host myocytes indicated by the arrow. **(G)** Quantification of engraftment efficiency of X-Gal positive cells. **p* <0.05 Dox 3 or 7days-E11.5 cells injection groups vs. all other groups, one-way ANOVA with Tukey's multiple comparison test. Results are mean ± SEM of 3 experiments/group. **(H)** Quantification of blood vessels per section in recipient hearts after systemic delivery of donor cells. **p* <0.05 Control (no cells) vs. all other groups, #*p* <0.05 E11.5 cell injection, 7 days Dox (D) vs. E14.5 cell injections from 3 or 7 days Dox (D) experiments, one-way ANOVA with Tukey's multiple comparison test. Results are mean ± SEM of 30 sections from 3 recipient hearts/group.

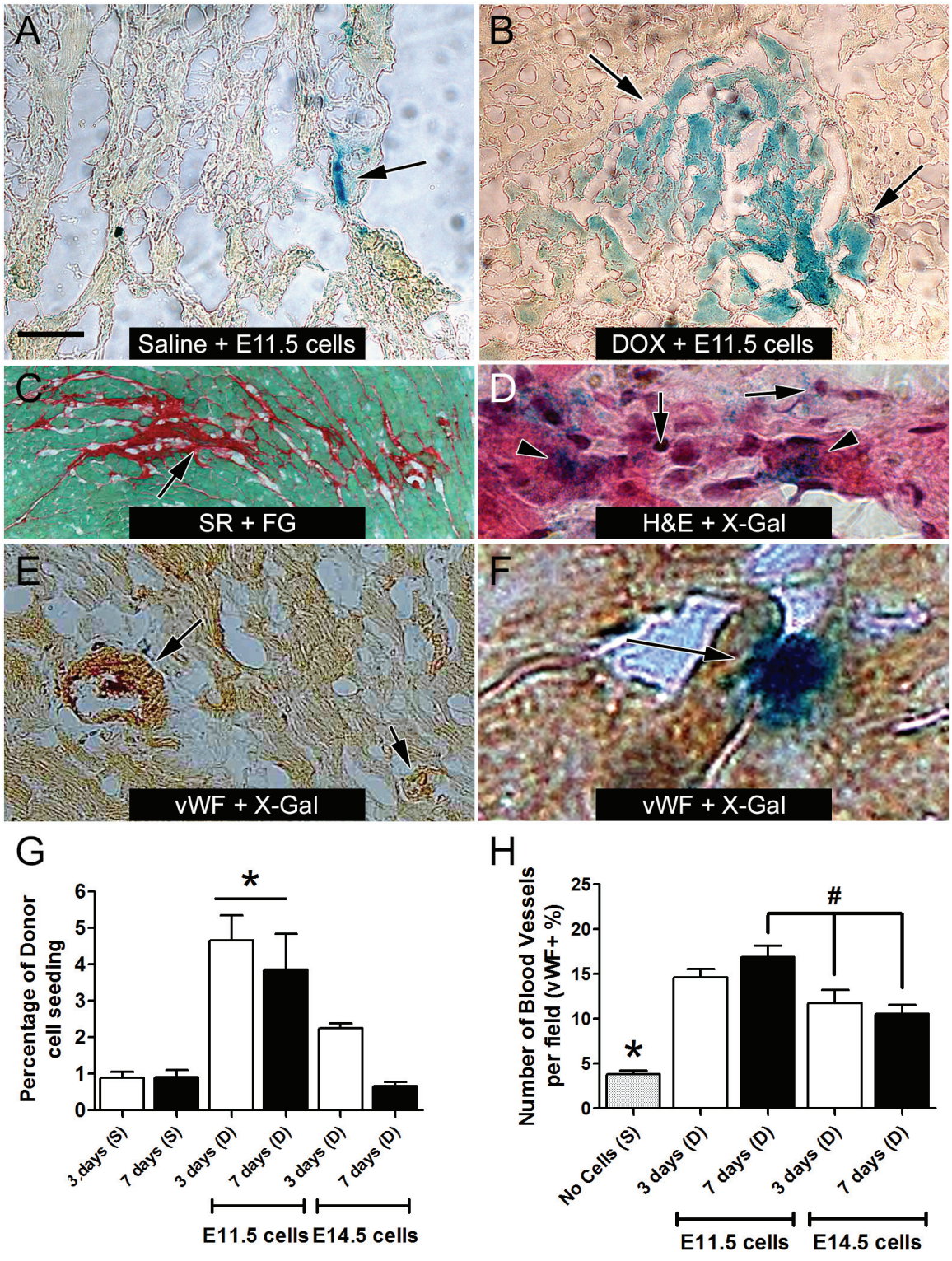
A
Saline + E11.5 cells
B
DOX + E11.5 cells
C
SR + FG
D
H&E + X-Gal
E
vWF + X-Gal
F
vWF + X-Gal
G
Percentage of Donor cell seeding
0
1
2
3
4
5
6
*
3 days (S)
7 days (S)
3 days (D)
7 days (D)
3 days (D)
7 days (D)
E11.5 cells
E14.5 cells
H
Number of Blood Vessels per field (vWF+ %)
0
5
10
15
20
25
*
#
No Cells (S)
3 days (D)
7 days (D)
3 days (D)
7 days (D)
E11.5 cells
E14.5 cells

4.3.5 Tail vein injection of mid-gestation embryonic ventricular cells can result in functional cardiac improvements in injured myocardium

Various studies have highlighted the importance of angiogenesis in improving cardiac function in MI and HF settings (Behfar et al., 2014; Sun et al., 2012; Ni et al., 2014). In the previous section (Section 4.3.4) tail vein injection of mid-gestation embryonic ventricular cells resulted in increased angiogenesis in diseased myocardium. Using echocardiogram and electrocardiogram (ECG) analysis, changes in the cardiac function of diseased mice injected (tail vein) with or without E11.5 ventricular cells was analyzed.

Lead II ECG traces were obtained from Saline, Dox and Dox+Ell.5 cells treated mice (Figure 4.9 A). Quantification of the ECG parameters indicated a significant increase in the QRS interval of Dox treated mice, compared to the Saline treated group and Dox+E11.5 cells treated group (Figure 4.9 B). Although, not significant, compared to the Saline treated group, a increases in heart rate (Figure 4.3.9 C), RR interval (Figure 4.9 D), PR interval (Figure 4.9 E) and QTc (Figure 4.9 F) were evident in the Dox treated group. Tail vain infusion of E11.5 ventricular cells in Dox treated animals, increased heart rate (Figure 4.9 C), decreased RR interval (Figure 4.9 D) and QTc (Figure 4.9 F) compared to the Dox treated group, however, the changes were not significant. In summary, tail vein infusion of E11.5 ventricular cells was able to normalize the deleterious QRS readings associated with Dox.

Short-axis echocardiogram images were obtained from Saline, Dox and Dox+Ell.5 cells treated groups (Figure 4.10). Compared to the Saline treated group, quantification of the echocardiogram parameters of Dox treated animals indicated a significant decrease in ejection fraction (Figure 4.11 A), percentage of fractional

shortening (Figure 4.11 B), stroke volume (Figure 4.11 C), LV posterior wall during diastole and systole (Figure 4.11 E, I), left ventricular internal diameter during diastole (Figure 4.11 F), end diastolic volume (Figure 4.11 G), and a significant increase in intraventricular septum during diastole (Figure 4.11 D) was evident. Tail vein infusion of E11.5 ventricular cells in Dox treated animals significantly increased the ejection fraction and percentage of fractional shortening compared to the Dox treated animals. Although, the LV posterior wall during diastole and systole was still significantly lower compared to the Saline treated group, no significant changes were evident in any other parameters.

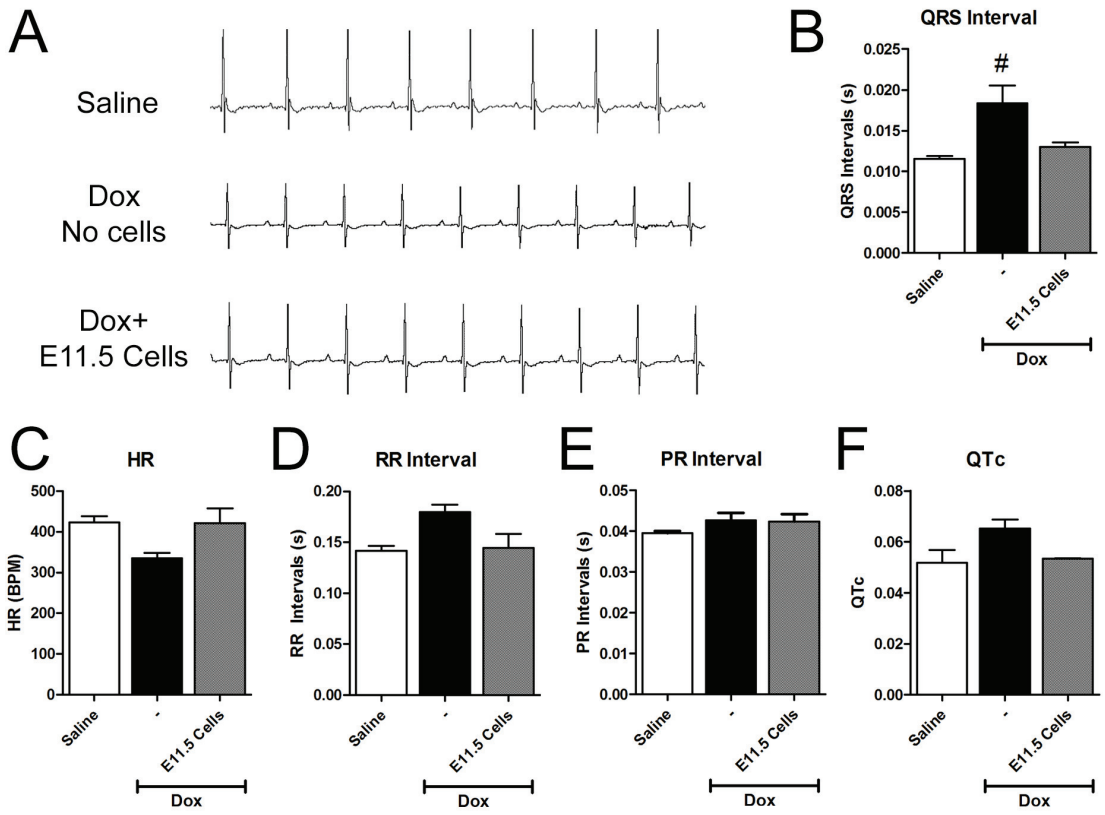

Figure 4.9 Electrocardiographic analysis of Saline or Doxorubicin treated mice treated with or without tail injection of E11.5 ventricular cells.
(A) Representative electrocardiogram (ECG) traces of different treatment groups of recipient mice. Quantification of ECG parameters, **(B)** QRS interval, **(C)** heart rate (HR), **(D)** RR interval, **(E)** PR interval, and **(F)** QTc of untreated and Doxorubicin (Dox) treated C57BL/6 mice treated with and without tail vein injection of embryonic day (E) 11.5 ventricular cells. #p <0.05 vs. Saline, one-way ANOVA with Tukey's multiple comparison test. Results are mean ± SEM of 3-4 experiments/group. Panel C-F: no significant differences observed between groups.

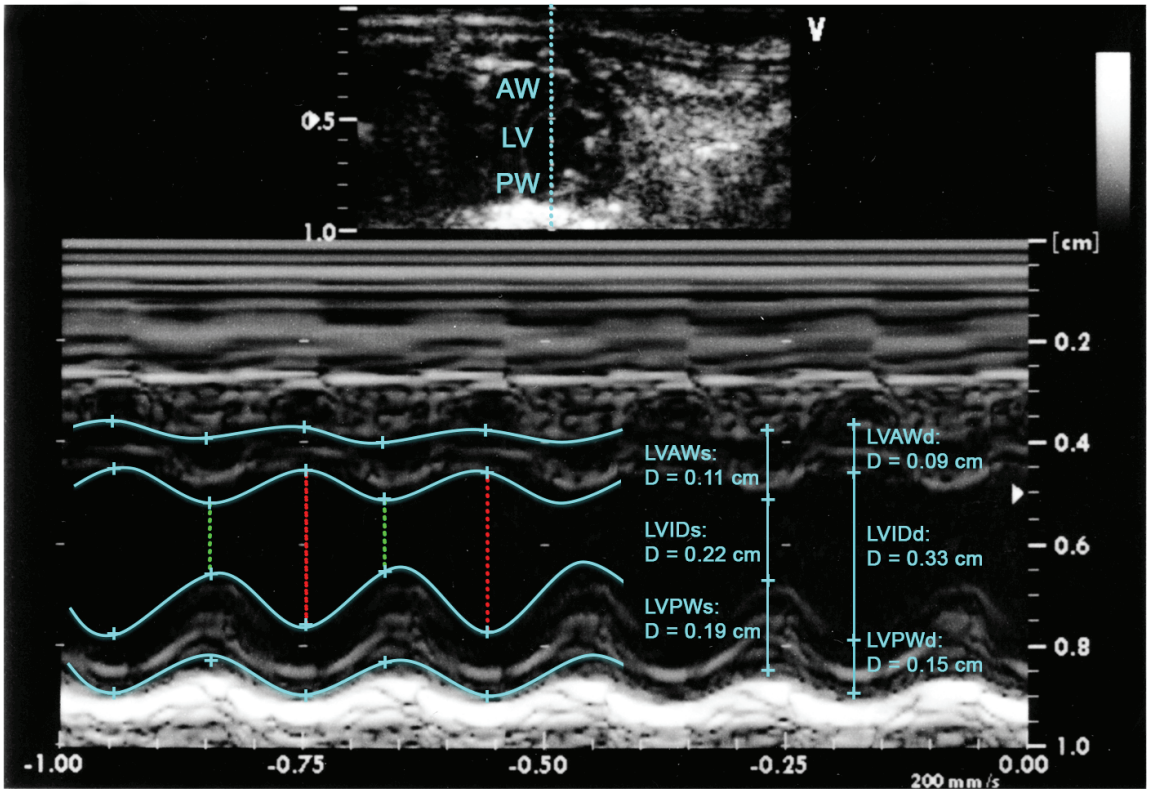

Figure 4.10 Short axis M-mode imaging of mouse left ventricle.
Representative micrograph of short axis M-mode imaging of left ventricle (LV) illustrating dimensions of LV wall, cavity and cardiac functional measurements. The y-axis indicates the distance from transducer (in mm) and the x-axis indicates time (in ms). M-Mode images illustrate LV anterior wall (AW) and posterior wall (PW) along with the ventricular chamber, through systole (s) and diastole (d). LVID, s, LV internal diameter during systole; LVID, d, LV internal diameter during diastole.

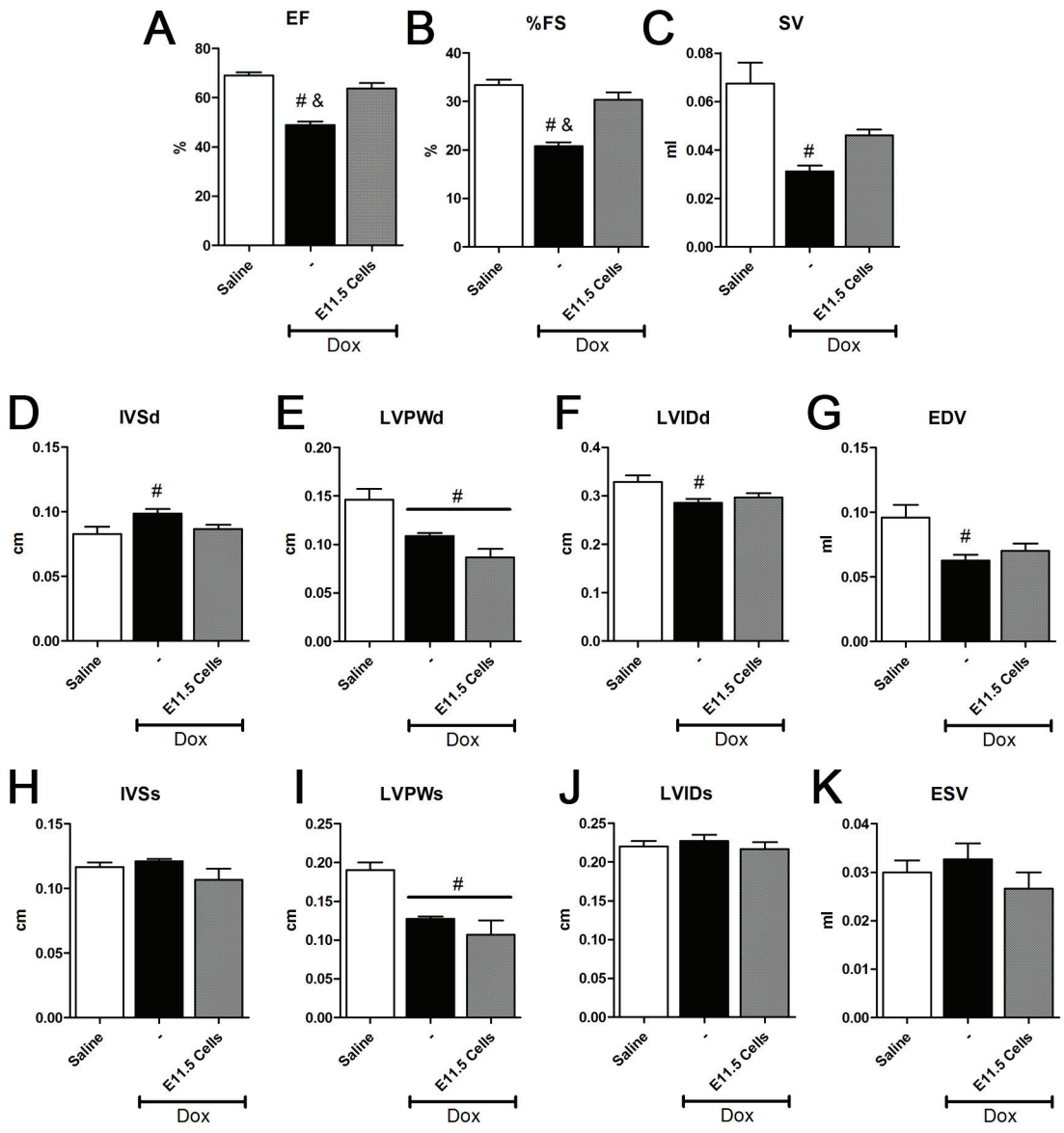

Figure 4.11 Echocardiogram analysis of Saline or Doxorubicin injected mice treated with or without tail injection of E11.5 ventricular cells.

Quantification of short-axis M-mode echocardiogram parameters of untreated and Doxorubicin (Dox) treated C57BL/6 mice treated with and without tail vein injection of embryonic day (E) 11.5 ventricular cells. **(A)** EF, **(B)** %FS, **(C)** SV, **(D)** IVSd, **(E)** LVPWd, **(F)** LVIDd, **(G)** EDV, **(H)** IVSs, **(I)** LVPWs, **(J)** LVIDs and **(K)** ESV. EF, ejection fraction; %FS, percent fractional shortening; SV, stroke volume; IVSd, intraventricular septum during diastole; LVPWd, left ventricular posterior wall during diastole; LVIDd, left ventricular internal diameter during diastole; EDV, end diastolic volume; IVSs, intraventricular septum during systole; LVPWs, left ventricular posterior wall during systole; LVIDs, left ventricular internal diameter during systole; ESV, end systolic volume; *#p* <0.05 vs. Saline, *&p* <0.05 vs. E11.5 cells, one-way ANOVA with Tukey's multiple comparison test. Results are mean ± SEM of 3-4 experiments/group.

CHAPTER 5 ENRICHMENT OF CARDIAC PROGENITOR CELLS FROM A MIXED POPULATION OF EMBRYONIC VENTRICULAR CELLS AND EVALUATION OF THEIR DIFFERENTIATION POTENTIAL IN VITRO

5.1 Background and Hypothesis

Transplantation of undifferentiated cells has been shown to result in formation of teratomas (Zhang et al., 2011). Thus, there is a clear need for the development of novel methods for enrichment of optimal donor cells with no risk for recipient's health. Previous studies from our laboratory showed that E11.5 ventricles contain a large number of cardiomyogenic CPCs, which can give rise to functional cardiomyocytes (McMullen, Zhang & Pasumarthi, 2009). In chapter 3 of this thesis, we showed that CPCs possess higher cell cycle activity compared to CMs (see Section 3.3.5). Further, we showed that E11.5 ventricular cells form larger intracardiac grafts compared to ventricular cells isolated from later developmental stages possibly owing to higher cell cycle activity and cardiomyogenic ability of CPCs (see Section 4.3.2). Based on these attributes, it is likely that fractionated E11.5 CPCs may serve as better donor cells compared to more differentiated CMs. However, currently there is no information available on cell surface markers for E11.5 ventricular cells for fractionation of pure populations of CPCs and CMs.

Fukuda and colleagues showed that CMs have high mitochondrial content compared to other cell types and can be purified using a fluorescent dye (tetramethylrhodamine methyl ester perchlorate; TMRM) that labels mitochondria (Hattori et al., 2010). Notably, they used TMRM staining to FACS sort cardiomyocytes (fraction 1; TMRM-high), nonmyocytes (fraction 2; TMRM-low) and dead cell (fraction 3; TMRM-negative) populations from early rat embryos or differentiated stem cell

cultures (Hattori et al., 2010). Earlier studies from our laboratory also found that E11.5 CMs contain a large number of mitochondria compared to undifferentiated cell population in E11.5 mouse ventricles using transmission electron microscopy (Zhang & Pasumarthi, 2007), Since there is no evidence for development of cardiac fibroblasts at E11.5 stage (Ieda et al., 2009), **we hypothesized that TMRM based FACS sorting of E11.5 ventricular cells would yield CMs in TMRM-high and CPCs in TMRM-low cell fractions. Further, we also hypothesized that the use of cardiogenic compounds may be necessary to increase the myogenic differentiation potential of fractionated CPCs.**

5.2 Specific Aims

1. Fractionate CMs and CPCs from embryonic mouse ventricles using TMRM staining and FACS sorting techniques.
2. Determine the differentiation potential of TMRM-low fraction into mature CMs overtime.
3. Examine the effects of cardiomyogenic induction factors such as DMSO, Dynorphin B, Retinoic Acid and 5-Azacytidine on differentiation of TMRM-low fraction into mature CMs.

5.3 Results

5.3.1 Fractionation of CPCs and CMs from a mixed population of E11.5 and E17.5 embryonic ventricular cells based on mitochondrial content

E11.5 or E17.5 ventricular cells dispersed from the non-transgenic CD1 embryos and stained with TMRM were subjected to FACS sorting analysis (Figure 5.1). As additional controls, unstained E11.5 ventricular cells as well as adult cardiac fibroblasts stained with or without TMRM were also processed for FACS analysis (Figure 5.1). Scatter plots gathered from the FACS analysis indicated three distinct populations of cells

in the TMRM stained E11.5 and E17.5 ventricular cells (Figure 5.1 panel#1) compared to both unstained cell preparations (Figure 5.1 panel#2). Unstained cell preparations (E11.5 ventricular cells or adult CFs) exhibited only background fluorescence in TMRM channel and this background signal was generally attributed to the presence of lipo-pigments and flavins (Hattori et al., 2010; Monici, 2005). Notably, TMRM high and low fractions from E11.5 and E17.5 ventricular cells could be readily cultured *in vitro*. In contrast, TMRM negative cells (fraction 3) contained dead cells and debris and thus could not be cultured *in vitro* (data not shown). Quantitative analysis revealed that TMRM stained E11.5 ventricular cells consisted of 27.0±1.5% TMRM-high and 73.0±1.5% TMRM-low cell populations (Figure 5.2 A). In contrast, TMRM stained E17.5 ventricular cells consisted of 57.0±0.6% TMRM-high and 42.0±0.6 TMRM low cell populations (Figure 5.2 B). These results also indicate that the TMRM-low fraction is significantly larger than the TMRM-high fraction in E11.5 ventricular cells, whereas the relative distribution of these fractions is reversed in E17.5 ventricular cells (Figure 5.2 A-B). In order to further validate our FACS findings regarding the mitochondrial content of TMRM high and low fractions, FAC sorted E11.5 ventricular cells were, cultured and stained with TMRM and a cell viability marker, Calcein. Using confocal imaging, it became clear that the cells in TMRM high fraction contain a larger mitochondrial content (Figure 5.2 C-E) compared to the cells in TMRM low fraction (Figure 5.2 F-H).

To determine the CM and non-CM cell (NMC) distribution within each sub-population of TMRM positive cells, FACS sorted cells were cultured on fibronectin coated chamber slides for 4hrs, fixed and processed for immunolabelling with differentiation marker sarcomeric myosin heavy chain (MF20). Cells positive for MF20

were noted as CMs ($MF20^+$) and those negative for MF20 were noted as NMCs ($MF20^-$) (Figure 5.3 A-F). The $MF20^+$ and $MF20^-$ cell densities were quantified per square millimeter area. Immunolabelling of fractionated TMRM-high and low E11.5 ventricular cells indicated that the number of CMs is significantly higher in the TMRM-high sub-population (97.3±9.9 cells/mm^2) compared to that of the TMRM low sub-population (1.2±0.3 cells/mm^2) (Figure 5.3 G). Inversely, the number of NMCs was significantly lower in the TMRM high sub-population (1.0±0.5 cells/mm^2) compared to the TMRM low sub-population (48.5±2.0 cells/mm^2) (Figure 5.3 H). Immunolabelling of fractionated TMRM high and low E17.5 ventricular cells indicated that the number of CMs is significantly higher in the TMRM high sub-population (201.1±17.9 cells/mm^2) compared to the TMRM low sub-population (1.2±0.5 cells/mm^2) (Figure 5.3 I). Inversely, the number of E17.5 NMCs was significantly lower in the TMRM high sub-population (0.6±0.3 cells/mm^2) compared to the TMRM low sub-population (41.2±8.5 cells/mm^2) (Figure 5.3 J).

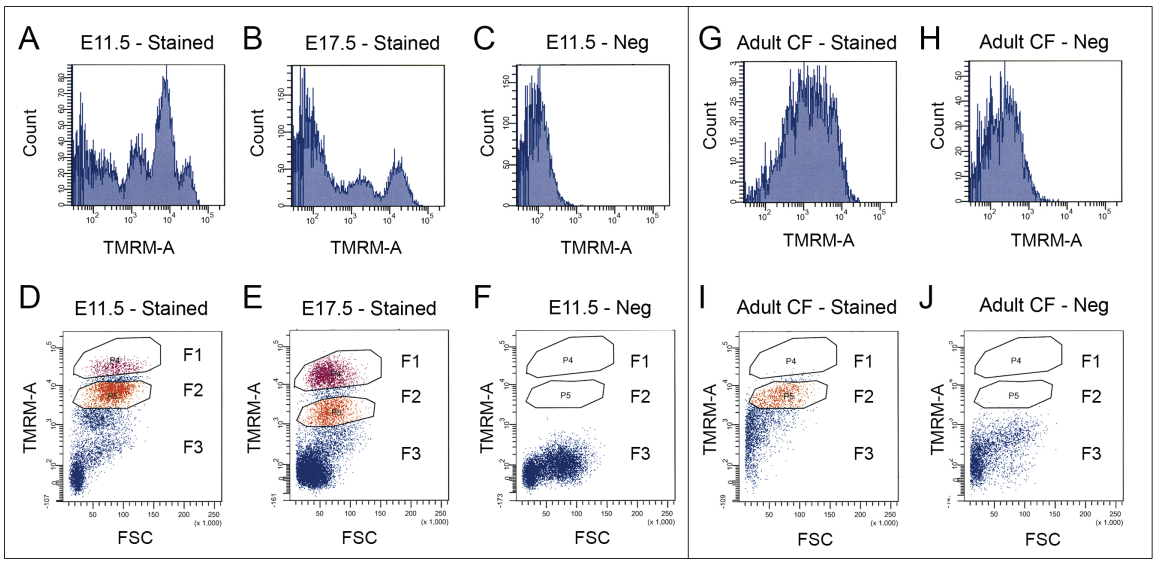

Figure 5.1 Representative FACS experiments for mitochondrial content marker TMRM in unfixed and unpermeabilized embryonic ventricular cells and adult cardiac fibroblasts.

The upper panels represent histograms representing the number of cells and their tetramethylrhodamine methyl ester (TMRM) fluorescence intensity and the lower panels are dot plots indicating measured fluorescence of each individual cell represented as an individual dot. Results from negative control experiments **(C, F and H, J)** were used to set threshold for level of TMRM intensity **(A, B D, E and H, J)**. Compared to the unstained embryonic (E) 11.5 ventricular cells **(C)** a shift to the right was evident in stained E11.5 **(A)** and E17.5 **(B)** ventricular cells indicating a positive TMRM stain. In TMRM stained ventricular cells **(D, E)**, three distinct fractions were visible, TMRM high (F1), TMRM low (F2) and TMRM negative **(**F3**)**. Adult cardiac fibroblasts (CF) were also used to test the assay's capability to sort cells according to their mitochondrial content **(G, H and I, J)**. Compared to the unstained adult CF **(H)**, in adult CF cells stained with TMRM **(G)**, a shift to the right occurred indicating that cells were positive for the stain. In addition, the majority of adult CFs stained were either TMRM low (F2) or TMRM negative with no cells in TMRM high region (F1; see panel I).

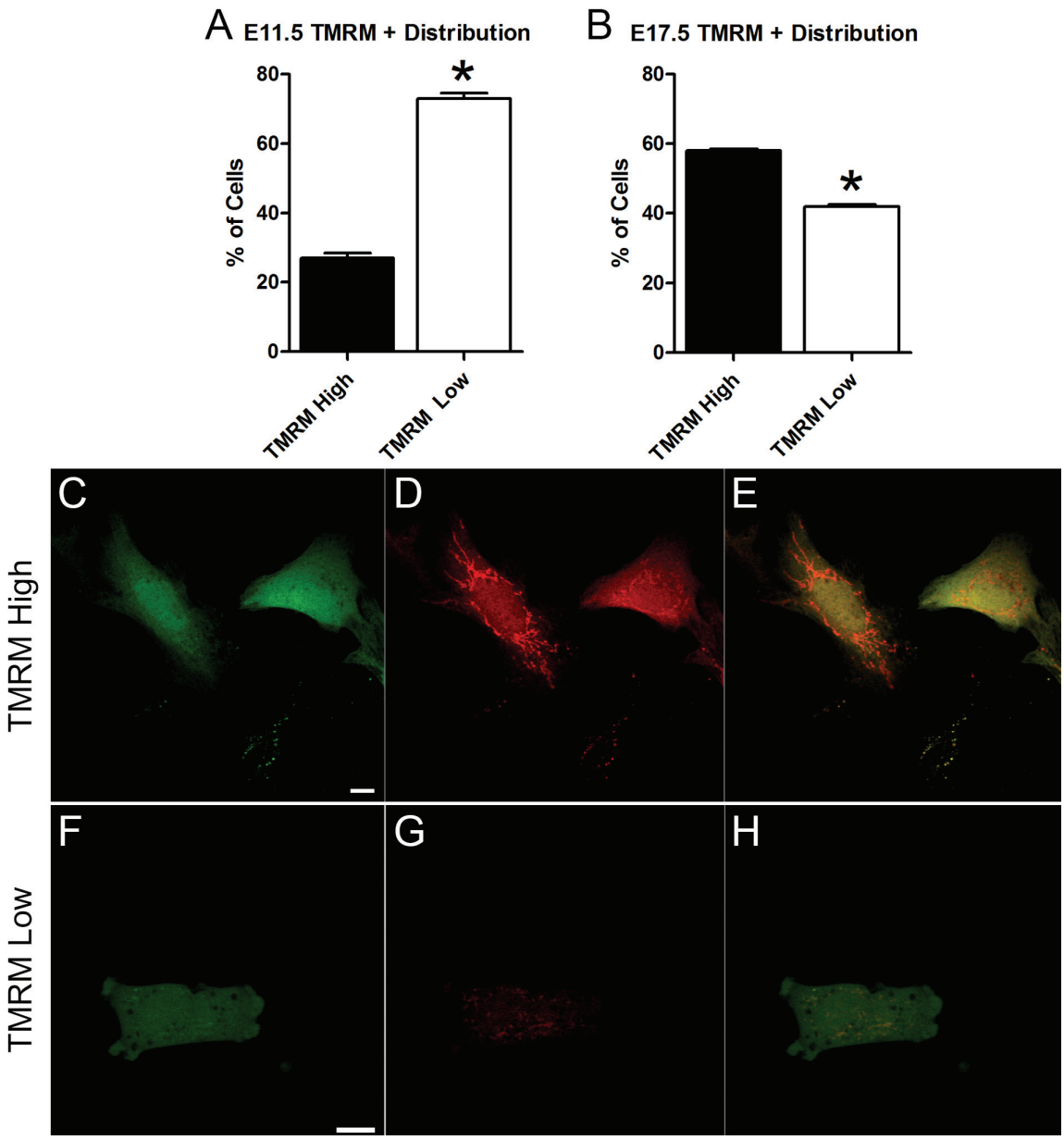

Figure 5.2 E11.5 and E17.5 embryonic ventricular cells fractions stained with mitochondrial content marker TMRM.
Data from Fluorescent activated cell sort (FACS) analysis of embryonic ventricular myocytes stained with tetramethylrhodamine methyl ester (TMRM) indicated that there are two distinct TMRM positive fractions, TMRM high and TMRM low. **(A, B)** Quantification of FAC sorted TMRM fractions of **(A)** embryonic day (E) 11.5 and **(B)** E17.5 ventricular cells. *p <0.001 vs. TMRM high fraction, unpaired student's t-test. Results are mean ± SEM of 4 independent experiments/group. Representative images of **(C-E)** TMRM high and **(F-G)** TMRM low fractions stained with Calcein (green) and TMRM (red). First row indicates cells stained with Calcein, second row are cells stained with TMRM and the third row is a merged image. Scale bars = 10μm

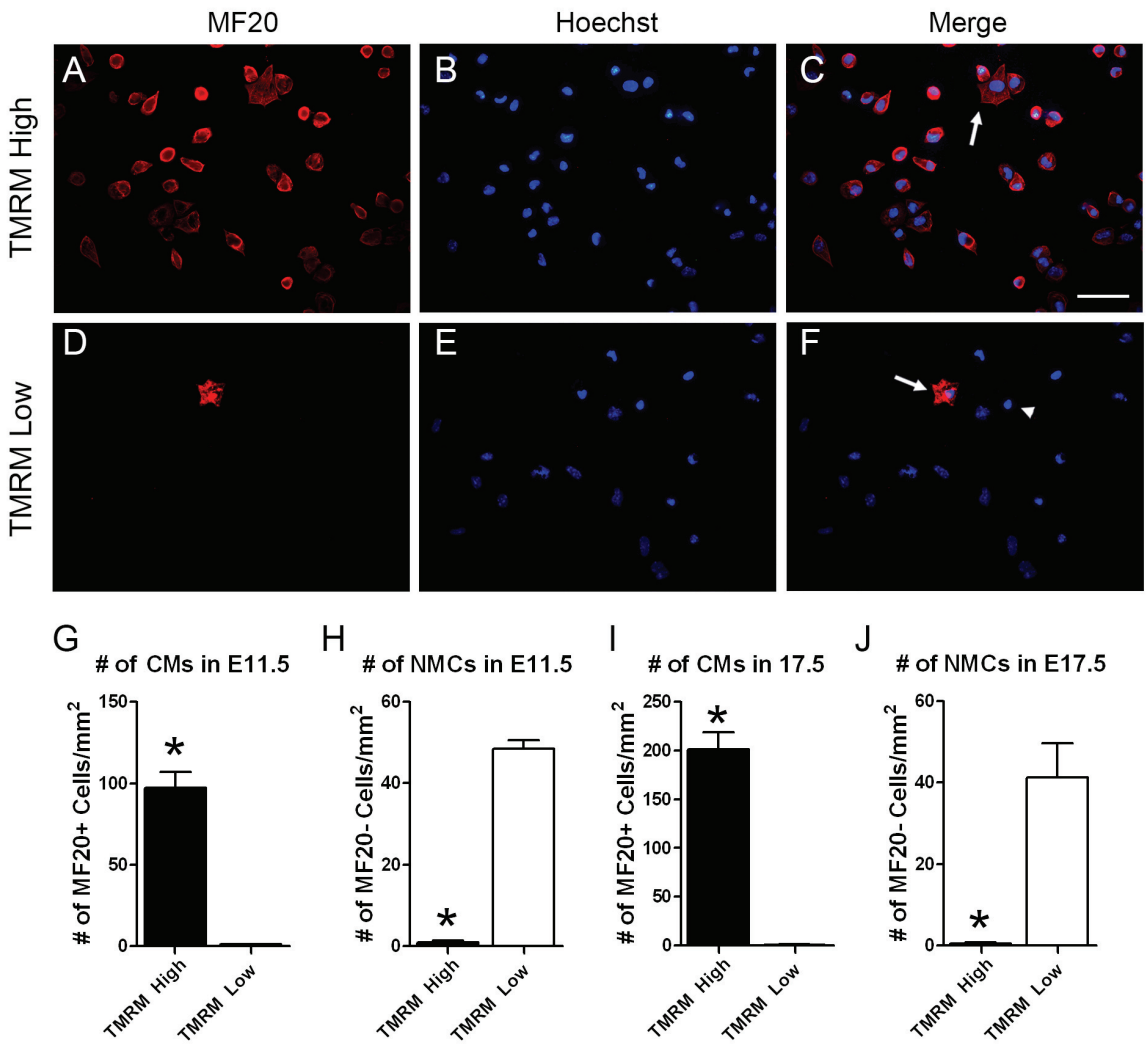

Figure 5.3 Characterization of FACS sorted E11.5 and E17.5 ventricular cells stained with the mitochondrial content marker TMRM.
Fluorescent activated cell sorted (FACS) embryonic day (E) 11.5 and E17.5 ventricular cells were cultured and immunolabelled with the sarcomeric myosin antibodies (MF20). **(A-F)** Representative images of $MF20^{+}$ and $MF20^{-}$ cells were used to quantify the number of cardiomyocytes (CMs; $MF20^{+}$) and nonmyocytes (NMCs; $MF20^{-}$) per square millimeters (mm^2). The first column represents FACS sorted E11.5 and E17.5 embryonic ventricular cells stained with MF20 **(A, D)**, the second column is the same field of cells stained with Hoechst nuclear stain **(B, E)**, and the last column shows merged images **(C, F)**. The top row is a representative image of tetramethylrhodamine methyl ester (TMRM) low fraction **(A-C)** and the second row is representative of TMRM high fractions **(D-F)**. Scale bars = 100µm. **(G-J)** Quantification of the number of CMs **(G and I)** and NMCs **(H and J)** in TMRM sorted fractions of E11.5 **(G, H)** and E17.5 **(I, J)** ventricular cells. Data is presented as number of cells per square millimeters. *p <0.05 vs. TMRM low fraction, unpaired student's t-test. Results are mean ± SEM of 4 independent experiments/group. CM: cardiomyocytes; NMC: Nonmyocyte/myogenic cells.

5.3.2 Differentiation potential of TMRM-low sub-population into mature cardiomyocytes in vitro

Since results from the previous section indicated very low number of differentiated CMs ($MF20^+$) in the FACS sorted E11.5 and E17.5 TMRM-low sub-populations 4 hrs post culturing, we next examined the differentiation capacity of $MF20^-$ cells into $MF20^+$ cells over time. To do so, E11.5 and E17.5 ventricular cells were FACS sorted according to their mitochondrial content and the TMRM-low sub-populations were cultured for 4, 24 and 48 hrs.

Immunostaining of the TMRM-low E11.5 ventricular cells revealed a very low number of $MF20^+$ 4 hrs post culturing (Figure 5.4 A). In contrast, the density of $MF20^+$ cells in cultured TMRM low sub-population progressively increased after 24-48 hrs (Figure 5.4 A-C) of culture period. Quantitative analysis revealed that compared to 4 hours (1.2±0.3 cells/mm^2), the number of $MF20^+$ CMs significantly increased by 24 hrs (15.6±1.4 cells/mm^2) and 48 hrs (29.6±2.3 cells/mm^2) (Figure 5.4 D). Quantification of MF20 negative cells indicated that compared to 4 hrs (48.5±2.0 cells/mm^2), the number of NMCs significantly increased 24 hrs after culturing (88.0±8.3 cells/mm^2) and 48 hrs (180.4±17.8 cells/mm^2) post culturing (Figure 5.4 E).

FACS sorted E11.5 TMRM low ventricular cells cultured for 72 hours indicated a significant increase in $MF20^+$ cells (93.8±13.3 cells/mm^2) compared to 4, 24, and 48 hrs, however, the culture was overtaken with an overwhelming number of $MF20^-$ cells (1071.0±139.0 cells/mm^2) (Figure 5.5 A-D). Thus, the 48-hour time point was used for further studies.

Immunolabelling of TMRM-low E17.5 ventricular cell cultures indicated that compared to 4 hrs (1.2±0.6 cells/mm^2), the number of CMs significantly increased after

24 hrs (11.5±2.3 cells/mm^2) and 48 hrs cultures (37.4±4.8 cells/mm^2) (Figure 5.3.4 F). Quantification of MF20 negative cells indicated that compared to the 4 hrs cultures (41.2±8.5 cells/mm^2), the number of NMCs significantly increased in 24 hrs (181.4±16.1 cells/mm^2) and 48 hrs cultures (150.5±8.6 cells/mm^2). The number of NMCs did not significantly change between the 24 hours and 48 hours cultures (Figure 5.4 G) in E17.5 TMRM-low cultures.

Collectively, these data suggest that TMRM-low sub-population contains CPCs capable of generating cardiomyocytes at both E11.5 and E17.5 stages of ventricular development. TMRM-low cells from both E11.5 and E17.5 stages appear to possess a similar magnitude of cardiomyogenic potential (E11.5: 29.6±2.3 cells/mm^2 Vs. E17.5: 37.4±4.8 cells/mm^2 at 48hr time points). Furthermore, NMC cells appear to expand exponentially in TMRM-low cultures from both developmental stages along with the newly formed cardiomyocytes.

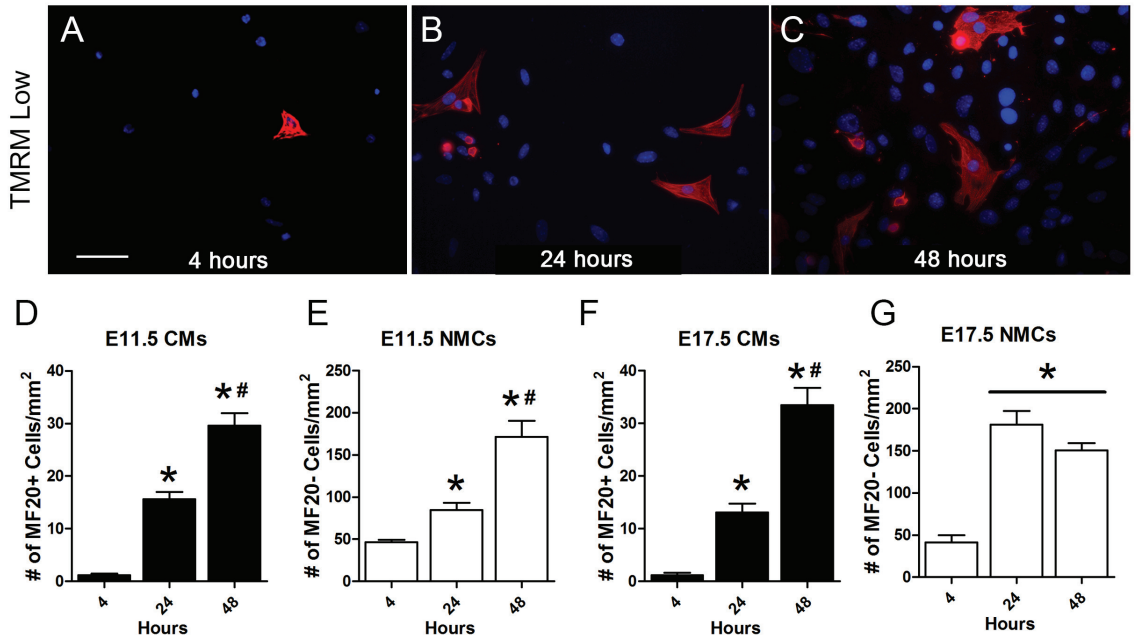

Figure 5.4 Myogenic differentiation potential of FACS sorted TMRM low E11.5 and E17.5 ventricular myocytes cells time.

To characterize the differentiation potential of fluorescent activated cell sorted (FACS) embryonic day (E) 11.5 and E17.5 tetramethylrhodamine methyl ester (TMRM) low fractions, FACS sorted cells were cultured for 4, 24 and 48 hours and immunolabelled with sarcomeric myosin (MF20) marker. **(A-C)** Representative images of $MF20^{+}$ and $MF20^{-}$ cells were used to quantify the number of cardiomyocytes (CMs; $MF20^{+}$) and nonmyocytes (NMCs; $MF20^{-}$) per square millimeters (mm^2). **(A-C)** Representative merged images of E11.5 TMRM low fraction cells cultured for times indicated and stained with MF20 (red) and Hoechst nuclear stain (blue). Scale bars = 100µm. Quantification of the number of CMs **(D, F)** and NMCs **(E, G)** in E11.5 **(D, E)** and E17.5 **(F, G)** TMRM low fractions per mm^2. *p <0.05 vs. 4 hours culture, #p <0.05 vs. 24 hours cultures, one-way ANOVA with Tukey's multiple comparison test. Results are mean ± SEM of 4 independent experiments/group. CM: cardiomyocytes; NMC: Nonmyocyte/myogenic cells.

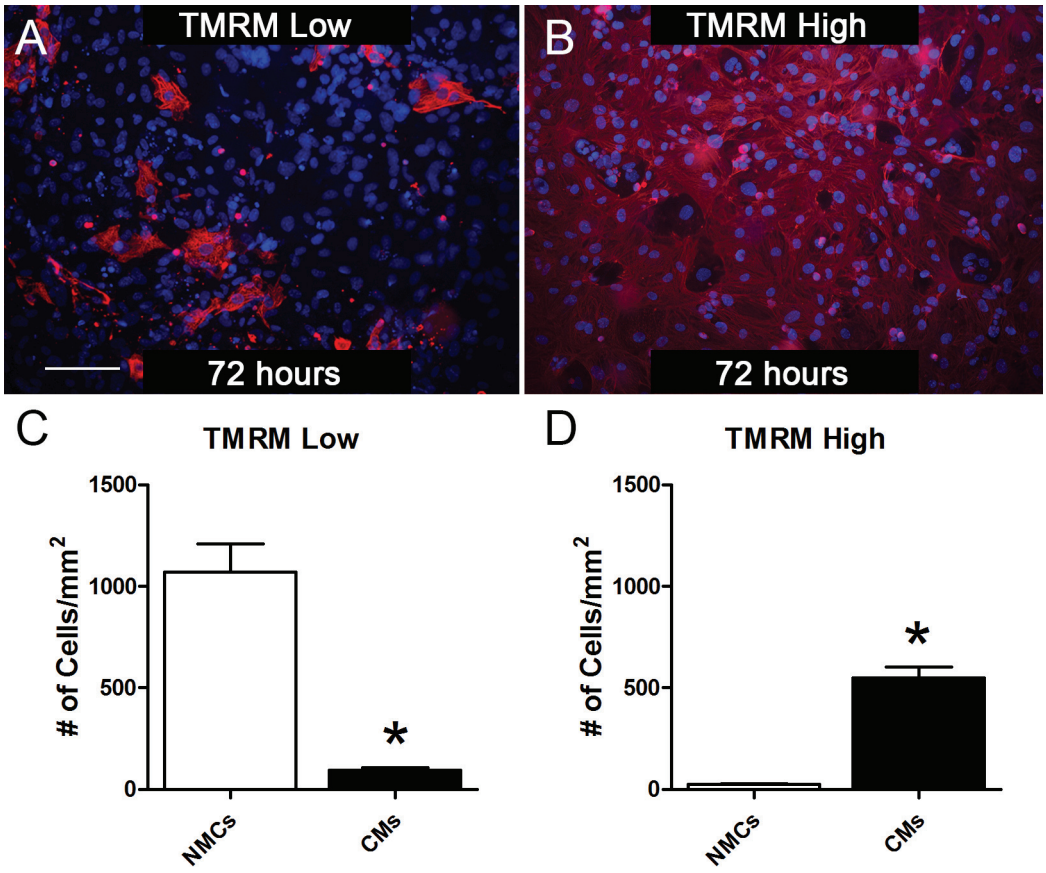

Figure 5.5 FACS sorted TMRM low and high fractions of E11.5 ventricular cells 72 hours post culturing.

(A, B) Representative image of tetramethylrhodamine methyl ester (TMRM) **(A)** low and **(B)** high fractions of fluorescent activated cell sorted (FACS) embryonic day (E) 11.5 ventricular cells immunolabelled with sarcomeric myosin heavy chain (MF20; red) marker. **(A, B)** $MF20^{+}$ and $MF20^{-}$ cells were used to quantify the number of cardiomyocytes (CMs; $MF20^{+}$) and nonmyocytes (NMCs; $MF20^{-}$) per square millimeters (mm^2). Scale bars = 100µm. **(C, D)** Quantification of the number of CMs and NMCs in the **(C)** TMRM low and **(D)** TMRM high fractions per square mm^2. *p <0.05 vs. NMCs unpaired t-test. Results are mean ± SEM of 4 independent experiments/group.

5.3.3 In vitro survival and expansion of TMRM-high CM cultures

In order to determine if there are any differences in viability and expansion characteristics of pure CM populations between E11.5 and E17.5 stages, FACS sorted TMRM-high cells were plated on fibronectin coated chamber slides and maintained for 4, 24 or 48 hrs culture periods (Figure 5.6 A-C). Immunolabelling of E11.5 TMRM-high cultures with MF20 antibodies indicated that compared to 4 hrs (97.3±9.9 cells/mm^2), the number of $MF20^+$ CMs did not significantly increase by 24 hrs (107.2±21.5 cells/mm^2) or 48 hrs (155.6±3.2 cells/mm^2) time points (Figure 5.6 D). Quantification of $MF20^-$ cells (NMC) indicated that compared to 4 hrs (0.96±0.5 cells/mm^2), the number of NMCs did not significantly increase at 24 hrs (4.1±2.4 cells/mm^2) and 48 hrs (7.3±2.4 cells/mm^2) post culturing (Figure 5.6 E).

Immunolabelling of E17.5 TMRM-high cells with MF20 antibodies indicated that compared to 4 hrs (201.1±17.8 cells/mm^2), the number of CMs did not significantly increase after 24 hrs (205.6±13.6 cells/mm^2) and 48 hrs (248.0±32.7 cells/mm^2) post culturing (Figure 5.3.6 F). Quantification of MF20 negative cells indicated that compared to 4 hrs (0.6±0.3 cells/mm^2), there was no significant increase in the number of NMCs 24 hrs (0.2±0.2 cells/mm^2) and 48 hrs (0.25±0.25 cells/mm^2) after culturing (Figure 5.6 G). In contrast to TMRM-low cultures, TMRM-high cultures could not be accurately analyzed for CM and NMC content in some fields at 72 hrs time points due to overcrowding of CMs.

These results indicate that TMRM-high cultures from both E11.5 and E17.5 ventricles can be maintained as pure CM populations (>98%) with a minimal expansion of NMC over 48-72 hrs culture periods.

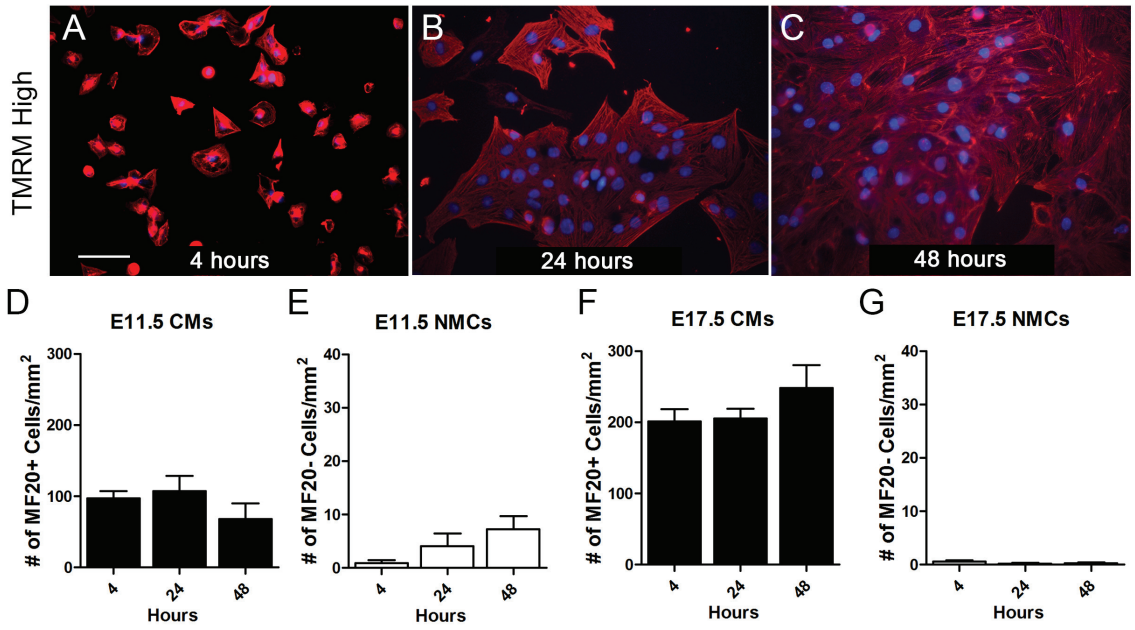

Figure 5.6 Characterization of FACS sorted TMRM high E11.5 and E17.5 ventricular myocytes over time.

To characterize the survival potential of fluorescent activated cell sorted (FACS) embryonic day (E) 11.5 and E17.5 tetramethylrhodamine methyl ester (TMRM) high fractions, FACS sorted cells were cultured for 4, 24 and 48 hours and immunolabelled with the sarcomeric myosin marker (MF20). **(A-C)** Representative merged images of E11.5 TMRM high cells stained with MF20 and Hoechst nuclear stain. These cells were cultured for various time periods as indicated on each panel. Representative images were used to quantify the number of CMs ($MF20^{+}$) and NMCs ($MF20^{-}$) per square millimeter. Scale bar = 100µm. (D-J) Quantification of the number of CMs **(D, F)** and NMCs **(E, G)** in E11.5 (D, E) and E17.5 (F, G) TMRM high cultures per square millimeter. One-way ANOVA with Tukey's multiple comparison test. Results are mean ± SEM of 4 experiments/group. CM: cardiomyocytes; NMC: Nonmyocyte/myogenic cells

5.3.4 Ventricular conduction system markers are expressed in a small number of cells in both TMRM-high and TMRM-low cell cultures

Ventricular conduction system (VCS) patterning is yet to develop at E11.5 stage (Franco & Icardo, 2001) and VCS cells can be identified by the presence of few myofilament bundles and expression of unique ion channel subunits (Han et al., 2002). We next sought to determine whether the TMRM-high and -low cell fractions also express VCS markers after culturing for 48 hrs. To this end, cultured TMRM cell fractions were immunolabelled with VCS specific markers HCN4 and Cx40. HCN4 is the fourth member of potassium/sodium hyperpolarization-activated cyclic nucleotide-gated channels and is predominantly expressed in both sinus nodal cells (Schulze-Bahr et al., 2003) and the Purkinje fibers of VCS (Han et al., 2002) in the mammalian heart. Our immunostaining results revealed that HCN4 was expressed in a small percentage (~20%) of TMRM-low (Figure 5.7 A-D) and TMRM-high (5.7 E-H) sub-populations. In E11.5 TMRM-low cells, HCN4 was expressed in both CMs ($MF20^{+}$) and NMCs ($MF20^{-}$) cells (Figure 5.7 D) 48 hours post culturing.

Cx40 is a member of the gap junction channels, which is responsible for coupling myocytes involved in mediating conduction in the heart. In the mouse heart, Cx40 expression is restricted to atrial and ventricular conductive myocytes (Miquerol et al., 2003). Cx40 was also expressed in a small percentage (~5%) of cells in TMRM-low (Figure 5.8 A-D) and TMRM-high (5.8 E-H) sub-populations.

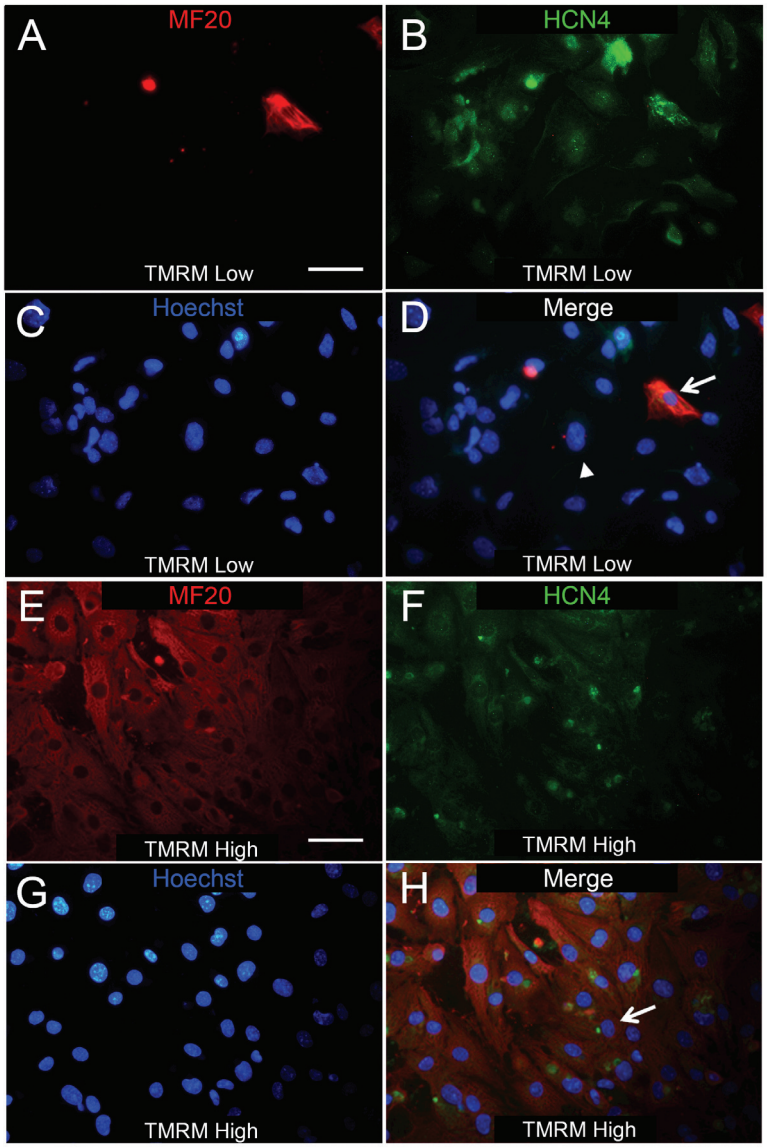

Figure 5.7 Subcellular localization of HCN4 in TMRM low and high fractions of FACS sorted E11.5 ventricular cells.
Embryonic day (E) 11.5 ventricular cells were fluorescent activated cell sorted (FACS) according to their mitochondrial content using tetramethylrhodamine methyl ester (TMRM) and cultured for 48 hours and then immunolabelled with Hoechst nuclear stain (blue), K^+/Na^+ hyperpolarization-activated cyclic nucleotide-gated channel (HCN4; green), sarcomeric myosin (MF20; red) to distinguish between cardiomyocytes (CMs; $MF20^+$) and nonmyocytes (NMCs; $MF20^-$). **(A-D)** In the TMRM low fraction HCN4 labeling was strong in the CMs (long arrow) localized mainly in the cytoplasm while less prominent in NMCs (arrow head). **(E-H)** Similarly, in the TMRM high fraction HCN4 labeling was strong in the MCs (long arrow) localized mainly in the cytoplasm. Scale bars = 50µm.

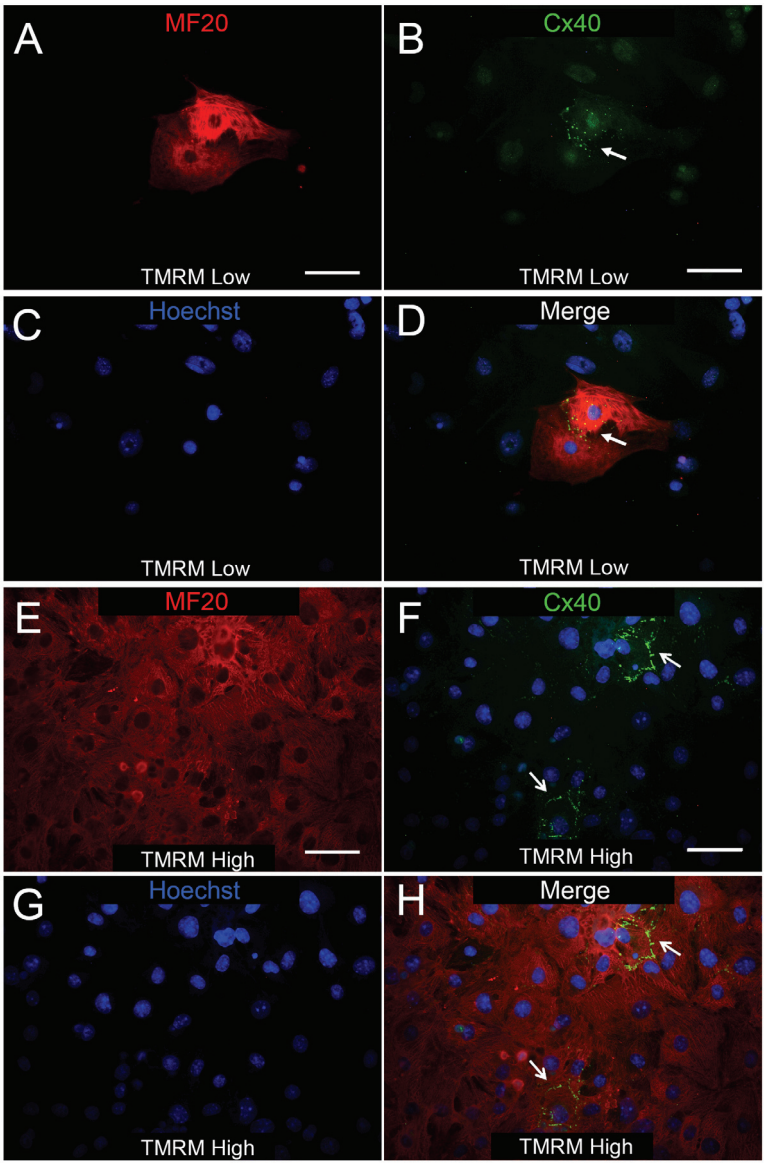

Figure 5.8 Subcellular localization of Cx40 in TMRM low and high fractions of FACS sorted E11.5 ventricular cells.
Embryonic day (E) 11.5 ventricular cells were fluorescent activated cell sorted (FACS) according to their mitochondrial content using tetramethylrhodamine methyl ester (TMRM) and cultured for 48 hours and then immunolabelled with Hoechst nuclear stain (blue), connexin 40 (Cx40; green), sarcomeric myosin (MF20; red) to distinguish between cardiomyocytes (CMs; $MF20^{+}$) and nonmyocytes (NMCs; $MF20^{-}$). **(A-D)** In the TMRM low fractions, Cx40 labeling was only visible in the CMs (long arrow) localized mainly in the membrane of adjacent cells. **(E-H)** Similarly, in the TMRM high fractions, Cx40 labeling was strong in the CMs (long arrow) localized mainly in the membrane of adjacent cells. Compared to the TMRM low fraction **(D)**, Cx40 labeling was more frequent in the TMRM high fraction **(H)**. Scale bars = 50μm.

5.3.5 Further characterization of NMCs from E11.5 TMRM labeled cell fractions

Our next goal was to characterize the NMCs of E11.5 TMRM-low fraction. To determine if there are any endothelial cells within the 48-hr TMRM-low cell cultures, we used the endothelial markers von Willebrand Factor (vWF) and CD31. The glycoprotein factor vWF is a protein involved in various vascular processes and is often used as a marker for endothelial cells involved in angiogenesis (Randi et al., 2013). Similarly, CD31 is an endothelial protein that is membrane glycoprotein enriched mainly at intercellular junctions of endothelial cells (Newman et al., 1990). Interestingly, E11.5 TMRM-low cultures were negative for vWF (Figure 5.9 A-C), yet, a small percentage (~0.1 %) of cells with positive staining for CD31 were seen (Figure 5.9 D-F). Further, the smooth muscle cell marker α-smooth muscle actin [α-SMA; (Skalli et al., 1989)] was used to determine the presence of smooth muscle cells in these cultures. However, immunolabelling did not reveal the presence of any smooth muscle cells within TMRM-low cultures (Figure 5.9 G-I). Although Nestin has generally been suggested as a neural stem cell marker (Rietze et al., 2001), its expression has been identified in mid-embryonic period of developing mouse heart (Calderone, 2012). Consistent with previous findings, immunolabelling of TMRM-low cultures revealed a prominent Nestin staining in the majority cells (Figure 5.9 J-L).

In a previous study, we showed that the majority of the differentiated and undifferentiated cells in the E11.5 myocardium express the transcription factor Nkx2.5 (Zhang & Pasumarthi, 2007). It has also been shown that cardiac fibroblasts are void of Nkx2.5 expression (Kasahara et al., 1998). To further examine whether the NMCs of E11.5 TMRM fractions also express Nkx2.5, the double transgenic NCRL mouse model

(Figure 3.6) was used. E11.5 NCRL embryonic ventricular heart cells were sorted according to their mitochondrial content, and cultured for 48 hours. Double immunolabelling of the NCRL cells from the TMRM-low fraction for β-galactosidase (β-gal) and MF20 indicated a strong expression of β-gal in both MF20- (NMCs) and $MF20^{+}$ (CMs) cells (Figure 5.3.10 A-D). Interestingly, β-gal expression was only evident in $MF20^{+}$ cells of the TMRM-high cultures (Figure 5.10 E-H).

Collectively, these results indicate that NMCs from TMRM-low cultures harbor $Nkx2.5^{+}$ CPCs that can give rise to working and conduction system myocytes but do not differentiate into other cell lineages under routine culture conditions. However, the presence of CD31 and Nestin positive cells also suggests that TMRM-low cells may harbor a small percentage of multi-potent progenitor cells, which may differentiate into other cell lineages under specialized culture conditions.

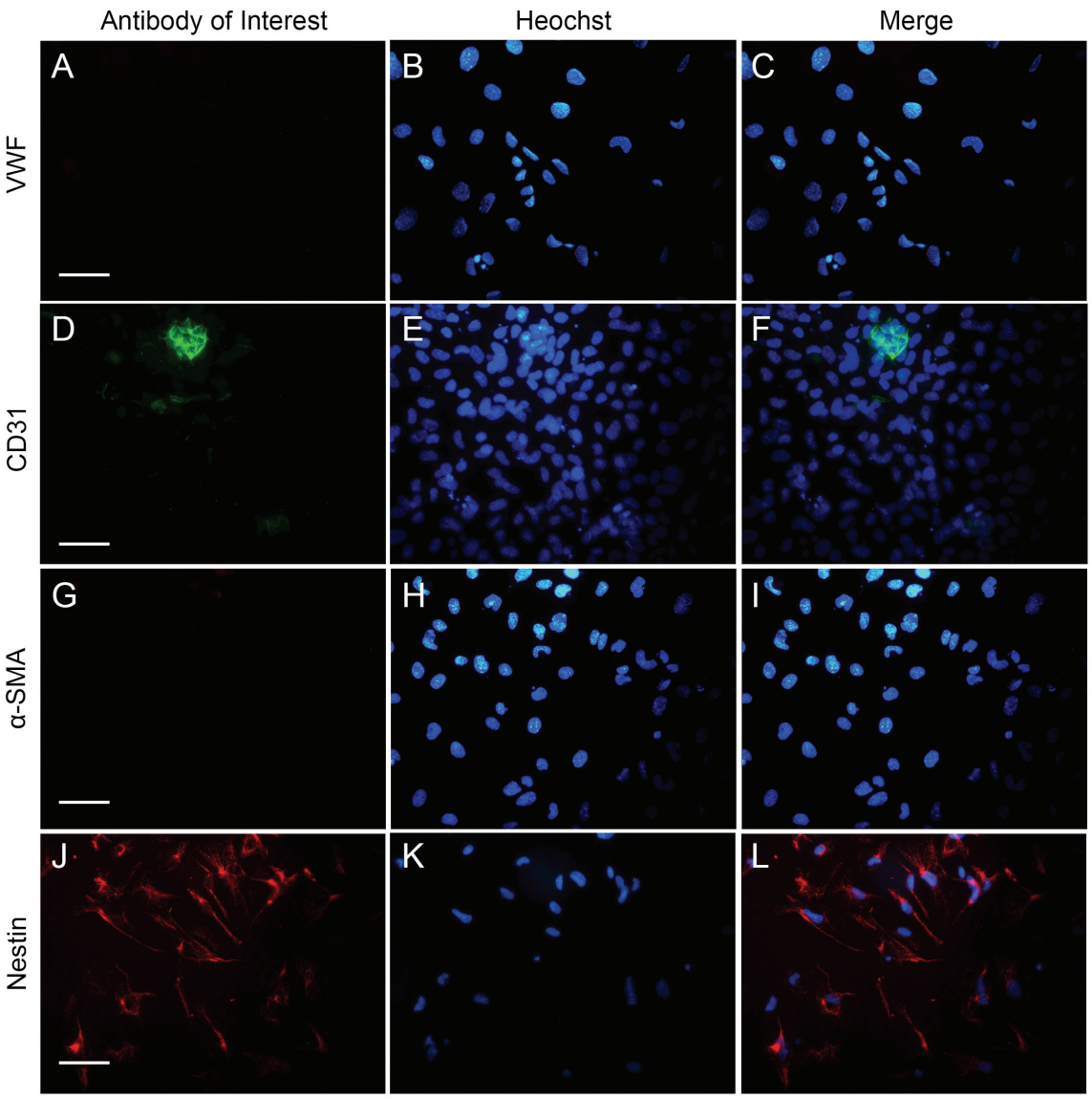

Figure 5.9 Characterization of NMCs of FACS sorted E11.5 TMRM low fractions of ventricular cells after a 48-hour culture period.
Embryonic day (E) 11.5 ventricular cells were fluorescent activated cell sorted (FACS) according to their mitochondrial content using tetramethylrhodamine methyl ester (TMRM) and cultured for 48 hours and then immunolabelled in order to characterize cell types present. The first column shows representative images of antibody of interest, second column shows the same fields stained with Hoechst nuclear stain, and the third column shows merged images. Cells were labeled with **(A-C)** von Willebrand factor (vWF), **(D-F)** cluster of differentiation 31 (CD31), **(G-I)** α-smooth muscle actin (α-SMA) and **(J-L)** Nestin to distinguish the phenotype of the nonmyocytes (NMCs) seen in cultures. CD31 and vWF were used to identify endothelial cells and α-SMA was used to identify smooth muscle cells. Nestin is generally considered as a marker for neural stem cells. Scale bars = 100μm.

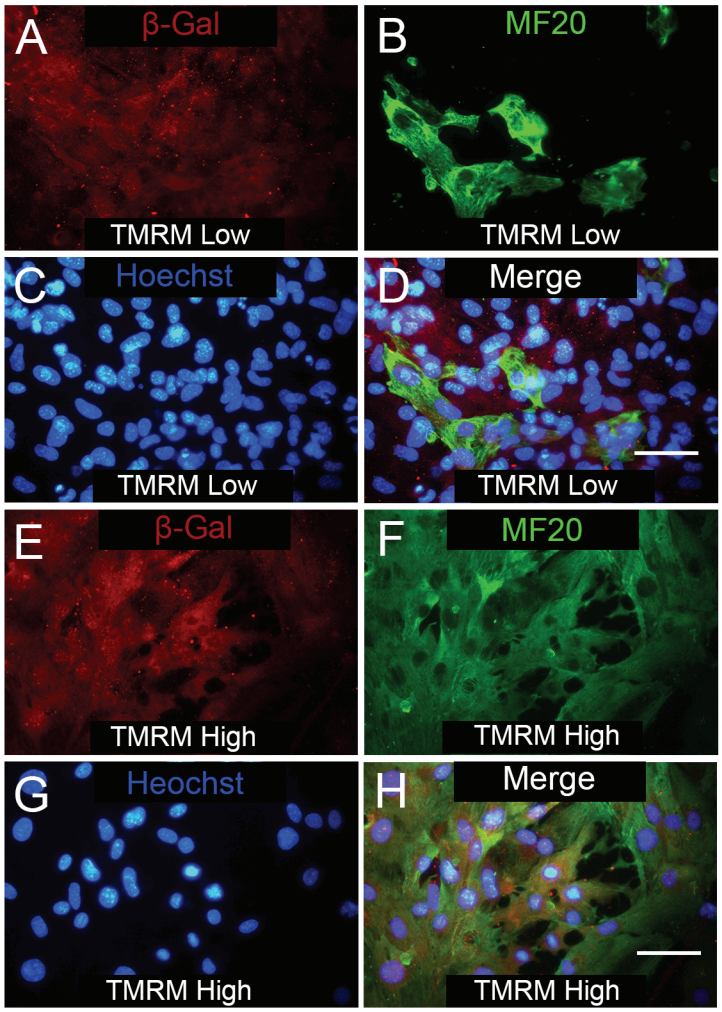

Figure 5.10 Further characterization of NMCs of E11.5 FACS sorted TMRM high and low fractions of ventricular cells in 48-hour cultures using double knockin mouse model NCRL.

Double knockin embryos (Nkx2.5 Cre X Rosa-lacZ) were generated in order to genetically label Nkx2.5^{+} lineage (express β-Gal) in embryonic day (E) 11.5 tetramethylrhodamine methyl ester (TMRM) high and low fraction cultured for 48 hours. **(A, E)** Cells were immunolebelled with β-galactosidase (β-Gal; red) in order to distinguish between Nkx2.5^{+} and Nkx2.5^{-} lineage, **(B, F)** sarcomeric myosin (MF20; green) to distinguish between cardiomyocytes (CMs; MF20^{+}) and nonmyocytes (NMCs; MF20^{-}) and **(C, G)** Hoechst nuclear stain (blue) of the same field and **(D, H)** images were also merged. Immunolabelling for β-Gal was prominent in both TMRM high and low fractions indicating that majority of the cells are from an Nkx2.5^{+} lineage. Scale bars = 50μm.

5.3.6 Exogenous treatment of E11.5 TMRM-low cultures with cardiomyogenic induction factors enhance cardiomyocyte formation in vitro

Previous studies have suggested that use of cardiomyogenic induction factors can induce differentiation of stem cells into cardiomyocytes. For instance, DMSO and Dynorphin B have been shown to induce cardiac differentiation and trigger expression of GATA4 and Nkx2.5 gene and appearance of α-myosin heavy chain and myosin light chain-2V which are markers for cardiac differentiation in murine P19 embryonal carcinoma cells (Gong et al., 2013; Ventura & Maioli, 2000). Furthermore, it has been shown that the hypomethylating agent 5-Azacytidine increased expression of cardiac-specific mRNA in human mesenchymal stem cells (Supokawej et al., 2013). While Retinoic acid has been shown to limit FGF signaling and reduce the size of the cardiac field in mice (Duester, 2013), it has also been shown to enhance cardiomyocyte differentiation from stem cell cultures (Wobus et al., 1997). Thus, we examined the effects of high and low concentrations of DMSO, Dynorphin B, Retinoic acid and high and low concentrations of 5-Azacytidine on differentiation of E11.5 TMRM-low cell cultures. Concentrations of exogenous factors were chosen based on the published literature as described earlier. We also examined the effects of TMRM-high cell conditioned media on differentiation of TMRM-low sub-population as CMs in TMRM-high cultures may release factors that could contribute to the differentiation of CPCs.

To examine the effects of various factors, TMRM-low cells were cultured for 48 hrs in the presence or absence of exogenous factors (Figure 5.11). Subsequently, cell were immunolabelled with MF20 and the CM ($MF20^+$) number was quantified and expressed as number of $MF20^+$ cells per squared millimeter. Quantification of the $MF20^+$ cells (CMs) indicated that compared to the untreated group (30.9±2.8 cells/mm^2), the

number of $MF20^+$ cells significantly increased in cultures treated with 1%DMSO (140mM) (68.8±8.6 cells/mm^2), 2.8nM DMSO (83.0±10.6 cells/mm^2) and 1μM Dynorphin B (76.5±5.9 cells/mm^2) (Figure 5.11 I). Further, no significant increase was evident in the number of $MF20^+$ cells in cultures treated with 10nM Retinoic acid (17.4±2.2 cells/mm^2), conditioned media of TMRM high sub-population (19.9±2.6 cells/mm^2) and 3μM 5-Azacytidine (14.7±1.6 cells/mm^2) or 10μM 5-Azacytidine (11.1±1.0 cells/mm^2) compared to the untreated group (Figure 5.11 I).

Since individual treatments of 2.8nM DMSO and 1μM Dynorphin B had such a strong effect on cardiomyogenic induction, we next examined the combined effect of these two factors on CM number in TMRM-low cultures (Figure 5.12 A-D). Compared to the untreated group (30.9±2.8 cells/mm^2), the number of $MF20^+$ cells did not significantly change in the cultures co-treated with both 2.8nM DMSO and 1μM Dynorphin B (38.2±2.6 cells/mm^2) (Figure 5.12 E). Further, the number of $MF20^+$ cells in individually treated 2.8nM DMSO and 1μM Dynorphin B were significantly higher compared to the cultures co-treated with both 2.8nM DMSO and 1μM Dynorphin B (Figure 5.12 E).

These results suggest that additional factors such as Dynorphin B or DMSO are necessary to increase cardiomyogenic induction in TMRM-low cultures in vitro. Although conditioned media from TMRM–high cells did not have any effect on the degree of myogenic induction in our experiments, secretion of induction factors from CMs cannot be ruled out since these factors may be labile under the conditions used in this study.

Figure 5.11 Differentiation potential of FACS sorted E11.5 TMRM low ventricular cells in response to cardiogenic compounds.
To characterize the differentiation potential of embryonic day (E) 11.5 tetramethylrhodamine methyl ester (TMRM) low cells in response to various cardiomyogenic compounds, fluorescent activated cell sorted cells were cultured for 48 hours in the **(A)** absence or presence of **(B)** 1% (or 10mM) and **(C)** 2.8mM dimethyl sufoxide (DMSO), **(D)** 1μM Dynorphin B, **(E)** 10nM Retinoic acid, **(F)** conditioned medial from TMRM high cells cultured for 48hrs, **(G, H)** 3μM and 10μM 5-Azacytidine and immunolabelled with sarcomeric myosin marker (MF20; red). **(I)** Quantification of the number of cardiomyocytes (CM) in different culture conditions per square millimeter area. **p* <0.05 vs. untreated culture, #*p* <0.05 vs. 1μM Dynorphin B treated cultures, &*p* <0.05 vs. 1% DMSO treated cultures, ^*p* <0.05 vs. 2.8mM DMSO treated cultures, ***p* <0.05 vs. 48-hour culture media of TMRM high fractions cultures, one-way ANOVA with Tukey's multiple comparison test. Results are mean ± SEM of 4 experiments/group. Scale bars = 100μm.

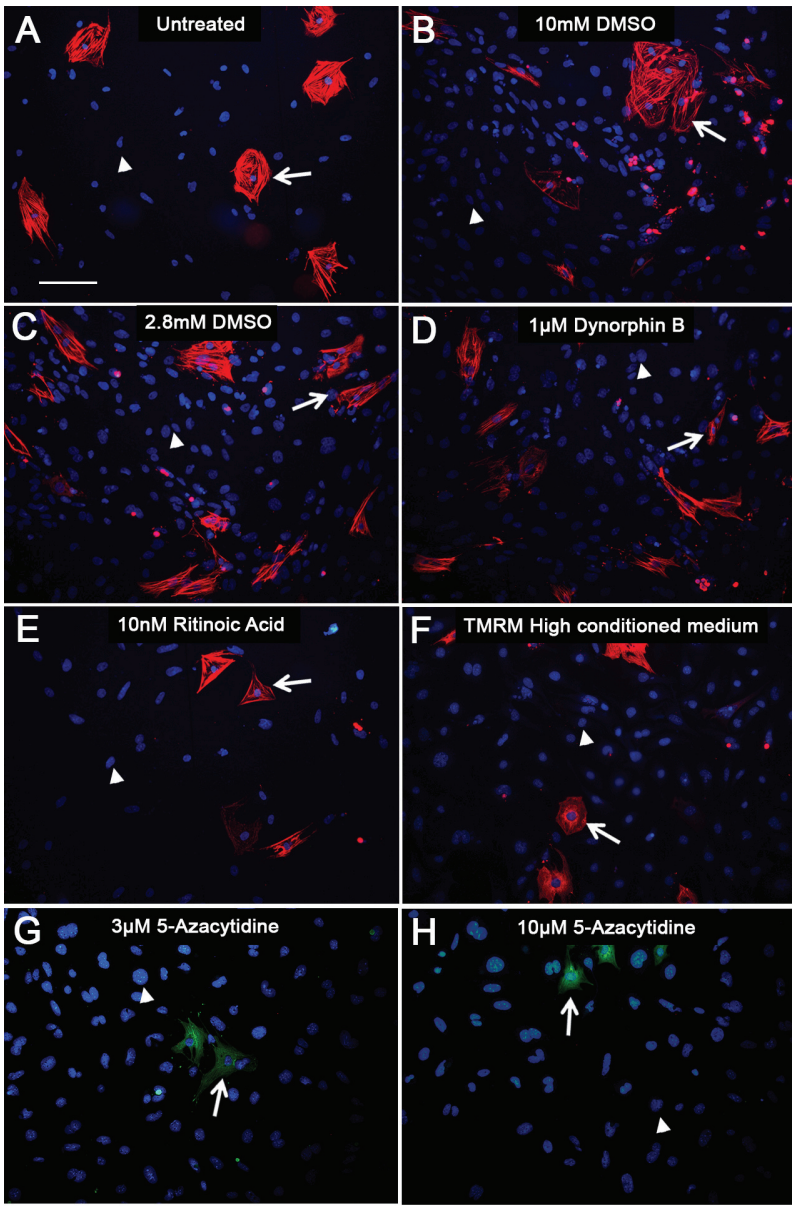
A
Untreated
B
10mM DMSO
C
2.8mM DMSO
D
1μM Dynorphin B
E
10nM Ritinoic Acid
F
TMRM High conditioned medium
G
3μM 5-Azacytidine
H
10μM 5-Azacytidine

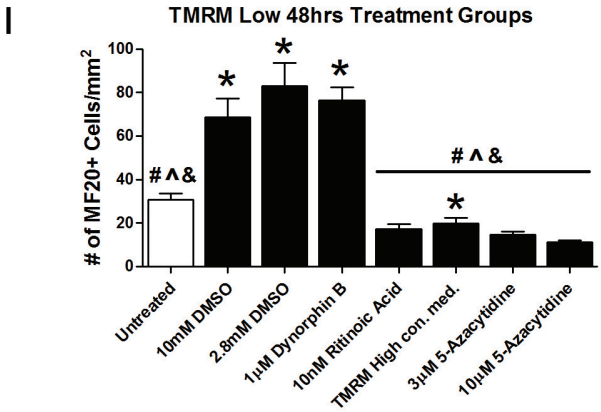
I
TMRM Low 48hrs Treatment Groups
# of MF20+ Cells/mm2
100
80
60
40
20
0
#∧&
*
*
*
#∧&
*
Untreated
10mM DMSO
2.8mM DMSO
1μM Dynorphin B
10nM Ritinoic Acid
TMRM High con. med.
3μM 5-Azacytidine
10μM 5-Azacytidine

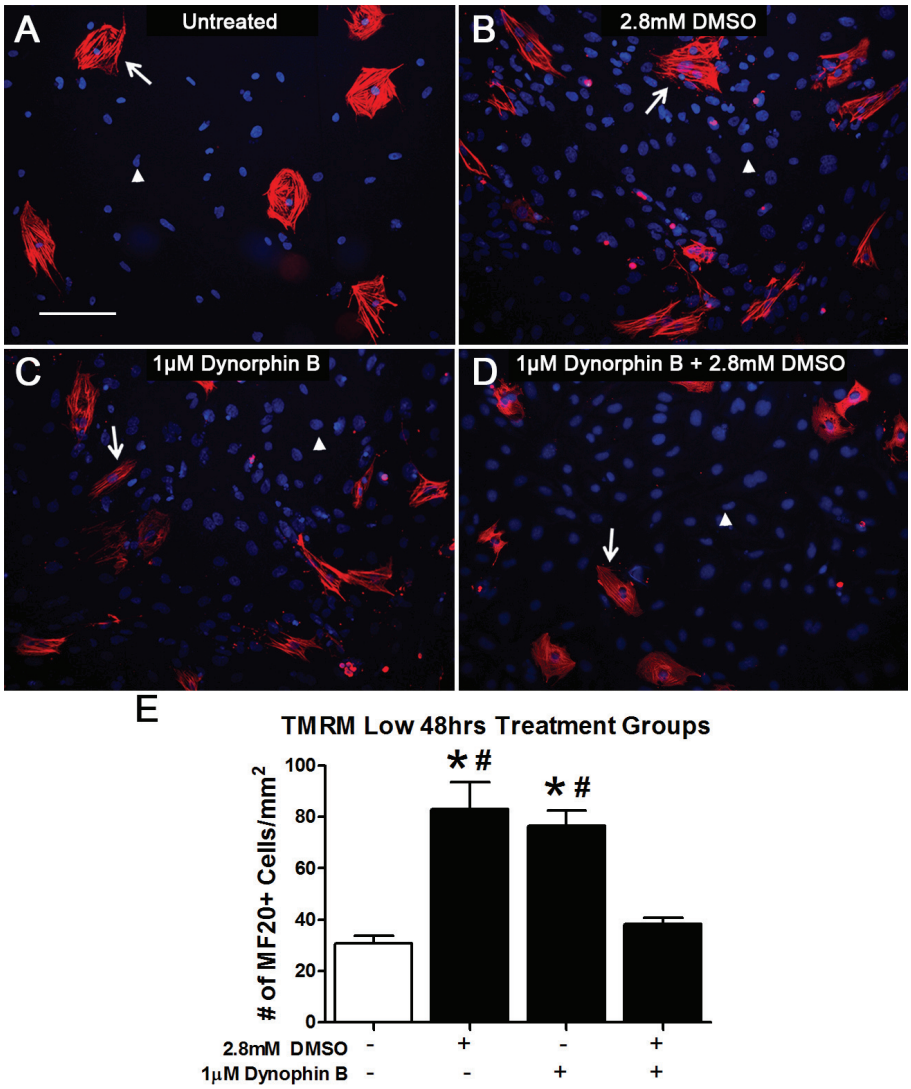

Figure 5.12 Differentiation potential of E11.5 TMRM low fraction ventricular in response to combination of 2.8mM DMSO and 1µM Dynorphin B.

To characterize the differentiation potential of embryonic day (E) 11.5 tetramethylrhodamine methyl ester (TMRM) low fraction ventricular myocytes in response to a combination of 2.8mM dimethyl sulfoxide (DMSO) and 1µM Dynorphin B, ventricular cells were cultured for 48 hours in the **(A)** absence of any treatment or in presence of **(B)** 2.8nM DMSO and **(C)** 1µM Dynorphin B alone and **(D)** 2.8mM DMSO and 1µM Dynorphin B and immunolabelled with sarcomeric myosin (MF20; red) marker. **(I)** Quantification of the number of cardiomyocytes (CMs; $MF20^{+}$) in different culture conditions per square millimeter area. *p <0.05 vs. untreated culture and #p <0.05 vs. 2.8mM DMSO and 1µM Dynorphin B treated cultures, one-way ANOVA with Tukey's multiple comparison test. Results are mean ± SEM of 4 experiments/group. Scale bars = 100µm.

CHAPTER 6 THE ROLE OF β-ADRENERGIC RECEPTOR SIGNALING AND CYCLIC AMP IN CARDIOMYOGENIC DIFFERENTIATION OF MID-GESTATION TMRM-LOW CARDIAC PROGENITOR CELLS

6.1 Background and Hypothesis

Previous studies have highlighted the importance of the β-adrenergic receptor (β-AR) signaling pathways in development of embryonic heart (Zhou et al., 1995; Kudlacz et al., 1990; Portbury et al., 2003; Thomas et al., 1995). Further, in chapter 3 we demonstrated that continuous β-AR stimulation of embryonic day 11.5 (E11.5) ventricular cells results in significant decrease in proliferation of both cardiomyocytes (CMs) and cardiac progenitor cells (CPCs), due to decreases in phosphorylation of ERK and AKT, leading to decreased expression of cell cycle genes. Although β-AR mediated cAMP responses are more robust in late stages of ventricular development (e.g. E14.5 and E17.5) compared to mid-gestational E11.5 stage, it is not known whether β-AR signaling and associated cAMP production plays any role in the differentiation of residual CPCs in E11.5 ventricles.

The combination of fluorescent dye Tetramethylrhodamine methyl ester perchlorate (TMRM) and fluorescent activated cell sorting which allowed for the enrichment of CPCs and CMs from a heterogeneous population of embryonic ventricular cells (see chapter 5.3.1) provided us with a platform to examine the role of β-adrenergic stimulation (Isoproterenol) in differentiation of CPCs into CMs. Furthermore, it is not known whether there are any differences in adrenergic drug responses and calcium handling capabilities between E11.5 CPCs and CMs. **In this study, we hypothesized that β-AR signaling mediates differentiation of CPCs in TMRM low fractions into**

CMs, and the TMRM high fraction cells will possess more prominent intracellular Ca^{2+} influx and fluctuations, compared to the TMRM low fraction.

6.2 Specific Aims

1. Compare the second messenger responses of β-AR stimulation between fractionated TMRM high and low fractions of E11.5 ventricular cells.
2. Compare and contrast the effects of β-adrenergic stimulation on intracellular Ca^{2+} levels of fractionated TMRM high and low fractions in response to isoproterenol stimulation.
3. Examine the role of β-adrenergic system in differentiation of TMRM low fraction.

6.3 Results

6.3.1 Assessment of second messenger responses in embryonic TMRM high and low fractions after β-adrenergic stimulation

Previous findings established that ISO acts more potently on E17.5 cells possibly due to higher percentage of ventricular CMs compared to E11.5 or E14.5 cells (Section 3.3.3). We next examined whether there are any differences in β-AR responses in TMRM high and low fractions of FACS sorted E11.5 ventricular cells. Cells of E11.5 TMRM high and low fractions were treated with different concentrations of ISO (0-100μM) and dose response curves were generated after normalizing responses to the cell number. Based on these responses, we determined the half maximal effective concentration (EC_{50}) of each TMRM fraction. The EC_{50} value for unfractionated E11.5 ventricular cells was previously found to be 1083±37nM (Figure 3.4 A). In contrast, the EC_{50} values for ISO responses of TMRM high and low fractions were found to be 800±13nM and 870±19

nM, respectively (Figure 6.1). These results suggest that ISO acts more potently on TMRM high compared to the TMRM low cells derived from E11.5 ventricles.

We next determined whether the ISO responses seen in embryonic ventricular cells were due to β_1 or β_2-AR activation. For these experiments, E11.5 TMRM high and low cells were treated with 1μM ISO (~EC_{50}) in the presence or absence of varying concentrations (0.1, 1 and 10μM) of the β_1-AR blocker Metoprolol (Meto) or the β_2-AR blocker ICI 188,551 (ICI) and the cAMP levels were measured (Figure 6.2). As expected, a significant increase in cAMP concentration was evident in TMRM high cells treated with 1μM ISO (~4.5-fold) compared to the basal untreated group. Although, co-treatment of TMRM-high cells with 1μM ISO and 1 or 10μM of the β_1-blocker Meto reduced the cAMP levels, it was not able to return cAMP levels back to basal levels (Figure 6.2 A). TMRM high cells co-treated with 1μM ISO and 1 and 10μM of the β_2-blocker ICI showed significant reduction in cAMP levels compared to the ISO only group (Figure 6.2 B). Similarly, a significant increase in cAMP concentration was evident in TMRM low cells treated with 1μM ISO (~3.5-fold) compared to the basal untreated group. Co-treatment of cells with 1μM ISO and 1 or 10μM of the β_1-blocker Meto reduced the cAMP levels back to basal values (Figure 6.2 C). TMRM low cells co-treated with 1μM ISO and 0.1, 1 and 10μM of the β_2-blocker ICI showed significant reduction in cAMP levels compared to the ISO only group (Figure 6.2 C). Collectively, these results suggest that both β_1-and β_2-ARs are involved in ISO mediated cAMP generation in TMRM high and low cells.

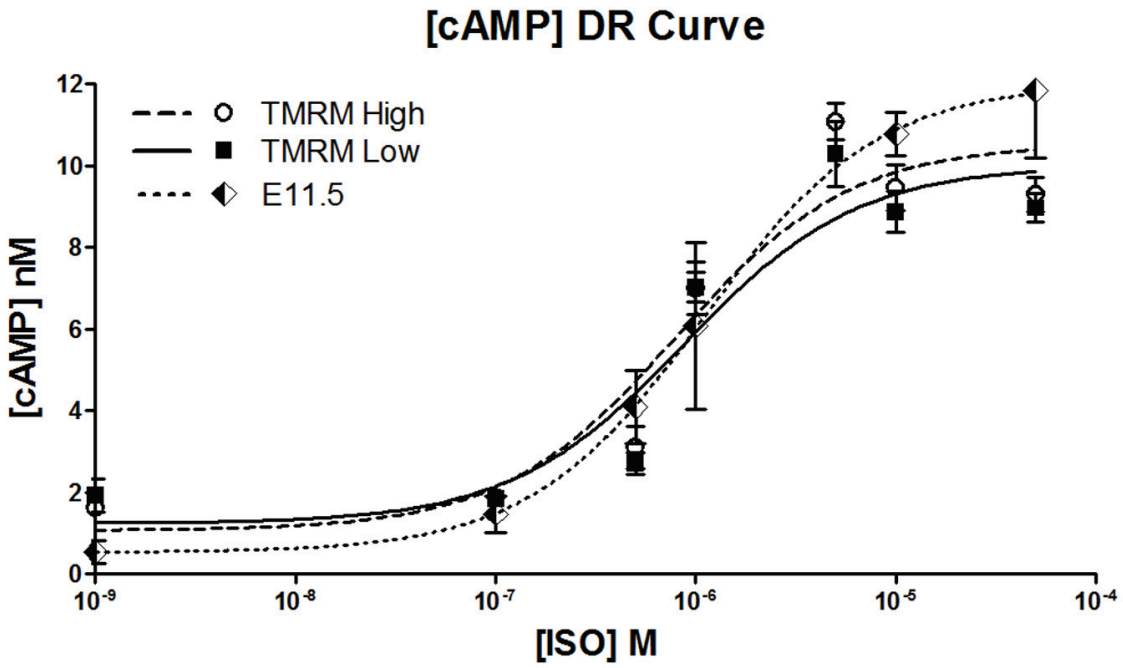

Figure 6.1 Isoproterenol, dose-response curve for E11.5 TMRM high and low fractions using heterogeneous time resolved fluorescence based cAMP assay.
Half maximal effective concentration (EC_{50}) of Isoproterenol (ISO) for unfractionated embryonic day 11.5 ventricular cells was found to be 1083nM. Similarly, the EC_{50} values of ISO for TMRM high and low fractions were found to be 800nM and 870nM, respectively. N= 3 - 5 independent experiments, performed in duplicate wells.

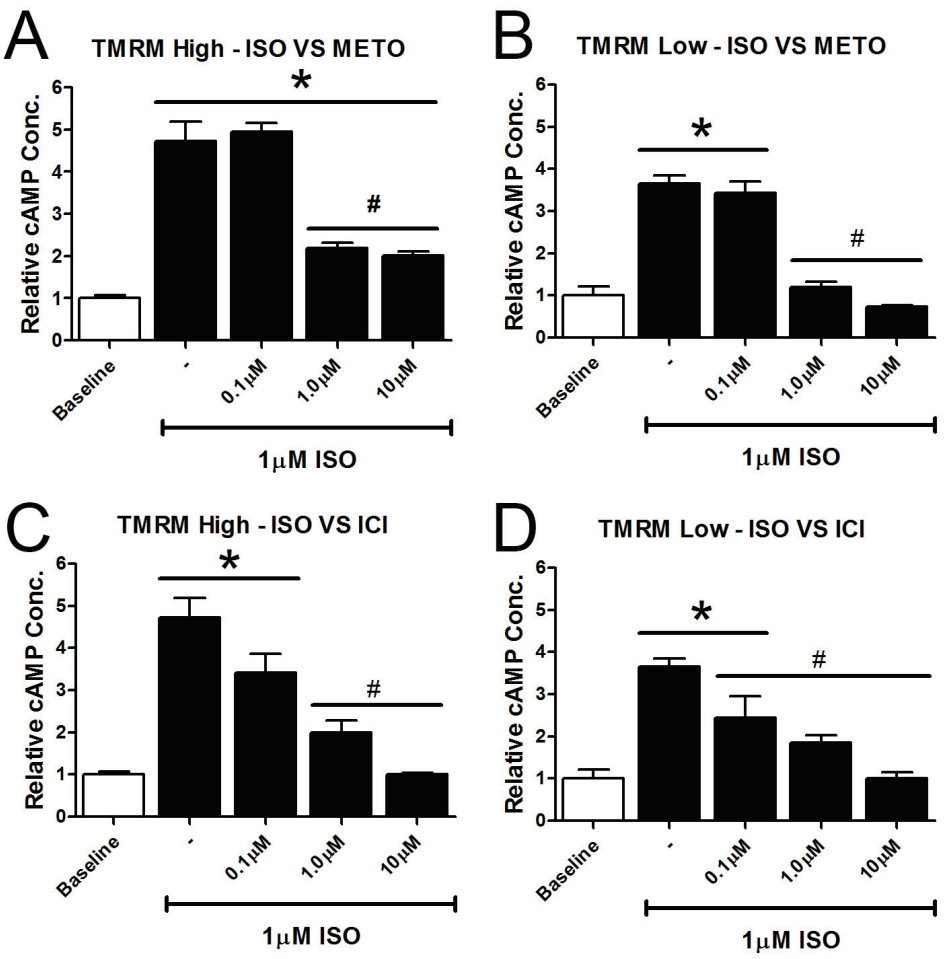

Figure 6.2 The effects of β-adrenergic receptor stimulation and inhibition on cAMP production in E11.5 TMRM high and low fractions.

Using a 3'-5'-cyclic adenosine monophosphate (cAMP) competitive immunoassay, basal cAMP levels were set to a value of 1.0 in untreated cultures. Data represent fold changes in cAMP in response to Isoproterenol (ISO) with or without blockers. **(A)** Stimulation with 1μM ISO was associated with ~4.5-fold increase in cAMP in tetramethylrhodamine methyl ester (TMRM) high fractions. Co-treatment of E11.5 TMRM high cells with ISO and the β_1-adrenergic receptor (AR) selective antagonist Metoprolol (Meto) abolished the increase in cAMP production observed with ISO alone. **(B)** Co-treatment of E11.5 TMRM high cells with ISO and the β_2-AR selective antagonist ICI-118,551 (ICI) also abolished the increase in cAMP production observed with ISO alone. **(C)** Stimulation with 1μM ISO was associated with ~3.5-fold increase in cAMP in TMRM low cells. Co-treatment of E11.5 TMRM low cells with ISO and Meto abolished the increase in cAMP production observed with ISO alone. **(D)** Co-treatment of E11.5 TMRM low cells with ISO and the ICI also abolished the increase in cAMP production observed with ISO alone. one-way ANOVA with Tukey's multiple comparison test N= 3 - 5 independent experiments, performed in duplicate wells *$p < 0.05$ vs. baseline, #$p < 0.05$ vs. ISO alone.

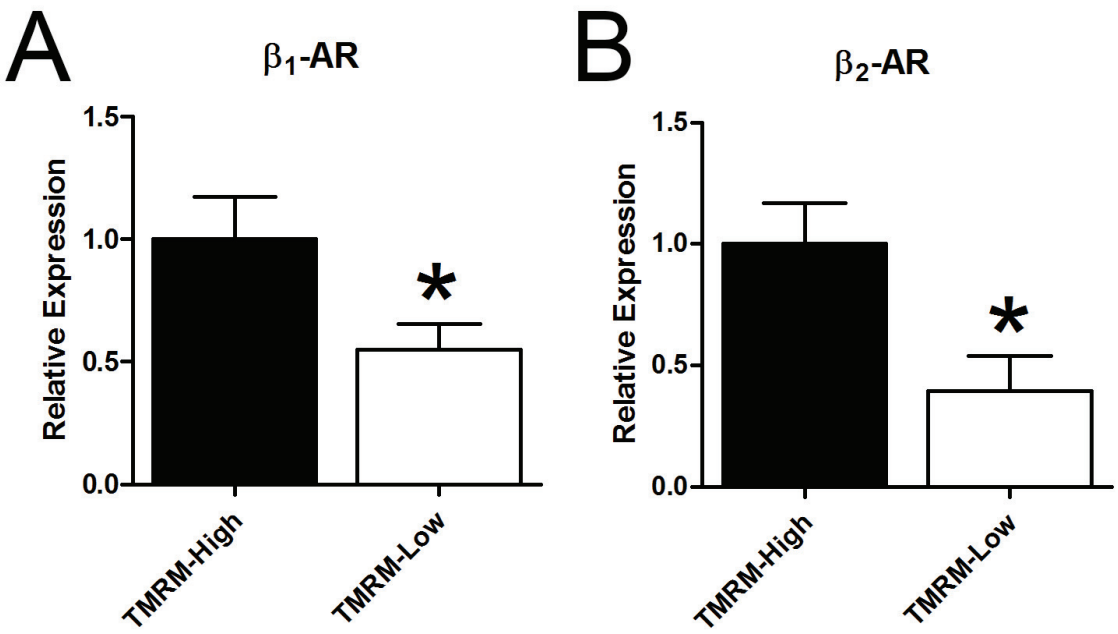

Figure 6.3 Comparison of β-adrenergic receptor gene expression between E11.5 TMRM-high and low fractions.

Quantitative polymerase chain reaction (qPCR) analysis representing relative gene expression of **(A)** β1-adrenergic receptor (AR) and **(B)** β2-AR in embryonic day (E) 11.5 tetramethylrhodamine methyl ester (TMRM) high and low fractions. N=3 experiments/ treatment group, analyzed in duplicate for each experiment, Two-tailed t-test, *$p<0.05$ vs. TMRM-high, results normalized to GAPDH.

6.3.2 Characterization of Ca^{2+} influx and intracellular Ca^{2+} fluctuations in Isoproterenol stimulated TMRM high and low fractions.

Adrenergic stimulation is coupled with the mobilization of Ca^{2+} from extracellular milieu to the cytoplasm in many cell types and also with the calcium induced calcium release from the sarcoplasmic reticulum in cardiomyocytes (Eisner et al., 2000). To determine whether the cells in TMRM high and low cultures have any differences in Ca^{2+} handling capacity, the Ca^{2+} sensitive indicator Fluo-8 AM was used to characterized Ca^{2+} influx and fluctuations in the presence of ISO. The Acetoxymethyl (AM) esters, attached to the Fluo-8 molecules, are capable of entering the cell and are quickly hydrolyzed by intracellular estrases generating charged groups that are retained within the cytoplasm. Once the Fluo-8 molecules bind to free intracellular Ca^{2+} ($[Ca^{2+}]_I$), they undergo a 200-fold increase in fluorescence intensity, which can be detected at a fluorescence intensity of 514nm and changes in fluorescence can be used to monitor intracellular Ca^{2+} fluctuations. In both TMRM low (Figure 6.4 A-D) and high (Figure 6.5 A-D) cultures, stimulation with 1μM ISO resulted in significant increase in $[Ca^{2+}]_I$ levels.

In order to quantify the total cellular Ca^{2+} influx, total cellular fluorescence was calculated using the Zeiss Zen 2012 microscope software. The change in $[Ca^{2+}]_I$ levels were calculated by setting the baseline intensity level at a value of 1.0 and changes in fluorescence intensity were calculated as fold-change compared to the baseline at 30, 60, and 90secs following stimulation. In TMRM low cultures, stimulation with 1μM ISO resulted in significant increase in $[Ca^{2+}]_I$ levels 60secs post stimulation (Figure 6.4 E). Similarly, in TMRM high cultures, stimulation with 1μM ISO resulted in significant increase in $[Ca^{2+}]_I$ levels only after 30secs post stimulation (Figure 6.5 E). These findings

indicate that compared to the TMRM low fraction, the TMRM high fraction has a more pronounced intracellular Ca^{2+} accumulation in response to β-AR stimulation.

Ca^{2+} sparks are local transient increases in intracellular calcium in resting single cardiomyocytes and represent the elementary events of SR Ca^{2+} release from SR calcium release channels or RyRs which is an underlying process for excitation-contraction coupling (Cheng et al., 1993). It has been shown that the frequency of Ca^{2+} sparks is significantly increased in response to EC coupling or opening of L-type calcium channels (Cannell et al., 1995; Cannell et al., 1994). We next examined whether there is any differences in the incidence of Ca^{2+} sparks in TMRM-low and TMRM-high cell preparations in response to ISO treatment. Using Fluo-8 and confocal microscopy, Ca^{2+} fluctuations were monitored in specific regions of interest (ROI) within the cells to determine changes in intensity due to β-AR stimulation. In both TMRM low (Figure 6.6 A-D) and high (Figure 6.7 A-D) cultures, stimulation with 1μM ISO resulted in intracellular Ca^{2+} sparks, however, the number of calcium sparks was much higher in the TMRM high cell cultures.

Quantification of fluorescence intensity in ROI limited to a single Ca^{2+} spark in TMRM low cultures treated with ISO indicated 1-2 unit changes in intensity compared to the baseline fluorescence overtime with approximately 10-12 peaks or oscillations over the 15sec interval (Figure 6.6 E). Similarly, quantification of fluorescence intensity in ROI limited to a single Ca^{2+} spark in TMRM high cultures treated with ISO also indicated 1-2 unit changes in intensity compared to the baseline fluorescence overtime with approximately 10-12 peaks over the 15sec interval (Figure 6.7 E). Collectively, these findings suggest that although TMRM low and high fractions posses similar

intracellular Ca^{2+} fluctuation capabilities, the number of regions with calcium sparks is much higher in the TMRM high fractions which could be due to their more mature differentiation nature, as CMs would possess more developed intracellular Ca^{2+} handling machinery.

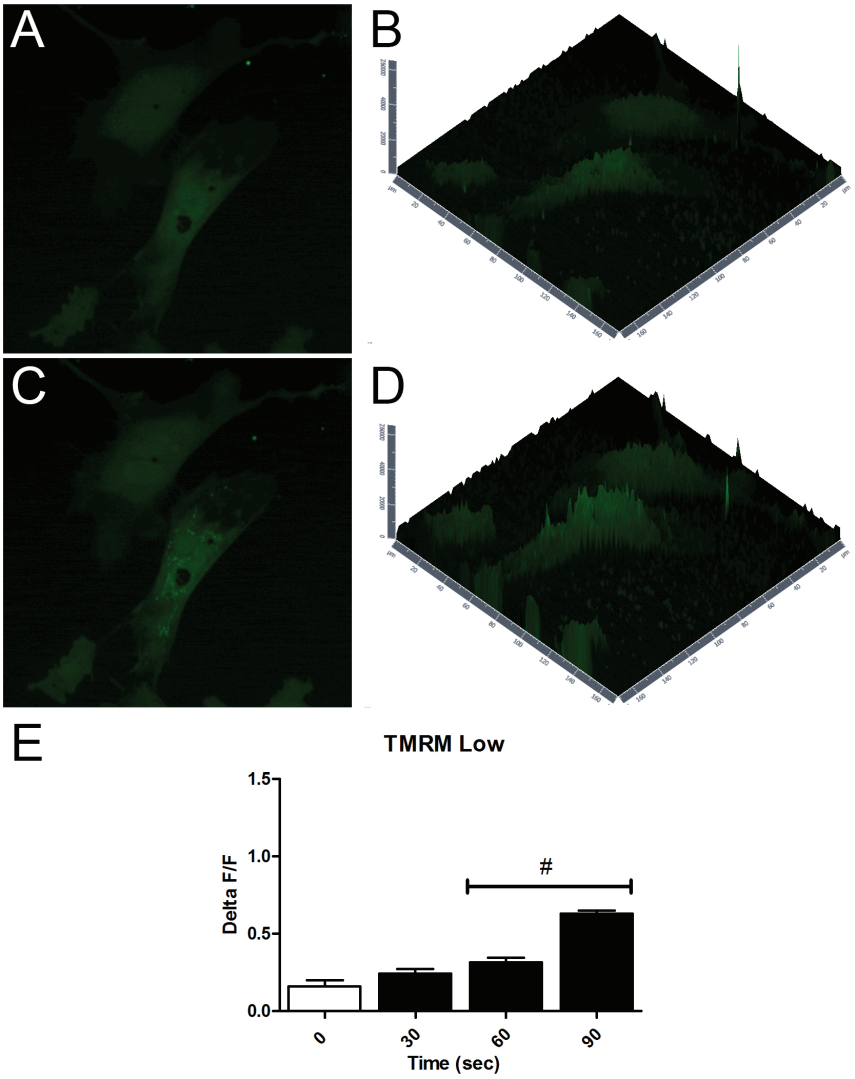

Figure 6.4 The effects of β-adrenergic receptor stimulation on intracellular Ca^{2+} fluctuations of E11.5 TMRM low cells cultured for 24 hrs.
(A) Representative micrograph of baseline fluorescence intensity in a tetramethylrhodamine methyl ester (TMRM) low cell and **(B)** represents the 2.5 dimensional (D) image of the same cell as in A, the z-axis indicates the intensity level of specific regions. **(C)** Representative micrograph of fluorescence intensity in the same TMRM low cell as seen in A post treatment with Isoproterenol (ISO) and **(D)** represent the 2.5 dimensional image of the same cell as in A post treatment with ISO, the z-axis indicates the intensity level of specific regions. **(E)** Quantification of changes in fluorescence intensity at 0, 30, 60 and 90secs time points that occurred in response to stimulation of cells with ISO. #p <0.05 vs. 0secs, one-way ANOVA with Tukey's multiple comparison test. Results are mean ± SEM, N=5 cells from 3 experiments.

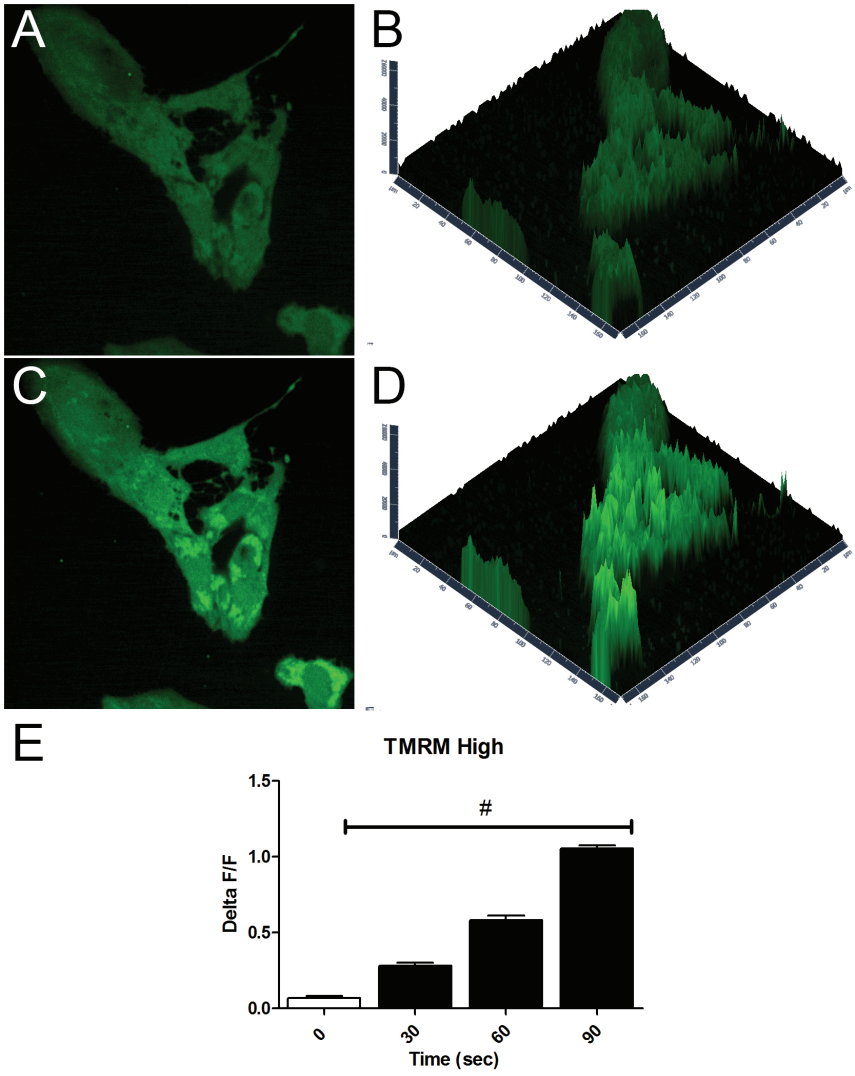

Figure 6.5 The effects of β-adrenergic receptor stimulation on intracellular Ca^{2+} fluctuations of E11.5 TMRM high cells cultured for 24 hrs.
(A) Representative micrograph of baseline fluorescence intensity in a tetramethylrhodamine methyl ester (TMRM) high cell and **(B)** represents the 2.5 dimensional (D) image of the same cell as in A, the z-axis indicates the intensity level of specific regions. **(C)** Representative micrograph of fluorescence intensity in the same TMRM high cell as seen in A post treatment with Isoproterenol (ISO) and **(D)** represent the 2.5 dimensional image of the same cell as in A post treatment with ISO, the z-axis indicates the intensity level of specific regions. **(E)** Quantification of changes in fluorescence intensity at 0, 30, 60 and 90secs time points that occurred in response to stimulation of cells with ISO. #p <0.05 vs. 0secs, one-way ANOVA with Tukey's multiple comparison test. Results are mean ± SEM, N=5 cells from 3 experiments.

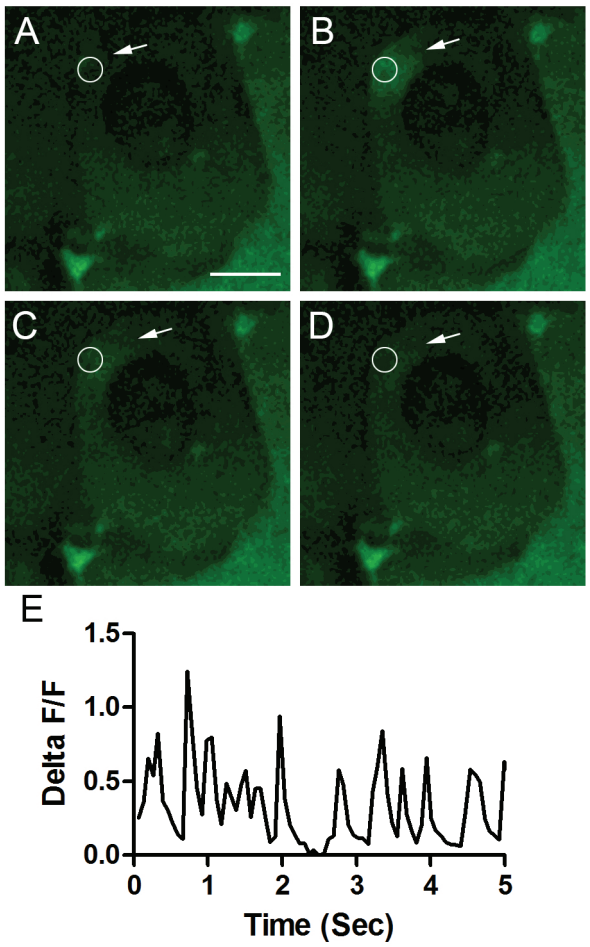

Figure 6.6 Intracellular Ca^{2+} fluctuations in E11.5 TMRM low cells cultured for 72 hrs.

(A-D) Representative sequential micrographs of Ca^{2+} fluctuation in a tetramethylrhodamine methyl ester (TMRM) high cell taken over a time frame of 1 second, arrow indicates the region of interest (ROI). **(E)** Quantification of changes in fluorescence intensity in ROI over a 15sec time period in response to stimulation of with Isoproterenol (ISO). Panel A-D: Scale bars = 10μm.

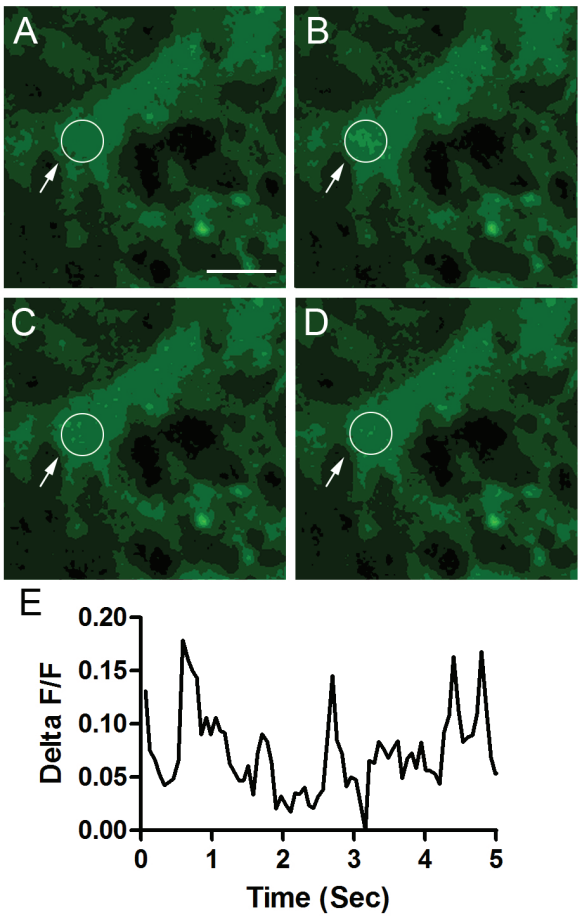

Figure 6.7 Intracellular Ca^{2+} fluctuations in E11.5 TMRM high cells cultured for 72 hrs.

(A-D) Representative sequential micrographs of Ca^{2+} fluctuation in a tetramethylrhodamine methyl ester (TMRM) high cell taken over a time frame of 1 second, arrow indicates the region of interest (ROI). **(E)** Quantification of changes in fluorescence intensity in ROI over a 15sec time period in response to stimulation of with Isoproterenol (ISO). Panel A-D: Scale bars = 10μm.

6.3.3 The role of β-AR signaling and cAMP in differentiation of E11.5 TMRM low cells into mature cardiomyocytes

Cyclic adenosine 3',5'-monophosphate (cAMP) is an important intracellular second messenger that plays a critical role in cardiac function (Zaccolo, 2009). The cAMP signaling pathway involves the activation of adenylyl cyclase (AC) leading to synthesis of cAMP from ATP (Zaccolo, 2011). Since β-AR stimulation led to increased levels of cAMP in E11.5 TMRM-low cultures, we further investigated the effects of β-adrenergic stimulation (using ISO) on cardiomyogenic differentiation of TMRM low cells.

To do so, E11.5 ventricular cells were FACS sorted according to their mitochondrial content and TMRM-low sub-populations were cultured for 48 hours in the presence or absence of 1μM ISO. Upon completion of the 48 hour time point, the TMRM low sub-population were immunolabelled with MF20 and the number of CMs ($MF20^+$) cells was quantified and expressed as number of $MF20^+$ cells per squared millimeter. Immunolabelling of TMRM low sub-populations indicated that compared to the untreated cultures (Figure 6.8 A), there may be an increase in number of CMs in 1μM ISO (Figure 6.8 B). Furthermore, the number of NMCs ($MF20^-$) in the 1μM ISO (Figure 6.8 B) also appeared to be higher compared to the untreated cultures (Figure 6.8 A).

Quantification of the CMs ($MF20^+$) indicated that compared to the untreated group (29.61±2.3 cells/mm^2), the number of $MF20^+$ cells significantly increased in cultures containing 1μM ISO (45.5±3.3 cells/mm^2). Furthermore, quantification of NMCs ($MF20^-$) indicated that compared to the untreated group (180.4±17.8 cells/mm^2), the number of NMCs was significantly higher in the 1μM ISO (452.7±31.8 cells/mm^2) cultures (Figure 6.8 E).

To further investigate whether ISO-induced myogenic differentiation of cultured TMRM low sub-population is due to the stimulation of β_1 or β_2-adrenergic receptors, cells were either cultured with 1μM of β_1-AR antagonist Meto or 1μM of β_2-AR antagonist ICI alone, and were also co-cultured with 1μM Meto or 1μM ICI in the presence of 1μM ISO. Similar to the previous experiments, the TMRM low sub-population were immunolabelled with MF20 and the number of CMs ($MF20^+$) was quantified and expressed as number of $MF20^+$ cells per squared millimeter. Immunolabelling results indicated that compared to the untreated cultures (Figure 6.9 A), the number of CMs in cultures treated with 1μM Meto alone (Figure 6.9 C) or co-treated with 1μM ISO and 1μM Meto (Figure 6.9 D) were very similar. However, compared to the untreated group, the number of CMs in cultures treated with 1μM ICI alone (Figure 6.9 E) or 1μM ISO and 1μM ICI (Figure 6.9 F) seemed noticeably lower. The number of CMs in cultures treated with 1μM ISO alone seemed higher compared to all treatment groups (Figure 6.9 B). Further, the number of NMCs in the cultures treated 1μM Meto alone, co-treated with 1μM ISO and 1μM Meto and 1μM ICI alone seemed larger compared to the untreated and those co-treated with 1μM ISO and 1μM ICI. Furthermore, cultures treated with 1μM ISO alone seemed to have a higher number of NMCs compared to all other treatment groups (Figure 6.9 F).

Quantification of the CMs ($MF20^+$) indicated that the number of MF20+ cells in cultures treated with 1μM ISO (45.5±3.3 cells/mm^2) was significantly higher compared to all treatment groups. Compared to the untreated group (29.6±2.3 cells/mm^2), the number of $MF20^+$ cells did not significantly change in cultures treated with 1μM Meto (31.3±2.6 cells/mm^2) and those co-treated with 1μM ISO and 1μM Meto (32.6±4.3 cells/mm^2)

(Figure 6.9 F). However, compared to the untreated group, the number of CMs was significantly lower in cultures treated with 1μM ICI (16.0±1.2 cells/mm^2) and also those co-treated with 1μM ISO and 1μM ICI (6.0±0.9 cells/mm^2) (Figure 6.9 F). Furthermore, the number of CMs in cultures treated with 1μM ICI and also those co-treated with 1μM ISO and 1μM ICI were significantly lower compared to the cultures treated with ISO alone and those co-treated with 1μM ISO and 1μM Meto. Quantification of NMCs ($MF20^-$) indicated that compared to the untreated group (180.4±17.8 cells/mm^2) and the group co-treated with 1μM ISO and 1μM ICI (189.3±35.7 cells/mm^2), the number of NMCs was significantly higher in those treated with 1μM ISO (452.7±31.8 cells/mm^2), 1μM Meto (334.0±26.0 cells/mm^2), co-treated with 1μM ISO and 1μM Meto (336.8±34.5 cells/mm^2), and those treated with 1μM ICI (311.0±33.9 cells/mm^2) (Figure 6.9 G).

Collectively, these results indicate that increased levels of intracellular cAMP or adrenergic stimulation can promote cardiomyogenic differentiation as well as expansion of undifferentiated cells in TMRM-low cultures. Both β_1- and β_2-ARs appear to play an important role in cardiomyogenic differentiation of TMRM-low cells.

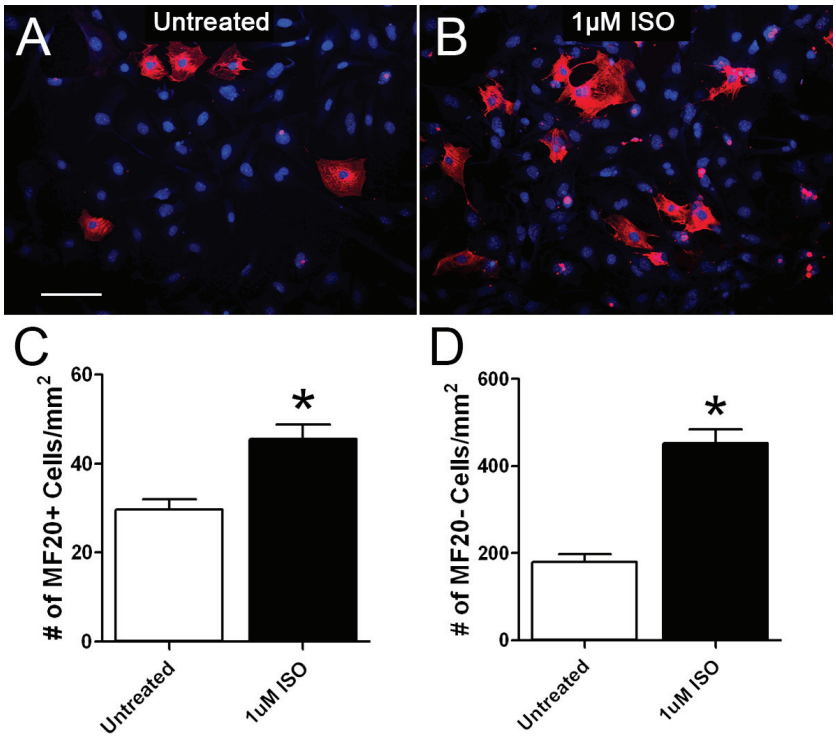

Figure 6.8 Cardiomyogenic differentiation potential of FACS sorted E11.5 TMRM low fraction ventricular cells in response to β-adrenergic stimulation.
(A, B) To characterize the differentiation potential of fluorescent activated cell sorted (FACS) embryonic day (E) 11.5 tetramethylrhodamine methyl ester (TMRM) low fraction in response to the β-adrenergic stimulation, cells were cultured for 48 hours in the **(A)** absence or **(B)** presence of 1μM Isoproterenol (ISO) and immunolabelled with sarcomeric myosin (MF20; red) marker. Representative images of were used to quantify the number of cardiomyocytes (CMs; $MF20^{+}$) and nonmyocytes (NMCs; $MF20^{-}$) per square millimeters (mm^2). **(C)** Quantification of CMs ($MF20^{+}$) cells in E11.5 TMRM low fraction indicated that compared to the untreated group, individual treatment of cells with 1μM ISO significantly increased the number of CMs. **(D)** Quantification of NMCs ($MF20^{-}$) cells in E11.5 TMRM low fraction indicated that compared to the untreated group, cultures treated with 1μM ISO showed significantly higher number of NMCs. *p <0.05 vs. untreated culture, Unpaired student's t-test. Results are mean ± SEM of 3 experiments/group. Panel A-B: Scale bars = 100μm.

Figure 6.9 Cardiomyogenic differentiation potential of FACS sorted E11.5 TMRM low fraction ventricular cells in response to β_1 and/or β_2-adrenergic stimulation.
(A-F) Embryonic day (E) 11.5 tetramethylrhodamine methyl ester (TMRM) low fraction ventricular cells were cultured for 48 hours in **(A)** the absence of any treatment or presence of **(B)** 1μM Isoproterenol (ISO), **(C)** 1μM Metoprolol (Meto), **(D)** co-treated with 1μM ISO and 1μM Meto, **(E)** 1μM ICI0118,551 (ICI), **(F)** 1μM ISO and 1μM ICI and immunolabelled with sarcomeric myosin (MF20) marker. Representative images of $MF20^+$ and $MF20^-$ cells were used to quantify the number of cardiomyocytes (CMs; $MF20^+$) and nonmyocytes (NMCs; $MF20^-$) per square millimeters (mm^2). **(G)** Quantification of CMs ($MF20^+$) cells in E11.5 TMRM low fraction indicated that compared to the untreated group, the number of CMs was significantly higher in cultures treated with 1μM ISO and significantly lower in cultures treated with 1μM ICI and co-treated with 1μM ISO and 1μM ICI. **(G)** The number of CMs in cultures treated with 1μM ISO was significantly higher compared to all cultures. **(G)** The number of CMs in cultures treated with 1μM ICI was significantly higher compared to the cultures co-treated with 1μM ISO and 1μM ICI. **(H)** Quantification of NMCs ($MF20^-$) indicated that compared to the untreated cultures and the cultures co-treated with 1μM ISO and 1μM ICI, the number of NMCs was significantly higher in all other cultures. Further, compared to the cultures treated with 1μM ISO alone the number of NMCs was significantly lower in cultures treated with 1μM ICI and co-treated with 1μM ISO and 1μM ICI. $*p < 0.05$ vs. untreated culture, $**p < 0.05$ vs. 1μM ISO, $\&p < 0.05$ vs. 1μM Meto, $\wedge p < 0.05$ vs. 1μM ISO and 1μM Meto, $\#p < 0.05$ vs. 1μM ISO and 1μM ICI, one-way ANOVA with Tukey's multiple comparison test. Results are mean ± SEM of 3 experiments/group. Panel's A-F: Scale bars = 100μm.

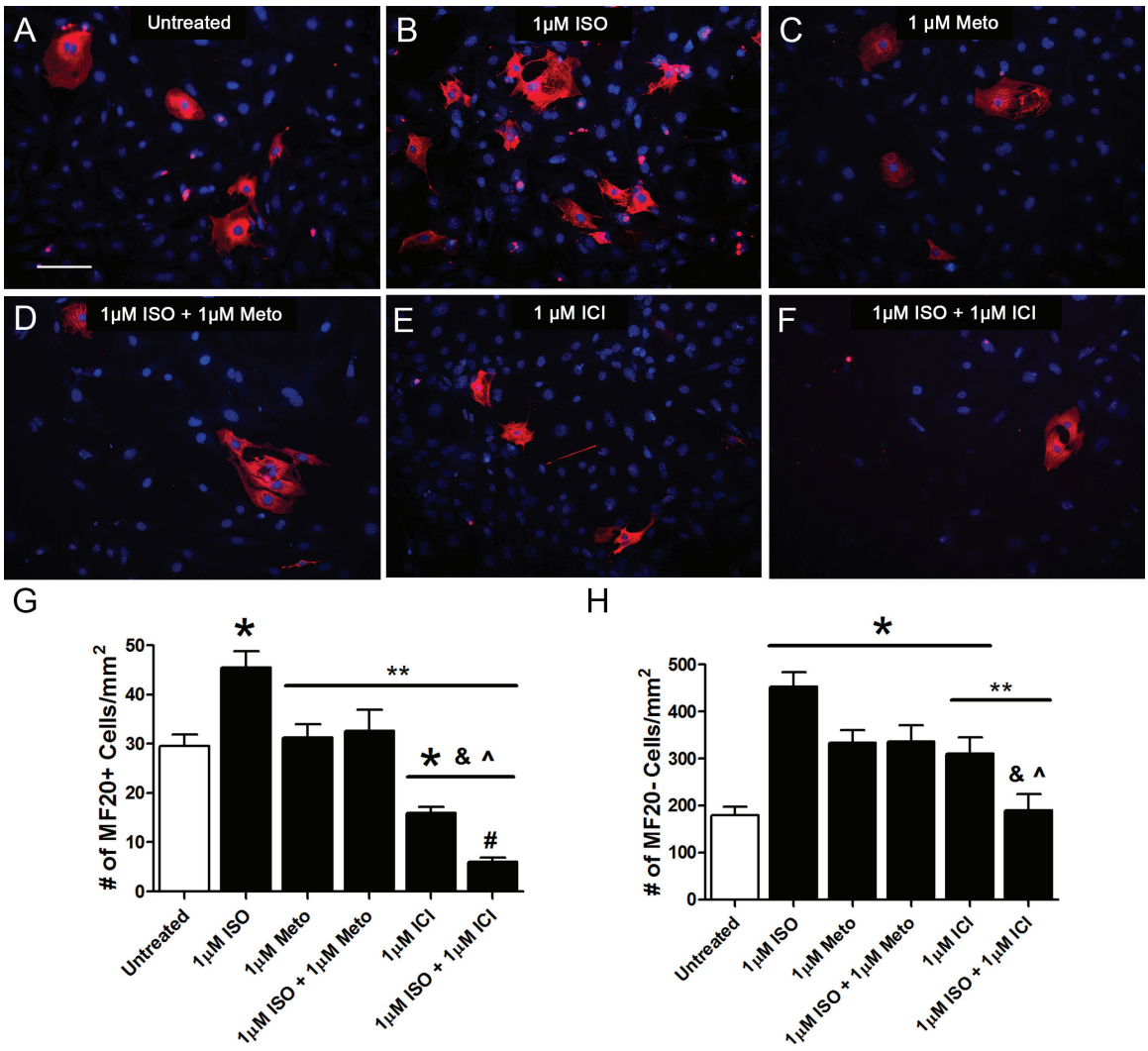
A
Untreated
B
1μM ISO
C
1 μM Meto
D
1μM ISO + 1μM Meto
E
1 μM ICI
F
1μM ISO + 1μM ICI
G
# of MF20+ Cells/mm2
0
10
20
30
40
50
*
**
* & ^
#
Untreated
1μM ISO
1μM Meto
1μM ISO + 1μM Meto
1μM ICI
1μM ISO + 1μM ICI
H
# of MF20- Cells/mm2
0
100
200
300
400
500
*
**
& ^
Untreated
1μM ISO
1μM Meto
1μM ISO + 1μM Meto
1μM ICI
1μM ISO + 1μM ICI

CHAPTER 7 DISCUSSION

7.1 Summary of results

The two primary aims of my doctoral work were to first, determine the role of β-adrenergic system in regulation of proliferation and differentiation of mid-gestation embryonic ventricular cells *in vitro* and *in vivo* and secondly, to identify a viable cell marker that could be used to enrich CPCs and CMs from a heterogeneous population of mid-gestation ventricular cells and to examine the effects of various cardiomyogenic compounds on the differentiation of CPCs *in vitro*. Our interest in gaining an understanding in the molecular mechanisms involved in regulating the proliferation and differentiation of CPCs is particularly important due to the potential use of CPCs in cell-based therapies for myocardial repair.

To date, there is limited information regarding the protective or detrimental effects of β-AR agonist and antagonists on donor cell transplantation. Results presented in this thesis demonstrated that exposure to β-AR agonist, Isoproterenol (ISO), is associated with significant decrease in cell cycle activity of mid-gestation (E11.5) CPCs and CMs *in vitro*. Furthermore, following intracardiac transplantation of E11.5 ventricular cells, a significant reduction in graft volume was observed in ventricles of recipient mice receiving a continuous dose of ISO compared to control untreated animals. Additionally, co-administration of β_1-AR antagonist, Metoprolol, was sufficient in attenuating the deleterious cell cycle effects associated with ISO, *in vitro* and *in vivo*.

Recent advancements in stem cell biology have provided scientists and clinicians with the possibility of generating functional CMs *in vitro*. However, the heterogeneous nature of such stem cell cultures is associated with increased risk of development of

teratomas upon transplantation. Hence, a clear need for the development of novel methods for enrichment of donor cells. Results presented in this thesis demonstrated that CMs and CPCs could be enriched according to their mitochondrial content using the mitochondrial content dye (tetramethylrhodamine methyl ester perchlorate; TMRM), and cells of cultured TMRM-low fraction consisting of mostly CPCs have the potential to differentiate into CMs, in presence and absence of recognized cardiomyogenic compounds.

7.2 The role of β-adrenergic receptor signaling in the regulation of cell cycle activity and differentiation in mid-gestation ventricular cells

7.2.1 Context

The role of catecholamines and β-ARs in cardiac development is quite intriguing. Catecholamines and their adrenergic receptors are present in mice as early as E8-9. Tyrosine hydroxylase knockout mice (*Th*$^{-/-}$) that lack dopamine, norepinephrine and epinephrine and dopamine-β-hydroxylase knockout mice (*Dbh*$^{-/-}$) that lack norepinephrine and epinephrine show similar patterns of lethality (75-100%) occurring during mid- to late-gestation (E11.5-E14.5) (Thomas et al., 1995; Kobayashi et al., 1995; Zhou et al., 1995). Cardiomyocytes of *Th*$^{-/-}$ and *Dbh*$^{-/-}$ mice are heterogeneous in size and are disorganized (Thomas et al., 1995; Kobayashi et al., 1995; Zhou et al., 1995). Mice lacking dopamine only are viable suggesting that dopamine may not play a significant role during embryonic heart development (Zhou & Palmiter, 1995). Collectively, these findings suggest that norepinephrine is an essential catecholamine required for embryonic development, and its activation of adrenergic receptors is essential for embryonic heart

development. Although, there is a large body of evidence suggesting the importance of norepinephrine in embryonic development, the molecular mechanisms involved in regulating the proliferation of CPCs and CMs during embryonic development are largely unknown. Thus, one of the primary aims of this thesis was to determine the role of β-ARs and the molecular pathways involved in proliferation of mid-gestation ventricular cells. Results presented in this thesis demonstrate that adrenergic stimulation of mid-gestation ventricular cells can result in decreased proliferation. This down regulation in proliferation could be attributed to decreased phosphorylation of ERK1/2 and AKT. Given the important role both of these mitogenic proteins play in the up-regulation of cyclin D1 and CDK4 gene expression, resulting in G_1/S phase cell cycle arrest of ventricular cells, supported by decreased DNA synthesis and cell proliferation data presented in this thesis.

7.2.2 Expression and function of β1 and β2-adrenergic receptors in cardiac ventricles from various development stages

Even though expression of β-AR during development has not been well studied, there is indirect evidence suggesting differences in β-AR regulation between mature and immature hearts (Hou et al., 1989). Catecholamines and their receptors have been shown to be present in rodents as early as E8 (Portbury et al., 2003). Furthermore, our findings regarding the increased expression of β-AR during embryonic development concur with previous findings, which have suggested that there is a gradual increase in β-AR density during pre- and post-natal development of the myocardium (Chen et al., 1982).

The gradual increase in the β-AR responsiveness during heart development is attributed to increased receptor expression, and AC activity, but not to the receptor's

affinity for the ligand (Chen et al., 1982). Furthermore, Kojima and colleagues have shown gradual increase in β-AR receptor binding of radio ligand [^{3}H]-dihydroalprenolol in rat ventricular myocytes starting from E16 and continuing to 20 days post-gestation (Kojima et al., 1990). These findings are in agreement with our current findings where we have shown an increase in the levels of the second messenger cAMP response in the presence of the β-AR agonist ISO in late-gestation compared to the mid-gestation ventricular cells. In agreement with our findings, where a higher concentration of the β_1-AR antagonist Metoprolol was required to inhibit ISO-induced increase in cAMP compared to β_2-AR antagonist ICI in E11.5 ventricular cells, others have shown an increase in responsiveness of β_1-AR accompanied with a decrease in β_2-AR responsiveness during post-natal development of mouse, rat, rabbit and human hearts (Roeske & Wildenthal, 1981; Whitsett et al., 1982; Schumacher et al., 1984; Kojima et al., 1990). These findings are interesting, as we did not observe any significant differences in β-AR surface protein expression between mid- and late-gestation ventricular cells, suggesting that the differences observed in cAMP production could be attributed to increased AC activity or possibly due to changes in expression pattern of AC isoforms in late-gestation ventricular cells (Hu et al., 2009). Lastly, the ablation of ISO-induced cAMP generation in response to either type of β-AR antagonist (β_1 or β_2) in our study can be explained by the β-AR's ability to dimerize (Lavoie et al., 2002). It has been suggested that β_1- and β_2-ARs require the support from each other to maintain optimal sympathetic control over their functionality, and thus, blocking one of the two receptors may be sufficient to block activation of the other receptor (Zhu et al., 2005).

Although our qPCR analysis indicated an increased expression of β_1-AR mRNA in developing embryonic hearts, our FACs analysis of surface expression of β_1-AR indicated that there is no significant different between mid- and late-gestation ventricular hearts. Gene expression is a complex multistep process, which involves transcription, translation and turnover of mRNAs and proteins. Recent studies using large scale proteome and transcriptome profiling experiments showed that relative abundance of proteins may or may not occur in proportion to their relative mRNA levels which could be due to various transcriptional, translational and protein degradation processes involved (Vogel & Marcotte, 2012). Secondly, our FACs analysis only quantified the number of cells positive for cell surface expression of β_1-AR in mid- and late-gestation ventricular cells, and did not account for cytosolic levels of β_1-ARs present within the cells. Previous studies have shown that the expression of β_1-AR is quite a dynamic event (Nakagawa & Asahi, 2013). Hence, the difference observed between the mRNA and cell surface protein expression of β_1-AR could be attributed to differences in transcriptional, translational and protein trafficking and degradation processes during cardiac development.

7.2.3 The role of β-adrenergic receptor stimulation in the proliferation of mid-gestation ventricular cells

Even though previous studies have explored the role of β-adrenergic signaling in proliferation of c-kit$^+$ adult cardiac progenitor cells (Khan et al., 2013), the effect of β-adrenergic drive on the proliferation of embryonic cardiac cells has not been studied. It is well established that changes in expression profiles of various cell cycle proteins play a pivotal role in heart development, however, the mechanisms underlying these changes in embryonic heart cells still remain unclear (Regula et al., 2004; Hotchkiss et al., 2012). As

described earlier, the β-adrenergic system response is mediated through the second messenger cAMP, which is responsible for various cardiac physiological functions (Keys & Koch, 2004).

Depending on the cell type, increased cAMP levels can result in inhibition or stimulation of cell proliferation. Our [^{3}H]-thymidine-incorporation assay and FACS findings indicated that ISO treatment results in increased number of mid-gestation ventricular cells arrested in G_1/S phase. These findings are contrary to a previous finding in which cAMP induced transition from G_0-G_1 in Swiss 3T3 fibroblasts (Schwartz & Rubin, 1983). Additionally, our thymidine-incorporation studies, combined with lineage marker analysis indicated significant decrease in proliferation of CPCs and CMs in ISO treated cultures. These findings are in agreement with other reports where increased cAMP levels resulted in decreased proliferation of NIH 3T3 fibroblasts (Mitsuzawa, 1994; Pastan et al., 1975) and smooth muscle cells (Indolfi et al., 1997; Assender et al., 1992). Further comparison of results from our [^{3}H]-thymidine-incorporation and CyQUANT assays indicated that the decreased [^{3}H]-thymidine-incorporation evident in CPCs and CMs (~50%) was not closely mirrored to changes in cell number using a CyQUANT assay (~15% decrease in cell number). This discrepancy could be attributed to the fact that while our [^{3}H]-thymidine assay allowed for quantification of [^{3}H]-thymidine incorporation specifically in CPCs and CMs, whereas the CyQUANT assay measured the overall cell number and did not distinguish between CPC, CM and NMC. It is possible that stimulation of cultures with ISO may have potentially increased the proliferation of NMCs in E11.5 cultures, which may account for a smaller change in cell number using CyQUANT assay. Alternatively, since the S-phase is the longest phase (15-

18 hrs) in mammalian cell cycle compared to the total duration required for completing one round of cell division (~24 hrs), it is possible that CyQUANT assay performed after 48-72 hr duration (as opposed to an 18 hr duration in this study) may mirror more closely to the results obtained using [^{3}H]-thymidine labeling assay. In our studies, the treatment of mid-gestation ventricular cells with ISO resulted in decrease in phosphorylation of mitogenic proteins ERK1/2 and AKT. Protein-serine/threonine kinases ERK1/2 and AKT have been shown to play a significant role in variety of cellular processes, including proliferation (Roskoski, 2012; Xu et al., 2012). Currently, it is not clear how β-AR activation leads to decreases in ERK and AKT phosphorylation in E11.5 ventricular cells. Several studies conducted on other cell types suggest potential mechanisms that may explain a connection between the cAMP pathway and ERK1/2 and AKT phosphorylation. For instance, decreased levels of phosphorylated ERK1/2 observed in ISO-treated mid-gestation ventricular cells could be attributed to, (1) inactivation of Ras via protein kinase A signaling (Indolfi et al., 1997), (2) hyperphosphorylation of MEK (Vogel et al., 2006), or (3) activation of Rap-1 and inactivation of Ras/MEK pathway (Schmitt & Stork, 2002). Additionally, it has been suggested that cAMP-induced deactivation of AKT could be attributed to blocking of membrane localization of phoinositide-dependent kinase-1 (PDK1) (Kim et al., 2001) and PKA-activated Rap1b (Lou et al., 2002). Nonetheless, additional experiments are required to precisely define the signaling events linking the β-AR activation to changes in ERK1/2 and AKT phosphorylation in mid-gestation ventricular cells.

In addition to decreased phosphorylation of ERK1/2 and AKT, ISO treatment of mid-gestation ventricular cells also resulted in significant decreases in Cyclin D1 and

CDK4 gene expression. During cardiac development, D-type cyclins are highly expressed during development and decrease after birth, suggesting that they play a critical role in regulating cell proliferation during cardiac development (Pasumarthi et al., 2005; Brooks et al., 1997). Cell cycle progression into S-phase is dependent upon the Cyclin D1/CDK4 complex's ability to link extracellular signals to cell cycle machinery, thus initiating cell cycle progression (Sherr & Roberts, 1999). Accordingly, elevated cAMP decreased phosphorylation of AKT and ERK1/2 and decreased levels of cyclin D1 and CDK4 form the basis for ISO-induced cell cycle exit in E11.5 ventricular cells. The activated AKT pathway is known to be involved in the induction of cyclin D1 expression in human fibroblasts and breast cancer cells via both transcriptional and post-transcriptional mechanisms (Muise-Helmericks et al., 1998; Ouyang et al., 2006). Contrary to these findings, activated AKT was also shown to repress the transcription of cyclin D1 gene in mouse embryonic fibroblasts (Vartanian et al., 2011). Given the down-regulation of cyclin D1 mRNA in response to decreased levels of activated AKT in our experiments, it is likely that activated AKT is necessary for the induction of cyclin D1 mRNA in E11.5 ventricular cells.

Similar to the AKT pathway, activation of ERK1/2 pathway was found to be necessary for the induction of the cyclin D1 gene (Weber et al., 1997; Lavoie et al., 1996). The precise mechanisms that connect ERK1/2 signaling to cyclin D1 transcription are not fully understood. Strong correlations exist between sustained ERK1/2 activity and expression of transcriptional regulators such as AP1, c-Jun, JunB, Fra-1 and Fra-2 (Balmanno & Cook, 1999; Murphy et al., 2002) and the cyclin D1 promoter region is known to harbor binding sites for many of these transcriptional regulators (Klein &

Assoian, 2008). Furthermore, the inhibitory effect of ISO treatment on CDK4 gene expression in E11.5 ventricular cells could be attributed to transcriptional mechanisms as reported in non-cardiac cell types. For instance, CDK4 transcription was shown to be positively regulated by the proto-oncogene, c-myc, via c-myc binding sequences in the CDK4 promoter region (Hermeking et al., 2000). In other studies, elevated intracellular cAMP was shown to significantly decrease the transcription of c-myc in myeloid cells undergoing G_1 phase (Williamson et al., 1997). Based on these studies, we speculate that ISO-induced cAMP in E11.5 ventricular cells may decrease CDK4 transcription by altering c-myc levels. At this stage, we cannot rule out the involvement of other novel mechanisms which may be responsible for the down regulation of cyclin D1 and CDK4 gene expression in ISO treated mid-gestation ventricular cells.

7.2.4 The role of β-adrenergic receptor signaling in regulation of mid-gestation ventricular cell differentiation

Recent studies suggest that the β-adrenergic system plays a significant role in maturation of cardiac stem cells. There is direct *in vivo* evidence that suggests that both depletion as well as over exposure of catecholamines can be detrimental for proper development and function of the heart. This suggests that there is a fine balance between the right type and amount of catecholamine and the period in which the myocardium is exposed to the catecholamine. For instance, extensive exposure of early (E4-5) chick embryos to epinephrine was shown to cause aortic arch anomalies (Hodach et al., 1974). Data from murine KO models suggested that E11.5-14.5 mouse embryonic development is dependent upon catecholamines, specifically norepinephrine, for proper cardiac

development and viability (Thomas et al., 1995; Kobayashi et al., 1995; Zhou et al., 1995).

Additionally, there have been *in vitro* studies demonstrating the importance of catecholamines and the β-ARs in differentiation of CPCs into CMs. For instance, Lehmann and colleagues demonstrated that catecholamine depletion of ES-derived cell cultures using reserpine, a vesicular monoamine transporter blocker, results in a significant decrease in cardiac-specific and mesodermal marker genes and proteins (Lehmann et al., 2013). Similar to reserpine treatment, pharmacological blockade of α- or β-ARs also led to a negative cardiogenic effect in ES cell cultures (Lehmann et al., 2013). In our studies with E11.5 ventricular cells, although no significant changes were evident in the expression of cardiomyogenic genes (MEF2c, GATA4, TBX4 and HAND2), ISO treatment significantly reduced the number of CPCs and significantly increased the number of CMs. In addition to effects on cardiomyogenic differentiation, our study also revealed that ISO treatment or β-AR activation does not have any significant effect on fibroblast or endothelial cell differentiation in E11.5 ventricular cultures. Collectively, our findings suggest that β-AR stimulation plays a significant role in differentiation of CPCs into CMs in of mid-gestation ventricular cell cultures.

7.3 Comparison of grafting efficiencies of mid- and late-gestation ventricular cells and the effects of β-adrenergic drugs on cell transplantation

7.3.1 Context

According to the 2014 Heart and Stroke Foundation Report on Health of Canadians, there are approximately 50,000 new patients diagnosed with heart failure.

Additionally, there is an occurrence of 70,000 new cases of heart attack patients each year. Recent advancements in management strategies, both pharmacological and surgical, have resulted in decreased mortality rates for patients suffering from major cardiovascular diseases (Lee & Ezekowitz, 2014). However, the risk factors involved in development of heart failure, such as coronary artery disease, diabetes and hypertension, are all increasing, potentially leading to a large increase in hospitalizations and burden on the health care system (Lee & Ezekowitz, 2014). Furthermore, the combination a severe shortage of cardiovascular pathologists (B. M. McManus et al., 1993) and human donors for heart transplantation (R. P. McManus et al., 1993) has increased the need for development of innovative new therapies. To this end, transplantation of donor cells in myocardial infarction and heart failure settings has emerged as a promising therapy, as most laboratory and clinical findings suggest initial improvements in cardiac function (Zhang & Pasumarthi, 2008).

Although BMMCs are the most popular choice due to their safety and ease of enrichment they have not been shown to be effective in long-term follow up studies. Additionally, low grafting efficiency and survival of intracardiac transplanted cells has also been identified as a limiting factor (Reinecke & Murry, 2002). Hence, currently, there is no consensus regarding the best cell type for transplantation. Furthermore, any patient suffering from cardiovascular disease who would require donor cell transplantation will also rely on a variety of pharmacological therapeutics (McKelvie et al., 2013). The depth of knowledge surrounding the effects of various cardiovascular drugs on the survival, proliferation and differentiation of intracardiac or intracoronary cell transplantation is quite shallow (McMullen & Pasumarthi, 2007). Cardiomyogenic

ability, higher cell cycle activity and an inability to form teratomas are all unique qualities that make CPCs an attractive candidate for intracoronary and intracardiac cell transplantation. With this in mind, one of the primary aims of this thesis was to first compare the intramuscular and intracardiac grafting efficiency of mid- and late-gestation ventricular cells. Secondly, to determine the effects of systemically administered β-AR agonist Isoproterenol and β_1-AR antagonist Metoprolol, on graft volume following transplantation of embryonic ventricular cells into adult recipient mice.

7.3.1 Grafting efficiencies of mid- and late-gestation ventricular cells in intramuscular and intracardiac transplantation models

Our findings from intramuscular and intracardiac transplantation of mid-gestation and late-gestation ventricular cells suggest that the stage of differentiation and the proliferative rate of the donor cell may play a significant role in the efficiency of myocardial repair, both in experimental and clinical studies. One of the unique qualities of CPCs, which makes them an attractive candidate for transplantation, is their high rate of proliferation, which translates into larger graft size formation. Our findings in this regard are in agreement with those obtained from embryonic striatal cell transplants in adult primate and rat brains (Fricker et al., 1997; Sladek et al., 1993). In primates, it was found that cells from an early developmental stage (E44) produced larger grafts compared to cells from a late developmental stage (E49) (Sladek et al., 1993). Furthermore, this study concluded that optimal cell survival in primates is dependent on the degree of post-germinal development of the transplanted cells (Sladek et al., 1993). Similarly, striatal primordial cells from younger donor stages (E14 and E16) resulted in larger grafts with a significantly higher number of striatal-like tissue compared to the

cells of later developmental stages (Fricker et al., 1997). Furthermore, Laflamme and colleagues demonstrated that intracardiac transplantation of ES-cell derived cardiomyocytes led to a 7-fold increase in size over a 4-week period (Laflamme et al., 2005). This increase of graft volume was also associated with increases in proliferation markers (Laflamme et al., 2005). Furthermore, our findings regarding proliferative potential of early gestation ventricular cells is in agreement with the documented regenerative ability of mid-gestation embryonic hearts, which have been shown to have an impressive capability to fully compensate for an effective loss of ~50% of cardiac tissue (Drenckhahn et al., 2008). Indeed, in both our intramuscular and intracardiac transplantation models, transplanted mid-gestation (E11.5) NCRL ventricular cells warranted larger grafts compared to the transplanted late-gestation (E14.5 and E17.5) cells. Collectively, the superior cell cycle kinetics of mid-gestation cells, along with their impressive transplantation efficiency, emphasize the importance of CPCs in post mid-gestation heart development and highlight their potential as an optimal donor cell candidate for myocardial repair.

Although the proliferation potential of a donor cell plays a significant role in graft formation, the differentiation level of the cell plays an equal part in proper graft formation. For instance, allogeneic transplantation of iPSC in the rat hearts was shown to result *in situ* tumorigenesis (Zhang et al., 2011). Similarly, transplantation of human ES derived CMs into infracted primate hearts has been show to lead to incomplete graft maturation and non-fatal arrhythmias (Chong et al., 2014). Although initial findings suggested that the engrafted myoblasts had trans-differentiated into cardiomyocytes, it was found that none of the transplanted cells expressed the gap-junction proteins required

for electromechanical coupling between one another and the host myocardium (Reinecke et al., 2002) and the majority of transplanted myoblasts were functionally isolated from the host myocardium (Leobon et al., 2003). Another unique quality of CPCs is their commitment to cardiomyogenic lineage, thus removing any concerns regarding tumorigenesis and arrhythmogenesis previously seen in undifferentiated transplanted cells.

Previous *in vitro* studies have been able to highlight the multipotency or bipotentency of mid-gestation ventricular cells based on their developmental stage. For instance, in the presence of appropriate cell growth and differentiation factors known to function during cardiogenesis, CPCs expressing the primitive streak marker *brachyury* and Flk-1 generated colonies that displayed cardiomyocyte, endothelial and vascular smooth muscle potential (Kattman et al., 2006). Furthermore, the majority of cardiac-specific Nkx2.5^{+} CPCs isolated from developing mouse embryos were shown to differentiate into CMs and conduction system cells, while, Isl-1^{+}/ c-kit^{+}/ Nkx2.5^{+} CPCs were shown to have bipotential differentiation capacity, as they were shown to differentiate into both CMs and smooth muscle cells (Wu et al., 2006). Additionally, intramuscular transplantation of undifferentiated ES-cells has been shown to result in progressively enlarging teratomas, while, transplantation of Nkx2.5^{+} CPCs resulted in generation of myofibrils expressing cardiac markers (Wu et al., 2006). These findings are congruent with our intramuscular transplantation of mid-gestation E11.5 ventricular cells, as the grafted cells maintained their Nkx2.5^{+} phenotype expressing cardiac specific markers. We have previously shown that the numbers of ventricular CPCs significantly decrease from the mid-gestation (E11.5) to late-gestation (E14.5 and E17.5) and there is a

significant increase in the population of mature CMs (McMullen, Zhang, Hotchkiss, et al., 2009). Intramuscular and intracardiac transplantation of mid-gestation (E11.5) cells resulted in significantly larger grafts containing $Nkx2.5^{+}$ CMs, expressing gap junction protein Cx43 and the cardiac differentiation marker α-CSA, but not other cell types. This data suggests that cues from the host myocardium plays a significant role in governing the differentiation of transplanted CPCs. Additionally, the absence of ECG abnormalities in recipient hearts, in addition to lack of cell fusion events seen in both intramuscular and intracardiac models, suggests that transplantation of large number of CPCs could be a safe alternative for myocardial repair.

7.3.2 Effects of non-selective β-AR agonist Isoproterenol and β_1-AR antagonist Metoprolol on graft size and differentiation of mid-gestation ventricular myocytes post-intracardiac transplantation

Increased sympathetic nerve activity associated with heart failure, has been shown to cause myocyte cell death (Lamba & Abraham, 2000). Thus, deleterious effects associated with increased norepinephrine signaling in a failing heart has provided the need for use of β-adrenergic blockers for the treatment of heart failure (Spargias et al., 1999). Further, given the reduction in cell proliferation of mid-gestation CPCs and CMs observed in response to continuous Isoproterenol (ISO) treatment, and Metoprolol's (Meto) ability to rescue CPCs and CMs from the deleterious cell cycle effects associated with ISO *in vitro*, we hypothesized that systemic administration of ISO would result in smaller grafts. However, co-administration of Meto could potentially rescue the reduced cell proliferation of intracardiac transplanted cells *in vivo*. As expected, our *in vivo* findings were in comparable with our *in vitro* findings. Results from our transplantation studies indicated that the total graft volume occupied by intracardiac transplanted NCRL

cells was significantly reduced in mice systemically treated with ISO. However, co-treatment of ISO-treated mice with Meto harbored larger graft volume occupied by intracardiac transplanted NCRL cells. These findings provide strong evidence that the interaction between systemically administered drugs and intracardiac transplanted cells should not be ignored. Based on our current experiments ISO-mediated reduction in graft volume is yet to be elucidated. We have not yet determined whether ISO-mediated reduced graft volume is attributed to reduced proliferation of intracardiac transplanted NCRL cells *in vivo*. Future work dedicated to assessing changes in cell cycle kinetics of intracardiac transplanted NCRL cells based on expression of cell cycle markers, such as PH3 or Bromodeoxyuridine (BrdU) incorporation, could be used to gain valuable insight into this important matter.

Current understanding surrounding the effects of pharmacological therapies on transplanted cells is quite shallow. It is imperative to gain insight into the beneficial or detrimental effects of pharmacological therapies on transplanted cells, as many patients who would benefit from regenerative therapies would most likely be taking multiple drugs (McKelvie et al., 2013). There is some evidence that interactions between pharmacological therapies and transplanted cells have significant impact on effectiveness of intracardiac transplantation therapies. For instance, use of heparin in the BOOST (Wollert et al., 2004) and CADUCEUS trial (Makkar et al., 2012) has come into question, as recent findings suggest that heparin interferes with the migration and homing potential of BMCs (Seeger et al., 2012). Additionally, the graft volume of intracardiac transplanted mid-gestation embryonic ventricular cells was significantly reduced in mice treated with the L-type Ca^{2+} blocker Nifedipine (Hotchkiss et al., 2014). Even though the

use of heparin and Nifedipine was deemed detrimental to grafting of transplanted cells, luckily, our results indicate that the use of Meto seems beneficial in rescuing the graft volume in recipient mice.

CV patients that would benefit from cell transplantation would be prescribed a multitude of pharmacological drugs. Hence, our findings raise the question regarding the effects of multitude of pharmacological drugs on intracardiac transplanted grafts. From a practical standpoint, our current model of cell transplantation approach would not be feasible to evaluate the effects of large number of drug combinations on engrafted cells. Based on this knowledge, higher throughput technologies need to be utilized for analyzing the effects of combinational drug therapies on transplanted cells. For instance, generation of engineered heart tissue has provided an efficient and predictive strategy for screening large numbers of parameters that may impact cell transplantation, including combinational drug therapies (Song et al., 2010). Initially, this method was used to test transplantation conditions and specific cell populations (ESC-derived CMs and CPCs) for their potential to functionally integrate within the host tissue (Song et al., 2010).

7.3.3 Potential of tail vein infusion of mid- and late-gestation ventricular cells in angiogenesis and improvement of cardiac function in doxorubicin-induced heart failure model

Evidence suggests that transplanted cells are capable of improving the function of scarred myocardium by inducing angiogenesis, myogenesis and secretion of paracrine factors, which may result in attenuation of the ventricular scar tissue (Dai et al., 2005; Orlic et al., 2003). In fact, in all studies where cardiac function and angiogenesis were scored, a positive correlation was evident with transplanted cells (Dowell et al., 2003). Kocher and colleagues have suggested that adult human BMMCs contain endothelial

precursors that could be used to directly induce new blood vessel formation in the infarct zone (vasculogenesis) and induce proliferation of preexisting vasculature (angiogenesis) (Kocher et al., 2001). For instance, transplantation of BMSCs post-AMI has been shown to increase the expression levels of HGF (hepatocyte growth factor) receptor, in male rats (Liu et al., 2004). Furthermore, intracardiac transplantation of homologous skeletal myoblasts and human derived AC-133^{+} cells was associated with increased levels of VEGF-A and TGF- β in MI-induced nude rats (Bonaros et al., 2008). Consistent with earlier reports, our findings suggest that both E11.5 and E14.5 ventricular cells can significantly improve angiogenic response in hearts of recipient mice. Additionally, fate-mapping analysis of E11.5 and E13.5 myocardium revealed that Nfatc1^{+} endocardial cells play a role in generating coronary vasculature (Wu et al., 2012). Thus, due to the heterogeneous nature of our cell preparations, the possibility that the noncardiomyogenic cells present in these preparations could contribute to the angiogenic response. Additionally, our findings suggested that tail vein infusion of E11.5 ventricular cells reduced IVSd in Dox-treated mice. However, there was no significant change in the EDV in the Dox-treated groups with or without E11.5 cells. One explanation for this phenomena could be that three day time period post Dox treatment is not sufficient for the compensatory dilation of the ventricles to take place.

Clinical analysis of patients suffering from ischemic heart disease, whom received intramyocardial autologous BMMNCs implantation, showed improved myocardial perfusion, which resulted in improved cardiac function represented by increased ejection fraction (Tse et al., 2003). These findings are in congruent with the improved cardiac function associated with tail vein infusion of mid- and late-gestation ventricular cells in

Dox-treated mice. Collectively, these findings suggest that intracardiac and intravenous transplantation of CPCs could not only harbor larger graft volume due to higher proliferative rate, but could also release cytokines and paracrine factors that could induce vasculogenesis and angiogenesis.

7.4 Enrichment of cardiac progenitor cells from a mixed population of embryonic ventricular cells and evaluation of their differentiation potential

7.4.1 Context

Our recent increased understanding of human embryonic stem cells (hESC) and induced pluripotent stem (iPSC) cell biology has provided researchers with an unlimited source of cardiomyocytes. For instance, several studies have been able to directly differentiate mouse, monkey and human ESCs into cardiomyocytes (Yuasa et al., 2005; Nemir et al., 2006; Mummery et al., 2003). Although, some protocols have achieved up to 60% differentiation efficiency, researchers have had to rely on genetic selection methods to enrich CMs from stem cell cultures (Anderson et al., 2007). From a clinical perspective, it is imperative to purify ESC-derived cardiomyocytes prior to transplantation, as transplantation of undifferentiated ESC cells has been shown to result in formation of teratomas (Kolossov et al., 2006).

Although genetic selection methods are powerful, they are not clinically feasible due to the prior requirement of genetic modification of cells using tedious techniques (Anderson et al., 2007; Kolossov et al., 2006; Hidaka et al., 2003; Fijnvandraat et al., 2003; Gassanov et al., 2004; Huber et al., 2007; Klug et al., 1996). In other studies, discontinuous Percoll density gradient centrifugation has been suggested as an alternate

method for enrichment of ESC-derived cardiomyocytes; however, the purity of this enrichment method is relatively low (Laflamme et al., 2007; Xu et al., 2006). Clearly, current methods for purification of ESC-derived cardiomyocytes are not clinically feasible; hence, there is an acute need for the development and validation of novel non-genetic selection methods for enrichment of optimal donor cells with no risk for the recipient's health. Thus, one of the main aims of this thesis was to develop and validate a novel method for the purification of CMs and CPCs from embryonic ventricular cells, and also to further characterize the effects of cardiomyogenic compounds on the differentiation of CPCs into CMs.

7.4.2 Fractionation of CMs and CPCs from embryonic ventricular cells using TMRM staining and FACs sorting techniques

Earlier findings from our laboratory established that E11.5 CMs contain a large number of mitochondria compared to undifferentiated cell population in E11.5 mouse ventricles using transmission electron microscopy (Zhang & Pasumarthi, 2007). Furthermore, Fukuda and colleagues showed that CMs have high mitochondrial content compared to other cell types and can be purified using a fluorescent dye that labels mitochondria (Hattori et al., 2010). Currently, there are various types of mitochondrial dyes that could potentially be used for enrichment of CPCs and CMs, including, MitoTracker (Green, Red, Orange, and Deep Red), Rho 123, JC-1, 10-Nonyl Acridine Orange (NAO), and tetramethylrhodamine methyl ester (TMRM). Fukuda and colleagues examined the efficacy and effects on cell viability of both marker on neonatal rat hearts and whole embryos, and concluded that TMRM possessed favorable qualities, such as (1) highest level of intensity, (2) most effective in separating CMs from NMCs and (3) no

effect on cell viability, making TMRM a great candidate for cell enrichment. Similar to the findings of Fukuda's group on TMRM labeled neonatal rat heart cells (Hattori et al., 2010), our findings also revealed three distinct populations of TMRM-labeled cells in mid- and late-gestation mouse ventricular cells after FACS sorting. These fractions consisted of mainly CMs (TMRM-high), NMCs (TMRM-low), and red blood cells and dead cells (TMRM negative). Similar to pervious findings, culturing of mid- and late-gestation TMRM low and high fractions indicated that fractionated cells from both populations are viable for at least 48-72 hrs post-culturing. In addition to these findings, we demonstrated for the first time that the cells from the mid- and late-gestation TMRM-low fractions have the potential to differentiate into CMs without any external stimulus, suggesting that the cells of TMRM-low fractions have cardiomyogenic potential.

Previous lineage tracking studies have shown that the $Nkx2.5^{+}$ cells are multipotent in nature and are able to give rise to cardiac, smooth muscle, endothelial, and conduction system cells (Moretti et al., 2006; Wu et al., 2006). Using our NCRL double transgenic mouse model, we were able to demonstrate that the majority of the cells from the TMRM-low fraction are derived from the $Nkx2.5^{+}$ cell lineage. Under routine culture conditions, mid-gestation TMRM-low fractions do not express markers for smooth muscle and endothelial cells. Furthermore, characterization of TMRM fractions using ventricular conduction system cell (VCS) markers, HCN4 and Cx40, provided evidence that cells of mid-gestation TMRM-low fractions possess the ability to differentiate into VCS, which has yet to develop during that time (Franco & Icardo, 2001).

There are two advantages of using mitochondrial content marker TMRM to enrich CPCs and CMs from embryonic ventricular cell cultures. Firstly, the TMRM method

does not require genetic modification of cells. In contrast, along with low efficiency, there are various disadvantages associated with the use of nonviral and viral systems for genetic selection methodologies. For instance, lentiviral-based genes could potentially silence genes of interest, bicistronic vector genes are inconsistent and do not allow uncoupled expression of two genes, and dual promoter vectors are driven by one promoter and may be disrupted by the other promoter (Gropp & Reubinoff, 2006). Further, transduced hESCs with lentiviral vectors have been shown to retain their self-renewal and pluripotent potential (Gropp & Reubinoff, 2006), suggesting a potential risk for tumorigenesis (Recchia et al., 2006; Tsukahara et al., 2006). Secondly, the TMRM method of purification can be highly useful for studying developmental interactions and molecular pathways involved in differentiation of CPCs into various cell-types responsible for giving rise to the myocardium. Further, this method provides the tools for studying the effects of various cardiomyogenic compounds on differentiation of CPCs into CMs and other cardiac-specific cell types.

Previous findings have indicated that fetal and neonatal rat cardiomyocytes and bone marrow mesenchymal and ESC-derived cardiomyocytes have a better chance of survival in recipient hearts (van Laake et al., 2007; Reinecke et al., 1999; Hattan et al., 2005). In Chapter 4 of this thesis, we found that the developmental stage of embryonic ventricular cells plays a critical role in graft formation. Our findings indicated that transplantation of mid-gestation ventricular cells form larger grafts compared to cells from late-gestation ventricles. However, it is not clear whether the high engraftment efficiency of mid-gestation ventricular cells is mainly due to high CPC content or due to higher cell cycle kinetics of both CPCs and CMs at that stage compared to later

development stages. Given the high enrichment efficiency associated with the TMRM staining technique, which allows for efficient fractionation of cardiomyogenic CPCs and CMs into TMRM low and high fractions, it should be feasible to examine engraftment efficiencies of CPC and CM fractions from E11.5 ventricles in future studies. Similarly, TMRM high fractions from different stages of ventricular development can be used to compare the engraftment efficiencies of CMs without the confounding effect of cardiomyogenic CPCs in transplantation experiments.

7.4.3 Effects of cardiomyogenic induction factors such as DMSO, Dynorphin B, Retinoic Acid and 5-Azacytidine on differentiation of TMRM-low fractions into CMs

Recent remarkable advances in the field of cardiac development has been attributed to the use of genetic, molecular, and biological factors to gain an understanding regarding the role of various genetic and molecular pathways involved in CPC differentiation. Several genes that regulate this process have been identified, and both *in vitro* and *in vivo* models have been used to identify their function (Srivastava & Olson, 2000). Our data suggests that cells of TMRM-low fraction have the potential of differentiating into CMs overtime, as the number of cells expressing sarcomeric myosin marker (MF20) significantly increased 24-72hrs post-culturing. Although the TMRM-low fraction revealed several cells with cardiomyogenic potential under normal culture conditions, rapid expansion of NMCs over time in these cultures clearly suggests that proliferative potential of TMRM-low cells may remain unchecked in the absence of a large number of TMRM-high CMs. This notion is further supported by the fact that a small number of NMCs observed in TMRM-high cultures did not expand significantly over time in our experiments. It is likely that growth factors or chemokines secreted from

differentiated cardiomyocytes and possibly other cell types (e.g. endocardial and epicardial cells, neurons, blood cells etc.) in embryonic ventricles may control the proliferative potential as well as cardiomyogenic fate of undifferentiated cells in TMRM-low fraction. It would be interesting to examine the effect of conditioned medium from TMRM-high cultures as well as the effect of co-culturing TMRM-low cultures with different proportions of TMRM-high CMs on the expansion of NMCs in future studies.

Subsequently, we attempted to increase the efficiency of cardiomyocyte differentiation in TMRM-low cultures by changing culture conditions. In addition to modifying the physiological conditions of the culture media, addition of cardiomyogenic induction factors have also been shown to be beneficial in increasing the efficiency of differentiation of stem cells into cardiomyocytes (Niebruegge et al., 2009). Further, different stem-cell cell lines have been shown to respond differently to similar cardiomyogenic compounds. Results obtained from this study indicate that treatment of TMRM-low fraction with low (2.8mM) and high (1% or 10mM) concentration of DMSO can significantly induce cardiac differentiation. The cardiogenic properties associated with DMSO observed in this study correlate with various other studies, that have demonstrated that this agent is capable of inducing cardiac differentiation in both P19 and ES cell lines (Jasmin et al., 2010; Edwards et al., 1983; van der Heyden et al., 2003). Treatment of P19-αMHC-EGFP cells with 1%DMSO (10mM) resulted in significant increases in both the number of beating clusters and the expression of α-MHC-promoter driven EGFP fluorochrome and cardiac transcription factors Nkx2.5, GATA4, MEF2c, and TBX5 (Gong et al., 2013). Furthermore, gap junction protein Cx43 was present in spontaneous beating clusters of P19 DMSO treated groups, suggesting that DMSO-

induced P19 cells are capable of differentiating into functionally mature CMs with the ability to propagate calcium waves (Jasmin et al., 2010).

Our findings regarding use of nuclear opioid receptor agonist Dynorphin B were quite similar to DMSO, in which the number of CMs significantly increased in TMRM-low cultures treated with this agent. Increased expression of pro-Dynorphin and Dynorphin B gene has been shown to orchestrate cardiac differentiation in P19 embryonal carcinoma cells (Ventura & Maioli, 2000). It has been suggested that the cardiomyogenic characteristics associated with Dynorphin B are attributed to its ability to activate subcellular and nuclear PKC isoenzyme activity, resulting in increased expression of cardiomyogenic genes GATA4 and Nkx2.5 (Ventura & Maioli, 2000; Ventura, Zinellu, Maninchedda & Maioli, 2003; Ventura, Zinellu, Maninchedda, Fadda, et al., 2003). These findings suggest that, similar to P19 cells, recruitment of PKC signaling in response to the dynorphinergic system and changes in expression and subcellular localization of specific PKC isoenzymes may play a significant role in the commitment of TMRM-low CPCs into CMs.

Treatment of TMRM-low fraction with retinoic acid (RA) resulted in a significant decrease in number of CMs. While previous studies suggested that RA plays an essential role in the differentiation of ventricular cell phenotype and proper development of ventricular trebeculae (Niederreither et al., 2001; Lin et al., 2010), RA treatment was also shown to limit FGF signaling and reduce the size of the cardiac field in mice (Duester, 2013). Contrary to our findings, RA was also shown to increase the number of CMs with Purkinje- and ventricular-like phenotype in ES-cell cultures (Wobus et al., 1997). This difference can be attributed to the time-sensitive role of RA in differentiation of CPCs

into CMs. It has been suggested that early-stage treatment of ES-cell cultures with RA resulted in preferential atrial cell-like phenotype, whereas late-stage treatment did not affect cardiogenic differentiation (Gassanov et al., 2008). Additionally, RA has been shown to play an essential role in regulating expression of extracellular matrix genes (fibronectin, Type IV collagen and LamininB1) required for cell seeding (Means & Gudas, 1995). Thus, a decrease in CM number in our RA treated TMRM-low cultures could be due to RA-induced reductions in the expression of (1) CM differentiation markers and/or (2) extracellular matrix markers required for cell seeding in cell culture.

Several studies have highlighted the cardiomyogenic potential of 5-Azacytidine (5-Aza) in various cell lines. For instance, 5-Aza was shown to induce expression of cardiac-specific gene markers in hESCs (sarcomeric α-actinin, cardiac troponin I and T and desmin) and P19 EC-cells (Isl-1, BMP-2, GATA4, and α-MHC) (López-Ruiz et al., 2014; Abbey & Seshagiri, 2013). Additionally, 5-Aza was shown to promote expression of both cardiac-specific genes (α-cardiac actinin, Troponin T) and skeletal myoblast-specific genes (MyoD, and myogenin) in MSC-treated cell cultures (Supokawej et al., 2013). Interestingly, our findings regarding the cardiogenic potential of 5-Aza are contrary to previously mentioned findings, as low (3μM) and high (10μM) concentrations of 5-Aza concentrations did not induce cardiac differentiation of CPCs in TMRM-low fractions. To induce further CM-differentiation in TMRM-low fraction, co-administration of exogenous growth and cardiomyogenic factors in combination with 5-Aza may be necessary. Previous findings have demonstrated that addition of other cardiomyogenic factors (such as cardiotropin-1 and oxytocin), in addition to 5-Aza, can enhance CM-induction in P19 embryonic stem cells (Paquin et al., 2002; Xinyun et al., 2010).

Cardiogenesis and CM-differentiation is governed by various intricate signaling, and transcriptional and translational mechanisms, some of which may be regulated by secreted paracrine factors (Srivastava, 2006b). In order to determine whether CMs of TMRM-high fraction released any paracrine factors that would induce differentiation of CPCs into CMs, TMRM-low fractions were cultured with 48hr-conditioned media of TMRM-high cultures. Interestingly, the number of CMs was significantly lower in TMRM-low fractions treated with 48hr TMRM high media compared to the untreated cultures. During cardiogenesis, the position of progenitor cells allows exposure of cells to various factors (such as FGF, BMP, Dkk-1and GSK3β) which are involved in regulating the proliferation and differentiation of embryonic CPCs (Reifers et al., 2000; Schultheiss et al., 1997; Marvin et al., 2001). Although it is very difficult to speculate, one could assume that the combination of released factors present in 48hr TMRM high conditioned media inhibited CM-differentiation. Exposure of embryonic CPCs to previously listed factors results in differentiation of progenitors into CMs and smooth muscle cells which is marked by the expression of key lineage regulator markers, such as Nkx2.5, GATA4, Mef2b/c, Hand1/2, Tbx5 (Lints et al., 1993; Molkentin, 2000; Guo et al., 2014; Srivastava et al., 1995; Bruneau et al., 1999). Even though our findings suggest that 48hr TMRM high conditioned media inhibits CM-differentiation, it is possible that the factors released may induce CPCs to differentiate into smooth muscle cells. Thus, future studies are necessary to characterize the NMCs present in the TMRM-low cultures treated with the conditioned media. On a similar note, it would also be important to examine the effects of different cardiomyogenic factors on NMC differentiation profiles in TMRM-low cultures.

7.5 The role of β-adrenergic receptor signaling and cyclic AMP in cardiomyogenic differentiation of mid-gestation TMRM-low cardiac progenitor cells

7.5.1 Context

We demonstrated that adrenergic stimulation of mid-gestation ventricular cells resulted in decreased proliferation and increased differentiation of CPCs in heterogeneous cultures (See Chapter 3). As previously indicated, the unique qualities of CPCs make them an attractive candidate for intracoronary and intracardiac cell transplantation, and we demonstrated that compared to late-gestation ventricular cells, transplantation of mid-gestation ventricular cells result in larger graft volumes due to higher percentage of CPCs (See Chapter 4). Further, in addition to these findings, the combination of the fluorescent dye TMRM and FACS allowed for successful enrichment of CPCs and CMs from a heterogeneous population of embryonic ventricular cells (See Chapter 5).

With this in mind, one of the primary aims of this chapter was first to compare and contrast the β-AR signaling between TMRM high and low fractions, and investigate the effects of β-adrenergic stimulation in differentiation of CPCs into CMs. Results presented in this thesis demonstrate that although the there is no significant difference with regards to cAMP accumulation in response to β-adrenergic stimulation via ISO, there is a significant difference in Ca^{2+} influx and Ca^{2+} fluctuations between the TMRM high and low fractions. Additionally, we demonstrated that β-adrenergic stimulation of TMRM low cell cultures resulted in significant increases in the number of CMs in culture.

7.5.2 β-adrenergic receptor responsiveness of FACS sorted TMRM high and low fractions of E11.5 ventricular cells

Initially, we found that compared to mid-gestation ventricular cells, cells from late-gestation ventricles respond more robustly to β-adrenergic stimulation (see Section 3.3.3). This result suggested that cAMP response to β-AR stimulation would be more prominent in TMRM high fraction compared to TMRM low fraction. Although ISO dose response curves indicated slightly different EC_{50} values for TMRM high and low fractions, treatment with 1μM ISO indicated that there is no significant difference between ISO-induced cAMP accumulations in TMRM high and low fractions. Notably, equimolar concentration of β_2-AR antagonist ICI was sufficient in attenuating ISO-induced cAMP response in TMRM high cells. In contrast, even a 10-fold higher concentration of β_1-AR antagonist Metoprolol was not sufficient to completely block the ISO response in these cells. These observations suggest that TMRM high cells may have a more prominent β_1-AR activity compared to the TMRM low cells. Additionally, equimolar concentrations of Meto and ICI were sufficient in attenuating ISO-induced cAMP response in TMRM low fractions. Interestingly, previous reports documented an increase in β_1-AR responsiveness followed by a decrease in β_2-AR responsiveness during post-natal heart development in many mammalian species (Roeske & Wildenthal, 1981; Whitsett et al., 1982; Schumacher et al., 1984; Kojima et al., 1990). Consistent with these reports, our findings suggest that as CPCs differentiate into mature CMs, β_1-AR response predominates over the β_2-AR response.

In addition to our second messenger findings, we demonstrated that compared to the TMRM-low fraction, the TMRM-high fraction has a more pronounced intracellular Ca^{2+} accumulation response to β-AR stimulation. However, it is unclear whether the

increase in Fluo-8 intensity seen in TMRM-high fractions can be attributed to influx of Ca^{2+} from the cell membrane, or release from the sarcoplasmic reticulum, or a combination of both. Further, this difference in intensity could be due to the possibility of higher number of available spare/uncoupled β-AR receptors. Previous studies have demonstrated increased sensitivity to β-AR agonists in later stages of heart development due to more efficient coupling of β-ARs to their downstream effector AC (Brown et al., 1992; Hejnova et al., 2014). Further, treatment of TMRM high and low cultures with ISO resulted in increased Ca^{2+} influx in both fractions. In cardiomyocytes, the Ca^{2+} influx through the L-type Ca^{2+} channels (LTCC) is the main pathway for ISO-induced contractility via a cascade of events leading to PKA-mediated phosphorylation of LTCC components (Okumura et al., 2003; Cooper et al., 1995). Although we have not confirmed the presence of LTCCs in TMRM-low fractions in this work, previously we previously demonstrated that E11.5 ventricular CPCs ($Nkx2.5^{+}/MF20^{-}$) possess LTCCs (Hotchkiss et al., 2014). To further address this issue, extracellular Ca^{2+} influx could be blocked by using LTCC blocker nifedipine (Hotchkiss et al., 2014), or intracellular Ca^{2+} resources could be blocked by inhibiting SR Ca^{2+} release channels RyR using 4-(2-aminopropyl)-3,5-dichloro-N,N-dimethylaniline (FLA 365) (Ostrovskaya et al., 2007). Such experiments would answer whether TMRM low cells possess LTCCs. It will be of interest to determine whether TMRM low cells have other types of calcium channels. This can be addressed by quantifying the gene and protein expression for other calcium channel subtypes using qPCR and immunolabelling of TMRM low cells as reported previously (Hotchkiss et al., 2014).

7.5.3 The role of β-adrenergic receptor system in differentiation of TMRM low fractions

Initial findings in Chapter 3 (Section 3.3.9) indicated that treatment of mid-gestation ventricular cells with ISO results in significant decrease in CPCs and significant increase in CMs. These findings were further validated here as our results with fractioned cells indicated that compared to the untreated groups, treatment of TMRM low fractions with ISO resulted in a significant increase in CM number. Various studies have highlighted the importance of cAMP in differentiation of progenitor cells such as neuronal progenitor cells and mesenchymal stem cells (Stachowiak et al., 2003; Kim et al., 2005), however, whether the role of cAMP as a pro- or anti-differentiation agent in CPCs has not yet been studied. Our findings are consistent with recent studies, where cAMP was shown to induce the differentiation of murine pluripotent ES cells into cardiomyocytes *in vitro* (Chen et al., 2006). Further, these cardiomyocytes expressed cardiac cell specific genes such as GATA4, Nkx2.5, β-MHC, ANF, and α-actin (Chen et al., 2006). On the other hand, in H9c2 cells, it was shown that cAMP-elevating agents [Forskolin (FSK), IBMX and ISO] negatively affected the differentiation of H9c2 myoblasts (Pagano et al., 2004). Collectively, our findings highlight the importance of the β-adrenergic system and cAMP in the differentiation of CPCs into CMs. Although our findings indicated a significant increase in CMs in ISO-treated TMRM low cultures, future studies are required to characterize the NMCs present, to determine whether β-AR stimulation plays a role in differentiation of NMCs into other cell types such as smooth muscle cells, endothelial cells and fibroblasts.

7.6 Limitations and future directions

The findings in this thesis indicated that the treatment of mid-gestation ventricular cells with ISO resulted in decreases in phosphorylation of mitogenic proteins ERK1/2 and AKT, leading to decrease in cell cycle activity attributed to a reduction in the expression of cell cycle genes Cyclin D1 and CDK4. Further, the ISO-induced decrease in cell cycle activity was verified using various cell proliferation assays (FACs, CyQUANT and [^{3}H]-thymidine-incorporation assay). However, our study has not further addressed the cellular mechanisms involved in ISO-induced reductions in phosphorylation status of ERK1/2 and AKT. As previously indicated, there have been several studies which have highlighted possible mechanisms of cAMP-induced reduction of cell cycle activity such as, (1) inactivation of Ras via protein kinase A signaling (Indolfi et al., 1997), (2) hyperphosphorylation of MEK (Vogel et al., 2006), (3) activation of Rap-1 and inactivation of Ras/MEK pathway (Schmitt & Stork, 2002), or (4) blockage of membrane localization of phoinositide-dependent kinase-1 (PDK1) (Kim et al., 2001) and PKA-activated Rap1b (Lou et al., 2002). Nonetheless, additional experiments are required to precisely define the signaling events linking the β-AR activation to changes in ERK 1/2 and AKT phosphorylation in mid-gestation ventricular cells.

Our findings regarding the protective effect of Metoprolol on cell cycle in the presence of ISO was quite intriguing. Thus, future work examining the effects of co-treatment of mid-gestation ventricular cells with ISO and Metoprolol on cell cycle machinery and mitogenic proteins would provide valuable insight into the molecular mechanisms involved in regulation of proliferation and differentiation of mid-gestation ventricular cells. For instance, it would be interesting to find whether protective cell cycle

effects associated with Meto *in vitro* are attributed to its ability to normalize p-ERK1/2 or p-AKT levels or both.

Given the ISO-induced reduction in cell proliferation observed in CPCs and CMs *in vitro*, we hypothesized that systemic administration of ISO would also result in significant reduction in graft volume in recipient hearts *in vivo*. As expected, results from our transplantation findings indicated a reduction in graft volume in ISO-treated recipient mice. Although our in vivo findings provided strong evidence regarding interactions between intracardiac transplanted cells and systemically administered drugs, our findings do not elucidate whether reduced graft volume is attributed to reduced cell cycle activity of transplanted cells *in vivo*. Additional experiments dedicated to assessing differences in cell cycle kinetics in ISO-treated and untreated recipient grafts should be performed using bromodexoyuridine or thymidine labeling techniques as well as immunostaining for cell proliferation markers such as PH3 or Ki-67. Our intracardiac transplantation model provided evidence that transplantation of mid-gestation ventricular cells results in a larger graft volume compared to late-gestation ventricular cells. Although we rationalized that the observed differences between graft volumes is attributed to higher cell cycle activity of E11.5 CPCs and CMs, we have not directly monitored the cell cycle profiles of intracardiac grafts in vivo and this limitation should be addressed by performing further cell cycle analysis as discussed earlier.

While TMRM based fractionation of mid-gestation ventricular cells confirmed the presence of cardiomyogenic CPCs in TMRM low fraction, it is important to identify the factor or combination of factors responsible for maximal cardiomyogenic induction as well as those responsible for prevention of NMC expansion in TMRM-low cultures. On a

similar note, it is yet to be confirmed whether purified fraction of E11.5 TMRM-low cells would form a larger intracardiac graft compared to TMRM-high cells. We could address this issue by using TMRM staining on NCRL ventricular cells to fractionate E11.5 CPCs (TMRM-low NCRL) and CMs (TMRM-high NCRL) and engraft them into recipient hearts. NCRL donor cells can be readily tracked using X-Gal or β-Gal antibody staining in the recipient hearts and graft volumes for these two cell fractions can be monitored as described in chapter 4. Additionally, our *in vitro* data demonstrated that various cardiomyogenic factors can induce differentiation of CPCs into CMs. Thus, it would be interesting to examine the effects of environment of the recipient myocardium on the differentiation of intracardiac transplanted NCRL TMRM-low CPCs.

7.7 Clinical significance

Overall, it is our hope that the findings from this thesis have provided meaningful insight into the molecular mechanisms involved in mediating proliferation and differentiation of mid-gestation ventricular cells. Further, we hope that the findings have provided a feasible and safe method for the isolation of CPCs and CMs and also, increased the knowledge regarding the molecular mechanisms underlying cell cycle regulation in donor cells. Collectively, these findings could help advance the development of effective cell-based therapies and possibly aid in the development of new cell-based therapies for treating patients with heart disease. Although recent advances in stem cell research with regards to generation of functional cardiomyocytes from induced pluripotent stem (iPS) cell cultures is quite exciting, there is still a greater degree of cellular heterogeneity in the iPS-derived cardiomyocytes. Hence, development of optimal methods for enrichment of CPCs from a mixed population of heart cells and

understanding the effects of widely used clinical drugs hold great clinical significance and could bridge the gap between the basic research and clinical use of iPS-derived myocardial cells.

REFERENCES

Abbey, D. & Seshagiri, P.B., 2013. Aza-induced cardiomyocyte differentiation of P19 EC-cells by epigenetic co-regulation and ERK signaling. *Gene*, 526(2), pp.364–73.

Ahlquist, R.P., 1980. Historical perspective. Classification of adrenoreceptors. *Journal of autonomic pharmacology*, 1(1), pp.101–6.

Ai, D. et al., 2007. Canonical Wnt signaling functions in second heart field to promote right ventricular growth. *Proceedings of the National Academy of Sciences of the United States of America*, 104(22), pp.9319–24.

Akhter, S.A. et al., 1999. In vivo inhibition of elevated myocardial beta-adrenergic receptor kinase activity in hybrid transgenic mice restores normal beta-adrenergic signaling and function. *Circulation*, 100(6), pp.648–53.

Alvarez-Dolado, M. et al., 2003. Fusion of bone-marrow-derived cells with Purkinje neurons, cardiomyocytes and hepatocytes. *Nature*, 425(6961), pp.968–73.

Amit, M. et al., 2000. Clonally derived human embryonic stem cell lines maintain pluripotency and proliferative potential for prolonged periods of culture. *Developmental biology*, 227(2), pp.271–8.

Anderson, D. et al., 2007. Transgenic enrichment of cardiomyocytes from human embryonic stem cells. *Molecular therapy : the journal of the American Society of Gene Therapy*, 15(11), pp.2027–36.

Angers, S., Salahpour, A. & Bouvier, M., 2002. Dimerization: an emerging concept for G protein-coupled receptor ontogeny and function. *Annual review of pharmacology and toxicology*, 42, pp.409–35.

Armstrong, P.W., Chiong, M.A. & Parker, J.O., 1977. Effects of propranolol on the hemodynamic, coronary sinus blood flow and myocardial metabolic response to atrial pacing. *The American journal of cardiology*, 40(1), pp.83–9.

Assender, J.W. et al., 1992. Inhibition of proliferation, but not of Ca2+ mobilization, by cyclic AMP and GMP in rabbit aortic smooth-muscle cells. *The Biochemical journal*, 288 (Pt 2, pp.527–32.

Assmus, B. et al., 2006. Transcoronary transplantation of progenitor cells after myocardial infarction. *The New England journal of medicine*, 355(12), pp.1222–32.

Assmus, B. et al., 2002. Transplantation of Progenitor Cells and Regeneration Enhancement in Acute Myocardial Infarction (TOPCARE-AMI). *Circulation*, 106(24), pp.3009–17.

Atoui, R. & Chiu, R.C.J., 2012. Concise review: immunomodulatory properties of mesenchymal stem cells in cellular transplantation: update, controversies, and unknowns. *Stem cells translational medicine*, 1(3), pp.200–5.

Baguma-Nibasheka, M. et al., 2007. Selective cyclooxygenase-2 inhibition suppresses basic fibroblast growth factor expression in human esophageal adenocarcinoma. *Molecular carcinogenesis*, 46(12), pp.971–80.

Baker, J.G., 2005. The selectivity of beta-adrenoceptor antagonists at the human beta1, beta2 and beta3 adrenoceptors. *British journal of pharmacology*, 144(3), pp.317–22.

Balmanno, K. & Cook, S.J., 1999. Sustained MAP kinase activation is required for the expression of cyclin D1, p21Cip1 and a subset of AP-1 proteins in CCL39 cells. *Oncogene*, 18(20), pp.3085–97.

Balsam, L.B. & Robbins, R.C., 2005. Haematopoietic stem cells and repair of the ischaemic heart. *Clinical science (London, England : 1979)*, 109(6), pp.483–92.

Barile, L. et al., 2007. Endogenous cardiac stem cells. *Progress in cardiovascular diseases*, 50(1), pp.31–48.

Bartunek, J. et al., 2013. Cardiopoietic stem cell therapy in heart failure: the C-CURE (Cardiopoietic stem Cell therapy in heart failURE) multicenter randomized trial with lineage-specified biologics. *Journal of the American College of Cardiology*, 61(23), pp.2329–38.

Behfar, A. et al., 2014. Cell therapy for cardiac repair--lessons from clinical trials. *Nature reviews. Cardiology*, 11(4), pp.232–46.

Beltrami, A.P. et al., 2003. Adult cardiac stem cells are multipotent and support myocardial regeneration. *Cell*, 114(6), pp.763–76.

Beltrami, A.P. et al., 2001. Evidence that human cardiac myocytes divide after myocardial infarction. *The New England journal of medicine*, 344(23), pp.1750–7.

Bergmann, O. et al., 2009. Evidence for cardiomyocyte renewal in humans. *Science (New York, N.Y.)*, 324(5923), pp.98–102.

Bergwerff, M. et al., 1998. Neural crest cell contribution to the developing circulatory system: implications for vascular morphology? *Circulation research*, 82(2), pp.221–31.

Berridge, M.J., 1997. Elementary and global aspects of calcium signalling. *The Journal of experimental biology*, 200(Pt 2), pp.315–9.

Bers, D.M., 2002. Cardiac excitation-contraction coupling. *Nature*, 415(6868), pp.198–205.

Billingham, M.E. et al., 1978. Anthracycline cardiomyopathy monitored by morphologic changes. *Cancer treatment reports*, 62(6), pp.865–72.

Bilski, A.J. et al., 1983. The pharmacology of a beta 2-selective adrenoceptor antagonist (ICI 118,551). *Journal of cardiovascular pharmacology*, 5(3), pp.430–7.

Bisognano, J.D. et al., 2000. Myocardial-directed overexpression of the human beta(1)-adrenergic receptor in transgenic mice. *Journal of molecular and cellular cardiology*, 32(5), pp.817–30.

Bittira, B. et al., 2002. In vitro preprogramming of marrow stromal cells for myocardial regeneration. *The Annals of thoracic surgery*, 74(4), pp.1154–9; discussion 1159–60.

Bolli, R. et al., 2011. Cardiac stem cells in patients with ischaemic cardiomyopathy (SCIPIO): initial results of a randomised phase 1 trial. *Lancet*, 378(9806), pp.1847–57.

Bonaros, N. et al., 2008. Neoangiogenesis after combined transplantation of skeletal myoblasts and angiopoietic progenitors leads to increased cell engraftment and lower apoptosis rates in ischemic heart failure. *Interactive cardiovascular and thoracic surgery*, 7(2), pp.249–55.

Bondue, A. & Blanpain, C., 2010. Mesp1: a key regulator of cardiovascular lineage commitment. *Circulation research*, 107(12), pp.1414–27.

Bookman, D.E. et al., 1987. Effect of neural crest ablation on development of the heart and arch arteries in the chick. *American Journal of Anatomy*, 180(4), pp.332–341.

Boudoulas, H. et al., 1977. Hypersensitivity to adrenergic stimulation after propranolol withdrawal in normal subjects. *Annals of internal medicine*, 87(4), pp.433–6.

Brade, T. et al., 2013. Embryonic heart progenitors and cardiogenesis. *Cold Spring Harbor perspectives in medicine*, 3(10), p.a013847.

Bristow, M.R. et al., 1986. Beta 1- and beta 2-adrenergic-receptor subpopulations in nonfailing and failing human ventricular myocardium: coupling of both receptor subtypes to muscle contraction and selective beta 1-receptor down-regulation in heart failure. *Circulation research*, 59(3), pp.297–309.

Bristow, M.R. et al., 1998. The role of third-generation beta-blocking agents in chronic heart failure. *Clinical cardiology*, 21(12 Suppl 1), pp.I3–13.

Brixius, K. et al., 2007. Chronic treatment with carvedilol improves Ca(2+)-dependent ATP consumption in triton X-skinned fiber preparations of human myocardium. *The Journal of pharmacology and experimental therapeutics*, 322(1), pp.222–7.

Brixius, K. et al., 2002. Increased Ca2+-sensitivity of myofibrillar tension in heart failure and its functional implication. *Basic research in cardiology*, 97 Suppl 1, pp.I111–7.

Brodde, O.E. et al., 1998. Diminished responsiveness of Gs-coupled receptors in severely failing human hearts: no difference in dilated versus ischemic cardiomyopathy. *Journal of cardiovascular pharmacology*, 31(4), pp.585–94.

Brodde, O.E. et al., 2001. Presence, distribution and physiological function of adrenergic and muscarinic receptor subtypes in the human heart. *Basic research in cardiology*, 96(6), pp.528–38.

Brodde, O.E. et al., 1986. Regional distribution of beta-adrenoceptors in the human heart: coexistence of functional beta 1- and beta 2-adrenoceptors in both atria and ventricles in severe congestive cardiomyopathy. *Journal of cardiovascular pharmacology*, 8(6), pp.1235–42.

Brooks, G. et al., 1997. Expression and activities of cyclins and cyclin-dependent kinases in developing rat ventricular myocytes. *Journal of molecular and cellular cardiology*, 29(8), pp.2261–71.

Brown, L. et al., 1992. Spare receptors for beta-adrenoceptor-mediated positive inotropic effects of catecholamines in the human heart. *Journal of cardiovascular pharmacology*, 19(2), pp.222–32.

Bruneau, B.G. et al., 1999. Chamber-specific cardiac expression of Tbx5 and heart defects in Holt-Oram syndrome. *Developmental biology*, 211(1), pp.100–8.

Brzostowski, J.A. & Kimmel, A.R., 2001. Signaling at zero G: G-protein-independent functions for 7-TM receptors. *Trends in biochemical sciences*, 26(5), pp.291–7.

Bu, L. et al., 2009. Human ISL1 heart progenitors generate diverse multipotent cardiovascular cell lineages. *Nature*, 460(7251), pp.113–7.

Buckingham, M., Meilhac, S. & Zaffran, S., 2005. Building the mammalian heart from two sources of myocardial cells. *Nature reviews. Genetics*, 6(11), pp.826–35.

Bühler, F.R. et al., 1972. Propranolol inhibition of renin secretion. A specific approach to diagnosis and treatment of renin-dependent hypertensive diseases. *The New England journal of medicine*, 287(24), pp.1209–14.

Bünemann, M. et al., 1999. Desensitization of G-protein-coupled receptors in the cardiovascular system. *Annual review of physiology*, 61, pp.169–92.

Cai, C.-L. et al., 2003. Isl1 identifies a cardiac progenitor population that proliferates prior to differentiation and contributes a majority of cells to the heart. *Developmental cell*, 5(6), pp.877–89.

Calderone, A., 2012. Nestin+ cells and healing the infarcted heart. *American journal of physiology. Heart and circulatory physiology*, 302(1), pp.H1–9.

Califf, R.M. et al., 2002. Integrating quality into the cycle of therapeutic development. *Journal of the American College of Cardiology*, 40(11), pp.1895–901.

Canaves, J.M. & Taylor, S.S., 2002. Classification and phylogenetic analysis of the cAMP-dependent protein kinase regulatory subunit family. *Journal of molecular evolution*, 54(1), pp.17–29.

Cannell, M.B., Cheng, H. & Lederer, W.J., 1994. Spatial non-uniformities in [Ca2+]i during excitation-contraction coupling in cardiac myocytes. *Biophysical journal*, 67(5), pp.1942–56.

Cannell, M.B., Cheng, H. & Lederer, W.J., 1995. The control of calcium release in heart muscle. *Science (New York, N.Y.)*, 268(5213), pp.1045–9.

Caprioli, A. et al., 2011. Nkx2-5 represses Gata1 gene expression and modulates the cellular fate of cardiac progenitors during embryogenesis. *Circulation*, 123(15), pp.1633–41.

Carafoli, E., 2002. Calcium signaling: a tale for all seasons. *Proceedings of the National Academy of Sciences of the United States of America*, 99(3), pp.1115–22.

Carreira, R.S. et al., 2006. Carvedilol: just another Beta-blocker or a powerful cardioprotector? *Cardiovascular & hematological disorders drug targets*, 6(4), pp.257–66.

Castro, R.F. et al., 2002. Failure of bone marrow cells to transdifferentiate into neural cells in vivo. *Science (New York, N.Y.)*, 297(5585), p.1299.

Chen, F.C., Yamamura, H.I. & Roeske, W.R., 1982. Adenylate cyclase and beta adrenergic receptor development in the mouse heart. *The Journal of pharmacology and experimental therapeutics*, 222(1), pp.7–13.

Chen, Y. et al., 2006. Cyclic adenosine 3',5'-monophosphate induces differentiation of mouse embryonic stem cells into cardiomyocytes. *Cell biology international*, 30(4), pp.301–7.

Cheng, H., Lederer, W.J. & Cannell, M.B., 1993. Calcium sparks: elementary events underlying excitation-contraction coupling in heart muscle. *Science (New York, N.Y.)*, 262(5134), pp.740–4.

Cheng, Y. & Zhang, C., 2010. MicroRNA-21 in cardiovascular disease. *Journal of cardiovascular translational research*, 3(3), pp.251–5.

Chiu, R.C., Zibaitis, A. & Kao, R.L., 1995. Cellular cardiomyoplasty: myocardial regeneration with satellite cell implantation. *The Annals of thoracic surgery*, 60(1), pp.12–8.

Chong, J.J.H. et al., 2014. Human embryonic-stem-cell-derived cardiomyocytes regenerate non-human primate hearts. *Nature*, 510(7504), pp.273–7.

Christoforou, N. & Gearhart, J.D., 2007. Stem cells and their potential in cell-based cardiac therapies. *Progress in cardiovascular diseases*, 49(6), pp.396–413.

Chruscinski, A.J. et al., 1999. Targeted disruption of the beta2 adrenergic receptor gene. *The Journal of biological chemistry*, 274(24), pp.16694–700.

Chugh, A.R. et al., 2012. Administration of cardiac stem cells in patients with ischemic cardiomyopathy: the SCIPIO trial: surgical aspects and interim analysis of myocardial function and viability by magnetic resonance. *Circulation*, 126(11 Suppl 1), pp.S54–64.

Cockcroft, J.R. et al., 1995. Nebivolol vasodilates human forearm vasculature: evidence for an L-arginine/NO-dependent mechanism. *The Journal of pharmacology and experimental therapeutics*, 274(3), pp.1067–71.

Colston, J.T. et al., 1994. Altered sarcolemmal calcium channel density and Ca(2+)-pump ATPase activity in tachycardia heart failure. *Cell calcium*, 16(5), pp.349–56.

Cooper, D.M., Mons, N. & Karpen, J.W., 1995. Adenylyl cyclases and the interaction between calcium and cAMP signalling. *Nature*, 374(6521), pp.421–4.

Costello, I. et al., 2011. The T-box transcription factor Eomesodermin acts upstream of Mesp1 to specify cardiac mesoderm during mouse gastrulation. *Nature cell biology*, 13(9), pp.1084–91.

Dai, W. et al., 2005. Allogeneic mesenchymal stem cell transplantation in postinfarcted rat myocardium: short- and long-term effects. *Circulation*, 112(2), pp.214–23.

Dambrot, C. et al., 2011. Cardiomyocyte differentiation of pluripotent stem cells and their use as cardiac disease models. *The Biochemical journal*, 434(1), pp.25–35.

Dawn, B. et al., 2005. Cardiac stem cells delivered intravascularly traverse the vessel barrier, regenerate infarcted myocardium, and improve cardiac function. *Proceedings of the National Academy of Sciences of the United States of America*, 102(10), pp.3766–71.

Dib, N. et al., 2005. Safety and feasibility of autologous myoblast transplantation in patients with ischemic cardiomyopathy: four-year follow-up. *Circulation*, 112(12), pp.1748–55.

Dimmeler, S., Burchfield, J. & Zeiher, A.M., 2008. Cell-based therapy of myocardial infarction. *Arteriosclerosis, thrombosis, and vascular biology*, 28(2), pp.208–16.

Dixon, R.A. et al., 1987. Structural features required for ligand binding to the beta-adrenergic receptor. *The EMBO journal*, 6(11), pp.3269–75.

Dobrzynski, H. et al., 2013. Structure, function and clinical relevance of the cardiac conduction system, including the atrioventricular ring and outflow tract tissues. *Pharmacology & therapeutics*, 139(2), pp.260–88.

Doetschman, T.C. et al., 1985. The in vitro development of blastocyst-derived embryonic stem cell lines: formation of visceral yolk sac, blood islands and myocardium. *Journal of embryology and experimental morphology*, 87, pp.27–45.

Dohlman, H.G., Caron, M.G. & Lefkowitz, R.J., 1987. A family of receptors coupled to guanine nucleotide regulatory proteins. *Biochemistry*, 26(10), pp.2657–64.

Doss, M.X., Sachinidis, A. & Hescheler, J., 2008. Human ES cell derived cardiomyocytes for cell replacement therapy: a current update. *The Chinese journal of physiology*, 51(4), pp.226–9.

Dowell, J.D. et al., 2003. Myocyte and myogenic stem cell transplantation in the heart. *Cardiovascular research*, 58(2), pp.336–50.

Drenckhahn, J.-D. et al., 2008. Compensatory growth of healthy cardiac cells in the presence of diseased cells restores tissue homeostasis during heart development. *Developmental cell*, 15(4), pp.521–33.

Du, X.J. et al., 2000. beta(2)-adrenergic receptor overexpression exacerbates development of heart failure after aortic stenosis. *Circulation*, 101(1), pp.71–7.

Duester, G., 2013. Retinoid signaling in control of progenitor cell differentiation during mouse development. *Seminars in cell & developmental biology*, 24(10-12), pp.694–700.

Dunlop, D. & Shanks, R.G., 1968. Selective blockade of adrenoceptive beta receptors in the heart. *British journal of pharmacology and chemotherapy*, 32(1), pp.201–18.

Dzurba, A. et al., 1984. Alterations in the heart sarcolemmal Ca2+ transport activity by some beta-adrenergic antagonists. *Basic research in cardiology*, 79(6), pp.620–6.

Edwards, M.K., Harris, J.F. & McBurney, M.W., 1983. Induced muscle differentiation in an embryonal carcinoma cell line. *Molecular and cellular biology*, 3(12), pp.2280–6.

Eichhorn, E.J. & Bristow, M.R., 1997. Practical guidelines for initiation of beta-adrenergic blockade in patients with chronic heart failure. *The American journal of cardiology*, 79(6), pp.794–8.

Eisner, D.A. et al., 2000. Integrative analysis of calcium cycling in cardiac muscle. *Circulation research*, 87(12), pp.1087–94.

Van Empel, V.P.M. et al., 2005. Myocyte apoptosis in heart failure. *Cardiovascular research*, 67(1), pp.21–9.

Engelhardt, S. et al., 1999. Progressive hypertrophy and heart failure in beta1-adrenergic receptor transgenic mice. *Proceedings of the National Academy of Sciences of the United States of America*, 96(12), pp.7059–64.

Evans, S.M. et al., 2010. Myocardial lineage development. *Circulation research*, 107(12), pp.1428–44.

Fabiato, A., 1983. Calcium-induced release of calcium from the cardiac sarcoplasmic reticulum. *The American journal of physiology*, 245(1), pp.C1–14.

Ferguson, D.W., Berg, W.J. & Sanders, J.S., 1990. Clinical and hemodynamic correlates of sympathetic nerve activity in normal humans and patients with heart failure: evidence from direct microneurographic recordings. *Journal of the American College of Cardiology*, 16(5), pp.1125–34.

Ferguson, J.A., 1975. Fissure-in-ano and anal stenosis. Part II: radical surgical management. *Clinics in gastroenterology*, 4(3), pp.629–34.

Feridooni, T. et al., 2011. Cardiomyocyte Specific Ablation of p53 Is Not Sufficient to Block Doxorubicin Induced Cardiac Fibrosis and Associated Cytoskeletal Changes C. Gaetano, ed. *PLoS ONE*, 6(7), p.12.

Fijnvandraat, A.C. et al., 2003. Cardiomyocytes purified from differentiated embryonic stem cells exhibit characteristics of early chamber myocardium. *Journal of molecular and cellular cardiology*, 35(12), pp.1461–72.

Filippatos, T.D. & Elisaf, M.S., 2013. Hyponatremia in patients with heart failure. *World journal of cardiology*, 5(9), pp.317–328.

Flesch, M. et al., 1999. Effect of beta-blockers on free radical-induced cardiac contractile dysfunction. *Circulation*, 100(4), pp.346–53.

Ford, E.S. et al., 2007. Explaining the decrease in U.S. deaths from coronary disease, 1980-2000. *The New England journal of medicine*, 356(23), pp.2388–98.

Formgren, H., 1976. The effect of metoprolol and practolol on lung function and blood pressure in hypertensive asthmatics. *British journal of clinical pharmacology*, 3(6), pp.1007–14.

Forrest, I.S. et al., 1970. Fluorescent labeling of psychoactive drugs. *Agressologie: revue internationale de physio-biologie et de pharmacologie appliquées aux effets de l'agression*, 11(2), pp.127–33.

Franco, D. & Icardo, J.M., 2001. Molecular characterization of the ventricular conduction system in the developing mouse heart: topographical correlation in normal and congenitally malformed hearts. *Cardiovascular research*, 49(2), pp.417–29.

Francou, A. et al., 2013. Second heart field cardiac progenitor cells in the early mouse embryo. *Biochimica et biophysica acta*, 1833(4), pp.795–8.

Fricker, R.A., Torres, E.M. & Dunnett, S.B., 1997. The effects of donor stage on the survival and function of embryonic striatal grafts in the adult rat brain. I. Morphological characteristics. *Neuroscience*, 79(3), pp.695–710.

Frielle, T. et al., 1988. Structural basis of beta-adrenergic receptor subtype specificity studied with chimeric beta 1/beta 2-adrenergic receptors. *Proceedings of the National Academy of Sciences of the United States of America*, 85(24), pp.9494–8.

Frishman, W.H., 2013. β-Adrenergic blockade in cardiovascular disease. *Journal of cardiovascular pharmacology and therapeutics*, 18(4), pp.310–9.

Gaffney, T.E. & Braunwald, E., 1963. Importance of the adrenergic nervous system in the support of circulatory function in patients with congestive heart failure. *The American journal of medicine*, 34, pp.320–4.

Garcia-Martinez, V. & Schoenwolf, G.C., 1993. Primitive-streak origin of the cardiovascular system in avian embryos. *Developmental biology*, 159(2), pp.706–19.

Gaspard, G.J. & Pasumarthi, K.B.S., 2008. Quantification of cardiac fibrosis by colour-subtractive computer-assisted image analysis. *Clinical and experimental pharmacology & physiology*, 35(5-6), pp.679–86.

Gassanov, N. et al., 2004. Endothelin induces differentiation of ANP-EGFP expressing embryonic stem cells towards a pacemaker phenotype. *FASEB journal : official publication of the Federation of American Societies for Experimental Biology*, 18(14), pp.1710–2.

Gassanov, N. et al., 2008. Retinoid acid-induced effects on atrial and pacemaker cell differentiation and expression of cardiac ion channels. *Differentiation; research in biological diversity*, 76(9), pp.971–80.

Gerhardstein, B.L. et al., 1999. Identification of the sites phosphorylated by cyclic AMP-dependent protein kinase on the beta 2 subunit of L-type voltage-dependent calcium channels. *Biochemistry*, 38(32), pp.10361–70.

Gessert, S. & Kühl, M., 2010. The multiple phases and faces of wnt signaling during cardiac differentiation and development. *Circulation research*, 107(2), pp.186–99.

Gilman, A.G., 1987. G proteins: transducers of receptor-generated signals. *Annual review of biochemistry*, 56, pp.615–49.

Gong, J. et al., 2013. SRC kinase family inhibitor PP2 promotes DMSO-induced cardiac differentiation of P19 cells and inhibits proliferation. *International journal of cardiology*, 167(4), pp.1400–5.

Greenstein, J.L. & Winslow, R.L., 2002. An integrative model of the cardiac ventricular myocyte incorporating local control of Ca2+ release. *Biophysical journal*, 83(6), pp.2918–45.

Grieskamp, T. et al., 2011. Notch signaling regulates smooth muscle differentiation of epicardium-derived cells. *Circulation research*, 108(7), pp.813–23.

Gropp, M. & Reubinoff, B., 2006. Lentiviral vector-mediated gene delivery into human embryonic stem cells. *Methods in enzymology*, 420, pp.64–81.

Guo, Y. et al., 2014. Comparative analysis reveals distinct and overlapping functions of Mef2c and Mef2d during cardiogenesis in Xenopus laevis. *PloS one*, 9(1), p.e87294.

Hall, R.A. & Lefkowitz, R.J., 2002. Regulation of G protein-coupled receptor signaling by scaffold proteins. *Circulation research*, 91(8), pp.672–80.

Hall, R.A., Premont, R.T. & Lefkowitz, R.J., 1999. Heptahelical receptor signaling: beyond the G protein paradigm. *The Journal of cell biology*, 145(5), pp.927–32.

Han, W. et al., 2002. Comparison of ion-channel subunit expression in canine cardiac Purkinje fibers and ventricular muscle. *Circulation research*, 91(9), pp.790–7.

Hansen, A. et al., 2001. Prognostic value of Doppler echocardiographic mitral inflow patterns: implications for risk stratification in patients with chronic congestive heart failure. *Journal of the American College of Cardiology*, 37(4), pp.1049–55.

Hare, J.M. et al., 2012. Comparison of allogeneic vs autologous bone marrow–derived mesenchymal stem cells delivered by transendocardial injection in patients with ischemic cardiomyopathy: the POSEIDON randomized trial. *JAMA : the journal of the American Medical Association*, 308(22), pp.2369–79.

Hattan, N. et al., 2005. Purified cardiomyocytes from bone marrow mesenchymal stem cells produce stable intracardiac grafts in mice. *Cardiovascular research*, 65(2), pp.334–44.

Hattori, F. et al., 2010. Nongenetic method for purifying stem cell-derived cardiomyocytes. *Nature methods*, 7(1), pp.61–6.

Hayes, A. & Cooper, R.G., 1971. Studies on the absorption, distribution and excretion of propranolol in rat, dog and monkey. *The Journal of pharmacology and experimental therapeutics*, 176(2), pp.302–11.

Hejnova, L. et al., 2014. Adenylyl cyclase signaling in the developing chick heart: the deranging effect of antiarrhythmic drugs. *BioMed research international*, 2014, p.463123.

Heldman, A.W. et al., 2014. Transendocardial mesenchymal stem cells and mononuclear bone marrow cells for ischemic cardiomyopathy: the TAC-HFT randomized trial. *JAMA : the journal of the American Medical Association*, 311(1), pp.62–73.

Hermeking, H. et al., 2000. Identification of CDK4 as a target of c-MYC. *Proceedings of the National Academy of Sciences of the United States of America*, 97(5), pp.2229–34.

Van der Heyden, M.A.G. et al., 2003. P19 embryonal carcinoma cells: a suitable model system for cardiac electrophysiological differentiation at the molecular and functional level. *Cardiovascular research*, 58(2), pp.410–22.

Hidaka, K. et al., 2003. Chamber-specific differentiation of Nkx2.5-positive cardiac precursor cells from murine embryonic stem cells. *FASEB journal : official publication of the Federation of American Societies for Experimental Biology*, 17(6), pp.740–2.

Hierlihy, A.M. et al., 2002. The post-natal heart contains a myocardial stem cell population. *FEBS letters*, 530(1-3), pp.239–43.

Hirsch, A. et al., 2011. Intracoronary infusion of mononuclear cells from bone marrow or peripheral blood compared with standard therapy in patients after acute myocardial infarction treated by primary percutaneous coronary intervention: results of the randomized controlled HEBE . *European heart journal*, 32(14), pp.1736–47.

Hodach, R.J., Gilbert, E.F. & Fallon, J.F., 1974. Aortic arch anomalies associated with the administration of epinephrine in chick embryos. *Teratology*, 9(2), pp.203–9.

Hotchkiss, A. et al., 2012. Role of D-type cyclins in heart development and disease. *Canadian journal of physiology and pharmacology*, 90(9), pp.1197–207.

Hotchkiss, A. et al., 2014. The effects of calcium channel blockade on proliferation and differentiation of cardiac progenitor cells. *Cell calcium*, 55(5), pp.238–51.

Hou, Q.C., Seidler, F.J. & Slotkin, T.A., 1989. Development of the linkage of beta-adrenergic receptors to cardiac hypertrophy and heart rate control: neonatal sympathectomy with 6-hydroxydopamine. *Journal of developmental physiology*, 11(5), pp.305–11.

Hu, C.-L. et al., 2009. Adenylyl cyclase type 5 protein expression during cardiac development and stress. *American journal of physiology. Heart and circulatory physiology*, 297(5), pp.H1776–82.

Huber, I. et al., 2007. Identification and selection of cardiomyocytes during human embryonic stem cell differentiation. *FASEB journal : official publication of the Federation of American Societies for Experimental Biology*, 21(10), pp.2551–63.

Huikuri, H. V et al., 2008. Effects of intracoronary injection of mononuclear bone marrow cells on left ventricular function, arrhythmia risk profile, and restenosis after thrombolytic therapy of acute myocardial infarction. *European heart journal*, 29(22), pp.2723–32.

Ieda, M. et al., 2009. Cardiac fibroblasts regulate myocardial proliferation through beta1 integrin signaling. *Developmental cell*, 16(2), pp.233–44.

Indolfi, C. et al., 1997. Activation of cAMP-PKA signaling in vivo inhibits smooth muscle cell proliferation induced by vascular injury. *Nature medicine*, 3(7), pp.775–9.

Janssens, S. et al., 2006. Autologous bone marrow-derived stem-cell transfer in patients with ST-segment elevation myocardial infarction: double-blind, randomised controlled trial. *Lancet*, 367(9505), pp.113–21.

Jasmin et al., 2010. Chemical induction of cardiac differentiation in p19 embryonal carcinoma stem cells. *Stem cells and development*, 19(3), pp.403–12.

Jazbutyte, V. & Thum, T., 2010. MicroRNA-21: from cancer to cardiovascular disease. *Current drug targets*, 11(8), pp.926–35.

Jiang, Y. et al., 2002. Pluripotency of mesenchymal stem cells derived from adult marrow. *Nature*, 418(6893), pp.41–9.

Johnson, L.L. et al., 1988. Hemodynamic effects of labetalol in patients with combined hypertension and left ventricular failure. *Journal of cardiovascular pharmacology*, 12(3), pp.350–6.

Joyner, R.W., Wilders, R. & Wagner, M.B., 2007. Propagation of pacemaker activity. *Medical & biological engineering & computing*, 45(2), pp.177–87.

Kametani, R. et al., 2006. Carvedilol inhibits mitochondrial oxygen consumption and superoxide production during calcium overload in isolated heart mitochondria.

Circulation journal : official journal of the Japanese Circulation Society, 70(3), pp.321–6.

Kamp, T.J. & Hell, J.W., 2000. Regulation of cardiac L-type calcium channels by protein kinase A and protein kinase C. *Circulation research*, 87(12), pp.1095–102.

Kang, P.M. & Izumo, S., 2003. Apoptosis in heart: basic mechanisms and implications in cardiovascular diseases. *Trends in molecular medicine*, 9(4), pp.177–82.

Kasahara, H. et al., 1998. Cardiac and extracardiac expression of Csx/Nkx2.5 homeodomain protein. *Circulation research*, 82(9), pp.936–46.

Kattman, S.J., Huber, T.L. & Keller, G.M., 2006. Multipotent flk-1+ cardiovascular progenitor cells give rise to the cardiomyocyte, endothelial, and vascular smooth muscle lineages. *Developmental cell*, 11(5), pp.723–32.

Kelly, R.G., 2012. The second heart field. *Current topics in developmental biology*, 100, pp.33–65.

Keys, J.R. & Koch, W.J., 2004. The adrenergic pathway and heart failure. *Recent progress in hormone research*, 59, pp.13–30.

Keyte, A. & Hutson, M.R., 2012. The neural crest in cardiac congenital anomalies. *Differentiation; research in biological diversity*, 84(1), pp.25–40.

Khan, M. et al., 2013. β-Adrenergic regulation of cardiac progenitor cell death versus survival and proliferation. *Circulation research*, 112(3), pp.476–86.

Kim, S. et al., 2001. Cyclic AMP inhibits Akt activity by blocking the membrane localization of PDK1. *The Journal of biological chemistry*, 276(16), pp.12864–70.

Kim, S.-S. et al., 2005. cAMP induces neuronal differentiation of mesenchymal stem cells via activation of extracellular signal-regulated kinase/MAPK. *Neuroreport*, 16(12), pp.1357–61.

Kimelman, D., 2006. Mesoderm induction: from caps to chips. *Nature reviews. Genetics*, 7(5), pp.360–72.

Kimura, K., Ieda, M. & Fukuda, K., 2012. Development, maturation, and transdifferentiation of cardiac sympathetic nerves. *Circulation research*, 110(2), pp.325–36.

Kléber, A.G. & Rudy, Y., 2004. Basic mechanisms of cardiac impulse propagation and associated arrhythmias. *Physiological reviews*, 84(2), pp.431–88.

Klein, E.A. & Assoian, R.K., 2008. Transcriptional regulation of the cyclin D1 gene at a glance. *Journal of cell science*, 121(Pt 23), pp.3853–7.

Klug, M.G. et al., 1996. Genetically selected cardiomyocytes from differentiating embronic stem cells form stable intracardiac grafts. *The Journal of clinical investigation*, 98(1), pp.216–24.

Kobayashi, K. et al., 1995. Targeted disruption of the tyrosine hydroxylase locus results in severe catecholamine depletion and perinatal lethality in mice. *The Journal of biological chemistry*, 270(45), pp.27235–43.

Koch, W.J. et al., 1995. Cardiac function in mice overexpressing the beta-adrenergic receptor kinase or a beta ARK inhibitor. *Science (New York, N.Y.)*, 268(5215), pp.1350–3.

Koch, W.J. et al., 1994. Cellular expression of the carboxyl terminus of a G protein-coupled receptor kinase attenuates G beta gamma-mediated signaling. *The Journal of biological chemistry*, 269(8), pp.6193–7.

Kocher, A.A. et al., 2001. Neovascularization of ischemic myocardium by human bone-marrow-derived angioblasts prevents cardiomyocyte apoptosis, reduces remodeling and improves cardiac function. *Nature medicine*, 7(4), pp.430–6.

Koh, G.Y. et al., 1993. Differentiation and long-term survival of C2C12 myoblast grafts in heart. *The Journal of clinical investigation*, 92(3), pp.1548–54.

Kohout, T.A. et al., 2001. Augmentation of cardiac contractility mediated by the human beta(3)-adrenergic receptor overexpressed in the hearts of transgenic mice. *Circulation*, 104(20), pp.2485–91.

Kojima, M. et al., 1990. Developmental changes in beta-adrenoceptors, muscarinic cholinoceptors and Ca2+ channels in rat ventricular muscles. *British journal of pharmacology*, 99(2), pp.334–9.

Kolossov, E. et al., 2006. Engraftment of engineered ES cell-derived cardiomyocytes but not BM cells restores contractile function to the infarcted myocardium. *The Journal of experimental medicine*, 203(10), pp.2315–27.

Kouskoff, V. et al., 2005. Sequential development of hematopoietic and cardiac mesoderm during embryonic stem cell differentiation. *Proceedings of the National Academy of Sciences of the United States of America*, 102(37), pp.13170–5.

Kraus, F., Haenig, B. & Kispert, A., 2001. Cloning and expression analysis of the mouse T-box gene Tbx18. *Mechanisms of development*, 100(1), pp.83–6.

Kruithof, B.P.T. et al., 2006. BMP and FGF regulate the differentiation of multipotential pericardial mesoderm into the myocardial or epicardial lineage. *Developmental biology*, 295(2), pp.507–22.

Kudlacz, E.M. et al., 1990. Prenatal exposure to propranolol via continuous maternal infusion: effects on physiological and biochemical processes mediated by beta adrenergic receptors in fetal and neonatal rat lung. *The Journal of pharmacology and experimental therapeutics*, 252(1), pp.42–50.

Kunst, G. et al., 2000. Myosin binding protein C, a phosphorylation-dependent force regulator in muscle that controls the attachment of myosin heads by its interaction with myosin S2. *Circulation research*, 86(1), pp.51–8.

Van Laake, L.W. et al., 2007. Human embryonic stem cell-derived cardiomyocytes survive and mature in the mouse heart and transiently improve function after myocardial infarction. *Stem cell research*, 1(1), pp.9–24.

Laflamme, M.A. et al., 2007. Cardiomyocytes derived from human embryonic stem cells in pro-survival factors enhance function of infarcted rat hearts. *Nature biotechnology*, 25(9), pp.1015–24.

Laflamme, M.A. et al., 2005. Formation of human myocardium in the rat heart from human embryonic stem cells. *The American journal of pathology*, 167(3), pp.663–71.

Lamba, S. & Abraham, W.T., 2000. Alterations in adrenergic receptor signaling in heart failure. *Heart failure reviews*, 5(1), pp.7–16.

Laugwitz, K.-L. et al., 2005. Postnatal isl1+ cardioblasts enter fully differentiated cardiomyocyte lineages. *Nature*, 433(7026), pp.647–53.

Lavine, K.J. & Ornitz, D.M., 2008. Fibroblast growth factors and Hedgehogs: at the heart of the epicardial signaling center. *Trends in genetics : TIG*, 24(1), pp.33–40.

Lavoie, C. et al., 2002. Beta 1/beta 2-adrenergic receptor heterodimerization regulates beta 2-adrenergic receptor internalization and ERK signaling efficacy. *The Journal of biological chemistry*, 277(38), pp.35402–10.

Lavoie, J.N. et al., 1996. Cyclin D1 expression is regulated positively by the p42/p44MAPK and negatively by the p38/HOGMAPK pathway. *The Journal of biological chemistry*, 271(34), pp.20608–16.

Lee, D.S. & Ezekowitz, J.A., 2014. Risk stratification in acute heart failure. *The Canadian journal of cardiology*, 30(3), pp.312–9.

Lefkowitz, R.J., 2003. A magnificent time with the “magnificent seven” transmembrane spanning receptors. *Circulation research*, 92(4), pp.342–4.

Lehmann, L.H., Stanmore, D.A. & Backs, J., 2014. The role of endothelin-1 in the sympathetic nervous system in the heart. *Life sciences*.

Lehmann, M. et al., 2013. Evidence for a critical role of catecholamines for cardiomyocyte lineage commitment in murine embryonic stem cells. *PloS one*, 8(8), p.e70913.

Lennard, M.S. et al., 1982. Oxidation phenotype--a major determinant of metoprolol metabolism and response. *The New England journal of medicine*, 307(25), pp.1558–60.

Leobon, B. et al., 2003. Myoblasts transplanted into rat infarcted myocardium are functionally isolated from their host. *Proceedings of the National Academy of Sciences of the United States of America*, 100(13), pp.7808–11.

Li, Z. et al., 2003. Effects of two Gbetagamma-binding proteins--N-terminally truncated phosducin and beta-adrenergic receptor kinase C terminus (betaARKct)--in heart failure. *Gene therapy*, 10(16), pp.1354–61.

Liggett, S.B. et al., 2000. Early and delayed consequences of beta(2)-adrenergic receptor overexpression in mouse hearts: critical role for expression level. *Circulation*, 101(14), pp.1707–14.

Lin, S.-C. et al., 2010. Endogenous retinoic acid regulates cardiac progenitor differentiation. *Proceedings of the National Academy of Sciences of the United States of America*, 107(20), pp.9234–9.

Lints, T.J. et al., 1993. Nkx-2.5: a novel murine homeobox gene expressed in early heart progenitor cells and their myogenic descendants. *Development (Cambridge, England)*, 119(2), pp.419–31.

Liu, Y. et al., 2004. Bone marrow mononuclear cell transplantation into heart elevates the expression of angiogenic factors. *Microvascular research*, 68(3), pp.156–60.

Løkkegaard, E.C. et al., 2004. [Relation between postmenopausal hormone replacement therapy and ischemic heart based on a Danish prospective cohort study]. *Ugeskrift for laeger*, 166(20), pp.1892–4.

López-Ruiz, E. et al., 2014. Cardiomyogenic differentiation potential of human endothelial progenitor cells isolated from patients with myocardial infarction. *Cytotherapy*.

Losordo, D.W. et al., 2011. Intramyocardial, autologous CD34+ cell therapy for refractory angina. *Circulation research*, 109(4), pp.428–36.

Lou, L. et al., 2002. cAMP inhibition of Akt is mediated by activated and phosphorylated Rap1b. *The Journal of biological chemistry*, 277(36), pp.32799–806.

Lowes, B.D. et al., 2002. Myocardial gene expression in dilated cardiomyopathy treated with beta-blocking agents. *The New England journal of medicine*, 346(18), pp.1357–65.

Lunde, K. et al., 2006. Intracoronary injection of mononuclear bone marrow cells in acute myocardial infarction. *The New England journal of medicine*, 355(12), pp.1199–209.

Maack, C. et al., 2000. Different intrinsic activities of bucindolol, carvedilol and metoprolol in human failing myocardium. *British journal of pharmacology*, 130(5), pp.1131–9.

MacLellan, W.R. & Schneider, M.D., 2000. Genetic dissection of cardiac growth control pathways. *Annual review of physiology*, 62, pp.289–319.

Maczewski, M. & Mackiewicz, U., 2008. Effect of metoprolol and ivabradine on left ventricular remodelling and Ca2+ handling in the post-infarction rat heart. *Cardiovascular research*, 79(1), pp.42–51.

Madamanchi, A., 2007. Beta-adrenergic receptor signaling in cardiac function and heart failure. *McGill journal of medicine : MJM : an international forum for the advancement of medical sciences by students*, 10(2), pp.99–104.

Mahan, D.C. & Mangan, L.T., 1975. Evaluation of various protein sequences on the nutritional carry-over from gestation to lactation with first-litter sows. *The Journal of nutrition*, 105(10), pp.1291–8.

Maillet, M., van Berlo, J.H. & Molkentin, J.D., 2013. Molecular basis of physiological heart growth: fundamental concepts and new players. *Nature reviews. Molecular cell biology*, 14(1), pp.38–48.

Makino, S. et al., 1999. Cardiomyocytes can be generated from marrow stromal cells in vitro. *The Journal of clinical investigation*, 103(5), pp.697–705.

Makkar, R.R. et al., 2012. Intracoronary cardiosphere-derived cells for heart regeneration after myocardial infarction (CADUCEUS): a prospective, randomised phase 1 trial. *Lancet*, 379(9819), pp.895–904.

Mangi, A.A. et al., 2003. Mesenchymal stem cells modified with Akt prevent remodeling and restore performance of infarcted hearts. *Nature medicine*, 9(9), pp.1195–201.

Männer, J. et al., 2001. The origin, formation and developmental significance of the epicardium: a review. *Cells, tissues, organs*, 169(2), pp.89–103.

Martin, C.M. et al., 2004. Persistent expression of the ATP-binding cassette transporter, Abcg2, identifies cardiac SP cells in the developing and adult heart. *Developmental biology*, 265(1), pp.262–75.

Marvin, M.J. et al., 2001. Inhibition of Wnt activity induces heart formation from posterior mesoderm. *Genes & development*, 15(3), pp.316–27.

Marx, S.O. et al., 2000. PKA phosphorylation dissociates FKBP12.6 from the calcium release channel (ryanodine receptor): defective regulation in failing hearts. *Cell*, 101(4), pp.365–76.

Masri, C. & Chandrashekhar, Y., 2008. Apoptosis: a potentially reversible, meta-stable state of the heart. *Heart failure reviews*, 13(2), pp.175–9.

Matsuda, T. et al., 1990. Regulation of L-type pyruvate kinase gene expression by dietary fructose in normal and diabetic rats. *Journal of biochemistry*, 107(4), pp.655–60.

McKelvie, R.S. et al., 2013. The 2012 Canadian Cardiovascular Society heart failure management guidelines update: focus on acute and chronic heart failure. *The Canadian journal of cardiology*, 29(2), pp.168–81.

McManus, B.M., Wilson, J.E. & Struve, L.C., 1993. Manpower deficiencies in cardiovascular pathology. Implications for medical care of cardiovascular diseases. *Archives of pathology & laboratory medicine*, 117(6), pp.584–8.

McManus, R.P. et al., 1993. Immunosuppressant combinations in primate cardiac xenografts. A review. *Annals of the New York Academy of Sciences*, 696, pp.281–4.

McMullen, N.M., Zhang, F., Hotchkiss, A., et al., 2009. Functional characterization of cardiac progenitor cells and their derivatives in the embryonic heart post-chamber formation. *Developmental dynamics : an official publication of the American Association of Anatomists*, 238(11), pp.2787–99.

McMullen, N.M. & Pasumarthi, K.B.S., 2007. Donor cell transplantation for myocardial disease: does it complement current pharmacological therapies? *Canadian journal of physiology and pharmacology*, 85(1), pp.1–15.

McMullen, N.M., Zhang, F. & Pasumarthi, K.B.S., 2009. Assessment of embryonic myocardial cell differentiation using a dual fluorescent reporter system. *Journal of cellular and molecular medicine*, 13(9A), pp.2834–42.

Means, A.L. & Gudas, L.J., 1995. The roles of retinoids in vertebrate development. *Annual review of biochemistry*, 64, pp.201–33.

Meilhac, S.M. et al., 2003. A retrospective clonal analysis of the myocardium reveals two phases of clonal growth in the developing mouse heart. *Development (Cambridge, England)*, 130(16), pp.3877–89.

Meins, M. et al., 2000. Characterization of the human TBX20 gene, a new member of the T-Box gene family closely related to the Drosophila H15 gene. *Genomics*, 67(3), pp.317–32.

Menasché, P. et al., 2003. Autologous skeletal myoblast transplantation for severe postinfarction left ventricular dysfunction. *Journal of the American College of Cardiology*, 41(7), pp.1078–83.

Menasché, P. et al., 2008. The Myoblast Autologous Grafting in Ischemic Cardiomyopathy (MAGIC) trial: first randomized placebo-controlled study of myoblast transplantation. *Circulation*, 117(9), pp.1189–200.

Mendelowitz, D., 1999. Advances in Parasympathetic Control of Heart Rate and Cardiac Function. *News in physiological sciences : an international journal of physiology*

produced jointly by the International Union of Physiological Sciences and the American Physiological Society, 14, pp.155–161.

Metra, M., Nodari, S. & Dei Cas, L., 2001. Beta-blockade in heart failure: selective versus nonselective agents. *American journal of cardiovascular drugs : drugs, devices, and other interventions*, 1(1), pp.3–14.

Milligan, G. & White, J.H., 2001. Protein-protein interactions at G-protein-coupled receptors. *Trends in pharmacological sciences*, 22(10), pp.513–8.

Miquerol, L. et al., 2003. Gap junctional connexins in the developing mouse cardiac conduction system. *Novartis Foundation symposium*, 250, pp.80–98; discussion 98–109, 276–9.

Miquerol, L. & Kelly, R.G., 2013. Organogenesis of the vertebrate heart. *Wiley interdisciplinary reviews. Developmental biology*, 2(1), pp.17–29.

Mitsuzawa, H., 1994. Increases in cell size at START caused by hyperactivation of the cAMP pathway in Saccharomyces cerevisiae. *Molecular & general genetics : MGG*, 243(2), pp.158–65.

Mjaatvedt, C.H. et al., 2001. The outflow tract of the heart is recruited from a novel heart-forming field. *Developmental biology*, 238(1), pp.97–109.

Mochizuki, M. et al., 2007. Scavenging free radicals by low-dose carvedilol prevents redox-dependent Ca2+ leak via stabilization of ryanodine receptor in heart failure. *Journal of the American College of Cardiology*, 49(16), pp.1722–32.

Molenaar, P., Sarsero, D. & Kaumann, A.J., 1997. Proposal for the interaction of non-conventional partial agonists and catecholamines with the "putative beta 4-adrenoceptor" in mammalian heart. *Clinical and experimental pharmacology & physiology*, 24(9-10), pp.647–56.

Molkentin, J.D., 2000. The zinc finger-containing transcription factors GATA-4, -5, and -6. Ubiquitously expressed regulators of tissue-specific gene expression. *The Journal of biological chemistry*, 275(50), pp.38949–52.

Von Möllendorff, E., Reiff, K. & Neugebauer, G., 1987. Pharmacokinetics and bioavailability of carvedilol, a vasodilating beta-blocker. *European journal of clinical pharmacology*, 33(5), pp.511–3.

Monici, M., 2005. Cell and tissue autofluorescence research and diagnostic applications. *Biotechnology annual review*, 11, pp.227–56.

Moretti, A. et al., 2006. Multipotent embryonic isl1+ progenitor cells lead to cardiac, smooth muscle, and endothelial cell diversification. *Cell*, 127(6), pp.1151–65.

Muise-Helmericks, R.C. et al., 1998. Cyclin D expression is controlled post-transcriptionally via a phosphatidylinositol 3-kinase/Akt-dependent pathway. *The Journal of biological chemistry*, 273(45), pp.29864–72.

Mummery, C. et al., 2003. Differentiation of human embryonic stem cells to cardiomyocytes: role of coculture with visceral endoderm-like cells. *Circulation*, 107(21), pp.2733–40.

Mummery, C.L. et al., 2012. Differentiation of human embryonic stem cells and induced pluripotent stem cells to cardiomyocytes: a methods overview. *Circulation research*, 111(3), pp.344–58.

Murphy, L.O. et al., 2002. Molecular interpretation of ERK signal duration by immediate early gene products. *Nature cell biology*, 4(8), pp.556–64.

Murry, C.E. et al., 2004. Haematopoietic stem cells do not transdifferentiate into cardiac myocytes in myocardial infarcts. *Nature*, 428(6983), pp.664–8.

Najafi, F. & Medina, J.F., 2013. Beyond "all-or-nothing" climbing fibers: graded representation of teaching signals in Purkinje cells. *Frontiers in neural circuits*, 7, p.115.

Nakagawa, T. & Asahi, M., 2013. β1-adrenergic receptor recycles via a membranous organelle, recycling endosome, by binding with sorting nexin27. *The Journal of membrane biology*, 246(7), pp.571–9.

Nemir, M. et al., 2006. Induction of cardiogenesis in embryonic stem cells via downregulation of Notch1 signaling. *Circulation research*, 98(12), pp.1471–8.

Neugebauer, G. et al., 1987. Pharmacokinetics and disposition of carvedilol in humans. *Journal of cardiovascular pharmacology*, 10 Suppl 1, pp.S85–8.

Neves, S.R., Ram, P.T. & Iyengar, R., 2002. G protein pathways. *Science (New York, N.Y.)*, 296(5573), pp.1636–9.

Newman, P.J. et al., 1990. PECAM-1 (CD31) cloning and relation to adhesion molecules of the immunoglobulin gene superfamily. *Science (New York, N.Y.)*, 247(4947), pp.1219–22.

Ni, N.C., Li, R.-K. & Weisel, R.D., 2014. The promise and challenges of cardiac stem cell therapy. *Seminars in thoracic and cardiovascular surgery*, 26(1), pp.44–52.

Nichols, A.J., Gellai, M. & Ruffolo, R.R., 1991. Studies on the mechanism of arterial vasodilation produced by the novel antihypertensive agent, carvedilol. *Fundamental & clinical pharmacology*, 5(1), pp.25–38.

Niebruegge, S. et al., 2009. Generation of human embryonic stem cell-derived mesoderm and cardiac cells using size-specified aggregates in an oxygen-controlled bioreactor. *Biotechnology and bioengineering*, 102(2), pp.493–507.

Niederreither, K. et al., 2001. Embryonic retinoic acid synthesis is essential for heart morphogenesis in the mouse. *Development (Cambridge, England)*, 128(7), pp.1019–31.

Nies, A.S. & Shand, D.G., 1975. Clinical pharmacology of propranolol. *Circulation*, 52(1), pp.6–15.

O'Donnell, S.R. & Wanstall, J.C., 1980. Evidence that ICI 118, 551 is a potent, highly Beta 2-selective adrenoceptor antagonist and can be used to characterize Beta-adrenoceptor populations in tissues. *Life sciences*, 27(8), pp.671–7.

Oh, H. et al., 2003. Cardiac progenitor cells from adult myocardium: homing, differentiation, and fusion after infarction. *Proceedings of the National Academy of Sciences of the United States of America*, 100(21), pp.12313–8.

Okumura, S. et al., 2003. Type 5 adenylyl cyclase disruption alters not only sympathetic but also parasympathetic and calcium-mediated cardiac regulation. *Circulation research*, 93(4), pp.364–71.

Olivey, H.E. & Svensson, E.C., 2010. Epicardial-myocardial signaling directing coronary vasculogenesis. *Circulation research*, 106(5), pp.818–32.

Olshansky, B. et al., 2008. Parasympathetic nervous system and heart failure: pathophysiology and potential implications for therapy. *Circulation*, 118(8), pp.863–71.

Olson, E.N., 2004. A decade of discoveries in cardiac biology. *Nature medicine*, 10(5), pp.467–74.

Orlic, D. et al., 2001. Bone marrow cells regenerate infarcted myocardium. *Nature*, 410(6829), pp.701–5.

Orlic, D. et al., 2003. Bone marrow stem cells regenerate infarcted myocardium. *Pediatric transplantation*, 7 Suppl 3, pp.86–8.

Ostrovskaya, O. et al., 2007. Inhibition of ryanodine receptors by 4-(2-aminopropyl)-3,5-dichloro-N,N-dimethylaniline (FLA 365) in canine pulmonary arterial smooth

muscle cells. *The Journal of pharmacology and experimental therapeutics*, 323(1), pp.381–90.

Ottervanger, J.P. et al., 2001. Long-term recovery of left ventricular function after primary angioplasty for acute myocardial infarction. *European heart journal*, 22(9), pp.785–90.

Ouyang, W. et al., 2006. Essential roles of PI-3K/Akt/IKKbeta/NFkappaB pathway in cyclin D1 induction by arsenite in JB6 Cl41 cells. *Carcinogenesis*, 27(4), pp.864–73.

Packer, M. et al., 1996. The effect of carvedilol on morbidity and mortality in patients with chronic heart failure. U.S. Carvedilol Heart Failure Study Group. *The New England journal of medicine*, 334(21), pp.1349–55.

Pagano, M. et al., 2004. Differentiation of H9c2 cardiomyoblasts: The role of adenylate cyclase system. *Journal of cellular physiology*, 198(3), pp.408–16.

Paquin, J. et al., 2002. Oxytocin induces differentiation of P19 embryonic stem cells to cardiomyocytes. *Proceedings of the National Academy of Sciences of the United States of America*, 99(14), pp.9550–5.

Pastan, I.H., Johnson, G.S. & Anderson, W.B., 1975. Role of cyclic nucleotides in growth control. *Annual review of biochemistry*, 44, pp.491–522.

Pasumarthi, K.B.S. et al., 2005. Targeted expression of cyclin D2 results in cardiomyocyte DNA synthesis and infarct regression in transgenic mice. *Circulation research*, 96(1), pp.110–8.

Pérez-Pomares, J.M. et al., 2002. Experimental studies on the spatiotemporal expression of WT1 and RALDH2 in the embryonic avian heart: a model for the regulation of myocardial and valvuloseptal development by epicardially derived cells (EPDCs). *Developmental biology*, 247(2), pp.307–26.

Perin, E.C. et al., 2012. Effect of transendocardial delivery of autologous bone marrow mononuclear cells on functional capacity, left ventricular function, and perfusion in chronic heart failure: the FOCUS-CCTRN trial. *JAMA : the journal of the American Medical Association*, 307(16), pp.1717–26.

Pietschmann, P. et al., 1991. Bone metabolism in patients with functioning kidney grafts: increased serum levels of osteocalcin and parathyroid hormone despite normalisation of kidney function. *Nephron*, 59(4), pp.533–6.

Pitcher, J.A. et al., 1992. Role of beta gamma subunits of G proteins in targeting the beta-adrenergic receptor kinase to membrane-bound receptors. *Science (New York, N.Y.)*, 257(5074), pp.1264–7.

Pittenger, M.F. et al., 1999. Multilineage potential of adult human mesenchymal stem cells. *Science (New York, N.Y.)*, 284(5411), pp.143–7.

Portbury, A.L. et al., 2003. Catecholamines act via a beta-adrenergic receptor to maintain fetal heart rate and survival. *American journal of physiology. Heart and circulatory physiology*, 284(6), pp.H2069–77.

Prall, O.W.J. et al., 2007. An Nkx2-5/Bmp2/Smad1 negative feedback loop controls heart progenitor specification and proliferation. *Cell*, 128(5), pp.947–59.

Pralong, D. et al., 2005. A novel method for somatic cell nuclear transfer to mouse embryonic stem cells. *Cloning and stem cells*, 7(4), pp.265–71.

Qian, L. et al., 2012. In vivo reprogramming of murine cardiac fibroblasts into induced cardiomyocytes. *Nature*, 485(7400), pp.593–8.

Quaini, F. et al., 2002. Chimerism of the transplanted heart. *The New England journal of medicine*, 346(1), pp.5–15.

Randi, A.M., Laffan, M.A. & Starke, R.D., 2013. Von Willebrand Factor, Angiodysplasia and Angiogenesis. *Mediterranean journal of hematology and infectious diseases*, 5(1), p.e2013060.

Recchia, A. et al., 2006. Retroviral vector integration deregulates gene expression but has no consequence on the biology and function of transplanted T cells. *Proceedings of the National Academy of Sciences of the United States of America*, 103(5), pp.1457–62.

Regårdh, C.G. et al., 1974. Pharmacokinetic studies on the selective beta1-receptor antagonist metoprolol in man. *Journal of pharmacokinetics and biopharmaceutics*, 2(4), pp.347–64.

Regula, K.M. et al., 2004. Therapeutic opportunities for cell cycle re-entry and cardiac regeneration. *Cardiovascular research*, 64(3), pp.395–401.

Reifers, F. et al., 2000. Induction and differentiation of the zebrafish heart requires fibroblast growth factor 8 (fgf8/acerebellar). *Development (Cambridge, England)*, 127(2), pp.225–35.

Reiken, S. et al., 2003. Beta-blockers restore calcium release channel function and improve cardiac muscle performance in human heart failure. *Circulation*, 107(19), pp.2459–66.

Reinecke, H. et al., 1999. Survival, integration, and differentiation of cardiomyocyte grafts: a study in normal and injured rat hearts. *Circulation*, 100(2), pp.193–202.

Reinecke, H. & Murry, C.E., 2002. Taking the death toll after cardiomyocyte grafting: a reminder of the importance of quantitative biology. *Journal of molecular and cellular cardiology*, 34(3), pp.251–3.

Reinecke, H., Poppa, V. & Murry, C.E., 2002. Skeletal muscle stem cells do not transdifferentiate into cardiomyocytes after cardiac grafting. *Journal of molecular and cellular cardiology*, 34(2), pp.241–9.

Rietze, R.L. et al., 2001. Purification of a pluripotent neural stem cell from the adult mouse brain. *Nature*, 412(6848), pp.736–9.

Rindt, H., Subramaniam, A. & Robbins, J., 1995. An in vivo analysis of transcriptional elements in the mouse alpha-myosin heavy chain gene promoter. *Transgenic research*, 4(6), pp.397–405.

Rios, M. et al., 1999. Catecholamine synthesis is mediated by tyrosinase in the absence of tyrosine hydroxylase. *The Journal of neuroscience : the official journal of the Society for Neuroscience*, 19(9), pp.3519–26.

Rockman, H.A. et al., 1998. Expression of a beta-adrenergic receptor kinase 1 inhibitor prevents the development of myocardial failure in gene-targeted mice. *Proceedings of the National Academy of Sciences of the United States of America*, 95(12), pp.7000–5.

Rockman, H.A., Koch, W.J. & Lefkowitz, R.J., 2002. Seven-transmembrane-spanning receptors and heart function. *Nature*, 415(6868), pp.206–12.

Roell, W. et al., 2007. Engraftment of connexin 43-expressing cells prevents post-infarct arrhythmia. *Nature*, 450(7171), pp.819–24.

Roeske, W.R. & Wildenthal, K., 1981. Responsiveness to drugs and hormones in the murine model of cardiac ontogenesis. *Pharmacology & therapeutics*, 14(1), pp.55–66.

Rohrer, D.K. et al., 1998. Alterations in dynamic heart rate control in the beta 1-adrenergic receptor knockout mouse. *The American journal of physiology*, 274(4 Pt 2), pp.H1184–93.

Rohrer, D.K. et al., 1999. Cardiovascular and metabolic alterations in mice lacking both beta1- and beta2-adrenergic receptors. *The Journal of biological chemistry*, 274(24), pp.16701–8.

Rohrer, D.K. et al., 1996. Targeted disruption of the mouse beta1-adrenergic receptor gene: developmental and cardiovascular effects. *Proceedings of the National Academy of Sciences of the United States of America*, 93(14), pp.7375–80.

Rosenthal, N., 2001. High hopes for the heart. *The New England journal of medicine*, 344(23), pp.1785–7.

Roskoski, R., 2012. ERK1/2 MAP kinases: structure, function, and regulation. *Pharmacological research : the official journal of the Italian Pharmacological Society*, 66(2), pp.105–43.

Ross, J.J. et al., 2006. Cytokine-induced differentiation of multipotent adult progenitor cells into functional smooth muscle cells. *The Journal of clinical investigation*, 116(12), pp.3139–49.

Rubart, M. et al., 2003. Physiological coupling of donor and host cardiomyocytes after cellular transplantation. *Circulation research*, 92(11), pp.1217–24.

Ruffolo, R.R. & Feuerstein, G.Z., 1997. Pharmacology of carvedilol: rationale for use in hypertension, coronary artery disease, and congestive heart failure. *Cardiovascular drugs and therapy / sponsored by the International Society of Cardiovascular Pharmacotherapy*, 11 Suppl 1, pp.247–56.

Sanada, F. et al., 2014. c-Kit-positive cardiac stem cells nested in hypoxic niches are activated by stem cell factor reversing the aging myopathy. *Circulation research*, 114(1), pp.41–55.

Sandow, A., 1952. Excitation-contraction coupling in muscular response. *The Yale journal of biology and medicine*, 25(3), pp.176–201.

Schächinger, V. et al., 2006. Intracoronary bone marrow-derived progenitor cells in acute myocardial infarction. *The New England journal of medicine*, 355(12), pp.1210–21.

Schlaich, M.P. et al., 2003. Relation between cardiac sympathetic activity and hypertensive left ventricular hypertrophy. *Circulation*, 108(5), pp.560–5.

Schmitt, J.M. & Stork, P.J.S., 2002. PKA phosphorylation of Src mediates cAMP's inhibition of cell growth via Rap1. *Molecular cell*, 9(1), pp.85–94.

Schneider, V.A. & Mercola, M., 2001. Wnt antagonism initiates cardiogenesis in Xenopus laevis. *Genes & development*, 15(3), pp.304–15.

Scholl, A.M. & Kirby, M.L., 2009. Signals controlling neural crest contributions to the heart. *Wiley interdisciplinary reviews. Systems biology and medicine*, 1(2), pp.220–7.

Schultheiss, T.M., Burch, J.B. & Lassar, A.B., 1997. A role for bone morphogenetic proteins in the induction of cardiac myogenesis. *Genes & development*, 11(4), pp.451–62.

Schulze-Bahr, E. et al., 2003. Pacemaker channel dysfunction in a patient with sinus node disease. *The Journal of clinical investigation*, 111(10), pp.1537–45.

Schumacher, W., Mirkin, B.L. & Sheppard, J.R., 1984. Biological maturation and beta-adrenergic effectors: development of beta-adrenergic receptors in rabbit heart. *Molecular and cellular biochemistry*, 58(1-2), pp.173–81.

Schwartz, D.A. & Rubin, C.S., 1983. Regulation of cAMP-dependent protein kinase subunit levels in Friend erythroleukemic cells. Effects of differentiation and treatment with 8-Br-cAMP and methylisobutyl xanthine. *The Journal of biological chemistry*, 258(2), pp.777–84.

Schwartz, R.E. et al., 2002. Multipotent adult progenitor cells from bone marrow differentiate into functional hepatocyte-like cells. *The Journal of clinical investigation*, 109(10), pp.1291–302.

Schwartz, Y. & Kornowski, R., 2003. Progenitor and embryonic stem cell transplantation for myocardial angiogenesis and functional restoration. *European heart journal*, 24(5), pp.404–11.

Scicchitano, P. et al., 2012. HCN channels and heart rate. *Molecules (Basel, Switzerland)*, 17(4), pp.4225–35.

Seeger, F.H. et al., 2012. Heparin disrupts the CXCR4/SDF-1 axis and impairs the functional capacity of bone marrow-derived mononuclear cells used for cardiovascular repair. *Circulation research*, 111(7), pp.854–62.

Shake, J.G. et al., 2002. Mesenchymal stem cell implantation in a swine myocardial infarct model: engraftment and functional effects. *The Annals of thoracic surgery*, 73(6), pp.1919–25; discussion 1926.

Shand, D.G. & Rangno, R.E., 1972. The disposition of propranolol. I. Elimination during oral absorption in man. *Pharmacology*, 7(3), pp.159–68.

Sherr, C.J. & Roberts, J.M., 1999. CDK inhibitors: positive and negative regulators of G1-phase progression. *Genes & development*, 13(12), pp.1501–12.

Shiba, Y. et al., 2012. Human ES-cell-derived cardiomyocytes electrically couple and suppress arrhythmias in injured hearts. *Nature*, 489(7415), pp.322–5.

Shintaro Nakano, T.M.S.N. and T.S., 2012. *Current Basic and Pathological Approaches to the Function of Muscle Cells and Tissues - From Molecules to Humans* H. Sugi, ed., InTech.

Showell, C., Binder, O. & Conlon, F.L., 2004. T-box genes in early embryogenesis. *Developmental dynamics : an official publication of the American Association of Anatomists*, 229(1), pp.201–18.

Silverman, M.E., 1999. A view from the millennium: the practice of cardiology circa 1950 and thereafter. *Journal of the American College of Cardiology*, 33(5), pp.1141–51.

Siminiak, T. et al., 2004. Autologous skeletal myoblast transplantation for the treatment of postinfarction myocardial injury: phase I clinical study with 12 months of follow-up. *American heart journal*, 148(3), pp.531–7.

Simmerman, H.K. & Jones, L.R., 1998. Phospholamban: protein structure, mechanism of action, and role in cardiac function. *Physiological reviews*, 78(4), pp.921–47.

Skalli, O. et al., 1989. Alpha-smooth muscle actin, a differentiation marker of smooth muscle cells, is present in microfilamentous bundles of pericytes. *The journal of histochemistry and cytochemistry : official journal of the Histochemistry Society*, 37(3), pp.315–21.

Sladek, J.R. et al., 1993. Fetal dopamine cell survival after transplantation is dramatically improved at a critical donor gestational age in nonhuman primates. *Experimental neurology*, 122(1), pp.16–27.

Smart, N. & Riley, P.R., 2008. The stem cell movement. *Circulation research*, 102(10), pp.1155–68.

Song, H. et al., 2010. Interrogating functional integration between injected pluripotent stem cell-derived cells and surrogate cardiac tissue. *Proceedings of the National Academy of Sciences of the United States of America*, 107(8), pp.3329–34.

Soriano, P., 1999. Generalized lacZ expression with the ROSA26 Cre reporter strain. *Nature genetics*, 21(1), pp.70–1.

Spann, J.F. et al., 1966. Cardiac norepinephrine stores and the contractile state of heart muscle. *Circulation research*, 19(2), pp.317–25.

Spargias, K.S. et al., 1999. beta blocker treatment and other prognostic variables in patients with clinical evidence of heart failure after acute myocardial infarction: evidence from the AIRE study. *Heart (British Cardiac Society)*, 81(1), pp.25–32.

Srivastava, D., 2006a. Genetic regulation of cardiogenesis and congenital heart disease. *Annual review of pathology*, 1, pp.199–213.

Srivastava, D., 2006b. Making or breaking the heart: from lineage determination to morphogenesis. *Cell*, 126(6), pp.1037–48.

Srivastava, D., Cserjesi, P. & Olson, E.N., 1995. A subclass of bHLH proteins required for cardiac morphogenesis. *Science (New York, N.Y.)*, 270(5244), pp.1995–9.

Srivastava, D. & Olson, E.N., 2000. A genetic blueprint for cardiac development. *Nature*, 407(6801), pp.221–6.

Stachowiak, E.K. et al., 2003. cAMP-induced differentiation of human neuronal progenitor cells is mediated by nuclear fibroblast growth factor receptor-1 (FGFR1). *Journal of neurochemistry*, 84(6), pp.1296–312.

Stanley, E.G. et al., 2002. Efficient Cre-mediated deletion in cardiac progenitor cells conferred by a 3'UTR-ires-Cre allele of the homeobox gene Nkx2-5. *The International journal of developmental biology*, 46(4), pp.431–9.

Steinberg, S.F. & Brunton, L.L., 2001. Compartmentation of G protein-coupled signaling pathways in cardiac myocytes. *Annual review of pharmacology and toxicology*, 41, pp.751–73.

Stephen, S.A., 1966. Unwanted effects of propranolol. *The American journal of cardiology*, 18(3), pp.463–72.

Stiles, G.L. & Lefkowitz, R.J., 1984. Cardiac adrenergic receptors. *Annual review of medicine*, 35, pp.149–64.

Sulakhe, P. V & Vo, X.T., 1995. Regulation of phospholamban and troponin-I phosphorylation in the intact rat cardiomyocytes by adrenergic and cholinergic stimuli: roles of cyclic nucleotides, calcium, protein kinases and phosphatases and depolarization. *Molecular and cellular biochemistry*, 149-150, pp.103–26.

Sun, Y.-L. et al., 2005. Effect of beta-blockers on cardiac function and calcium handling protein in postinfarction heart failure rats. *Chest*, 128(3), pp.1812–21.

Sun, Z. et al., 2012. Neonatal transfer of membrane-bound stem cell factor improves survival and heart function in aged mice after myocardial ischemia. *Human gene therapy*, 23(12), pp.1280–9.

Supokawej, A. et al., 2013. Cardiogenic and myogenic gene expression in mesenchymal stem cells after 5-azacytidine treatment. *Turkish journal of haematology : official journal of Turkish Society of Haematology*, 30(2), pp.115–21.

Takahashi, K. et al., 2007. Induction of pluripotent stem cells from adult human fibroblasts by defined factors. *Cell*, 131(5), pp.861–72.

Talwar, K.K. et al., 1996. Hemodynamic predictors of early intolerance and long-term effects of propranolol in dilated cardiomyopathy. *Journal of cardiac failure*, 2(4), pp.273–7.

Tam, P.P. et al., 1997. The allocation of epiblast cells to the embryonic heart and other mesodermal lineages: the role of ingression and tissue movement during gastrulation. *Development (Cambridge, England)*, 124(9), pp.1631–42.

Taylor, D.A. et al., 1998. Regenerating functional myocardium: improved performance after skeletal myoblast transplantation. *Nature medicine*, 4(8), pp.929–33.

Temple, I.P. et al., 2013. Connexins and the atrioventricular node. *Heart rhythm : the official journal of the Heart Rhythm Society*, 10(2), pp.297–304.

Tenero, D. et al., 2000. Steady-state pharmacokinetics of carvedilol and its enantiomers in patients with congestive heart failure. *Journal of clinical pharmacology*, 40(8), pp.844–53.

Thomas, S.A., Matsumoto, A.M. & Palmiter, R.D., 1995. Noradrenaline is essential for mouse fetal development. *Nature*, 374(6523), pp.643–6.

Tocci, A. & Forte, L., 2003. Mesenchymal stem cell: use and perspectives. *The hematology journal : the official journal of the European Haematology Association / EHA*, 4(2), pp.92–6.

Tomita, Y. et al., 2005. Cardiac neural crest cells contribute to the dormant multipotent stem cell in the mammalian heart. *The Journal of cell biology*, 170(7), pp.1135–46.

Traverse, J.H. et al., 2011. Effect of intracoronary delivery of autologous bone marrow mononuclear cells 2 to 3 weeks following acute myocardial infarction on left ventricular function: the LateTIME randomized trial. *JAMA : the journal of the American Medical Association*, 306(19), pp.2110–9.

Traverse, J.H. et al., 2012. Effect of the use and timing of bone marrow mononuclear cell delivery on left ventricular function after acute myocardial infarction: the TIME randomized trial. *JAMA : the journal of the American Medical Association*, 308(22), pp.2380–9.

Tse, H.-F. et al., 2003. Angiogenesis in ischaemic myocardium by intramyocardial autologous bone marrow mononuclear cell implantation. *Lancet*, 361(9351), pp.47–9.

Tsukahara, T. et al., 2006. Murine leukemia virus vector integration favors promoter regions and regional hot spots in a human T-cell line. *Biochemical and biophysical research communications*, 345(3), pp.1099–107.

Tzahor, E. & Evans, S.M., 2011. Pharyngeal mesoderm development during embryogenesis: implications for both heart and head myogenesis. *Cardiovascular research*, 91(2), pp.196–202.

Ueno, S. et al., 2007. Biphasic role for Wnt/beta-catenin signaling in cardiac specification in zebrafish and embryonic stem cells. *Proceedings of the National Academy of Sciences of the United States of America*, 104(23), pp.9685–90.

Ungerer, M. et al., 1993. Altered expression of beta-adrenergic receptor kinase and beta 1-adrenergic receptors in the failing human heart. *Circulation*, 87(2), pp.454–63.

Vartanian, R. et al., 2011. AP-1 regulates cyclin D1 and c-MYC transcription in an AKT-dependent manner in response to mTOR inhibition: role of AIP4/Itch-mediated JUNB degradation. *Molecular cancer research : MCR*, 9(1), pp.115–30.

Vatner, S.F., Vatner, D.E. & Homcy, C.J., 2000. beta-adrenergic receptor signaling: an acute compensatory adjustment-inappropriate for the chronic stress of heart failure? Insights from Gsalpha overexpression and other genetically engineered animal models. *Circulation research*, 86(5), pp.502–6.

Ventura, C., Zinellu, E., Maninchedda, E. & Maioli, M., 2003. Dynorphin B is an agonist of nuclear opioid receptors coupling nuclear protein kinase C activation to the transcription of cardiogenic genes in GTR1 embryonic stem cells. *Circulation research*, 92(6), pp.623–9.

Ventura, C., Zinellu, E., Maninchedda, E., Fadda, M., et al., 2003. Protein kinase C signaling transduces endorphin-primed cardiogenesis in GTR1 embryonic stem cells. *Circulation research*, 92(6), pp.617–22.

Ventura, C. & Maioli, M., 2000. Opioid peptide gene expression primes cardiogenesis in embryonal pluripotent stem cells. *Circulation research*, 87(3), pp.189–94.

Vincent, S.D. & Buckingham, M.E., 2010. How to make a heart: the origin and regulation of cardiac progenitor cells. *Current topics in developmental biology*, 90, pp.1–41.

Vogel, C. & Marcotte, E.M., 2012. Insights into the regulation of protein abundance from proteomic and transcriptomic analyses. *Nature reviews. Genetics*, 13(4), pp.227–32.

Vogel, S. et al., 2006. MEK hyperphosphorylation coincides with cell cycle shut down of cultured smooth muscle cells. *Journal of cellular physiology*, 206(1), pp.25–34.

Waagstein, F. et al., 1993. Beneficial effects of metoprolol in idiopathic dilated cardiomyopathy. Metoprolol in Dilated Cardiomyopathy (MDC) Trial Study Group. *Lancet*, 342(8885), pp.1441–6.

Wagers, A.J. et al., 2002. Little evidence for developmental plasticity of adult hematopoietic stem cells. *Science (New York, N.Y.)*, 297(5590), pp.2256–9.

Weber, J.D. et al., 1997. Sustained activation of extracellular-signal-regulated kinase 1 (ERK1) is required for the continued expression of cyclin D1 in G1 phase. *The Biochemical journal*, 326 (Pt 1, pp.61–8.

Welt, F.G.P. et al., 2013. Effect of cardiac stem cells on left-ventricular remodeling in a canine model of chronic myocardial infarction. *Circulation. Heart failure*, 6(1), pp.99–106.

Wenzel-Seifert, K. & Seifert, R., 2000. Molecular analysis of beta(2)-adrenoceptor coupling to G(s)-, G(i)-, and G(q)-proteins. *Molecular pharmacology*, 58(5), pp.954–66.

Wess, J., 1997. G-protein-coupled receptors: molecular mechanisms involved in receptor activation and selectivity of G-protein recognition. *FASEB journal : official publication of the Federation of American Societies for Experimental Biology*, 11(5), pp.346–54.

Wessels, A. & Pérez-Pomares, J.M., 2004. The epicardium and epicardially derived cells (EPDCs) as cardiac stem cells. *The anatomical record. Part A, Discoveries in molecular, cellular, and evolutionary biology*, 276(1), pp.43–57.

Westfall, M. V et al., 1997. Ultrastructure and cell-cell coupling of cardiac myocytes differentiating in embryonic stem cell cultures. *Cell motility and the cytoskeleton*, 36(1), pp.43–54.

White, D.C. et al., 2000. Preservation of myocardial beta-adrenergic receptor signaling delays the development of heart failure after myocardial infarction. *Proceedings of the National Academy of Sciences of the United States of America*, 97(10), pp.5428–33.

Whitsett, J.A., Noguchi, A. & Moore, J.J., 1982. Developmental aspects of alpha- and beta-adrenergic receptors. *Seminars in perinatology*, 6(2), pp.125–41.

Van Wijk, B. & van den Hoff, M., 2010. Epicardium and myocardium originate from a common cardiogenic precursor pool. *Trends in cardiovascular medicine*, 20(1), pp.1–7.

Williamson, E.A. et al., 1997. Cyclic AMP negatively controls c-myc transcription and G1 cell cycle progression in p210 BCR-ABL transformed cells: inhibitory activity exerted through cyclin D1 and cdk4. *Leukemia*, 11(1), pp.73–85.

Wobus, A.M. et al., 1997. Retinoic acid accelerates embryonic stem cell-derived cardiac differentiation and enhances development of ventricular cardiomyocytes. *Journal of molecular and cellular cardiology*, 29(6), pp.1525–39.

Wollert, K.C. et al., 2004. Intracoronary autologous bone-marrow cell transfer after myocardial infarction: the BOOST randomised controlled clinical trial. *Lancet*, 364(9429), pp.141–8.

Wollert, K.C. & Drexler, H., 2010. Cell therapy for the treatment of coronary heart disease: a critical appraisal. *Nature reviews. Cardiology*, 7(4), pp.204–15.

Wu, B. et al., 2012. Endocardial cells form the coronary arteries by angiogenesis through myocardial-endocardial VEGF signaling. *Cell*, 151(5), pp.1083–96.

Wu, S.M. et al., 2006. Developmental origin of a bipotential myocardial and smooth muscle cell precursor in the mammalian heart. *Cell*, 127(6), pp.1137–50.

Xiao, R.P., 2001. Beta-adrenergic signaling in the heart: dual coupling of the beta2-adrenergic receptor to G(s) and G(i) proteins. *Science's STKE : signal transduction knowledge environment*, 2001(104), p.re15.

Xiao, R.P. et al., 1999. Coupling of beta2-adrenoceptor to Gi proteins and its physiological relevance in murine cardiac myocytes. *Circulation research*, 84(1), pp.43–52.

Xiao, R.P., Ji, X. & Lakatta, E.G., 1995. Functional coupling of the beta 2-adrenoceptor to a pertussis toxin-sensitive G protein in cardiac myocytes. *Molecular pharmacology*, 47(2), pp.322–9.

Xinyun, C. et al., 2010. Effects of cardiotrophin-1 on differentiation and maturation of rat bone marrow mesenchymal stem cells induced with 5-azacytidine in vitro. *International journal of cardiology*, 143(2), pp.171–7.

Xu, C. et al., 2006. Cardiac bodies: a novel culture method for enrichment of cardiomyocytes derived from human embryonic stem cells. *Stem cells and development*, 15(5), pp.631–9.

Xu, C. et al., 2002. Characterization and enrichment of cardiomyocytes derived from human embryonic stem cells. *Circulation research*, 91(6), pp.501–8.

Xu, N. et al., 2012. Akt: a double-edged sword in cell proliferation and genome stability. *Journal of oncology*, 2012, p.951724.

Yao, A. et al., 2003. Characteristic effects of alpha1-beta1,2-adrenergic blocking agent, carvedilol, on [Ca2+]i in ventricular myocytes compared with those of timolol and atenolol. *Circulation journal : official journal of the Japanese Circulation Society*, 67(1), pp.83–90.

Yoshikawa, T. et al., 1996. Cardiac adrenergic receptor effects of carvedilol. *European heart journal*, 17 Suppl B, pp.8–16.

Yu, J. et al., 2007. Induced pluripotent stem cell lines derived from human somatic cells. *Science (New York, N.Y.)*, 318(5858), pp.1917–20.

Yu, J. et al., 2010. SDF-1/CXCR4-mediated migration of transplanted bone marrow stromal cells toward areas of heart myocardial infarction through activation of PI3K/Akt. *Journal of cardiovascular pharmacology*, 55(5), pp.496–505.

Yuasa, S. et al., 2005. Transient inhibition of BMP signaling by Noggin induces cardiomyocyte differentiation of mouse embryonic stem cells. *Nature biotechnology*, 23(5), pp.607–11.

Zaccolo, M., 2009. cAMP signal transduction in the heart: understanding spatial control for the development of novel therapeutic strategies. *British journal of pharmacology*, 158(1), pp.50–60.

Zaccolo, M., 2011. Spatial control of cAMP signalling in health and disease. *Current opinion in pharmacology*, 11(6), pp.649–55.

Zaffran, S. et al., 2004. Right ventricular myocardium derives from the anterior heart field. *Circulation research*, 95(3), pp.261–8.

Zamah, A.M. et al., 2002. Protein kinase A-mediated phosphorylation of the beta 2-adrenergic receptor regulates its coupling to Gs and Gi. Demonstration in a reconstituted system. *The Journal of biological chemistry*, 277(34), pp.31249–56.

Zhang, F. & Pasumarthi, K.B.S., 2008. Embryonic stem cell transplantation: promise and progress in the treatment of heart disease. *BioDrugs : clinical immunotherapeutics, biopharmaceuticals and gene therapy*, 22(6), pp.361–74.

Zhang, F. & Pasumarthi, K.B.S., 2007. Ultrastructural and immunocharacterization of undifferentiated myocardial cells in the developing mouse heart. *Journal of cellular and molecular medicine*, 11(3), pp.552–60.

Zhang, Y. et al., 2011. Intramyocardial transplantation of undifferentiated rat induced pluripotent stem cells causes tumorigenesis in the heart. *PloS one*, 6(4), p.e19012.

Zhou, B., Ma, Q., et al., 2008. Epicardial progenitors contribute to the cardiomyocyte lineage in the developing heart. *Nature*, 454(7200), pp.109–13.

Zhou, B., von Gise, A., et al., 2008. Nkx2-5- and Isl1-expressing cardiac progenitors contribute to proepicardium. *Biochemical and biophysical research communications*, 375(3), pp.450–3.

Zhou, Q.Y. & Palmiter, R.D., 1995. Dopamine-deficient mice are severely hypoactive, adipsic, and aphagic. *Cell*, 83(7), pp.1197–209.

Zhou, Q.Y., Quaife, C.J. & Palmiter, R.D., 1995. Targeted disruption of the tyrosine hydroxylase gene reveals that catecholamines are required for mouse fetal development. *Nature*, 374(6523), pp.640–3.

Zhu, W.-Z. et al., 2005. Heterodimerization of beta1- and beta2-adrenergic receptor subtypes optimizes beta-adrenergic modulation of cardiac contractility. *Circulation research*, 97(3), pp.244–51.

Zou, C. et al., 2007. [Effects of metoprolol on cardiac function and myocyte calcium regulatory protein expressions in rabbits with experimental heart failure]. *Zhonghua xin xue guan bing za zhi*, 35(5), pp.476–9.

Zucker, I.H., Patel, K.P. & Schultz, H.D., 2012. Neurohumoral stimulation. *Heart failure clinics*, 8(1), pp.87–99.

Zucker, I.H., Xiao, L. & Haack, K.K. V, 2014. The central renin-angiotensin system and sympathetic nerve activity in chronic heart failure. *Clinical science (London, England : 1979)*, 126(10), pp.695–706.